Stem Cells International

Ex Vivo and *In Vivo* Stem Cells-Based Tissue Engineering Strategies for Their Use in Regenerative Medicine

Lead Guest Editor: Víctor Carriel
Guest Editors: Heidi Declercq, Stefano Geuna, and Miguel Alaminos

Ex Vivo and *In Vivo* Stem Cells-Based Tissue Engineering Strategies for Their Use in Regenerative Medicine

Stem Cells International

Ex Vivo and *In Vivo* Stem Cells-Based Tissue Engineering Strategies for Their Use in Regenerative Medicine

Lead Guest Editor: Víctor Carriel
Guest Editors: Heidi Declercq, Stefano Geuna, and Miguel Alaminos

Copyright © 2018 Hindawi. All rights reserved.

This is a special issue published in "Stem Cells International." All articles are open access articles distributed under the Creative Commons Attribution License, which permits unrestricted use, distribution, and reproduction in any medium, provided the original work is properly cited.

Editorial Board

James Adjaye, Germany
Cinzia Allegrucci, UK
Stefan Arnhold, Germany
Andrea Ballini, Italy
Dominique Bonnet, UK
Philippe Bourin, France
Daniel Bouvard, France
Silvia Brunelli, Italy
Stefania Bruno, Italy
Bruce A. Bunnell, USA
Kevin D. Bunting, USA
Benedetta Bussolati, Italy
Leonora Buzanska, Poland
A. C. Campos de Carvalho, Brazil
Stefania Cantore, Italy
Yilin Cao, China
Alain Chapel, France
Isotta Chimenti, Italy
Mahmood S. Choudhery, Pakistan
Pier Paolo Claudio, USA
Gerald A. Colvin, USA
Mihaela Crisan, UK
Marcus-André Deutsch, Germany
Varda Deutsch, Israel
Valdo Jose Dias Da Silva, Brazil
Massimo Dominici, Italy
Leonard M. Eisenberg, USA
Georgina Ellison, UK
Alessandro Giacomello, Italy
Maria M. Estima Gomes, Portugal
Cristina Grange, Italy
Stan Gronthos, Australia
Jacob H. Hanna, Israel
David A. Hart, Canada
Yohei Hayashi, Japan
Tong-Chuan He, USA
Boon C. Heng, Hong Kong
Xiao J. Huang, China
Thomas Ichim, USA
Joseph Itskovitz-Eldor, Israel
Elena Jones, UK
Diana Klein, Germany
Valerie Kouskoff, UK
Andrzej Lange, Poland
Laura Lasagni, Italy
Renke Li, Canada
Tao-Sheng Li, Japan
Shinn-Zong Lin, Taiwan
Yupo Ma, USA
Marcin Majka, Poland
Giuseppe Mandraffino, Italy
Athanasios Mantalaris, UK
Cinzia Marchese, Italy
Katia Mareschi, Italy
Hector Mayani, Mexico
Jason S. Meyer, USA
Eva Mezey, USA
Susanna Miettinen, Finland
Toshio Miki, USA
Claudia Montero-Menei, France
Christian Morsczeck, Germany
Federico Mussano, Italy
Mustapha Najimi, Belgium
Norimasa Nakamura, Japan
Karim Nayernia, UK
Krisztian Nemeth, USA
Sue O'Shea, USA
Kishore B. S. Pasumarthi, Canada
Stefan Przyborski, UK
Bruno Pèault, USA
Peter J. Quesenberry, USA
Pranela Rameshwar, USA
Bernard A. J. Roelen, Netherlands
Peter Rubin, USA
Hannele T. Ruohola-Baker, USA
Benedetto Sacchetti, Italy
Ghasem Hosseini Salekdeh, Iran
Antonio Salgado, Portugal
Fermin Sanchez-Guijo, Spain
Heinrich Sauer, Germany
Coralie Sengenes, France
Dario Siniscalco, Italy
Shimon Slavin, Israel
Sieghart Sopper, Austria
Valeria Sorrenti, Italy
Giorgio Stassi, Italy
Ann Steele, USA
Alexander Storch, Germany
Bodo Eckehard Strauer, Germany
Hirotaka Suga, Japan
Gareth Sullivan, Norway
Masatoshi Suzuki, USA
Kenichi Tamama, USA
Corrado Tarella, Italy
Daniele Torella, Italy
Hung-Fat Tse, Hong Kong
Marc L. Turner, UK
Dominik Wolf, Austria
Qingzhong Xiao, UK
Takao Yasuhara, Japan
Zhaohui Ye, USA
Holm Zaehres, Germany
Elias T. Zambidis, USA
Ewa K. Zuba-Surma, Poland
Maurizio Zuccotti, Italy

Contents

Hindawi
Stem Cells International
Volume 2018, Article ID 7143930, 2 pages
https://doi.org/10.1155/2018/7143930

Editorial

Ex Vivo and In Vivo Stem Cells-Based Tissue Engineering Strategies for Their Use in Regenerative Medicine

Víctor Carriel,[1] **Stefano Geuna**,[2] **and Miguel Alaminos**[1]

[1]*Department of Histology, Tissue Engineering Group, University of Granada and Instituto de Investigación Biosanitaria, Ibs, Granada, Spain*
[2]*Dipartimento di Scienze Cliniche e Biologiche, Università di Torino, Torino, Italy*

Correspondence should be addressed to Víctor Carriel; vcarriel@ugr.es

Received 13 February 2018; Accepted 13 February 2018; Published 15 April 2018

Copyright © 2018 Víctor Carriel et al. This is an open access article distributed under the Creative Commons Attribution License, which permits unrestricted use, distribution, and reproduction in any medium, provided the original work is properly cited.

Tissue engineering is an emergent discipline focused on the generation of bioartificial tissue-like substitutes through the combination of biomaterials, cells, and growth factors. In this context, stem cell-based strategies have made substantial contributions in the field. Researchers worldwide have demonstrated that stem cells have an extraordinary capability to differentiate into different cell lineages, promote tissue regeneration, release a wide range of growth factors, and modulate the host immune response. Based on the current impact of tissue engineering and stem cells in medicine, *Stem Cells International* set out to publish a special issue focused on the "Ex Vivo and In Vivo Stem Cell-Based Tissue Engineering Strategies for Their Use in Regenerative Medicine." This special issue resulted in a collection of nine outstanding articles which include two reviews and seven original studies made by recognized researchers from seven countries across Europe, Asia, South America, and North America.

Concerning the review articles, M. Cimino et al. contributed with a complete review entitled "Xeno-Free Strategies for Safe Human Mesenchymal Stem/Stromal Cell Expansion: Supplements and Coatings," where authors suggest that culture/expansion of human mesenchymal stem cells under xeno-free conditions is still needed to improve their clinical translation. The review made by A. Owczarczyk-Saczonek et al. discussed "The Use of Adipose-Derived Stem Cells in Selected Skin Diseases (Vitiligo, Alopecia, and Nonhealing Wounds)," highlighting that these stem cells are promising alternatives to generate new engineered or stem cell-based strategies to treat skin diseases.

In the field of cartilage tissue engineering, two interesting *in vivo* studies were published in this special issue. On the one hand, M. Mata et al. published the article entitled "In Vivo Articular Cartilage Regeneration Using Human Dental Pulp Stem Cells Cultured in an Alginate Scaffold: A Preliminary Study" in which they demonstrated, through different histological approaches, that human dental pulp stem cells have a positive impact on the regeneration of articular cartilage in rabbits. On the other hand, V. Chapman et al. demonstrated that late passage marrow-derived mesenchymal stem cells were more efficient than early passage cells in the treatment of osteoarthritis on their article entitled "Therapeutic Benefit for Late, but Not Early, Passage Mesenchymal Stem Cells on Pain Behaviour in an Animal Model of Osteoarthritis." These articles provide new evidence related to the usefulness of stem cells in cartilage tissue engineering.

Currently, adipose-derived mesenchymal stem cells are considered one of the most promising mesenchymal stem cells by several and well-supported reasons. Within this special issue, N. Garcia-Honduvilla et al. demonstrated that a natural extract purified from *Cryptomphalus aspersa's* eggs induced the differentiation of adipose stem cells to myofibroblast on their study entitled "High Sensitivity of Human Adipose Stem Cells to Differentiate into Myofibroblasts in the Presence of C. aspersa Egg Extract." In another interesting ex vivo approach, E. Oliveira et al. on their article "Influence of Different ECM-Like Hydrogels on Neurite Outgrowth Induced by Adipose Tissue-Derived Stem Cells" demonstrated the synergetic effect of the correct combination of bio-

materials and adipose stem cells to increase the neurite outgrowth from DRG explants. In these articles, the usefulness and versatility of adipose stem cells in tissue engineering were well demonstrated.

Extraembryonic tissues are an important source of stem cells and natural scaffolds. In this regard, G. P. Liao et al. successfully repaired diaphragmatic defects in rats by using decellularized rat diaphragm containing human amniotic fluid-derived stem cells on their article entitled "Tissue Engineering to Repair Diaphragmatic Defect in a Rat Model." In addition, in order to solve the problem associated to the expansion of epithelial cells, S. M. Nam et al. investigated the use two stem cells sources as feeder cells of corneal epithelial cells on their article entitled "Ex Vivo Expansion of Human Limbal Epithelial Cells Using Human Placenta-Derived and Umbilical Cord-Derived Mesenchymal Stem Cells." In an *in vivo* approach, M. Garrido et al. demonstrate the potential clinical application of amniotic membrane in digestive surgery on their article "Transplantation of Human Amniotic Membrane over the Liver Surface Reduces Hepatic Fibrosis in a Cholestatic Model in Young Rats." These three articles highlight the potential clinical usefulness of extraembryonic-derived cells and scaffolds in tissue engineering.

Finally, in these nine articles, authors rigorously discussed and demonstrated the high versatility of different kinds of stem cells to differentiate, promote tissue healing, modulate host immune response, and serve as feeder platform for the ex vivo expansion of differentiated cells. In conclusion, the articles published in this special issue provide new tissue engineered-based strategies and scientific evidence that support the potential clinical usefulness of stem cells in regenerative medicine.

Víctor Carriel
Stefano Geuna
Miguel Alaminos

Hindawi
Stem Cells International
Volume 2018, Article ID 6169546, 9 pages
https://doi.org/10.1155/2018/6169546

Research Article

Transplantation of Human Amniotic Membrane over the Liver Surface Reduces Hepatic Fibrosis in a Cholestatic Model in Young Rats

M. Garrido,[1,2] C. Escobar,[1] C. Zamora,[1] C. Rejas,[1] J. Varas,[1] C. Córdova,[1] C. Papuzinski,[3] M. Párraga,[1] S. San Martín,[1] and S. Montedonico[1,2]

[1]*Centro de Investigaciones Biomédicas, Universidad de Valparaíso, Valparaíso, Chile*
[2]*Servicio de Cirugía Pediátrica, Hospital Carlos van Buren, Valparaíso, Chile*
[3]*Departamento de Salud Pública, Universidad de Valparaíso, Valparaíso, Chile*

Correspondence should be addressed to S. San Martín; sebastian.sanmartin@uv.cl

Received 25 April 2017; Accepted 9 December 2017; Published 25 February 2018

Academic Editor: Stefano Geuna

Copyright © 2018 M. Garrido et al. This is an open access article distributed under the Creative Commons Attribution License, which permits unrestricted use, distribution, and reproduction in any medium, provided the original work is properly cited.

Purpose. Biliary atresia precedes liver cirrhosis and liver transplantation. Amniotic membrane (AM) promotes tissue regeneration, inhibits fibrosis, and reduces inflammation. Here, we test amniotic membrane potential as a therapeutic tool against cholestatic liver fibrosis. *Methods*. Three groups of rats were used: sham surgery (SS), bile duct ligature (BDL), and bile duct ligature plus human amniotic membrane (BDL + AM). After surgery, animals were sacrificed at different weeks. Biochemical and histopathological analyses of liver tissue were performed. Collagen was expressed as a percentage of total liver tissue area. qPCR was performed to analyse gene expression levels of transforming growth factor-β1 (*Tgfb1*) and apelin (*Apln*). Statistical analysis performed considered $p < 0.05$ was significant. *Results*. Groups undergoing BDL developed cholestasis. Biochemical markers from BDL + AM group improved compared to BDL group. Ductular reaction, portal fibrosis, and bile plugs were markedly reduced in the BDL + AM group compared to BDL group. Collagen area in BDL + AM group was statistically decreased compared to BDL group. Finally, expression levels of both *Apln* and *Tgfb1* mRNA were statistically downregulated in BDL + AM group versus BDL group. *Conclusion*. AM significantly reduces liver fibrosis in a surgical animal model of cholestasis. Our results suggest that AM may be useful as a therapeutic tool in liver cirrhosis.

1. Background and Purpose

Biliary atresia is a neonatal disease of unknown etiology characterized by progressive, inflammatory, and fibrosclerosing cholangiopathy resulting in obstruction of both extrahepatic and intrahepatic bile ducts. Despite Kasai portoenterostomy, 68–80% of patients affected by biliary atresia develop progressive fibrosis leading to biliary cirrhosis and portal hypertension [1]. Biliary atresia constitutes the first cause of pediatric liver transplantation, accounting for half of cases [2]. In the last two decades, strategies to improve liver function in biliary atresia have been focused in early diagnosis and in developing methods to prevent progressive liver fibrosis.

Animal models play a key role in our understanding of the molecular basis and natural history of human diseases. Bile duct ligature (BDL) is a surgical model of cholestasis that provokes a progressive liver fibrosis leading to liver cirrhosis [3–5].

In the least years, stem cells have been successfully used for regenerative therapies against human diseases. The amniotic membrane retains pluripotential properties from

epiblastic cells offering anti-inflammatory and antifibrotic properties; it modulates angiogenesis and favours healing process. Amniotic membrane has unlimited availability and has not ethical or legal barriers. Preclinical studies have demonstrated that amniotic membrane reduces lung and liver fibrosis in animal models, but only adult animals have been tested [6–11].

The aim of this study was to test human amniotic membrane as a potential therapeutic tool against cholestatic liver fibrosis in young rats.

2. Methods

2.1. Animals. The study was approved by the Institutional Bioethics Committee for Animal Research of Universidad de Valparaíso (BEA029-2014). It was carried out according to the International Guiding Principles regarding the use of laboratory animals [12].

Sixty-three 3-week-old Sprague-Dawley rats were divided into three groups: sham surgery (SS, $n = 21$), bile duct ligature (BDL, $n = 19$), and bile duct ligature plus human amniotic membrane (BDL + AM, $n = 20$). Numbers are different because two rats from the BDL group and one rat from the BDL + AM group died after surgery and were not analyzed. They had access to drink and food ad libitum, circadian cycle of light-darkness 12 : 12 h, controlled humidity (40–70%), and temperature ($21 \pm 2^{\circ}$C), with ventilation of 10 changes air/h.

2.2. Donor Selection and Procurement of Amniotic Membrane. Full-term placentas were collected from caesarean section delivery of healthy women donor under informed consent. Institutional Ethic Committee approved the protocol of placenta and amniotic membrane donation (88-04.09.2013).

Placenta and amniotic membrane were processed under sterile conditions; in a laminar flow hood, blood clots were removed with saline solution 0.09% plus penicillin [50 μg/mL], streptomycin [50 μg/mL], and amphotericin B [2.5 μg/mL]. Amniotic membrane was isolated from chorion through blind dissection. These samples were cultured in order to rule out bacterial or fungal infection. If cultures were negative, amniotic membranes were frozen in sterile Petri dish with Dulbecco's modified Eagle medium at −80°C and glycerol in 1 : 1 proportion.

2.3. Surgical Procedure. One hour before the operation, acetaminophen 0.1 mL (10 g/100 mL) was administered to 3-week-old rats by oral route. The rat was placed in a transparent acrylic box for anesthetic induction. The rat was preoxygenated with 99.5 ± 0.5 pure oxygen at 1 L/min for 30 s and then anesthetized with isoflurane at 3-4% with a funnel-fill vaporizer (Harvard Apparatus, Holliston, MA, USA) until assessed by the absence of voluntary movements, muscle relaxation, and loss of response to stimuli reflexes. After that, the rat was placed in a heating small-animal operating table (Harvard Apparatus, Holliston, MA, USA). Anesthesia was maintained with a facial mask with oxygen and isoflurane 2%. The surgical procedure was performed under clean conditions, using surgical loupes (magnification 2.5x) and microsurgical instruments. A superior midline abdominal incision was performed. The viscera were exposed, the duodenum was exteriorized, and the common bile duct was identified and dissected. After that, the common bile duct was ligated into two parts: a distal ligature was placed just before the entrance to the pancreas, and a proximal ligature was placed below the hepatic duct junction, both with 7-0 polypropylene. After that, the common bile duct was sectioned in the middle. In the BDL + AM group, human amniotic membrane was sutured to the hepatic surface with 7-0 polypropylene covering the whole liver (Figure 1). The abdomen was then closed in two layers. In the SS group, the common bile duct was dissected, but it was not ligated. During anesthetic recovery, the rats were exposed to infrared light to prevent hypothermia for 30 min and received oxygen until awake. After surgery, the rats were allowed to feed normally. After the surgical procedure, rats were followed up on a daily basis until their sacrifice.

Figure 1: After the completion of bile duct ligature procedure, in the BDL + AM group, human amniotic membrane was sutured to the hepatic surface covering the whole liver.

2.4. Euthanasia and Collection of Samples. Rats from each group were sacrificed in subgroups of 7 on the 2nd, 4th, and 6th postoperative weeks, under general anesthesia with isoflurane 4% according to the International Guiding Principles regarding the use of laboratory animals [12]. Weight gain (grams) was recorded before euthanized. A laparotomy was performed describing the intra-abdominal anatomy focusing in liver aspect and biliary duct changes.

2.5. Biochemical Liver Function Analysis. Blood samples were collected by puncture with a 21-gauge needle from the infrahepatic inferior cava vein at time of euthanasia. These were centrifuged at 1000 rpm by 3 min and analyzed

Table 1: The sequences of the primers.

Gene	Sense primer	Antisense primer
Tgfb1	5′-AGAGCCCTGGATACCAACTA-3′	5′-GACCTTGCTGTACTGTGTGT-3′
Apln	5′-TGTCCTCATCCCGTGTGTTC-3′	5′-AAGCACTCACCTCCCTACA-3′
B2m	5′-CAGTTCCACCCACCTCAGAT-3′	5′-TTTTGGGCTCCTTCAGAGTG-3′

by VetTest® Chemistry Analyzer (IDEXX Laboratories, Westbrook, ME, USA). Albumin, alkaline phosphatase, alanine transaminase, gamma-glutamyl transpeptidase, and total bilirubin were studied.

2.6. Determination of Spleen Index. The spleen was extracted and weighed (grams) in order to obtain an indirect measurement of portal hypertension expressed as "spleen index": spleen weight/body weight × 100 [3].

2.7. Histopathological Examination. The left lateral lobe of the liver from each rat was subject to histological evaluation. A sample of the lobe was divided into two samples: the first sample was kept at 4% buffered paraformaldehyde, embedded in paraffin, sectioned, and stained with hematoxylin-eosin. The second sample was fixed in methacarn solution (methanol, chloroform, and acetic acid: 6 : 3 : 1) during 4 h at 4°C. After that, samples were dehydrated by submerging into 100% ethanol 3 times for 30 minutes each, cleared in xylol 3 times for 15 minutes each, and embedded in liquid paraffin at 60°C 3 times for 30 minutes each, and finally included in a solid paraffin block. From these blocks, 10 histological sections of 5 μm thick were cut, and number 11 was the selected section for analysis. Another 10 sections of 5 μm were cut, and number 11 was again selected for analysis. At the end, two sections, 5 μm each, separated by 50 μm of tissue were analyzed. This makes a total number of 42 sections from group SS, 38 sections from group BDL, and 40 sections from group BDL + AM. This procedure was carried out with every liver. Selected sections were stained in a sirius red solution during 1 h for collagen evaluation. The slides were analyzed in a light microscope (Olympus® CX81, Olympus, Tokyo, Japan) and photographed (DP71 camera, Olympus, Tokyo, Japan). Images at 40x, 100x, and 400x magnification were captured.

2.8. Collagen Quantification. Ten nonoverlapping photographs from random fields for each selected section as described above were taken from two slides per specimen at 100x magnification. We obtained $42 \times 10 = 420$ images from group SS, $38 \times 10 = 380$ images from group BDL, and $40 \times 10 = 400$ images from group BDL + AM. Images were exported in .JPG format with a resolution of 1200×900 pixels in RGB color palette. They were then converted in TIFF format and processed to enhance the positive marking, adjusted using the hue-saturation-brightness (HSB) combination with a graphic editor (Adobe Photoshop CC version 16.1.0, Adobe Systems, San José, CA, USA). Images were processed in an automated image analyzer (ImageJ version 1.48, US National Institutes of Health, Bethesda, MA, USA). Threshold colors were adjusted using HSB combination to select all the positive sirius red marking according to controls. Selected area was measured in square pixels, and the staining intensity was measured in an 8-bit gray scale (0 to 256). The positive area fraction considering a complete picture of the same resolution was calculated. The process of analysis was automated using macrocode to process 10 images per cycle. Data were expressed as a percentage of total liver tissue area.

2.9. Gene Expression. A sample of 100 mg from left lateral lobe of the liver was frozen in liquid nitrogen and used for gene expression analysis. Total RNA was extracted using TRIzol® RNA Isolation Reagent (Ambion, Thermo Fisher Scientific, Waltham, MA, USA) according to the manufacturer's recommendations. Template cDNA was obtained by reverse transcription of 2 μg of total RNA using MMLV retrotranscriptase (NEB, Ipswich, MA, USA). Reaction mixtures were incubated at 25°C for 10 min, 42°C for 50 min, and 70°C for 10 min.

Relative quantification of gene expression levels for transforming growth factor-β1 (*Tgfb1*) and apelin (*Apln*) genes was carried out by real-time quantitative PCR (RT-PCR) on EcoPCR real-time system (Illumina, San Diego, CA, USA) using cDNA samples obtained as described before. For this purpose, SYBR® Select Master Mix (Thermo Fisher Scientific, Waltham, MA, USA) was used according to manufacturer's instructions. Specific primers were designed for amplification of each gene, and their sequences are described below. Comparative cycle threshold (Ct) values were obtained after RT-PCR reaction was performed. We used the Ct method to calculate relative mRNA expression. All quantifications were normalized by the corresponding expression of β2 microglobulin (*B2m*) mRNA that served as housekeeping gene. In addition, results were corrected with the expression of the same normalized genes in control tissue. Finally, gene expression differences were calculated using data obtained from groups according to the time elapsed after surgery. These differences were shown as "fold change" in the level of expression of both *Apln* and *Tgfb1* at 2, 4, and 6 weeks after surgery.

The sequences of the primers used in this study were presented in Table 1.

2.10. Statistical Analysis. Data are expressed as mean ± standard deviation. ANOVA test was used for comparison of initial weights between three groups. Nonparametric Mann–Whitney Rank Sum Test was applied to evaluate other

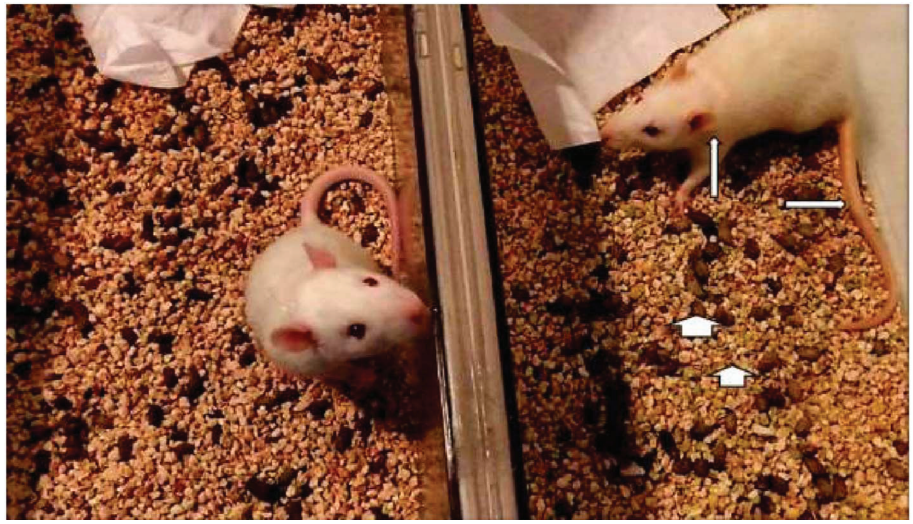

Figure 2: In comparison with the control group, in both the BDL groups, cholestasis was clinically evident, characterized by icteric coloration of face, legs, and tail (arrows). Additionally, yellowish pigmentation was observed in the gravel of boxes (choluria), and stools were clearly pale (acholia) (arrowheads).

Table 2: Preoperative and postoperative weight and spleen index.

		Preoperative	2nd PO week	4th PO week	6th PO week
SS ($n = 21$)	Weight	52.65 ± 6.68 g	129.46 ± 12.97 g	213.74 ± 37.74 g	235.19 ± 37.17 g
	Spleen index		0.42 ± 0.03	0.31 ± 0.06	0.26 ± 0.05
BDL ($n = 19$)	Weight	54.16 ± 9.41 g	85.29 ± 38.90 g*	154.37 ± 27.68 g*	219.64 ± 47.99 g
	Spleen index		0.38 ± 0.34	0.60 ± 0.11	0.54 ± 0.24*
BDL + AM ($n = 20$)	Weight	51.37 ± 12.95 g	62.08 ± 15.92 g†	116.74 ± 25.26 g††‡	241.30 ± 48.67 g
	Spleen index		0.38 ± 0.14	0.53 ± 0.15**	0.54 ± 0.28*

Weight is measured in grams (g), and spleen index in absolute values.
PO: postoperative; SS: sham surgery; BDL: bile duct ligature; AM: amniotic membrane.
$^{*}p < 0.05$ sham versus BDL/BDL + AM.
$^{**}p < 0.01$ sham versus BDL/BDL + AM.
$^{\dagger}p < 0.05$ sham versus BDL + AM.
$^{\dagger\dagger}p < 0.01$ sham versus BDL + AM.
$^{\ddagger}p < 0.01$ BDL versus BDL + AM.

differences among groups. A p value < 0.05 was considered statistically significant. Statistical analysis was performed using STATA software version 12.0 (StataCorp LP, College Station, TX, USA).

3. Results

All the rats in the SS group survived the experiments, while the survival rate in the BDL group was 19/21 and in the BDL + AM group was 20/21. In both the BDL and BDL + AM groups, cystic dilatation of the bile duct was observed in all the rats studied and was a consequence of the surgical procedure of bile duct ligation model, demonstrating that the bile duct was effectively obstructed. Cholestasis was clinically evident and progressive in time, noted by icteric coloration of face, legs, and tail. Additionally, yellowish pigmentation was observed in the gravel of boxes (choluria), and stools were clearly pale (acholia) (Figure 2). At laparotomy, bile-stained tissues, ascites, and splenomegaly was observed in all the rats studied. All these findings were progressive in time and were more striking in the rats that were sacrificed on the 6th postoperative week. In addition, poor growth of hair in the surgical wound was observed. Table 2 shows preoperative and postoperative weight and spleen index in rats. No initial or postoperative differences were noted in the three groups. In both the BDL and BDL + AM groups, histological analysis of liver showed progressive ductular reaction and portal fibrosis with collagen deposition. However, on the 6th postoperative week, the BDL + AM group presented a marked reduction in these features (Figure 3 and Table 3). Biochemical liver function analysis is shown in Table 4. mRNA expression level of *Tgfb1* and *Apln* was significantly higher in the BDL group versus the BDL + AM group, with values for *Tgfb1* of 5.49 ± 3.7 versus 0.30 ± 0.25, respectively ($p < 0.01$), and values for *Apln* of 1.40 ± 0.6 versus 0.39 ± 0.8, respectively ($p < 0.05$) (Figure 4).

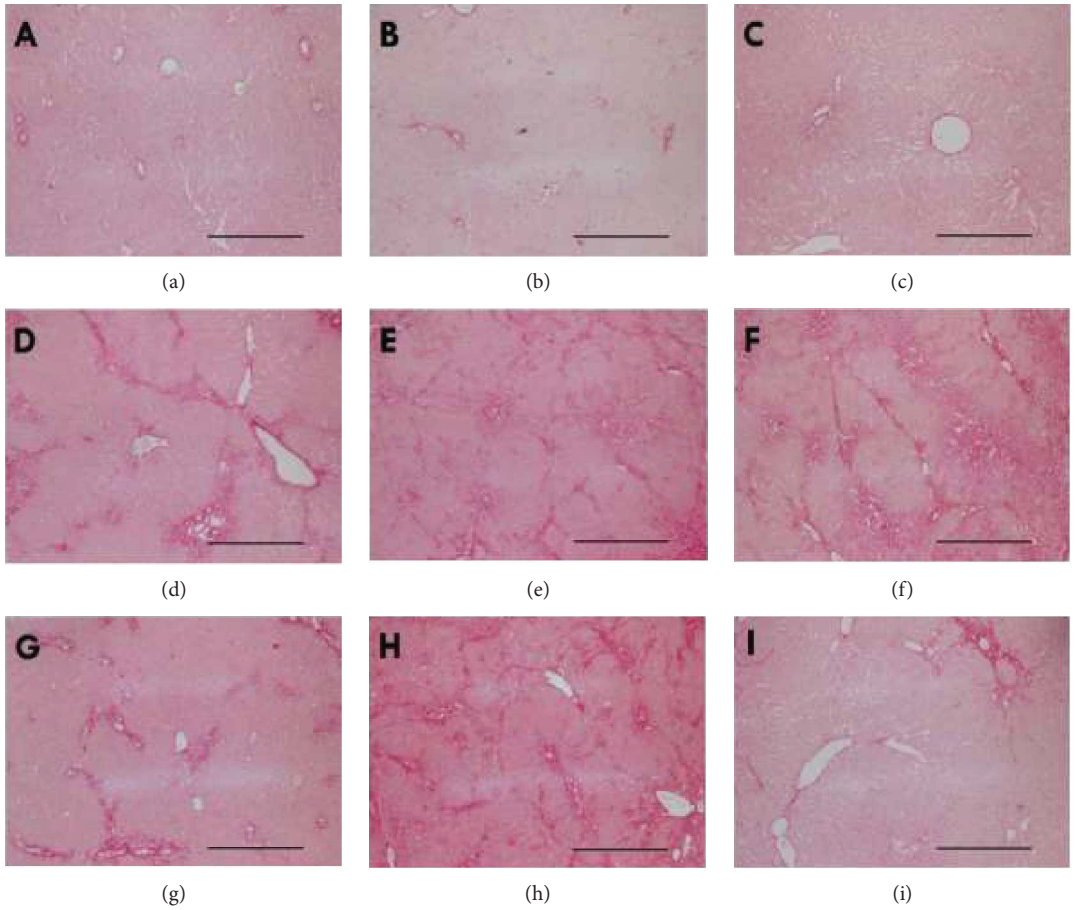

Figure 3: Representative histological sections stained with sirius red from the three studied groups on the 2nd, 4th, and 6th postoperative weeks. In the SS group, no changes were noticed (a–c). In the BDL group, a progressive ductular reaction and periportal fibrosis were evident along the postoperative weeks (d–f). In the BDL + AM group, a progressive ductular reaction and periportal fibrosis were noted on the 2nd and 4th postoperative weeks (g and h). However, a marked reduction in liver fibrosis was evident on the 6th postoperative week (i). SS: sham surgery; BDL: bile duct ligature; BDL + AM: bile duct ligature plus amniotic membrane; PO: postoperative. Scale bar represents 200 μm.

Table 3: Collagen quantification.

	2nd PO week	4th PO week	6th PO week
SS ($n = 21$)	4.81 ± 4.72%	3.05 ± 3.50%	4.80 ± 4.15%
BDL ($n = 19$)	14.25 ± 6.74%**	16.29 ± 9.46%**	26.96 ± 11.63%**
BDL + AM ($n = 20$)	14.70 ± 6.80%**	19.28 ± 9.33%**	14.57 ± 9.37%**††‡

PO: postoperative; SS: sham surgery; BDL: bile duct ligature; AM: amniotic membrane.
**$p < 0.01$ sham versus BDL/BDL + AM.
††$p < 0.01$ BDL versus BDL + AM.
‡$p < 0.05$ BDL + AM 4th PO week versus BDL + AM 6th PO week.

4. Discussion

Biliary atresia constitutes an important problem in pediatric surgery. The vast majority of patients would need a liver transplantation. Children undergoing liver transplantation for biliary atresia are younger than those engrafted for other conditions displaying a higher risk of complications and retransplantation [2]. Therefore, studying strategies to improve liver function secondary to biliary atresia is mandatory. Three types of animal models have been reported in biliary atresia: spontaneous, secondary to viral infection, and surgically created. The sea lamprey (*Petromyzon marinus*) is a jawless vertebrate that during metamorphosis from larvae to parasitic juveniles progressively loses the biliary system until complete biliary degeneration. However, sea lamprey does not develop cirrhosis during development of biliary atresia. Intraperitoneal inoculation of mice with rhesus rotavirus within the first 48 h of postnatal life leads

Table 4: Liver function tests.

	Sham ($n = 6$)	2nd PO week ($n = 3$)	4th PO week ($n = 4$)	6th PO week ($n = 5$)
Albumin (g/dL)	2.5 ± 0	BDL: 2.4 ± 0.37 BDL + AM: 2.85 ± 0.07	BDL: 1.88 ± 0.5* BDL + AM: 2.9 ± 0†	BDL: 1.99 ± 0.17 BDL + AM: 3.33 ± 0.36‡†
ALT (U/L)	70 ± 7.07	BDL: 79.75 ± 17.99 BDL + AM: 106 ± 0	BDL: 124.6 ± 58.8 BDL + AM: 76 ± 7.07	BDL: 79 ± 46.16 BDL + AM: 56.71 ± 35.5
Alkaline phosphatase (U/L)	573 ± 99	BDL: 420 ± 84 BDL + AM: 324 ± 0	BDL: 635.6 ± 197.53 BDL + AM: 419 ± 56.57	BDL: 421 ± 172.52 BDL + AM: 278 ± 171
GGT (U/L)	0 ± 0	BDL: 24.75 ± 28.93 BDL + AM: 79 ± 0	BDL: 35.8 ± 21.29 BDL + AM: 13.5 ± 19.09	BDL: 33 ± 27.4 BDL + AM: 1.86 ± 3.49††
Bilirubin (mg/dL)	0.1 ± 0	BDL: 2.73 ± 2.86 BDL + AM: 10.7 ± 5.23	BDL: 2.84 ± 1.68* BDL + AM: 2.65 ± 3.61	BDL: 4.23 ± 1.12 BDL + AM: 2.39 ± 2.50

ALT: alanine transaminase; GGT: gamma-glutamyl transpeptidase; PO: postoperative.
*$p < 0.05$ BDL versus sham.
‡$p < 0.05$ BDL + AM versus sham.
†$p < 0.05$ BDL versus BDL + AM.
††$p < 0.01$ BDL versus BDL + AM.

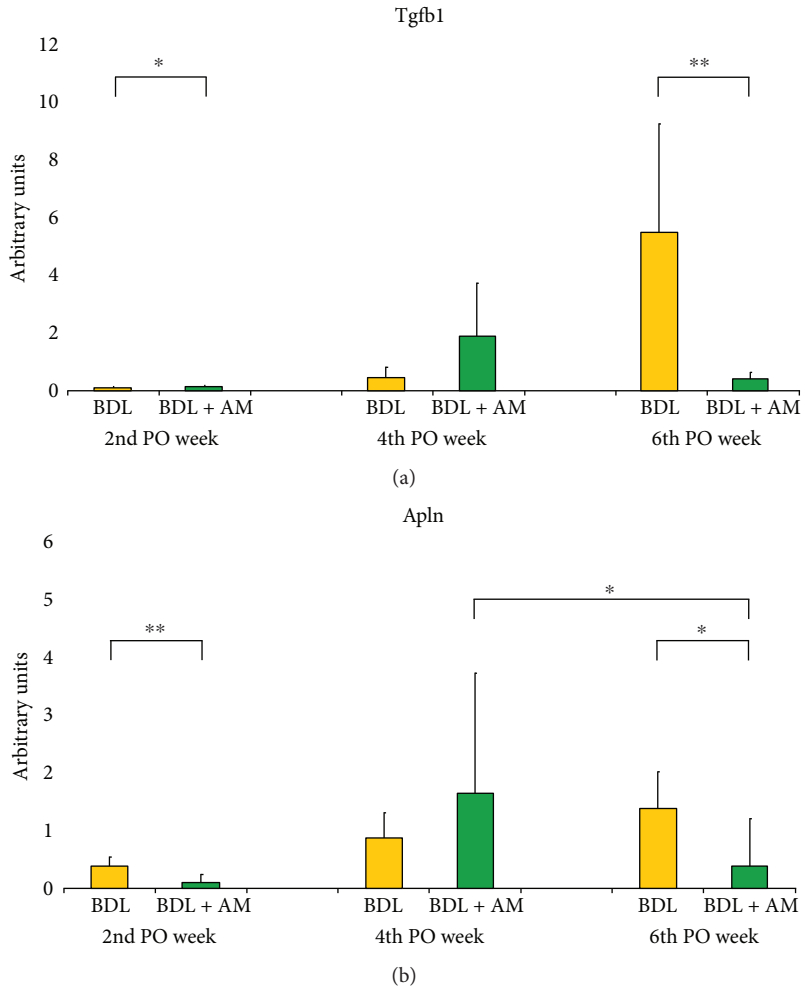

Figure 4: mRNA expression levels of profibrogenic genes in arbitrary units as "fold change." (a) mRNA expression levels of *Tgfb1*. In the BDL group, *Tgfb1* exponentially increased along the experiment. Marked differences were noted on the 6th postoperative week between the BDL group and the BDL + AM group. (b) mRNA expression levels of *Apln*. In the BDL group, *Apln* increased in a linear way over time. Marked differences were also noticed on the 6th postoperative week between the BDL group and the BDL + AM group. Additionally, a reduction in expression levels of *Apln* was noticed in the BDL + AM group among the 4th and 6th postoperative weeks. SS: sham surgery; BDL: bile duct ligature; BDL + AM: bile duct ligature plus amniotic membrane; PO: postoperative. *$p < 0.05$ BDL versus BDL + AM; **$p < 0.01$ BDL versus BDL + AM.

to injury of the biliary epithelium and subsequent extrahepatic biliary obstruction and intrahepatic bile duct proliferation. However, rhesus rotavirus model is limited by timing and dosing of virus application, injection-related injury to abdominal organs, cannibalization, and survival rate of pups. In addition, mice do not develop liver fibrosis and portal hypertension because they recover spontaneously [13]. Bile duct ligature (BDL) is a surgically created animal model developed by Cameron and Oakley in 1932 that consists in ligation and excision of the common bile duct, being the most utilized to replicate cholestasis. BDL is the only animal model that allows progressive liver damage with long-term follow-up and recreates associated complications such as portal hypertension and hepatopulmonary syndrome. Gibelli et al. demonstrated that histological and molecular findings in livers of newborn rats submitted to BDL were more similar to biliary atresia-related fibrosis pattern compared to adult rats [5]. However, operating on in rat pups is technically difficult because of the small size of biliary structures and mortality after the procedure was reported to be as high as 77% [3–5]. In the present study, we developed BDL in 3-week-old rats. At that age, ligature of the common bile duct is technically less complex to perform than in newborn rats, and animals can be kept without their mothers during the postoperative period avoiding cannibalism. Our study demonstrates that BDL in 3-week-old rats recreates all the histological and molecular features of biliary atresia, having the advantages of both neonatal and adult rat models of bile duct ligature. Additionally, our study demonstrates that the survival rate of young rats is superior to previous reports due to appropriate perioperative care in anesthesia and recovery, by controlled anesthetic delivery and avoiding hypothermia.

Regenerative medicine is an emerging multidisciplinary field focused on replacing or regenerating human cells, tissues, or organs in order to restore or establish normal function. A few reports have explored the use of stem cells in liver failure after biliary atresia. Gupta et al. injected autologous bone marrow mononuclear stem cells into hepatic artery and/or portal vein in eight patients demonstrating an initial improve in liver function [14]. After that experience, the authors included fifteen children with biochemical and scintigraphic improvement at 1-year follow-up [15]. Other authors reported a 1-year-old girl treated with hepatic progenitor cell infusion through the hepatic artery with decreased in serum bilirubin values and a scintigraphy showing increased liver cell function after 2 months [16].

However, the use of stem cells has some drawbacks. Embryonic stem cells collection implies important ethical barriers. Embryonic stem cells also have tumorigenic capacity. Adult mesenchymal stem cells are present in lower concentration, require invasive procedures for collection, and have limited proliferation [17]. In contrast, amniotic membrane, the innermost layer of fetal membranes, has many advantages over other sources of stem cells. Placenta is a readily available organ, with minimum ethical and legal barriers. There is no need for invasive procedures, and amniotic membrane stem cells are no tumorigenic. Moreover, stem cells from amniotic membrane induce apoptosis in neoplastic cells [18]. Amniotic stem cells have more plasticity and do not have accumulative damage in DNA, supporting better time lapse in preservation conditions [10]. Other properties of amniotic membrane include barrier mechanism and analgesic effects, when used as a biological dressing, preventing desiccation and excessive fluid loss, protecting exposed sensitive nerve ends in wound bed from the environment. Low immunogenicity is another property of amniotic membrane. This is explained by lack of human leukocyte antigen (HLA) class A, B, and DR and costimulatory molecules CD40, CD80, and CD86 in human amniotic cells [19]. Amniotic membrane promotes epithelization by releasing of growth factors and retains basement membrane components that influence proliferation, migration, and differentiation of epithelial cells. Additionally, amniotic membrane has antibacterial properties by production of human beta-3-defensin, elastase inhibitors, secretion of leukocyte proteinase inhibitor, lactoferrin, and IL-1RA. Finally, amniotic membrane has a role in angiogenesis modulation. It produces proangiogenic compounds such as vascular endothelial growth factor (VEGF) and basic fibroblastic growth factor (bFGF). On the other hand, amniotic membrane produces antiangiogenic factors as thrombospondin-1, IL-1RA, collagen XVIII, IL-10, some tissue metalloprotease inhibitors, and pigment epithelium-derived factor [19].

The use of amniotic membrane in hepatic disease models is emerging. A study demonstrated a reduction in proinflammatory cytokines IL-6 and TNFα after intravenous administration of human amniotic epithelial cells in a carbon tetrachloride toxic model [6]. Sant'Anna et al. demonstrated a reduction in liver fibrosis after amniotic membrane application on the liver surface in a bile duct ligature model; however, they used adult rats [8, 11]. In the present study, we demonstrated a reduction in hepatic fibrosis in young rats by liver function analysis, by collagen quantification, and by analysis of profibrotic genes.

Liver diseases are characterized by a catabolic state compromising nutrition. In our study, weight gain was recorded in the three groups along the experiments. At the end of study, no significant differences were noted among the three groups. These findings may be due to compensatory weight gain in both the BDL and BDL + AM groups by development of hepatosplenomegaly and ascites as a consequence of a progressive liver fibrosis and portal hypertension. Spleen index is a ratio between spleen weight and body weight that allows to study the presence of splenomegaly and secondary portal hypertension [3]. In our study, both the BDL and BDL + AM groups developed progressive increase in spleen index, without differences among them. Previous studies using amniotic membrane in liver diseases have not measured the spleen index [6–11].

Adult mice treated with injection of human amniotic epithelial cells showed lower levels of alanine transaminase after injection [6]. Similarly, our results show an improvement in liver function tests, but only albumin and gamma-glutamyl transpeptidase had a significant change most probably due to the limited number of samples studied.

Liver fibrogenesis is a dynamic wound healing-like process leading to progressive accumulation of extracellular matrix components. Histopathological liver changes in

biliary atresia include ductular reaction, portal fibrosis, and bile plugs. Ductular reaction consists in proliferation of small interanastomosing ductules located at the periphery of portal tracts and represents the most consistent indicator of the presence of biliary obstruction [20]. Portal fibrosis pattern is characterized by formation of portal–portal fibrotic septa surrounding liver nodules [21]. Collagen quantification by digital image analysis allows a more precise and objective measurement of fibrosis avoiding interobserver variations [22]. All ductular reaction and portal fibrosis were found in rat livers after BDL procedure and were clearly progressive in time, as demonstrated by collagen quantification. After six weeks of treatment with amniotic membrane, a significant reduction of liver fibrosis was evident. Manuelpillai et al. injected human amniotic epithelial cells into a carbon tetrachloride model of liver fibrosis. They demonstrated a reduction in one third of hepatic fibrosis assessed by image analysis of sirius red stained slides [6]. Sant'Anna et al. applied amniotic membrane in a bile duct ligature model of liver fibrosis in adult rats [8]. They demonstrated a reduction of a half in collagen deposition in the treated group assessed by image analysis of Goldner's modified Masson trichrome stained slides [8]. Recently, then same authors demonstrated similar results in a bile duct ligature model of liver fibrosis in adult rats using sirius red staining. Our results show the same reduction in collagen deposition after amniotic membrane treatment in young rats.

In order to explain the potential mechanism involved in fibrosis reduction by human amniotic membrane, we explored the expression levels of two profibrotic genes: an established major profibrogenic cytokine, *Tgfb1*, and a novel involved protein in liver fibrosis recently linked to prognosis of biliary atresia patients, *Apln*.

TGF-β is a central regulator in chronic liver diseases that contributes to all stages of disease progression from initial liver injury through inflammation and fibrosis to cirrhosis and hepatocellular carcinoma. TGF-β1 isoform is considered as a major profibrogenic cytokine. TGF-β1 regulates a wide variety of cellular processes in liver fibrogenesis, including apoptosis of hepatocytes, enhance hepatocyte destruction, hepatic stellate cell and fibroblast activation with type I collagen production, recruitment of inflammatory cells into injured liver, and transdifferentiation of some liver-resident cells. In our study, *Tgfb1* gene expression had an exponential overexpression on the 6th postoperative week in the BDL group in accordance with the previous reports [23]. TGF-β1 inactivation reduces collagen synthesis, and this pathway is indicated as accountable for reversion of liver fibrosis by amniotic membrane. This effect over *Tgfb1* expression and type I collagen deposition has also been implied in playing a role in scarless fetal wound healing [19]. In addition, collagen deposition reduction was observed in a lung fibrosis model by induction of a collagen-degrading environment with altered proteases levels [7]. Our results show that the BDL + AM group *Tgfb1* gene expression was significantly downregulated on the 6th postoperative week demonstrating that amniotic membrane reverses collagen deposition by inhibiting *Tgfb1* gene expression in cholestatic young rats.

Apelin, the endogenous ligand of angiotensin-like-receptor 1, is an emergent peptide involved in liver disease. Chen et al. demonstrated that *apelin* is overexpressed in livers of biliary atresia patients according to progression of disease and that is markedly activated in end-stage cirrhosis [24]. The authors demonstrated that *apelin* expression level accurately reflects the severity of hepatic fibrosis and proposed that it could be used as a prognostic factor in biliary atresia patients, to estimate the timing of liver transplantation [24]. Our results show a linear progressive overexpression of *Apln* in the BDL group. In the BDL + AM group, *Apln* showed a downregulation in association to reversion of collagen deposition. This study is the first to evaluate *Apln* expression in a cholestatic model in young animals. Our results support the use of apelin as a prognostic factor in biliary atresia.

In conclusion, human amniotic membrane applied over liver surface reverses by near 50% liver fibrosis in a surgical model of cholestasis in young animals. These results suggest that amniotic membrane may be useful as a therapeutic tool against liver fibrosis in neonatal and childhood cholestatic disorders.

Disclosure

This study was presented at the XXIXth International Symposium on Paediatric Surgical Research, 8–10 September, Frankfurt/Main, Germany.

Conflicts of Interest

The authors declare that they have no conflicts of interest.

Acknowledgments

The authors thank Paola Acuña from Obstetrics Unit of Hospital Carlos van Buren from Valparaíso, Chile, for the collection of placental tissues, Nicolas Cáceres for carrying out rat blood tests, and Uenis Tannuri's team from Department of Pediatric Surgery, Instituto da Criança, University of São Paulo Medical School, Brazil, for teaching bile duct ligature model. This project received financial support from Centro de Investigaciones Biomédicas (CI 05/2006) and Universidad de Valparaíso, Chile.

References

[1] J. L. Hartley, M. Davenport, and D. A. Kelly, "Biliary atresia," *Lancet*, vol. 374, no. 9702, pp. 1704–1713, 2009.

[2] A. C. A. Tannuri, N. E. M. Gibelli, L. R. S. Ricardi et al., "Orthotopic liver transplantation in biliary atresia: a single-center experience," *Transplantation Proceedings*, vol. 43, no. 1, pp. 181–183, 2011.

[3] M. A. Aller, M. Duran, L. Ortega et al., "Comparative study of macro- and microsurgical extrahepatic cholestasis in the rat," *Microsurgery*, vol. 24, no. 6, pp. 442–447, 2004.

[4] Y. Yang, B. Chen, Y. Chen, B. Zu, B. Yi, and K. Lu, "A comparison of two common bile duct ligation methods to establish hepatopulmonary syndrome animal models," *Laboratory Animals*, vol. 49, no. 1, pp. 71–79, 2015.

[5] N. E. M. Gibelli, U. Tannuri, E. S. de Mello, and C. J. Rodrigues, "Bile duct ligation in neonatal rats: is it a valid experimental model for biliary atresia studies?," *Pediatric Transplantation*, vol. 13, no. 1, pp. 81–87, 2009.

[6] U. Manuelpillai, J. Tchongue, D. Lourensz et al., "Transplantation of human amnion epithelial cells reduces hepatic fibrosis in immunocompetent CCl_4-treated mice," *Cell Transplantation*, vol. 19, no. 9, pp. 1157–1168, 2010.

[7] O. Parolini and M. Caruso, "Review: preclinical studies on placenta-derived cells and amniotic membrane: an update," *Placenta*, vol. 32, Supplement 2, pp. S186–S195, 2011.

[8] L. B. Sant'Anna, A. Cargnoni, L. Ressel, G. Vanosi, and O. Parolini, "Amniotic membrane application reduces liver fibrosis in a bile duct ligation rat model," *Cell Transplantation*, vol. 20, pp. 411–453, 2011.

[9] U. Manuelpillai, Y. Moodley, C. V. Borlongan, and O. Parolini, "Amniotic membrane and amniotic cells: potential therapeutic tools to combat tissue inflammation and fibrosis?," *Placenta*, vol. 32, Supplement 4, pp. S320–S325, 2011.

[10] E. Ricci, G. Vanosi, A. Lindenmair et al., "Anti-fibrotic effects of fresh and cryopreserved human amniotic membrane in a rat liver fibrosis model," *Cell and Tissue Banking*, vol. 14, no. 3, pp. 475–488, 2013.

[11] L. B. Sant'anna, R. Hage, M. A. G. Cardoso et al., "Anti-fibrotic effects of human amniotic membrane transplantation in established biliary fibrosis induced in rats," *Cell Transplant*, vol. 25, no. 12, pp. 2245–2257, 2016.

[12] National Research Council, *Guide for the Care and Use of Laboratory Animals*, National Academies Press, Washington D.C, 8th edition, 2011.

[13] C. Petersen, "Biliary atresia: the animal models," *Seminars in Pediatric Surgery*, vol. 21, no. 3, pp. 185–191, 2012.

[14] D. K. Gupta, S. Sharma, P. Venugopal, L. Kumar, S. Mohanty, and S. Dattagupta, "Stem cells as a therapeutic modality in pediatric malformations," *Transplantation Proceedings*, vol. 39, no. 3, pp. 700–702, 2007.

[15] S. Sharma, L. Kumar, S. Mohanty, R. Kumar, S. Datta Gupta, and D. K. Gupta, "Bone marrow mononuclear stem cell infusion improves biochemical parameters and scintigraphy in infants with biliary atresia," *Pediatric Surgery International*, vol. 27, no. 1, pp. 81–89, 2011.

[16] A. A. Khan, N. Parveen, V. S. Mahaboob et al., "Management of hyperbilirubinemia in biliary atresia by hepatic progenitor cell transplantation through hepatic artery: a case report," *Transplantation Proceedings*, vol. 40, no. 4, pp. 1153–1155, 2008.

[17] S. Ilancheran, Y. Moodley, and U. Manuelpillai, "Human fetal membranes: a source of stem cells for tissue regeneration and repair?," *Placenta*, vol. 30, no. 1, pp. 2–10, 2009.

[18] H. Niknejad, M. Khayat-Khoei, H. Peirovi, and H. Abolghasemi, "Human amniotic epithelial cells induces apoptosis of cancer cells: a new anti-tumor strategy," *Cytotherapy*, vol. 16, no. 1, pp. 33–40, 2014.

[19] N. G. Fairbairn, M. A. Randolph, and R. W. Redmond, "The clinical applications of human amnion in plastic surgery," *Journal of Plastic, Reconstructive & Aesthetic Surgery*, vol. 67, no. 5, pp. 662–675, 2014.

[20] P. Russo, J. C. Magee, J. Boitnott et al., "Design and validation of Biliary Atresia Research Consortium histological assessment system for cholestasis in infancy," *Clinical Gastroenterology and Hepatology*, vol. 9, no. 4, pp. 357–362.e2, 2011.

[21] E. Novo, S. Cannito, C. Paternostro, C. Bocca, A. Miglietta, and M. Parola, "Cellular and molecular mechanisms in liver fibrogenesis," *Archives of Biochemistry and Biophysics*, vol. 548, pp. 20–37, 2014.

[22] H. Tanano, T. Hasegawa, T. Kimura et al., "Proposal of fibrosis index using image analyzer as a quantitative histological evaluation of liver fibrosis in biliary atresia," *Pediatric Surgery International*, vol. 19, no. 1-2, pp. 52–56, 2003.

[23] J. O. Gonçalves, A. C. A. Tannuri, M. C. M. Coelho, I. Bendit, and U. Tannuri, "Dynamic expression of *desmin*, *α-SMA* and *TGF-β1* during hepatic fibrogenesis induced by selective bile duct ligation in young rats," *Brazilian Journal of Medical and Biological Research*, vol. 47, no. 10, pp. 850–857, 2014.

[24] W. Chen, T. Oue, T. Ueno, S. Uehara, N. Usui, and M. Fukuzawa, "Apelin is a marker of the progression of the liver fibrosis and portal hypertension in patients with biliary atresia," *Pediatric Surgery International*, vol. 29, no. 1, pp. 79–85, 2013.

Hindawi
Stem Cells International
Volume 2017, Article ID 9142493, 9 pages
https://doi.org/10.1155/2017/9142493

Research Article

High Sensitivity of Human Adipose Stem Cells to Differentiate into Myofibroblasts in the Presence of *C. aspersa* Egg Extract

Natalio García-Honduvilla,[1,2,3,4] Alberto Cifuentes,[1,2,3] Miguel A. Ortega,[1,2,3] Arancha Delgado,[5] Salvador González,[1,2,3] Julia Bujan,[1,2,3,4] and Melchor Alvarez-Mon[1,2,3,4,6]

[1]*Department of Medicine and Medical Specialties, Faculty of Medicine and Health Sciences, University of Alcalá, Alcalá de Henares, Madrid, Spain*
[2]*Networking Biomedical Research Center on Bioengineering, Biomaterials and Nanomedicine (CIBER-BBN), Alcalá de Henares, Madrid, Spain*
[3]*Ramón y Cajal Institute of Sanitary Research (IRYCIS), Madrid, Spain*
[4]*University Center of Defense of Madrid (CUD-ACD), Madrid, Spain*
[5]*Industrial Pharmacy Cantabria, Madrid, Spain*
[6]*Immune System Diseases-Rheumatology and Oncology Service, University Hospital Príncipe de Asturias, Alcalá de Henares, Madrid, Spain*

Correspondence should be addressed to Julia Bujan; mjulia.bujan@uah.es

Received 10 April 2017; Accepted 28 November 2017; Published 27 December 2017

Academic Editor: Stefano Geuna

Copyright © 2017 Natalio García-Honduvilla et al. This is an open access article distributed under the Creative Commons Attribution License, which permits unrestricted use, distribution, and reproduction in any medium, provided the original work is properly cited.

Introduction. Regeneration therapy using adipose-derived stem cells (ADSC) has been proposed in the treatment of skin aging. Myofibroblast plays a relevant role in the organization of the extracellular matrix of the damaged skin. A natural extract was derived from the eggs of the mollusk *Cryptomphalus aspersa* (e-CAF) that seems to play a role on skin repair. We have investigated the potential effects of e-CAF in the differentiation of ADSC. *Materials and methods*. ADSC were cultured in the absence or presence of e-CAF (50 and 200 μg/mL) for 24 hours and 7 days. Real-time cell assay, morphological, immunofluorescence, and RT-PCR techniques were used to evaluate the cell culture and expression of αSMA, collagen I, and tropoelastin. *Results*. e-CAF induced significant reduction in the rate of growth of ADSC from 24 hours to 7 days of culture. e-CAF also induced bigger sizes, higher levels of cytoplasmic refringence and complexity, and a more polyhedral morphological changes in the cultured ADSC. The protein and mRNA expression of αSMA was significantly increased in e-CAF-cultured ADSC. *Conclusion*. e-CAF promotes ADSC differentiation to myofibroblasts and should be considered as a potential agent for the prevention and treatment of skin aging.

1. Introduction

Aging is a complex physiological process which causes a progressive decrease in the functionality of all human tissues, including skin. In the course of aging, the skin is subject to a number of agents or conditions which, together, are known as exposome. The skin exposome consists of external and internal factors and their interactions, as well as the response of the human body to these factors that lead to biological and clinical signs of skin aging [1]. Among the internal factors, genetics, metabolism, and hormones should be highlighted, while the main environmental factors include solar radiation and pollution, which add up to trigger photoaging [2, 3].

The clinical signs of aged skin manifest as wrinkles, dermal atrophy, and impaired wound healing, in part due to alterations in the organization and remodeling process of the extracellular matrix (ECM). Its main components, collagen and elastin, provide strength and elasticity to the tissue. Their degradation, which is increased during aging, elicits loss of structural integrity and decreased repair ability [2, 4].

After the skin is injured, repair mechanisms are activated, including transforming growth factor-beta (TGFβ) expression, which induces fibroblast proliferation and migration to the wound site, and their differentiation towards myofibroblasts by increasing the expression of α-smooth muscle actin protein (α-SMA), promoting the secretion and assembly of new ECM components that renew the skin structural support and being responsible for tissue contractility during maturation [5, 6]. During aging, the loss of ECM compromises this process and impairs the competence of the skin to successfully ensure scar formation and wound healing [7–9].

New treatments approaching the endogenous regenerative properties of the skin have been under extensive research in the last years [10], being especially promising are those focused in the fields of tissue engineering and regenerative medicine. Adipose-derived stem cells (ADSC) have emerged as a particularly relevant cell population to be targeted for these purposes. Their abundance, accessibility, and minimally traumatic harvesting, along with their ability to differentiate into several cell lineages, make ADSC a great candidate for advanced therapeutic uses [11–14]. ADSC can act in a paracrine fashion by secreting an assortment of growth factors, including insulin-like growth factor (IGF), vascular endothelial growth factor (VEGF), transforming growth factor-beta 1 (TGF-β1), and hepatocyte growth factor (HGF) [15, 16]. Besides, in addition to the potential of these cells to differentiate to osteogenic, chondrogenic, and adipogenic lineages, several studies have shown their capability to transform into cells involved in cutaneous repair, such as endothelial cells, keratinocytes, fibroblasts, and myofibroblasts [15–19]. ADSC have wound-healing and antioxidant effects on human skin via secretion of growth factors and activation of dermal fibroblasts. Thus, ADSC and its secretory factors are effective in wrinkles resulting from photoaging. The antiwrinkle effect is mainly mediated by reducing UVB-induced apoptosis and stimulating collagen synthesis of human dermal fibroblasts [12–14]. However, it has been described that age can cause changes in the function and differentiation ability of ADSC [20]. Therefore, the use of agents able to attenuate these effects could be useful in the treatment of skin aging.

In this regard, natural ingredients derived from the mollusk *Cryptomphalus aspersa* have been developed and assessed as regenerative agents for cutaneous tissue [16–20]. Its secretion (SCA) has been demonstrated to possess antioxidant and skin regenerative properties, preserving the survival of keratinocytes and fibroblasts and ECM dynamics, while promoting their mitogenic and motogenic activities during wound healing [21–27]. Moreover, a novel ingredient derived from an extract of the eggs of *C. aspersa* (e-CAF) has been recently developed, showing promising effects for the treatment of skin aging. In a recent study using human keratinocytes (HaCaT), human dermal fibroblasts (HDF), and senescent fibroblasts (SHDF), it has been demonstrated that e-CAF is able to induce migration and ECM production in these cell lines, while improving cytoskeletal organization. Furthermore, e-CAF showed antiaging properties, reducing the expression of age-related markers and preventing cell death due to ultraviolet radiation [28]. Furthermore, e-CAF has shown to promote migration of human hair dermal papilla cells (HDDPCs), also increasing their migratory behaviour and modulating the expression of adhesion molecules, suggesting its possible role on skin regeneration and prevention of tissue damage and skin aging [29].

In the present work, the in vitro effects of e-CAF on human ADSC have been assessed. Firstly, the cell proliferation and morphology of the natural extract derived from the eggs of mollusk *Cryptomphalus aspersa*, e-CAF, was assayed. For that, real-time cell assay (RTCA) was used to assay the capacity of e-CAF to modulating ADSC growth and size from 24 hours to 7 days of cultures. Likewise, the extract showed signs of a prodifferentiation activity. Subsequent analysis of myofibroblast markers showed an increase of this cell type in treated ADSC, pointing to an inductive effect of e-CAF towards this cell lineage. For this determination, the selected markers were expression of αSMA, a cytoskeletal protein commonly used as a myofibroblast marker. These data suggest that e-CAF might modulate the effect in the ADSC differentiation. This activity could be considered as a potential photoaging agent due to capacity of tissue repair and prevention of aging.

2. Materials and Methods

2.1. Cell Culture. Human ADSC were purchased from a commercial supplier (StemPro®, Gibco®, Thermo Fisher Scientific, Waltham, MA, USA) and cultured in MesenPro RS™ medium (Gibco) in a humidified incubator at 37°C in a 5% CO_2 atmosphere. The cells were maintained at subconfluence and were subcultured when necessary. All experiments were carried out using cells from the second to the fourth passages.

2.2. Ingredient. e-CAF (Industrial Farmacéutica Cantabria, S.A., Madrid, Spain), an ingredient derived from the eggs of *C. aspersa*, was prepared as described by Espada et al. [28]. Briefly, the spawn was collected, rinsed at low pressure, immersed in saline solution, and kept at between 2°C and 8°C. Then, intact snail spawn was obtained by filtration through a mesh and lysed. e-CAF was homogenized in DMEM (Gibco) and filtered through 0.22 μm filters to create a stock solution, and total protein concentration was measured by Bradford, as elsewhere described. Treatment media were prepared by mixing 4/5 of MesenPro RS with 1/5 of the stock solution and/or basal DMEM, to a final concentration of 50 μg/mL (e-CAF-50 group), 200 μg/mL (e-CAF-200 group), and 0 μg/mL (CTRL group). Cells belonging to each of the study groups were cultured in the corresponding medium for 7 days, receiving a cell culture medium change at day 4.

2.3. Real-Time Cell Assay (RTCA) and Morphological Studies. The growth of the different groups was measured using a label-free, impedance-based RTCA system (xCELLigence RTCA SP, Roche Diagnostics, Basel, Switzerland). ADSC were seeded in 96-well E-plates at 2000 and 1000 cells per well and maintained in growth medium for 24 hours, before switching to the different treatment media. Subsequently, cell growth was studied for 7 days, before the cultures could reach confluence. Cell index (CI) was recorded every 30 minutes and normalized to the values at 24 h. For each group and cell concentration, the mean slope of the curves between the start of the treatment and the end of the experiment was calculated. Duplicate parallel plates were prepared in regular clear 96-well plates to allow the visualization and photography of the cultures during the experiment, using an Axiovert 40C inverted microscope equipped with an AxioCam ICc1 digital camera (Carl Zeiss, Oberkochen, Germany). Three independent experiments were carried out, each of them in triplicates.

To further assess the morphology and size of the cells, ADSC were seeded onto sterile 12 mm diameter glass coverslips and cultured as described above. Cells were fixed with 4% paraformaldehyde, subjected to standard haematoxylin-eosin staining and visualized in a Zeiss Axiophot microscope equipped with an AxioCam HRc digital camera (Carl Zeiss). The mean area of the cells in each group of three different experiments was measured in nine random high-magnification fields (10 cells/field) using ImageJ software (NIH, Bethesda, MD, USA).

2.4. Immunofluorescence. The presence of αSMA, a myofibroblast marker, was detected and quantified by immunofluorescent labelling. Fixed cells were permeabilized with 0.1% Triton X-100, blocked with 3% bovine serum albumin, and incubated with anti-αSMA monoclonal antibody (clone 1A4, Sigma-Aldrich, St. Louis, MO, USA). FITC-labelled anti-mouse antibody (Sigma-Aldrich) was used as secondary antibody, and nuclei were counterstained with DAPI as elsewhere described. Negative controls, exposed to 3% BSA instead of primary antibody, were included. Cells were observed using a Leica TCS SP5 confocal microscope (Leica Microsystems, Wetzlar, Germany), and the percentage of αSMA-positive cells of three independent experiments was evaluated in nine random high-magnification fields.

2.5. Real-Time PCR. Total RNA was isolated from the cultures by standard guanidinium thiocyanate-phenol-chloroform extraction procedures using TRIzol (Thermo Fisher Scientific). RNA was recovered from the aqueous phase by precipitation, and its quantity and purity were assessed by measuring optical density at 260/280 and 260/230 nm in a NanoDrop ND-1000 spectrophotometer (Thermo Fisher Scientific).

Complementary DNA was synthesized from 200 ng of total RNA by reverse transcription (RT) with oligo-dT primers and the M-MLV reverse transcriptase enzyme (Thermo Fisher Scientific). cDNA was quantified by real-time PCR, using the relative standard curve method, in a StepOnePlus™ System (Thermo Fisher Scientific). The following primers were used: αSMA (Fwd 5′-AGC GTG GCT ATT CCT TCG TT-3′ and Rev 5′-CCC ATC AGG CAA CTC GTA ACT-3′), collagen type I (Fwd 5′-CCA TGT GAA ATT GTC TCC CA-3′ and Rev 5′-GGG GCA AGA CAG TGA TTG AA-3′), tropoelastin (Fwd 5′-GTG TAT ACC CAG GTG GCG TG-3′ and Rev 5′-CGA ACT TTG CTG CTT TAG-3′), and GAPDH (Fwd 5′-GGA AGG TGA AGG TCG GAG TCA-3′ and Rev 5′-GTC ATT GAT GGC AAC AAT ATC CAC T-3′). The samples were subjected to an initial stage of 10 min at 95°C, followed by 40 cycles of 15 s at 95°C, 30 s at 59.5°C (TE), 59.9°C (αSMA) or 60.0°C (Col-I, GAPDH), and 1 min at 72°C. Four independent experiments were carried out, and each experiment was run in triplicates, including a no-template control in each reaction. GAPDH was used as reference gene.

2.6. Statistical Analysis. Statistical software GraphPad Prism 5 (GraphPad Software Inc., La Jolla, CA, USA) was used to analyse the data. Groups were compared using ANOVA followed by Tukey-Kramer test. Non-Gaussian data sets (RT-PCR) were normalized by logarithmic transformation prior to statistical testing. Data are expressed as mean ± standard error of the mean (SEM). Levels of significance were set at $^{*}p \leq 0.05$, $^{**}p \leq 0.01$, and $^{***}p \leq 0.001$.

3. Results

3.1. e-CAF Modulates ADSC Growth and Size. First, we investigated the effects of e-CAF on the growth of ADSC. RTCA experiments showed that the addition of e-CAF to culture media caused a significant reduction in the rate of growth of ADSC. This effect of e-CAF on ADSC cultures was observed at both concentrations (50 μg/mL and 200 μg/mL), as well as at two different densities of cell seeding. The significant inhibitory effect of e-CAF was patented as soon as 24 hours after the addition of the product to the cultures and remained for the following 7 days of the study (Figures 1(a)–1(d)). The disturbances in the curves observed at day 4 were caused by the medium change procedures. The analysis of the slopes corresponding to the interval of the experiment showed significant differences between the treated groups and control group, with greater values in the case of untreated ADSC curves.

Next, we investigated whether e-CAF had any effects on the morphology of ADSC. The presence of e-CAF in the culture media induced morphological changes in the cells at both concentrations. e-CAF-cultured cells presented bigger sizes and a more polyhedral shape at 7 days (Figure 1(e)). Changes in ADSC morphology were observed since day 5 (data not shown). Furthermore, at 7 days of culture, ADSC treated with e-CAF showed higher levels of cytoplasmic refringence and complexity, suggesting the presence of a more developed cytoskeleton. In contrast, ADSC cultivated in medium alone mainly showed a spindle-shaped, more numerous cells which covered more culture surface, near to confluence.

We also performed haematoxylin-eosin staining of the ADSC cultures in the presence or absence of e-CAF after 7 days of culture (Figure 2). There was no evidence of increased

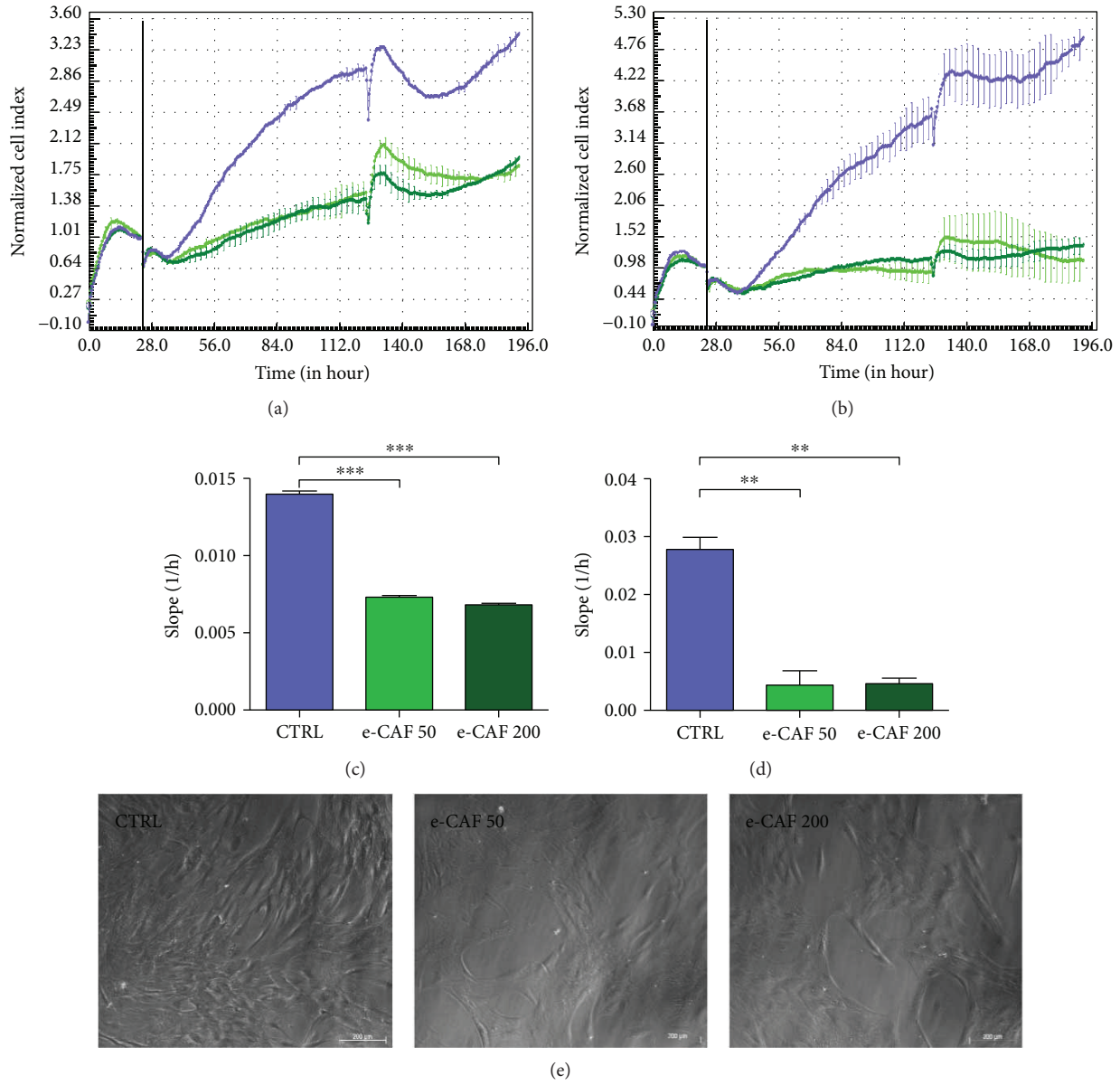

Figure 1: Effects of e-CAF on ADSC growth. RTCA graphs at two seeding densities, 2000 (a) and 1000 (b) cells/well. Normalization point was set at 24 h (vertical bar). Points represent the mean normalized cell index (CI) of three experiments run in triplicate ± SD for untreated ADSC (blue), cells treated with 50 μg/mL e-CAF (light green), and cells treated with 200 μg/mL e-CAF (dark green). Slope values computed from the RTCA between the normalization point (day 0) and the end of the experiment (day 7) at 2000 (c) and 1000 (d) cells/well seeding densities. $^{**}p \leq 0.01$ and $^{***}p \leq 0.001$. (e) Representative photographs of ADSC cultures from each group at day 7.

cell death in ADSC cultures due to the presence of e-CAF with any of the concentrations. The mean size of the cells, measured as cellular area, was higher in the ADSC treated with both concentrations of e-CAF than in the control group. Since the RTCA showed a higher growth of control cultures, and the cells of this group were markedly smaller, these results show a double effect of e-CAF upon ADSC, both reducing their proliferation and promoting the gain of cellular volume.

3.2. e-CAF Increases the Proportion of αSMA-Positive ADSC. Next, we investigated the effects of e-CAF on the differentiation of ADSC to myofibroblasts by immunofluorescent detection of the expression of αSMA, a cytoskeletal protein commonly used as a myofibroblast marker (Figure 3). The quantification of the proportion of positive cells showed significant differences in the treated groups. Although positive cells were also found in the control group (32.76% ± 4.11%), higher values were observed in both e-CAF-50 (48.59% ± 3.62%) and e-CAF-200 (49.80% ± 4.41%) groups, without significant differences between them.

Furthermore, we also investigated the morphology of ADSC expressing αSMA. In both e-CAF-treated and e-CAF-untreated ADSC, αSMA-positive cells showed aligned cytoskeletal microfilaments. It was also observed that these cells

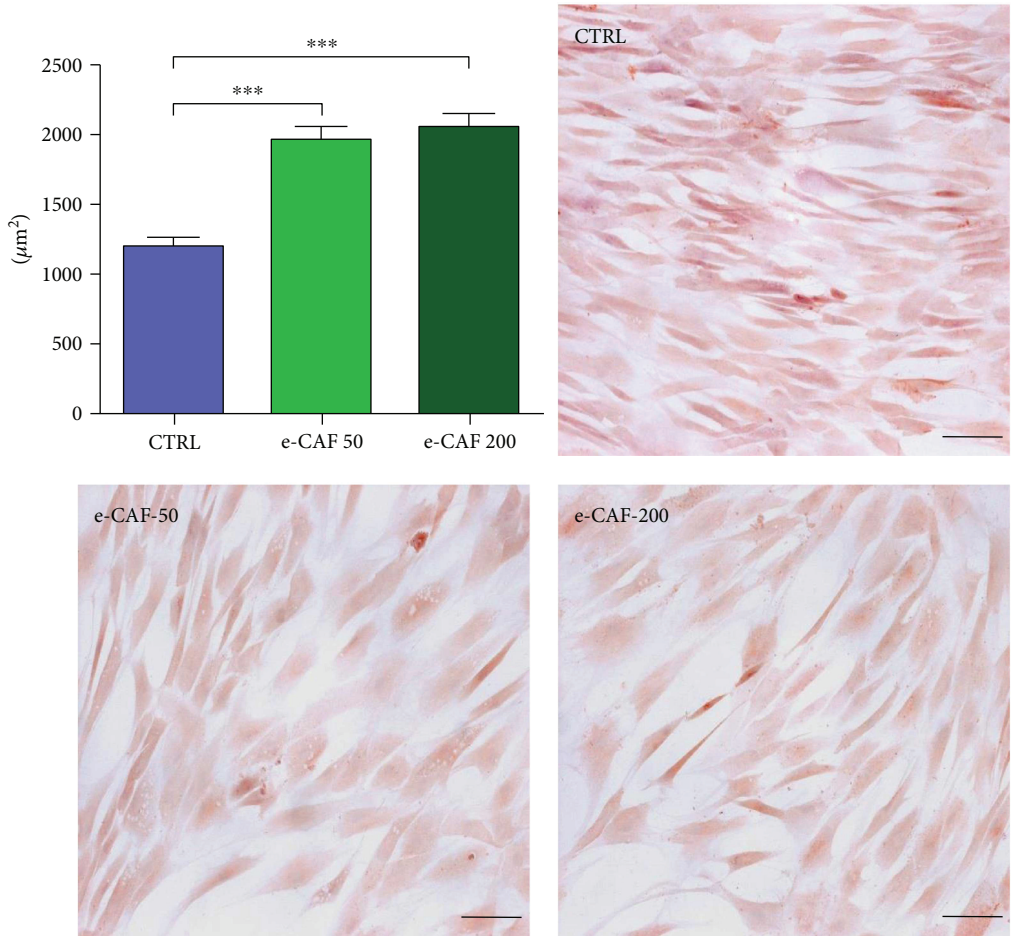

Figure 2: Effects of e-CAF on ADSC size and morphology. Morphometrical studies of the cells at culture day 7. Representative photographs of the study groups are shown (haematoxylin-eosin, bars: 100 μm). Graph represents the mean area of cells in each group, measured within nine fields (10 cells/field) of three experiments. An increase of the cellular size in groups exposed to 50 μg/mL e-CAF and 200 μg/mL e-CAF can be observed. $^{***}p \leq 0.001$.

tended to possess a greater extent of cytoplasm, frequently concurrent with polyhedral shapes.

3.3. e-CAF Upregulates the Expression of αSMA in ADSC. To further assess the extension to which e-CAF induces ADSC differentiation, mRNA levels of myofibroblast markers, such as αSMA, type I collagen, and tropoelastin, were measured by real-time quantitative PCR in ADSC cultured in the presence and absence of e-CAF for 7 days (Figure 4). The expression of αSMA showed an increase in the treated groups compared to the control group, reaching statistical significance in the e-CAF-200 group. No significant differences were observed in the expression of the extracellular matrix proteins type I collagen and tropoelastin, although in both cases, the e-CAF-200 group showed a clear trend to express higher mean values of these proteins than the control group.

4. Discussion

Aging causes changes in the structure and physiology of all tissues and organs. However, being the outermost part of the organism, the skin is exposed to additional aggressions that aggravate this process, leading to the clinical condition of photoaging [8]. Extensive research has been carried out aiming to find suitable agents capable of overcoming these age-related effects on the skin. To this end, many natural products have been assessed as reparative agents, mainly due to their antioxidant and anti-inflammatory properties [30, 31]. In this work, an extract obtained from the eggs of the mollusk *Cryptomphalus aspersa* (e-CAF) has been tested on human ADSC cultures in order to assess its effects on this cell lineage which may give rise to cells with cutaneous phenotype.

The growth of the cultures exposed to e-CAF was measured by RTCA. This novel technology is based on the changes of impedance registered in a cell culture e-plate covered by electrodes, allowing a noninvasive and label-free monitoring of the cultures [32]. This system has proven to be a powerful tool in the evaluation of proliferation, migration, and invasion of different cell cultures [33, 34], in the measurement of cytotoxic effects of different substances [32, 35] and in the assessment of stem cell viability and optimal time of use for cell therapy [36]. In our study, two different concentrations of

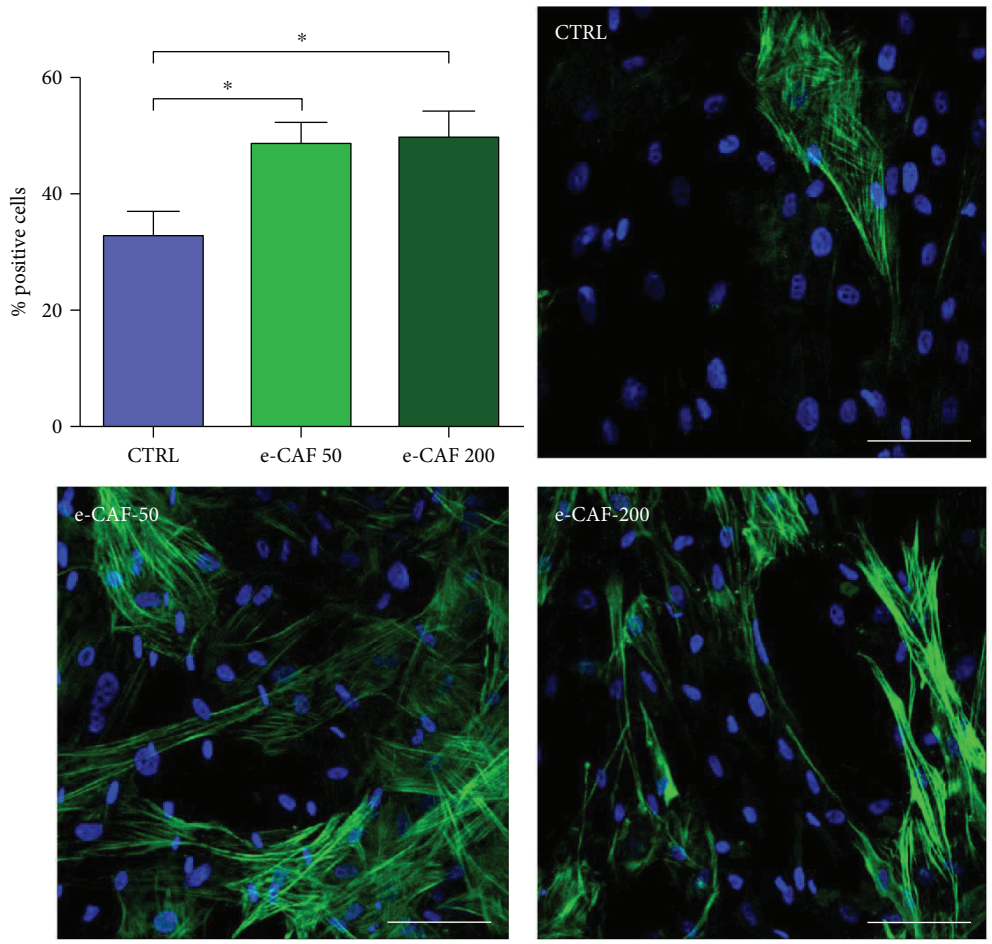

Figure 3: Effects of e-CAF on αSMA expression. Immunofluorescence detection of the myofibroblast marker αSMA (green) in the three groups (bars: 50 μm). Cell counts (graph) showed a higher percentage of positive cells for this marker in both e-CAF-treated groups. The results are expressed as the mean of positive cells per field, measured within nine fields of three experiments. $^{*}p \leq 0.05$.

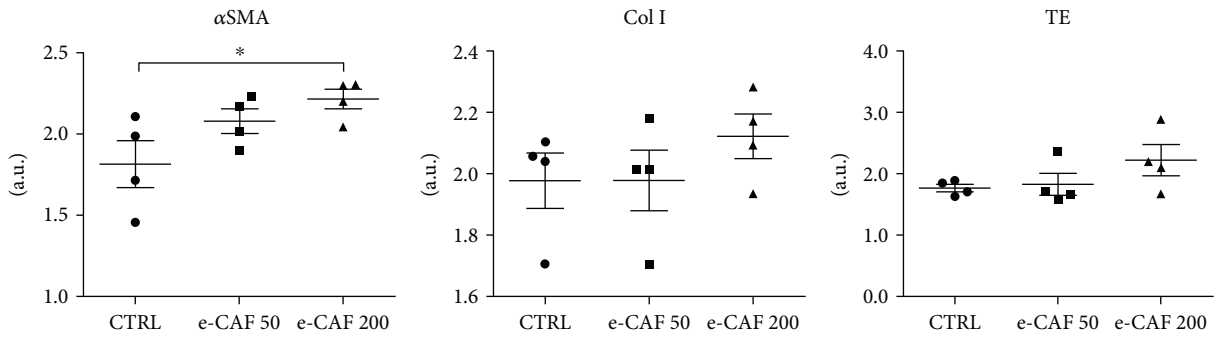

Figure 4: Effects of e-CAF on ADSC gene expression. Gene expression of α-smooth muscle actin (αSMA), collagen I (Col I), and tropoelastin (TE) in the three experimental groups, measured by RT-qPCR. GAPDH was used as reference gene. The results are log-transformed and are expressed as arbitrary units. A trend to an increase in the expression of the myofibroblast marker and the matrix proteins in e-CAF-treated groups was observed, with significant differences in αSMA expression between untreated and 200 μg/mL e-CAF groups. $^{*}p \leq 0.05$.

e-CAF caused a decrement of ADSC proliferation rate, without observing any cytotoxic effect. Instead, the monitoring of the replica plates showed morphological changes in the e-CAF groups compatible with a cell differentiation process compared to control cells, and these observations were also confirmed by quantification of cellular size. Since in the RTCA experiments, both cell proliferation and cell growth can contribute to an increase of the CI, the bigger sizes of treated cells indicate that the differences between the e-CAF and control groups in proliferation rates are

even more robust than those recorded. These results are aligned with the finding of Alameda et al. [29] that observed a significant decrease in proliferation of human hair dermal papilla stem cells (HHDPCs) with similar concentration of e-CAF (50 and 200 μg/mL).

The observed tendency to change the spindle-shaped characteristic of ADSC [15] to a more polyhedral one, with a prominent cytoskeleton, and the reduced proliferation rate suggested a possible effect of e-CAF favoring differentiation of ADSC towards myofibroblast lineage. Therefore, we examined the presence of αSMA, the most widely used marker to identify myofibroblasts [19, 37], in our cells. While positive cells were found in all groups, e-CAF treatment significantly increased the percentage of αSMA-positive cells compared to untreated cells, which confirmed our hypothesis. Accordingly, ADSC have been previously reported as capable to differentiate into αSMA-expressing cells, including vascular smooth muscle cells [38] and myofibroblasts, which also show high plasticity in the modulation of their contractile and migratory phenotypes [18]. This plasticity could partially explain the mild differences observed in collagen type I and tropoelastin mRNA levels, as the expression of ECM proteins is greatly upregulated in contractile myofibroblasts, induced mainly by TGF-β1 [18]. Additionally, these cultures lack many stimuli that are naturally present *in vivo* and cause ECM secretion by myofibroblasts, such as mechanical forces, and especially TGF-β1 and its interaction with many components of the matrix, which greatly modulates their action [37, 39, 40]. It must be noted, however, that the greatest level of expression for the three studied genes was found in the e-CAF-200 group, which could be suggestive of a more advanced differentiation in the group treated with the higher concentration. The observed effect of e-CAF favoring differentiation of ADSC towards myofibroblast lineage is not restricted to these stem cells. It has ben also shown that e-CAF exert differentiation effects of HHDPCs to the main skin cell lineages towards myofibroblast, a specific fibroblastoid phenotype [29]. The molecular mechanism of the myofibroblast differentiation promotion observed with e-CAF treatment has not been established, but it is possible to suggest it may be able to mimicry the TGF-β1 regulatory effects.

Aging has been related to a failure in fibroblast-to-myofibroblast differentiation, concurrent with lower generation of hyaluronic acid [41]. Being myofibroblasts as one of the main ECM-secreting cells, the inductive effect upon ADSC of e-CAF towards this lineage could be beneficial in the treatment of cutaneous aging. Related to this, recent studies have shown that e-CAF also has several proregenerative effects on other cutaneous cell types, such as keratinocytes and fibroblasts [28].

Moreover, functional stem cell units have been described throughout all layers of human skin: hair follicle bulge, interfollicular epidermis, dermal papillae, and perivascular hypodermal adipose tissue. Their secretome may be of great use due to the broad range of growth factors and other signalling molecules they produce [42]. However, in the course of aging, important changes occur in stem cell populations, reducing their pool, diminishing their functionality, and altering their niches [43–45], which in turn aggravate the aging process. Therefore, the existence of treatments capable of modulating stem cell activity and differentiation would be desirable.

In the last few years, ADSC have become a promising tool in the treatment of skin aging. Stem cell-based therapies offer tremendous potential for skin regeneration. ADSC have shown to paracrinally induce collagen synthesis and angiogenesis, while reducing the levels of matrix metalloproteinase-1 (MMP-1) and cell apoptosis [12, 13]. It has also been suggested that ADSC could play a role in preventing the accumulation of advanced glycation end-products (AGEs) associated with aging [14]. Since the activity of these stem cells can be so beneficial to ameliorate the effects of skin aging, resident ADSC from the perivascular hypodermis emerge as a potential target for antiaging treatments, such as e-CAF.

5. Conclusion

Our results show that e-CAF promotes ADSC differentiation to myofibroblasts and should be considered as a potential agent for the prevention and treatment of skin aging. These modulatory effects of e-CAF on ADSC expand those described on HHDPC differentiation and indicate that e-CAF could exert its activity on multiple types of skin cells and should be considered as a potential agent for the prevention and treatment of skin aging.

Disclosure

Julia Bujan and Melchor Alvarez-Mon shared senior authorship in this work.

Conflicts of Interest

The authors declared no potential conflicts of interest with respect to the research, authorship, and/or publication of this article.

Acknowledgments

This work was partially supported by a grant from IFC (Industrial Pharmacy Cantabria), Madrid (B2017/BMD-3804.MITIC-CM), and Instituto de Salud Carlos III (FIS-PI13/01413). e-CAF used in this research was kindly provided by Industrial Pharmacy Cantabria, S.A.

References

[1] J. Krutmann, A. Bouloc, G. Sore, B. A. Bernard, and T. Passeron, "The skin aging exposome," *Journal of Dermatological Science*, vol. 85, no. 3, pp. 152–161, 2017.

[2] C. López-Otín, M. A. Blasco, L. Partridge, M. Serrano, and G. Kroemer, "The hallmarks of aging," *Cell*, vol. 153, no. 6, pp. 1194–1217, 2013.

[3] E. Kohl, J. Steinbauer, M. Landthaler, and R. M. Szeimies, "Skin ageing," *Journal of the European Academy of Dermatology and Venereology*, vol. 25, no. 8, pp. 873–884, 2011.

[4] R. E. Watson and C. E. Griffiths, "Pathogenic aspects of cutaneous photoaging," *Journal of Cosmetic Dermatology*, vol. 4, no. 4, pp. 230–236, 2005.

[5] M. Valluru, C. A. Staton, M. W. R. Reed, and N. J. Brown, "Transforming growth factor-β and endoglin signaling orchestrate wound healing," *Frontiers in Physiology*, vol. 2, p. 89, 2011.

[6] V. J. Thannickal, D. Y. Lee, E. S. White et al., "Myofibroblast differentiation by transforming growth factor-β1 is dependent on cell adhesion and integrin signaling via focal adhesion kinase," *The Journal of Biological Chemistry*, vol. 278, no. 14, pp. 12384–12389, 2003.

[7] G. S. Ashcroft, M. A. Horan, and M. W. Ferguson, "The effects of ageing on cutaneous wound healing in mammals," *Journal of Anatomy*, vol. 187, Part 1, pp. 1–26, 1995.

[8] M. Yaar, M. S. Eller, and B. A. Gilchrest, "Fifty years of skin aging," *Journal of Investigative Dermatology Symposium Proceedings*, vol. 7, no. 1, pp. 51–58, 2002.

[9] T. A. Mustoe, K. O'Shaughnessy, and O. Kloeters, "Chronic wound pathogenesis and current treatment strategies: a unifying hypothesis," *Plastic and Reconstructive Surgery*, vol. 117, pp. 35S–41S, 2006.

[10] S. Fabi and H. Sundaram, "The potential of topical and injectable growth factors and cytokines for skin rejuvenation," *Facial Plastic Surgery*, vol. 30, no. 02, pp. 157–171, 2014.

[11] C. J. Tabit, G. C. Slack, K. Fan, D. C. Wan, and J. P. Bradley, "Fat grafting versus adipose-derived stem cell therapy: distinguishing indications, techniques, and outcomes," *Aesthetic Plastic Surgery*, vol. 36, no. 3, pp. 704–713, 2012.

[12] J.-H. Kim, M. Jung, H.-S. Kim, Y.-M. Kim, and E.-H. Choi, "Adipose-derived stem cells as a new therapeutic modality for ageing skin," *Experimental Dermatology*, vol. 20, no. 5, pp. 383–387, 2011.

[13] W. S. Kim, B. S. Park, S. H. Park, H. K. Kim, and J. H. Sung, "Antiwrinkle effect of adipose-derived stem cell: activation of dermal fibroblast by secretory factors," *Journal of Dermatological Science*, vol. 53, no. 2, pp. 96–102, 2009.

[14] S. Zhang, Z. Dong, Z. Peng, and F. Lu, "Anti-aging effect of adipose-derived stem cells in a mouse model of skin aging induced by D-galactose," *PLoS One*, vol. 9, no. 5, article e97573, 2014.

[15] W. U. Hassan, U. Greiser, and W. Wang, "Role of adipose-derived stem cells in wound healing," *Wound Repair and Regeneration*, vol. 22, no. 3, pp. 313–325, 2014.

[16] V. W. Wong, G. C. Gurtner, and M. T. Longaker, "Wound healing: a paradigm for regeneration," *Mayo Clinic Proceedings*, vol. 88, no. 9, pp. 1022–1031, 2013.

[17] V. Trottier, G. Marceau-Fortier, L. Germain, C. Vincent, and J. Fradette, "IFATS collection: using human adipose-derived stem/stromal cells for the production of new skin substitutes," *Stem Cells*, vol. 26, no. 10, pp. 2713–2723, 2008.

[18] V. D. Desai, H. C. Hsia, and J. E. Schwarzbauer, "Reversible modulation of myofibroblast differentiation in adipose-derived mesenchymal stem cells," *PLoS One*, vol. 9, pp. 1–12, 2014.

[19] B. Hinz, "The myofibroblast: paradigm for a mechanically active cell," *Journal of Biomechanics*, vol. 43, no. 1, pp. 146–155, 2010.

[20] B. M. Schipper, K. G. Marra, W. Zhang, A. D. Donnenberg, and J. P. Rubin, "Regional anatomic and age effects on cell function of human adipose-derived stem cells," *Annals of Plastic Surgery*, vol. 60, no. 5, pp. 538–544, 2008.

[21] A. Brieva, A. Guerrero, and J. P. Pivel, "Antioxidative properties of a mollusc secretion (SCA): a skin protective product," *Methods and Findings in Experimental and Clinical Pharmacology*, vol. 21, p. 175, 1999.

[22] A. Brieva, N. Philips, R. Tejedor et al., "Molecular basis for the regenerative properties of a secretion of the mollusk *Cryptomphalus aspersa*," *Skin Pharmacology and Physiology*, vol. 21, no. 1, pp. 15–22, 2008.

[23] M. Tribo-Boixareu, C. Parrado-Romero, B. Rais, E. Reyes, M. Vitale-Villarejo, and S. Gonzalez, "Clinical and histological efficacy of a secretion of the mollusk *Cryptomphalus aspersa* in the treatment of cutaneous photoaging," *Journal of Cosmetic Dermatology*, vol. 22, pp. 247–252, 2009.

[24] E. Ledo and A. Ledo, "Treatment of acute radiodermatitis with Cryptomphalus aspersa secretion," *Radioproteccion*, vol. 23, pp. 34–38, 1999.

[25] D. Tsoutsos, D. Kakagia, and K. Tamparopoulos, "The efficacy of helix aspersa muller extract in the healing of partial thickness burns: a novel treatment for open burn management protocols," *Journal of Dermatological Treatment*, vol. 20, no. 4, pp. 219–222, 2009.

[26] M. C. Cruz, F. Sanz-Rodriguez, A. Zamarron et al., "A secretion of the mollusc *Cryptomphalus aspersa* promotes proliferation, migration and survival of keratinocytes and dermal fibroblasts *in vitro*," *International Journal of Cosmetic Science*, vol. 34, no. 2, pp. 183–189, 2012.

[27] S. G. Fabi, J. L. Cohen, J. D. Peterson, M. G. Kiripolsky, and M. P. Goldman, "The effects of filtrate of the secretion of the *Cryptomphalus aspersa* on photoaged skin," *Journal of Drugs in Dermatology*, vol. 12, no. 4, pp. 453–457, 2013.

[28] J. Espada, M. Matabuena, N. Salazar et al., "*Cryptomphalus aspersa* mollusc eggs extract promotes migration and prevents cutaneous ageing in keratinocytes and dermal fibroblasts *in vitro*," *International Journal of Cosmetic Science*, vol. 37, no. 1, pp. 41–55, 2015.

[29] M. T. Alameda, E. Morel, C. Parrado, S. Gonzalez, and A. Juarranz, "*Cryptomphalus aspersa* mollusc egg extract promotes regenerative effects in human dermal papilla stem cells," *International Journal of Molecular Sciences*, vol. 18, no. 2, p. 463, 2017.

[30] W. P. Bowe and S. Pugliese, "Cosmetic benefits of natural ingredients," *Journal of Drugs in Dermatology*, vol. 13, no. 9, pp. 1021–1025, 2014.

[31] A. Budovsky, L. Yarmolinsky, and S. Ben-Shabat, "Effect of medicinal plants on wound healing," *Wound Repair and Regeneration*, vol. 23, no. 2, pp. 171–183, 2015.

[32] E. Urcan, U. Haertel, M. Styllou, R. Hickel, H. Scherthan, and F. X. Reichl, "Real-time xCELLigence impedance analysis of the cytotoxicity of dental composite components on human gingival fibroblasts," *Dental Materials*, vol. 26, no. 1, pp. 51–58, 2010.

[33] C. M. Dowling, C. H. Ors, and P. A. Kiely, "Using real-time impedance-based assays to monitor the effects of fibroblast-derived media on the adhesion, proliferation, migration and invasion of colon cancer cells," *Bioscience Reports*, vol. 34, no. 4, pp. 415–427, 2014.

[34] M. M. Roshan, A. Young, K. Reinheimer, J. Rayat, L. J. Dai, and G. L. Warnock, "Dynamic assessment of cell viability,

proliferation and migration using real time cell analyzer system (RTCA)," *Cytotechnology*, vol. 67, no. 2, pp. 379–386, 2015.

[35] R. Limame, A. Wouters, B. Pauwels et al., "Comparative analysis of dynamic cell viability, migration and invasion assessments by novel real-time technology and classic endpoint assays," *PLoS One*, vol. 7, no. 10, article e46536, 2012.

[36] I. Garzón, B. Pérez-Köhler, J. Garrido-Gómez et al., "Evaluation of the cell viability of human Wharton's jelly stem cells for use in cell therapy," *Tissue Engineering. Part C, Methods*, vol. 18, no. 6, pp. 408–419, 2012.

[37] F. Klingberg, B. Hinz, and E. S. White, "The myofibroblast matrix: implications for tissue repair and fibrosis," *The Journal of Pathology*, vol. 229, no. 2, pp. 298–309, 2013.

[38] A. M. Altman, Y. Yan, N. Matthias et al., "IFATS collection: human adipose-derived stem cells seeded on a silk fibroin-chitosan scaffold enhance wound repair in a murine soft tissue injury model," *Stem Cells*, vol. 27, no. 1, pp. 250–258, 2009.

[39] B. Hinz, "Formation and function of the myofibroblast during tissue repair," *The Journal of Investigative Dermatology*, vol. 127, no. 3, pp. 526–537, 2007.

[40] I. A. Darby, B. Laverdet, F. Bonté, and A. Desmoulière, "Fibroblasts and myofibroblasts in wound healing," *Clinical, Cosmetic and Investigational Dermatology*, vol. 7, pp. 301–311, 2014.

[41] R. M. Simpson, S. Meran, D. Thomas et al., "Age-related changes in pericellular hyaluronan organization leads to impaired dermal fibroblast to myofibroblast differentiation," *The American Journal of Pathology*, vol. 175, no. 5, pp. 1915–1928, 2009.

[42] V. W. Wong, B. Levi, J. Rajadas, M. T. Longaker, and G. C. Gurtner, "Stem cell niches for skin regeneration," *International Journal of Biomaterials*, vol. 2012, Article ID 926059, 8 pages, 2012.

[43] N. Gago, V. Pérez-López, J. P. Sanz-Jaka et al., "Age-dependent depletion of human skin-derived progenitor cells," *Stem Cells*, vol. 27, no. 5, pp. 1164–1172, 2009.

[44] J. Oh, Y. D. Lee, and A. J. Wagers, "Stem cell aging: mechanisms, regulators and therapeutic opportunities," *Nature Medicine*, vol. 20, no. 8, pp. 870–880, 2014.

[45] K. Lau, R. Paus, S. Tiede, P. Day, and A. Bayat, "Exploring the role of stem cells in cutaneous wound healing," *Experimental Dermatology*, vol. 18, no. 11, pp. 921–933, 2009.

Hindawi
Stem Cells International
Volume 2017, Article ID 2905104, 11 pages
https://doi.org/10.1155/2017/2905104

Research Article

Therapeutic Benefit for Late, but Not Early, Passage Mesenchymal Stem Cells on Pain Behaviour in an Animal Model of Osteoarthritis

Victoria Chapman,[1] Hareklea Markides,[2] Devi Rani Sagar,[1] Luting Xu,[1] James J. Burston,[1] Paul Mapp,[1] Alasdair Kay,[3] Robert H. Morris,[4] Oksana Kehoe,[3] and Alicia J. El Haj[2]

[1]*Arthritis Research UK Pain Centre and School of Life Sciences, University of Nottingham, Nottingham, UK*
[2]*Institute for Science and Technology in Medicine, Guy Hilton Research Centre, Keele University, Staffordshire, UK*
[3]*Institute for Science and Technology in Medicine, Keele University at RJAH Orthopaedic Hospital, Oswestry, UK*
[4]*School of Science and Technology, Nottingham Trent University, Nottingham, UK*

Correspondence should be addressed to Alicia J. El Haj; a.j.el.haj@keele.ac.uk

Received 26 May 2017; Accepted 7 September 2017; Published 24 December 2017

Academic Editor: Víctor Carriel

Copyright © 2017 Victoria Chapman et al. This is an open access article distributed under the Creative Commons Attribution License, which permits unrestricted use, distribution, and reproduction in any medium, provided the original work is properly cited.

Background. Mesenchymal stem cells (MSCs) have a therapeutic potential for the treatment of osteoarthritic (OA) joint pathology and pain. The aims of this study were to determine the influence of a passage number on the effects of MSCs on pain behaviour and cartilage and bone features in a rodent model of OA. *Methods*. Rats underwent either medial meniscal transection (MNX) or sham surgery under anaesthesia. Rats received intra-articular injection of either 1.5×10^6 late passage MSCs labelled with 10 μg/ml SiMAG, 1.5×10^6 late passage mesenchymal stem cells, the steroid Kenalog (200 μg/20 μL), 1.5×10^6 early passage MSCs, or serum-free media (SFM). Sham-operated rats received intra-articular injection of SFM. Pain behaviour was quantified until day 42 postmodel induction. Magnetic resonance imaging (MRI) was used to localise the labelled cells within the knee joint. *Results*. Late passage MSCs and Kenalog attenuated established pain behaviour in MNX rats, but did not alter MNX-induced joint pathology at the end of the study period. Early passage MSCs exacerbated MNX-induced pain behaviour for up to one week postinjection and did not alter joint pathology. *Conclusion*. Our data demonstrate for the first time the role of a passage number in influencing the therapeutic effects of MSCs in a model of OA pain.

1. Introduction

Osteoarthritis (OA) is the most common joint disease in adults, and current prevalence is 12% in the population > 60 years, which will escalate over the next 20 years [1, 2]. Although there is controversy in the field, it is acknowledged that a broad spectrum of proinflammatory pathways and catabolic factors contributes to the initiation of OA, which impacts upon both the joint cartilage, synovium, and bone [1]. Pain is one of the first symptoms of knee OA; it can progress to be continuous, reducing movement and quality of life [1].

The mechanisms underlying OA pain involve structural changes and alterations in peripheral transduction and central processing of painful sensory inputs. Current treatments for OA pain have limited efficacy [3], and total joint replacement (TJR) surgery is a common outcome [1]. TJR surgery often reverses central sensitization, indicating that nociceptive output from the joint is fundamental in driving central pain mechanisms [4]. However, surgery is not suitable for patients < 55 years [5], and it remains critical that numbers of people with OA pain reliant on joint replacement as a treatment are reduced.

An alternative approach is the development of more effective cell-based therapies that limit the joint pathology and reduce synovial inflammation, which is significantly associated with OA pain [6].

Mesenchymal stem cells (MSCs) have a potential as a therapy for OA [7–10]. MSCs readily differentiate into bone,

cartilage, and adipose cells and release soluble factors (such as growth factors and chemokines) which harbour a regenerative environment through a variety of mechanisms [9, 11]. Animal models mimicking pathological and pain components of OA are widely used [12–14]; intra-articular injection of rat bone marrow-derived MSCs reduced pain behaviour in the absence of an effect on joint pathology in the monosodium iodoacetate model of OA in the rat [15] and had significant chondroprotective and anti-inflammatory effects in a rat surgical model of OA, but pain was not assessed [16]. Similarly, local delivery of adult MSCs was associated with regeneration of meniscal tissue and reduced joint destruction in a caprine model of OA [17]. Increased passage number from 4 to 9 of human adipose-derived adult stem cells increases the chondrogenic potential of cells [18]; whether this translates into improved benefit *in vivo* has yet to be addressed.

Maximising the therapeutic potential of cell-based therapies for the treatment of OA pain requires further understanding of the conditions required to maximise the potential therapeutic effect of MSCs, and knowledge of their sites and mechanisms of action, which requires monitoring of implanted cells within the joint. The aim of the present study was to compare effects of early versus late passage MSCs on pain behaviour, structural changes to the knee joint, and circulating levels of tumor necrosis factor alpha (TNFα) and interleukin 10 (IL-10) in a surgical model of OA in the rat. Tracking and imaging of the MSCs within the joint were achieved using magnetic resonance imaging (MRI) of superparamagnetic iron oxide nanoparticles (SPION) internalised by MSCs in a subset of the groups within the study.

2. Materials and Methods

2.1. Cell Isolation, Expansion, and Characterisation. Early passage bone marrow murine MSCs (P3) were isolated from Balb/c mice, and late passage cells (P9) were isolated from C57Bl/6 mice as previously described [19]. Both sets of cells were fully characterised for membrane receptor expression of CD31, CD44, CD11b, CD45, CD105, and Ly-6A(Sca-1)PE, three lineage differentiation, and colony-forming unit fibroblast assay (CFU-F) (see Supplementary Information).

2.2. Magnetic Nanoparticle (MNPs) Labelling. MSCs were labelled with SiMAG (1000 nm; particle size) (Chemicell, Germany). These are commercially available MNPs consisting of a maghemite iron oxide core (Fe_2O_3) and an unmodified silica surface with terminal negatively charged silanol groups. Cell were labelled using a passive incubation method as described by Markides et al. [20]. In brief, MNPs were suspended in serum-free CIM (cell isolation media) and added directly to cells in culture. Following a 24-hour incubation period, cells were washed three times with phosphate buffered saline (PBS) to remove noninternalised MNPs.

2.3. CellTracker™ CM-DiI Fluorescent Dye Labelling. A 1 mg/ml stock solution of the red fluorescent CellTracker CM-DiI (Molecular Probes, UK) was prepared in dimethyl sulfoxide (DMSO). MSCs were trypsinized, washed with PBS, and incubated with CM-DiI (2.5 μl of stock per 1 ml of PBS) for 5 minutes at 37°C, and then for an additional 15 minutes at 4°C, in darkness.

Unincorporated dye was then removed by centrifugation at 300g for 5 minutes and 2 washes in PBS. Cells were resuspended in serum-free IMDM (Iscove's Modified Dulbecco's Medium) and maintained at 4° until injection.

2.4. MSC-Conditioned Medium Studies. Cells used for conditioned medium studies were previously isolated from C57Bl/6 and Balb/c mice and expanded *in vitro*. For testing, conditioned medium was prepared using murine bone marrow-derived MSC at P3 and P10. Conditioned medium was prepared using serum-free IMDM (SF-IMDM) (GIBCO, Life Technologies) with no supplements added as described previously [21]. Briefly, cells were expanded to confluence using cell expansion medium (CEM, comprising IMDM with 9% FBS, 9% Horse Serum, and 1% Pen/Strep). Flasks were then rinsed three times with DPBS and once with SF-IMDM before adding 12 ml SF-IMDM. Following this, flasks were incubated at 37°C, 5% CO_2 with SF-IMDM without cells used for controls. After 48-hour incubation, the medium was removed and centrifuged for 5 minutes at 1200g to remove cell debris. 11 ml supernatant was then passed through 3 kDa centrifugal filters (amicon ultra 15 centrifugal filter tubes, Merck Millipore, Hertfordshire, UK) at 4000g for 40 minutes at 4°C, and residual supernatant was removed from filters and immediately frozen to −80°C until testing.

2.5. Rat Model of Osteoarthritis Pain. Male Sprague Dawley rats (weighing 160–190 g) were purchased from Charles River UK. Studies were carried out in accordance with UK Home Office Animals (Scientific Procedures) Act (1986) and the guidelines of the International Association for the Study of Pain. Further, all works were conducted under Home Office project licence number 40-3647. Studies were undertaken in a blinded fashion. Rats underwent medial meniscal transection (MNX), or sham surgery, as previously described [22]. The surgical MNX model of OA in rats has been demonstrated to induce symptoms comparable to that seen in human OA for pain behaviour, weight-bearing asymmetry, and disease pathology, through synovitis, pathology of the subchondral bone, and chondropathology, as well as the development of osteophytes [13, 22–24]. Rats were anaesthetised with isoflurane (3% induction, 2–2.5% maintenance; 1 L/min O_2), and local anaesthetic EMLA cream was applied to the left hind limb. A full thickness cut through the medial meniscus of the left knee was performed. Sham-operated rats had their meniscus exposed, but not transected. Recovery from anaesthesia was monitored, and weight gain and general behaviour were monitored throughout the postinjury period.

2.6. Intervention Studies and Pain Behaviour. Baseline measurements were taken prior to surgery (day 0) and from day 3 onwards. Behavioural assessment of changes in weight distribution and sensitivity to mechanical stimuli applied to the hindpaw were performed for up to 42 days postsurgery

(see Supplementary Information). Two separate intervention studies were undertaken at 14 days postsurgery (MNX and sham). Prior to treatment, rats were stratified according to weight bearing and paw withdrawal thresholds (PWTs) (days 3–14) to ensure balanced groups. Under brief isoflurane anaesthesia (3% 1 L/min O_2), rats received one intra-articular injection.

2.6.1. Study 1: Late Passage MSCs (P.10). MNX rats received intra-articular injection of either 1.5×10^6 mesenchymal stem cells labelled with 10 μg/ml SiMAG (MSC-MNP; $n = 11$ rats), 1.5×10^6 mesenchymal stem cells (MSC-VEH; $n = 12$ rats), or serum-free media (SFM; $n = 12$ rats). Sham-operated rats received intra-articular injection of serum-free media (SFM; $n = 8$ rats).

2.6.2. Study 2: Early Passage MSCs (P.3) versus Steroid Treatment. MNX rats received intra-articular injection of 200 μg/20 μL Kenalog ($n = 8$), 1.5×10^6 MSC ($n = 10$ rats), or serum-free media ($n = 10$ rats). Sham-operated rats received serum-free media (SFM; $n = 8$ rats).

Following intra-articular injection, rats recovered from anaesthesia and were returned to the home cage. Weight bearing and PWTs were assessed on days 21, 28, 31, 35, and 38 post sham/MNX surgery. Experiments were terminated on day 42.

2.7. Magnetic Resonance Imaging (MRI). The *in vivo* MRI visibility threshold was determined previously by intra-articular injection of either 1×10^6 or 2×10^6 MSCs labeled with 0, 1, 5, and 10 μg/ml SiMAG into the joint of nonarthritic cadaveric 18-week-old Wistar rats. Rats were MR imaged using a Brucker 2.3 T animal scanner with the following sequence parameters; T2-weighted GEFI sequences, TR = 700 ms, TE = 5.5 ms, Flip angle = 30° and FoV = 7.9 × 7.9 cm, and matrix size = 256 × 192 to determine the location of the MNPs. MR images and signal loss profiles were compared to the untreated control groups and also between the treatment groups. Study 1 rats were sacrificed on day 42 and immediately MR imaged using the same system described above. Signal loss profiles were obtained and compared across all the groups. For details on data analysis, see Supplementary Information.

2.8. Histology. At sacrifice, tibiofemoral joints were removed and postfixed in neutral buffered formalin (4% formaldehyde) decalcified in ethylenediaminetetraacetic acid (EDTA) [24]. Histomorphometry was performed by an observer blinded to treatment. Coronal tissue sections (Osteoarthritis Research Society International (OARSI) guideline for histological assessment for OA in the rat) were cut at 5 μm [25].

Haematoxylin and eosin (H&E) stained sections were scored for joint morphology [26]. To validate the MRI results from study 1, midsagittal serial sections (4 μm) were obtained and stained with H&E and the fluorescent dye DAPI (1 : 200 dilution prepared in PBS) in order to visualise implanted CM-DiI-labelled MSCs (see Supplementary Information).

2.9. ELISA. At sacrifice, blood was taken via cardiac puncture, aliquots spun for 20 minutes at 1000 *g*, and serum supernatant was collected. Serum samples were diluted 2-fold, TNFα using 75 μl with calibrator diluent (R&D Systems, RD5-17), IL-10 using 50 μl with assay diluent (R&D Systems, RD1-21), and βNGF using assay diluent made up using 10% heat inactivated FBS (Life Technologies Ltd., 10500-064). Serum levels of TNFα and IL- 10 were determined using commercially available Enzyme-linked immunosorbant assay (ELISA) kits (RnD Systems, Minneapolis MN) as per manufacturer's instructions. Each serum sample was repeat tested $n = 2$, and absorption read at 450 nm with correction at 540 nm applied. Proprietary kits for measurement of βNGF in rat serum were not available, so components were sourced individually with the basic application using Duoset ELISA Development Kit (R&D Systems Europe, Ltd., DY556) and recommended components as per kit instructions (all R&D Systems Europe Ltd.) except for DPBS (GIBCO, Life Technologies, 14190-169).

2.10. Statistics. Data were analysed using GraphPad Prism 5.0. All data were tested for normality and for nonparametric testing; Kruskall-Wallis one way ANOVA with Dunn's post hoc testing or 2-way ANOVA with Tukey's post hoc testing was applied where appropriate, with probability values considered significant at $^*p < 0.05$, $^{**}p < 0.01$, and $^{***}p < 0.001$.

3. Results and Discussion Results

3.1. MSC Selection and Characterisation. Murine MSCs were freshly isolated and expanded *in vitro* to passage 3 (early passage) or passage 10 (late passage) with passaging taking place at 80–90% confluence. Stem cell properties were confirmed with flow cytometry for a panel of recognised MSC markers ($CD105^+$, $Sca\text{-}1^+$, $CD31^-$, $CD11b^-$, $CD45^-$, $CD44^+$, and $CD34^-$) (Supplementary Information Figure 1) and selected for use. Cells were successfully differentiated towards adipogenic, osteogenic, and chondrogenic lineages after 21 days in culture with relevant differentiation media (Supplementary Information Figure 2). CFU-F assay was used to assess the proliferative capacity of the cells being expanded in culture, and the results showed that late passage cells retained a high proliferation rate in culture (early passage 49 ± 18% versus late passage 51.5 ± 12%). Early and late passage cells were cultured for conditioned medium collection, and levels of key cytokines (IL-10, TNFα, and βNGF) were measured (Supplementary Information Figure 3). Levels of IL-10 in the conditioned medium were minimal and did not vary between early and late passage cells. Levels of βNGF were significantly higher in conditioned medium from late passage MSC, compared to early passage MSC (Student's *t*-test, $p < 0.05$, $n = 6$). TNFα was not detected in the conditioned medium under either condition (Supplementary Information Figure 3).

3.2. MRI of MSCs Labelled with SiMAG In Vivo. The presence of iron oxide MNPs was detected as a decrease in signal intensity when MR imaged using T2-weighted MRI sequences. This signal loss is portrayed visually as black areas on grey scale MR images, referred to as hypointense regions. The optimal cell number and SiMAG ratio to ensure good

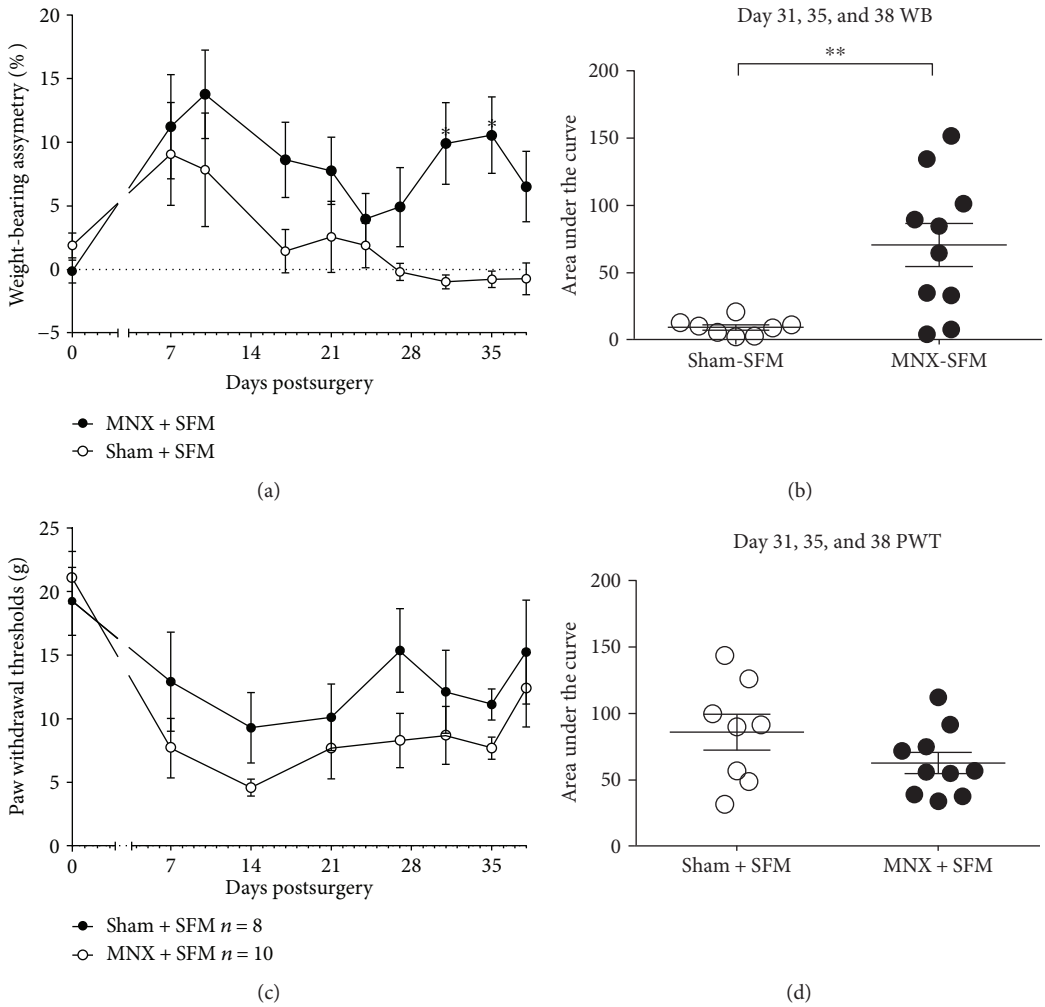

Figure 1: MNX surgery for induction of OA pain, or sham surgery, was performed on day 0. (a) MNX rats receiving SFM exhibited significant differences in weight-bearing asymmetry, compared to the sham-SFM rats. (b) Area under the curve (AUC) data calculated for days 31, 35, and 38 postsurgery revealed significant weight-bearing asymmetry in MNX rats at the later timepoints of the model. (c) Paw withdrawal thresholds were not significantly different in MNX rats, compared to sham controls at individual timepoints, or following AUC analysis. (d) Statistical comparison of the groups at each timepoint: two-way ANOVA with Bonferroni's post hoc. Comparison of AUC used a Mann–Whitney's nonparametric unpaired t-test. $^{*}p < 0.05$, $^{**}p < 0.01$ MNX versus sham. Data are mean ± SEM, $n = 8$–10 per group.

MRI visibility over a prolonged period of time were determined to be 1.5×10^6 cells labelled with 10 μg/ml of SiMAG (Supplementary Information Figure 4). This labelling combination allows for improved visibility thresholds over 1×10^6 whilst minimising excessive blooming as seen with 2×10^6 cells and was taken forward for subsequent *in vivo* MRI tracking studies.

3.3. Effects of MSC Treatment versus Steroid on Pain Behaviour in a Model of OA. Both sham surgery and MNX surgery resulted in early changes in weight bearing on the operated hindlimb. By day 14 postsurgery, there was a clear difference between the extent of weight-bearing asymmetry between the sham and MNX groups, indicative of pain behaviour in the MNX group. At days 28–38, weight-bearing asymmetry remained significantly increased in the MNX group, but had returned to baseline in the sham group (Figure 1(a)). Area under the curve analysis of the last three timepoints tested (days 31–38) revealed a significantly greater weight-bearing asymmetry in the MNX group compared to the sham control group. Consistent with the studies in our group, hindpaw withdrawal thresholds (PWTs) were lowered in both sham and MNX rats following surgery (Figure 1(c)). There were no significant differences in the PWTs between the two groups of rats (Figure 1(d)).

The effect of intra-articular injection of 1.5×10^6 of late passage MSCs on established pain behaviour in the MNX model was determined. MSC treatment did not alter weight-bearing asymmetry in the week (days 14–21) immediately following treatment (data not shown). By contrast, there was a significant reduction in weight-bearing asymmetry at later timepoints (days 31, 35, and 38) in the MNX group treated with late passage MSCs (Figure 2(a)). PWTs were not altered by the intra-articular injection of late passage MSCs (Figure 2(b)). The effects of intra-articular injection of early passage MSCs versus a steroid treatment

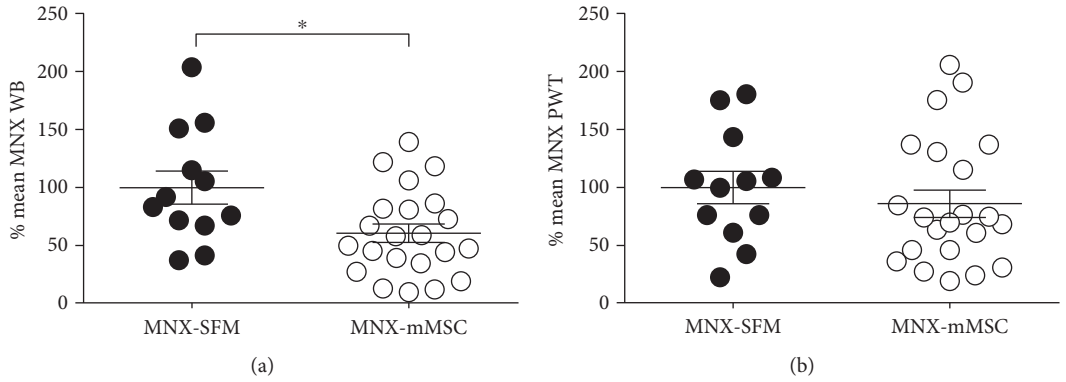

Figure 2: Rats received an intra-articular injection of 1.5×10^6 late passage mouse mesenchymal stem cells (mMSCs) from the bone marrow of Balb/c mice in 50 μL serum-free medium (SFM) or 50 μL SFM (vehicle) on day 14 post MNX surgery. (a) Intra-articular injection of MSCs significantly altered MNX-induced changes in the weight-bearing asymmetry. (b) Paw withdrawal thresholds in MNX rats were unaltered by the treatment. Data are expressed as a % of the mean MNX-SFM AUC for three timepoints (31, 35, and 38 days) postsurgery. Statistical analysis used a Mann–Whitney nonparametric unpaired t-test. Data are mean ± SEM, MNX-SFM ($n = 11$), MNX-MSC ($n = 22$). WB: weight-bearing asymmetry; PWT: paw withdrawal thresholds. $^*p < 0.05$ MNX-MSC versus MNX-SFM.

on pain behaviour in the MNX model were determined in separate groups of rats. Intra-articular injection of early passage MSC at day 14 resulted in a robust and significant increase in weight-bearing asymmetry at days 17 and 21 post model induction (Figure 3(a)). At later timepoints (days 29–38), weight-bearing asymmetry was comparable between the MNX-MSC group and the MNX-SFM group (Figure 3). Intra-articular injection of the steroid Kenalog at day 14 in MNX rats resulted in a complete reversal of weight-bearing asymmetry at days 17 and 21 (Figure 3). At later timepoints (days 29–38), Kenalog ceased to inhibit weight-bearing asymmetry and there were no differences between the MNX-SFM control group and the MNX Kenalog treatment group (Figure 3(b)).

3.4. Joint Pathology, Inflammation, and Pain-Related Cytokines. Analysis of joint histology at the end of the study revealed that MNX surgery resulted in a significant chondropathy score (Figure 4(a)), inflammation score of the synovium (Figure 4(b)), and an increase in the number of osteophytes (Figure 4(c)). At this final timepoint, none of the treatments significantly altered joint chondropathy or inflammation (Figures 4(a), 4(b), and 4(c)). Serum levels of three cytokines were measured in the different treatment groups at the end of the study (day 42 postsurgery). There were no differences in IL-10 expression between the treatment groups (Figure 4(d)). There was a significant increase in serum TNFα in the MNX-MSC early passage treatment group, compared to the sham-SFM controls and MNX-MSC late passage treatment group (Figure 4(e)). There were no significant differences in serum βNGF expression between the groups (Figure 4(f)).

3.5. MRI Tracking. A subset of rats received intra-articular injection of SiMAG-labelled MSCs (MSC-MNP) for terminal MRI imaging at 29 days post cell implantation. MRI revealed regions of increased hypointensity (black areas) localised to the synovial cavity of rats treated with MSC-MNP (Figure 5). In contrast, no hypointense regions were evident in the groups treated with MSCs (MSC-VEH) or serum-free media (SFM). To further validate these data, signal loss profiles were plotted for the different treatment groups and revealed a significant signal loss in the MSC-MNP group, compared to unlabelled MSCs (MSC-VEH) and SFM which had a relatively high signal intensity across the joint (Figure 5). In a subset of rats, it was confirmed that there were no differences between the effects of SiMAG-labelled MSCs and unlabelled MSCs on pain behaviour (data not shown). H&E staining was used to identify key structural features of the knee joint whilst identifying the location of the fluorescently labelled MSCs. CM-DiI-labelled MSCs were identified in the synovium of all MSC-treated groups (MSC-MNP and MSC-VEH) but not in the SFM-treated group (Figure 5).

4. Discussion

This study presents new evidence that passage number of MSCs markedly influences the effects of these cells on pain behaviour following their injection into the knee joint in a surgical model of OA pain. We report that late passage MSCs significantly reduced weight-bearing difference, a surrogate index of pain on loading, whereas early passage MSCs exacerbated weight-bearing difference for a period of 7 days postinjection in the MNX model. Despite the beneficial effects of the late passage MSCs on pain behaviour in the MNX model, there was no evidence for an alteration in the progression of joint pathology or inflammation at the end of the study. Nevertheless, a peripheral site of action of the MSCs was supported by the demonstration that SiMAG-labelled MSCs were detected within the synovial cavity at 29 days postinjection.

As joint degeneration progresses, a variety of surgical procedures can rebuild the degenerated cartilage lesions, but do not necessarily reduce the generalised joint inflammatory processes. Chondrocytes as a cell-based therapy (autologous chondrocyte implantation (ACI)) were successfully developed and used widely over the past 10 years, but

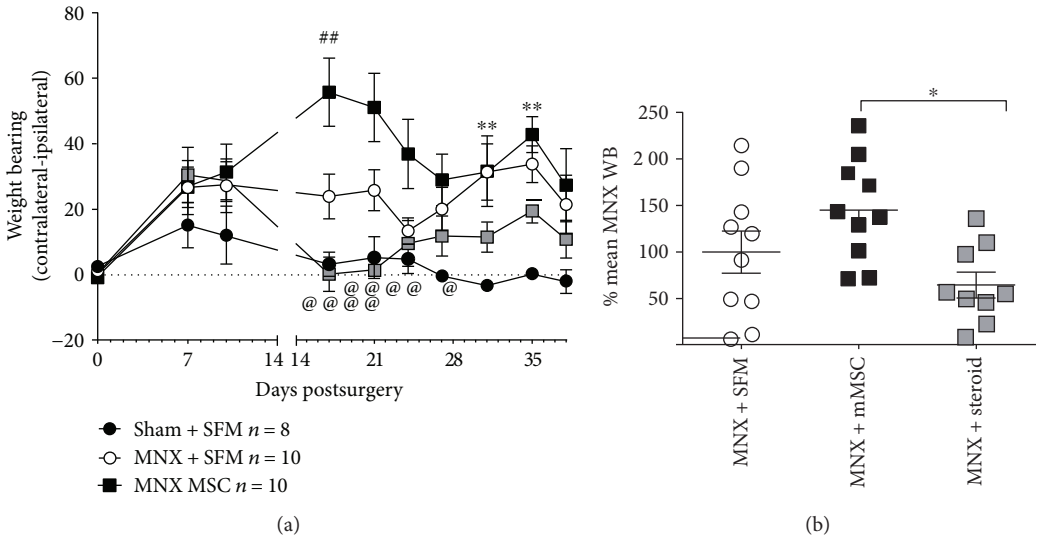

Figure 3: (a) Timecourse of the effects of intra-articular injection of the steroid Kenalog (200 μg/20 μL) versus 1.5×10^6 of early passage mMSC on weight-bearing asymmetry. Rats received the active treatments or 50 μL SFM (vehicle) on day 14 postsurgery. Kenalog had a rapid inhibitory effect on MNX-induced weight-bearing asymmetry at 17 and 21 days post model induction, compared to the MNX-SFM group. mMSC treatment significantly increased weight-bearing asymmetry at early timepoints (days 17 and 21) post model induction. At later timepoints, weight-bearing asymmetry was comparable between the MNX-MSC group and the MNX-SFM group. Data was analysed using a 2-way ANOVA with Tukey's post hoc test. $^{**}p < 0.01$ MNX-SFM versus sham-SFM, $\#\#p < 0.01$ MNX-MSC versus MNX-SFM; $@p < 0.05$, $@@@@p < 0.0001$ MNX steroid versus MNX-MSC. (b) Area under the curve (AUC) analysis of the effects of intra-articular injection of steroid Kenalog versus 1.5×10^6 of early passage mMSC on MNX-induced weight-bearing asymmetry for the last three timepoints (days 31, 35, and 38). mMSC treatment did not alter weight-bearing asymmetry in MNX rats. Although there was a trend towards an inhibition of weight-bearing asymmetry by Kenalog, this was only significantly compared to the MNX-mMSC group. Data are expressed as a % of the mean MNX-SFM AUC for timepoints 31, 35, and 38 days postsurgery. Statistical analysis used a Kruskal-Wallis test with Dunn's post hoc, $^{*}p < 0.05$. Data are mean ± SEM, $n = 9$-10 per group.

this treatment relies on damaging healthy cartilage to provide the cell sources. The therapeutic potential of alternate sources of cells, such as MSCs derived from the bone marrow, which have anti-inflammatory and immunosuppressive properties, has been investigated. Our finding that late passage MSCs attenuated established weight-bearing asymmetry in the MNX model is consistent with the report that intra-articular injection of MSCs reversed pain behaviour compared to pretreatment values, but did not alter structural damage or synovial inflammation in the chemical monosodium iodoacetate model of OA pain [27]. The clinical validity of animal models of OA continues to be debated, both in terms of the aetiology of the joint damage and the temporal progression of the structural changes seen in these models, compared to disease progression in patients. The MNX model of OA is believed to replicate some of the key biomechanical events that lead to clinical joint pathology, as well as displaying many of the features associated with joint pathology in OA (see refs in [28]). Our evidence that intra-articular injection of early passage MSCs exacerbated pain behaviour in the model of OA provides important new knowledge of the conditions under which the therapeutic potential of MSCs for OA pain can be harnessed.

Our data were built upon the previous studies that focused on the potential for MSCs to mediate joint repair. Indeed, therapeutic benefit of intra-articular injection of autologous MSCs has been reported in a surgical model of OA in the goat [17], and more recent studies report beneficial effects of MSCs from bone marrow and adipose in models of OA and extend the initial evidence by demonstrating reparative effects of the cells on the cartilage [29, 30]. The progression of MNX-induced joint pathology was not halted by intra-articular injection of late passage MSCs, suggesting that at least in this model the effects of MSC treatment on pain behaviour are not associated with increased joint repair. Despite this lack of effect on joint pathology, our study did provide evidence for changes in systemic inflammation. There was a trend towards an increase in serum TNFα in the MNX model of OA pain, compared to the sham control group at day 42 postsurgery. Interestingly, MNX rats treated with the early passage MSCs had significantly increased serum TNFα, compared to the sham group, consistent with the exacerbation of pain behaviour by this treatment. By contrast, serum TNFα was significantly lower in MNX rats treated with late passage MSCs, compared to early passage MSCs. These data are consistent with the ability of late passage, but not early passage, MSCs to reduce pain behaviour. Pharmacological studies using comparable methods demonstrated a significant increase in plasma TNFα in the MIA model of OA pain compared to control rats, with these changes reversed by an analgesic treatment [31]. Although both IL-10 and NGF were detected in the serum, there were no significant differences between the treatment groups, suggesting that changes in TNFα do not reflect a generalised change in inflammation.

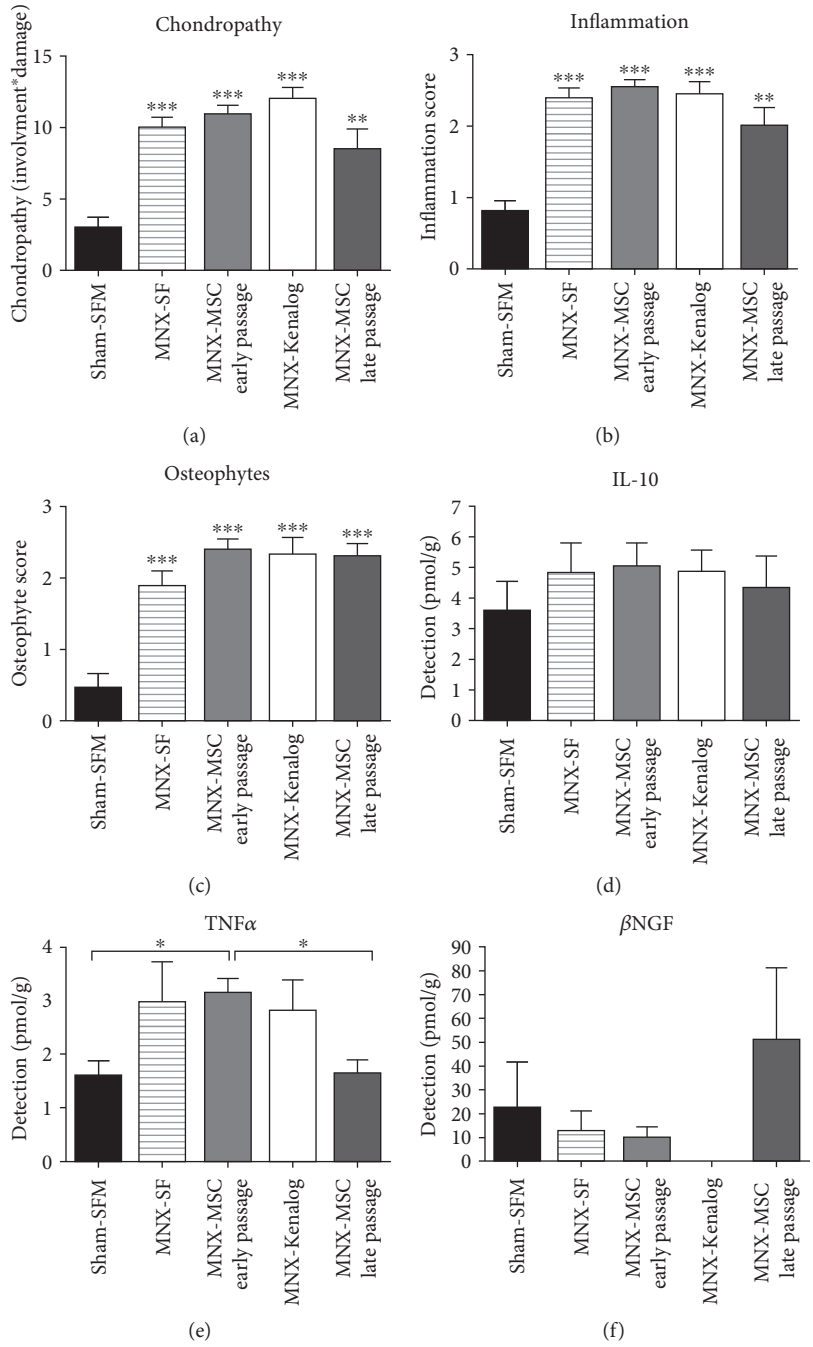

Figure 4: (a–c) MNX surgery was associated with significant chondropathy (a), joint inflammation (b), and increased presence of osteophytes (c), compared to sham controls at 42 days postsurgery. None of the treatments in MNX rats significantly altered the extent of chondropathy, inflammation, or osteophyte number. Statistical analysis used Kruskal-Wallis test with Dunn's post hoc, $^{**}p < 0.01$, $^{***}p < 0.001$. Data are mean ± SEM, 2–4 sections per rats were analysed, and total numbers of sections are sham-SFM: 37; MNX-SFM: 55; MNX-MSC early passage: 44; MNX Kenalog: 42; MNX-MSC late passage: 20. (d–f) Serum levels of cytokines in MNX- and sham-operated rats at 42 days postsurgery. There were no differences in IL-10 expression between the treatment groups (d). There was a significant increase in serum TNFα in the MNX-MSC early passage treatment group, compared to the sham-SFM controls and MNX-MSC late passage treatment group (e). There were no significant differences in serum βNGF expression between the groups. Statistical analysis used Kruskal-Wallis test with Dunn's post hoc, $^{*}p < 0.05$, $^{***}p < 0.001$. Data are overall mean ± SEM, whilst mean values from duplicate samples per rat were analysed; total numbers of mean values are sham-SFM: 15; MNX-SFM: 22; MNX-MSC early passage: 10; MNX Kenalog: 9; and MNX-MSC late passage: 23.

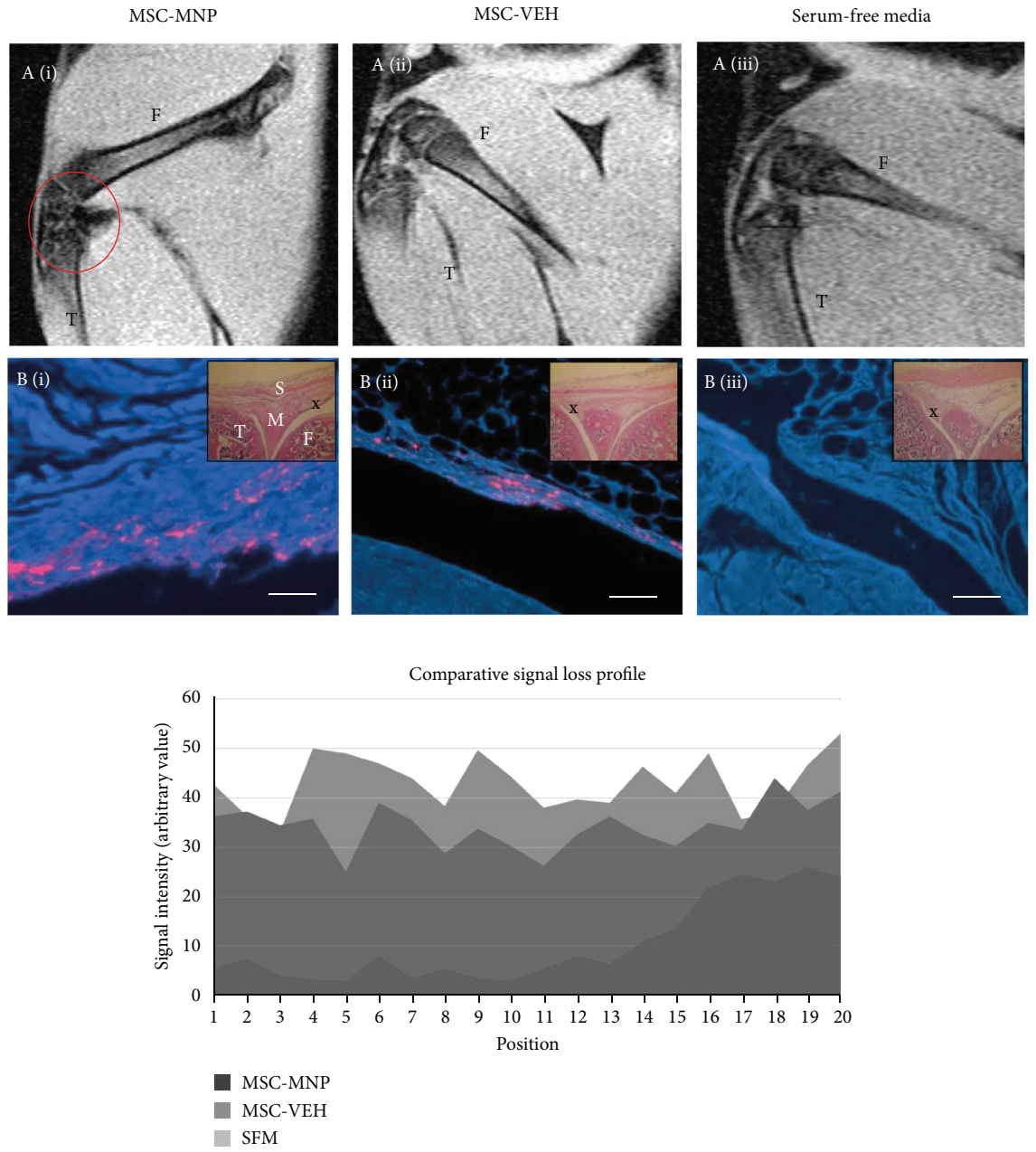

Figure 5: (a): Sagittal MRI scans; Location of SiMAG-labelled cells are depicted as areas of hypointense signal loss and highlighted by the red ring over the synovial cavity. (b) Corresponding histological sections. Fluorescent images correspond to location marked X on H&E images (inset). Implanted DiI-labelled MSCs are shown in red whilst all native materials are show by DAPI in blue. (c) Corresponding MRI signal loss profile. Groups include (i) SiMAG-labelled MSCs (MSC-MNP), (ii) MSCs only (MSC-VEH), and (iii) serum-free media. T: tibia; F: femur; S: synovial lining; M: meniscus. Scale bars = 100 μm.

Understanding the differences in properties of the early versus late passage MSCs that lead to the behavioural outcomes will help refine MSC treatment strategies. Prolonged *in vitro* culture of bone marrow-derived MSCs leads to a loss of MSC phenotype, multipotency, decreased wound homing properties [32], and self-renewal by around passage 15–20, associated with the onset of cellular senescence [33–36]. As a result, the use of early passage cells is recommended; however, early passage cell populations have increased likelihood of heterogeneity whilst late passage cells retain characteristic markers for MSC phenotype in a selectively more homogenous population [36, 37]. The immunomodulatory properties of MSCs in a long-term culture have been reported. Late passage MSCs of umbilical origin (passage 15) show significant upregulation of anti-inflammatory mediator HMOX-1, a modulator of IL-10 and NO activity [38, 39]; downregulation of proinflammatory IL-1α, IL-1β, and IFN-γ; reduced proliferation of PHA-stimulated peripheral blood mononuclear cells, implicated in expression of proinflammatory cytokines; and no change in expression of

TGF-β, a cytokine critical to the immunosuppressive capabilities of transfused MSC [39]. It may therefore follow in our study that IFN-γ production is impaired and macrophage balance shifts from M1 to M2, as seen previously with *in vivo* MSC transplantation [40]. Production of IL-6 is increased in the late passage human bone marrow-derived MSC compared to early passage cells, whilst CXCL8 levels fall [41]. IL-6 has both anti- and proinflammatory activities and may function here to activate IL-10 and bind to toll-like receptors to inhibit proinflammatory cytokine production, for example, TNF-α and IL-1, whilst also providing protection against bacterial proliferation [42, 43]. More analyses of the cytokine profile are needed to define exact pathways in the variation in potential immunomodulation between early and late passage MSCs in our model of OA pain.

There is evidence of other phenotypic shifts in MSCs with prolonged culture which may provide insight. For example, prolonged culture of MSCs reduces STRO-1 and BMP7 expression, changes alkaline phosphatase activity, and reduces osteogenic capability [36, 44, 45]. Earlier studies, examining passage-dependent differences to chondrogenic potential of MSCs, have produced varied results, with some studies reporting a maintenance of the chondrogenic potential of the cells up to passage 20 [46], or increase in COL2A1 and AGC1 expression from P4 to P9 in human adipose-derived adult stem [18]. Another study reported a reduction of chondrogenic capabilities of MSCs at late passage [33, 35, 47]. With an increasing passage number, MSC isolated from synovium shows migratory behaviour similar to chondrocytes, whilst at low passage ($p < 4$), a reduced ability to undergo chondrogenesis was observed [48]. Our results revealed that late passage MSCs attenuated established pain behaviour (weight-bearing asymmetry) in MNX rats, but did not alter MNX-induced joint pathology. This suggests that higher passage cells may have an increased potential for therapeutic application. What is clear is that selection of populations of cells for therapy will depend on the level of preculture with significant changes in phenotype and potential therapeutic activity as a result of prolonged culture. The trade-off between efficacy and cell number generated by scale-up of cell numbers will be an important consideration in a therapeutic design. Future studies of earlier experimental timepoints will shed light on the effects of treatments on the alleviation of pain and moderation of inflammatory response following MSC treatment.

The key to enabling the translation of MSC treatment for OA to the clinic is the tracking of the cells following injection into the knee joint to initially demonstrate effective delivery of cells and to monitor cell retention and biodistribution thereafter. Previously, we have shown that SiMAG, a commercially available superparamagnetic iron oxide nanoparticles (SPIONs), can be used to track the migration of MSCs over 7 days and localise them to the knee joint in a mouse model of rheumatoid arthritis (RA) [20]. Importantly, the same study demonstrated no adverse effects in terms of *in vitro* MSC properties, cell viability, and proliferation as a result of SiMAG labelling. Furthermore, the delivery of SiMAG-labelled MSCs was also well tolerated by mice thereby encouraging the use of SiMAG as an imaging and tracking agent in this current study. Although a number of noninvasive imaging modalities can be applied to track cells post implantation, SPION- and MRI-based tracking techniques benefit from relatively long-term and longitudinal monitoring of implanted cell populations. In a recent study by van Buul et al. [27], implanted MSC populations were monitored by bioluminescence and MRI with MSCs transfected with firefly luciferase and labelled with a particular SPION known as Endorem. A gradual and complete loss in bioluminescence signal was observed over a 3-week period. By contrast, the SPION-based component of this system has the potential to allow SPION-labelled cells to be monitored for up to 12 weeks as demonstrated by 2 independent studies by Jing et al. [49] and Chen et al. [50]. In these studies, Endorem-labelled MSCs and chondrocytes were monitored *in vivo* for up to 12 weeks within the knee joint [49, 50]. Nevertheless, unlike bioluminescence, the viability of implanted cells cannot be determined by MRI-based modalities. In our study, SiMAG-labelled cell was successfully observed up to 29 days post implantation.

5. Conclusions

We have demonstrated differences in pain responses in a rat surgical model of OA following cell therapy using populations of MSCs at early and late passages following isolation from the bone marrow. Late passage MSCs significantly reduced weight-bearing difference, a surrogate index of pain on loading (days 31, 35, and 38), whereas early passage MSCs exacerbated weight-bearing difference for a period of 7 days postinjection in the MNX model. Neither treatment altered progression of joint pathology nor inflammation quantified at the end of the study. Our data provide further evidence for the need for characterisation of this cell type prior to clinical use due to its multifunctional nature and the changing phenotype from repair to immunomodulation with time in culture.

Ethical Approval

All studies were approved by local ethics committee. Experiments were carried out in accordance with UK Home Office Animals (Scientific Procedures) Act (1986) and the guidelines of the International Association for the Study of Pain.

Conflicts of Interest

The authors declare that there is no conflict of interest regarding the publication of this article.

Acknowledgments

The authors thank the Arthritis Research UK for funding this work and thank Gemma Turner (Keele University) for the help with formatting the manuscript. This work was funded by Arthritis Research UK (Grant nos. 18769 and 19429). The work was partially funded through the ARUK Centre

for Tissue Engineering and the EPSRC IRC in manufacturing of regenerative medicine.

Supplementary Materials

Supplementary Figure 1: Cell marker profile for early and late passage MSC, characterised through $CD105^+$, $Sca\text{-}1^+$, $CD31^-$, $CD11b^-$, $CD45^-$, $CD44^+$, $CD34^-$. CD105 is known to vary in expression in murine MSC. In this study, cells at late passage expressed lower levels of CD105 whilst all other markers were consistently expressed. Supplementary Figure 2: Tri-lineage differentiation for early (A) and late (B) passage cells along adipogenic (1), osteogenic (2) and chondrogenic (3) lineages. Positive differentiation was detected for both early and late passage MSC. Scale bars = 200 μm. Supplementary Figure 3: Measurement of cytokines conditioned media from early and late passage cultured MSCs. There were no differences in IL10 levels between the two conditions. TNFα was not detected in conditioned medium. Expression of βNGF was significantly higher in late passage MSC compared to early passage MSC (Student's t-test, $p < 0.05$) ($n = 6$ for all samples). Supplementary Figure 4: In vivo dose response: Signal loss profiles and corresponding sagittal MR images following the implantation of (A) 1×10^6 and (B) 2×10^6 MSCs labelled with (i) 10 μg/ml, (ii) 5 μg/ml, and (iii) 1 μg/ml SiMAG into knee joints of cadaveric rats and compared to the (iv) untreated control. Location of SiMAG labelled cells is depicted as areas of hypointense signal loss and highlighted by the red ring over the synovial cavity. *(Supplementary Materials)*

References

[1] S. Glyn-Jones, A. J. R. Palmer, R. Agricola et al., "Osteoarthritis," *Lancet*, vol. 386, no. 9991, pp. 376–387, 2015.

[2] T. Neogi and Y. Zhang, "Epidemiology of osteoarthritis," *Rheumatic Diseases Clinics of North America*, vol. 39, no. 1, pp. 1–19, 2013.

[3] P. G. Conaghan, P. M. Peloso, S. V. Everett et al., "Inadequate pain relief and large functional loss among patients with knee osteoarthritis: evidence from a prospective multinational longitudinal study of osteoarthritis real-world therapies," *Rheumatology*, vol. 54, no. 2, pp. 270–277, 2015.

[4] T. Graven-Nielsen, T. Wodehouse, R. M. Langford, L. Arendt-Nielsen, and B. L. Kidd, "Normalization of widespread hyperesthesia and facilitated spatial summation of deep-tissue pain in knee osteoarthritis patients after knee replacement," *Arthritis & Rheumatism*, vol. 64, no. 9, pp. 2907–2916, 2012.

[5] S. Roberts, P. Genever, A. McCaskie, and C. De Bari, "Prospects of stem cell therapy in osteoarthritis," *Regenerative Medicine*, vol. 6, no. 3, pp. 351–366, 2011.

[6] B. J. de Lange-Brokaar, A. Ioan-Facsinay, E. Yusuf et al., "Association of pain in knee osteoarthritis with distinct patterns of synovitis," *Arthritis & Rheumatology*, vol. 67, no. 3, pp. 733–740, 2015.

[7] C. Bouffi, F. Djouad, M. Mathieu, D. Noël, and C. Jorgensen, "Multipotent mesenchymal stromal cells and rheumatoid arthritis: risk or benefit?," *Rheumatology*, vol. 48, no. 10, pp. 1185–1189, 2009.

[8] M. C. Kastrinaki, P. Sidiropoulos, S. Roche et al., "Functional, molecular and proteomic characterisation of bone marrow mesenchymal stem cells in rheumatoid arthritis," *Annals of the Rheumatic Diseases*, vol. 67, no. 6, pp. 741–749, 2008.

[9] J. Ringe and M. Sittinger, "Tissue engineering in the rheumatic diseases," *Arthritis Research & Therapy*, vol. 11, no. 1, p. 211, 2009.

[10] T. D. Henning, R. Gawande, A. Khurana et al., "Magnetic resonance imaging of ferumoxide-labeled mesenchymal stem cells in cartilage defects: in vitro and in vivo investigations," *Molecular Imaging*, vol. 11, no. 3, pp. 197–209, 2012.

[11] L. da Silva Meirelles, A. M. Fontes, D. T. Covas, and A. I. Caplan, "Mechanisms involved in the therapeutic properties of mesenchymal stem cells," *Cytokine & Growth Factor Reviews*, vol. 20, no. 5-6, pp. 419–427, 2009.

[12] A. M. Malfait, C. B. Little, and J. J. McDougall, "A commentary on modelling osteoarthritis pain in small animals," *Osteoarthritis and Cartilage*, vol. 21, no. 9, pp. 1316–1326, 2013.

[13] P. I. Mapp, D. R. Sagar, S. Ashraf et al., "Differences in structural and pain phenotypes in the sodium monoiodoacetate and meniscal transection models of osteoarthritis," *Osteoarthritis and Cartilage*, vol. 21, no. 9, pp. 1336–1345, 2013.

[14] T. L. Vincent, R. O. Williams, R. Maciewicz, A. Silman, and P. Garside, "Mapping pathogenesis of arthritis through small animal models," *Rheumatology*, vol. 51, no. 11, pp. 1931–1941, 2012.

[15] A. M. Suhaeb, S. Naveen, A. Mansor, and T. Kamarul, "Hyaluronic acid with or without bone marrow derived-mesenchymal stem cells improves osteoarthritic knee changes in rat model: a preliminary report," *Indian Journal of Experimental Biology*, vol. 50, no. 6, pp. 383–390, 2012.

[16] J. E. Kim, S. M. Lee, S. H. Kim et al., "Effect of self-assembled peptide–mesenchymal stem cell complex on the progression of osteoarthritis in a rat model," *International Journal of Nanomedicine*, vol. 9, Supplement 1, pp. 141–157, 2014.

[17] J. M. Murphy, D. J. Fink, E. B. Hunziker, and F. P. Barry, "Stem cell therapy in a caprine model of osteoarthritis," *Arthritis & Rheumatism*, vol. 48, no. 12, pp. 3464–3474, 2003.

[18] B. T. Estes, A. W. Wu, R. W. Storms, and F. Guilak, "Extended passaging, but not aldehyde dehydrogenase activity, increases the chondrogenic potential of human adipose-derived adult stem cells," *Journal of Cellular Physiology*, vol. 209, no. 3, pp. 987–995, 2006.

[19] A. Peister, J. A. Mellad, B. L. Larson, B. M. Hall, L. F. Gibson, and D. J. Prockop, "Adult stem cells from bone marrow (MSCs) isolated from different strains of inbred mice vary in surface epitopes, rates of proliferation, and differentiation potential," *Blood*, vol. 103, no. 5, pp. 1662–1668, 2004.

[20] H. Markides, O. Kehoe, R. H. Morris, and A. J. El Haj, "Whole body tracking of superparamagnetic iron oxide nanoparticle-labelled cells–a rheumatoid arthritis mouse model," *Stem Cell Research & Therapy*, vol. 4, no. 5, p. 126, 2013.

[21] M. Gnecchi and L. G. Melo, "Bone marrow-derived mesenchymal stem cells: isolation, expansion, characterization, viral transduction, and production of conditioned medium," *Methods in Molecular Biology*, vol. 482, pp. 281–294, 2009.

[22] S. Ashraf, P. I. Mapp, J. Burston, A. J. Bennett, V. Chapman, and D. A. Walsh, "Augmented pain behavioural responses to intra-articular injection of nerve growth factor in two animal models of osteoarthritis," *Annals of the Rheumatic Diseases*, vol. 73, no. 9, pp. 1710–1718, 2014.

[23] C. L. Christiansen and J. E. Stevens-Lapsley, "Weight-bearing asymmetry in relation to measures of impairment and functional mobility for people with knee osteoarthritis," *Archives of Physical Medicine and Rehabilitation*, vol. 91, no. 10, pp. 1524–1528, 2010.

[24] D. R. Sagar, S. Ashraf, L. Xu et al., "Osteoprotegerin reduces the development of pain behaviour and joint pathology in a model of osteoarthritis," *Annals of the Rheumatic Diseases*, vol. 73, no. 8, pp. 1558–1565, 2014.

[25] N. Gerwin, A. M. Bendele, S. Glasson, and C. S. Carlson, "The OARSI histopathology initiative–recommendations for histological assessments of osteoarthritis in the rat," *Osteoarthritis and Cartilage*, vol. 18, Supplement 3, pp. S24–S34, 2010.

[26] H. J. Mankin, H. Dorfman, L. Lippiello, and A. Zarins, "Biochemical and metabolic abnormalities in articular cartilage from osteo-arthritic human hips: II. Correlation of morphology with biochemical and metabolic data," *The Journal of Bone & Joint Surgery*, vol. 53, no. 3, pp. 523–537, 1971.

[27] G. M. van Buul, M. Siebelt, M. J. C. Leijs et al., "Mesenchymal stem cells reduce pain but not degenerative changes in a mono-iodoacetate rat model of osteoarthritis," *Journal of Orthopaedic Research*, vol. 32, no. 9, pp. 1167–1174, 2014.

[28] S. Ashraf, P. I. Mapp, and D. A. Walsh, "Contributions of angiogenesis to inflammation, joint damage, and pain in a rat model of osteoarthritis," *Arthritis and Rheumatism*, vol. 63, no. 9, pp. 2700–2710, 2011.

[29] A. N. Mokbel, O. S. el Tookhy, A. A. Shamaa, L. A. Rashed, D. Sabry, and A. M. el Sayed, "Homing and reparative effect of intra-articular injection of autologus mesenchymal stem cells in osteoarthritic animal model," *BMC Musculoskeletal Disorders*, vol. 12, no. 1, p. 259, 2011.

[30] M. ter Huurne, R. Schelbergen, R. Blattes et al., "Antiinflammatory and chondroprotective effects of intraarticular injection of adipose-derived stem cells in experimental osteoarthritis," *Arthritis & Rheumatism*, vol. 64, no. 11, pp. 3604–3613, 2012.

[31] J. J. Burston, D. R. Sagar, P. Shao et al., "Cannabinoid CB_2 receptors regulate central sensitization and pain responses associated with osteoarthritis of the knee joint," *PLoS One*, vol. 8, no. 11, article e80440, 2013.

[32] W. J. C. Rombouts and R. E. Ploemacher, "Primary murine MSC show highly efficient homing to the bone marrow but lose homing ability following culture," *Leukemia*, vol. 17, no. 1, pp. 160–170, 2003.

[33] A. Banfi, A. Muraglia, B. Dozin, M. Mastrogiacomo, R. Cancedda, and R. Quarto, "Proliferation kinetics and differentiation potential of ex vivo expanded human bone marrow stromal cells: implications for their use in cell therapy," *Experimental Hematology*, vol. 28, no. 6, pp. 707–715, 2000.

[34] I. Somasundaram, R. Mishra, H. Radhakrishnan, R. Sankaran, V. N. S. Garikipati, and D. Marappagounder, "Human adult stem cells maintain a constant phenotype profile irrespective of their origin, basal media, and long term cultures," *Stem Cells International*, vol. 2015, Article ID 146051, 29 pages, 2015.

[35] M. Bonab, K. Alimoghaddam, F. Talebian, S. Ghaffari, A. Ghavamzadeh, and B. Nikbin, "Aging of mesenchymal stem cell in vitro," *BMC Cell Biology*, vol. 7, no. 1, p. 14, 2006.

[36] T. Tondreau, L. Lagneaux, M. Dejeneffe et al., "Isolation of BM mesenchymal stem cells by plastic adhesion or negative selection: phenotype, proliferation kinetics and differentiation potential," *Cytotherapy*, vol. 6, no. 4, pp. 372–379, 2004.

[37] P. Tropel, D. Noël, N. Platet, P. Legrand, A. L. Benabid, and F. Berger, "Isolation and characterisation of mesenchymal stem cells from adult mouse bone marrow," *Experimental Cell Research*, vol. 295, no. 2, pp. 395–406, 2004.

[38] F. H. Bach, "Heme oxygenase-1: a therapeutic amplification funnel," *FASEB Journal*, vol. 19, no. 10, pp. 1216–1219, 2005.

[39] Y. Zhuang, D. Li, J. Fu, Q. Shi, Y. Lu, and X. Ju, "Comparison of biological properties of umbilical cord-derived mesenchymal stem cells from early and late passages: immunomodulatory ability is enhanced in aged cells," *Molecular Medicine Reports*, vol. 11, no. 1, pp. 166–174, 2015.

[40] M. Hajkova, E. Javorkova, A. Zajicova, P. Trosan, V. Holan, and M. Krulova, "A local application of mesenchymal stem cells and cyclosporine A attenuates immune response by a switch in macrophage phenotype," *Journal of Tissue Engineering and Regenerative Medicine*, vol. 11, no. 5, pp. 1456–1465, 2017.

[41] A. Briquet, S. Dubois, S. Bekaert, M. Dolhet, Y. Beguin, and A. Gothot, "Prolonged ex vivo culture of human bone marrow mesenchymal stem cells influences their supportive activity toward NOD/SCID-repopulating cells and committed progenitor cells of B lymphoid and myeloid lineages," *Haematologica*, vol. 95, no. 1, pp. 47–56, 2010.

[42] N. Nishimoto, "Interleukin-6 in rheumatoid arthritis," *Current Opinion in Rheumatology*, vol. 18, no. 3, pp. 277–281, 2006.

[43] T. van der Poll, C. V. Keogh, X. Guirao, W. A. Buurman, M. Kopf, and S. F. Lowry, "Interleukin-6 gene-deficient mice show impaired defense against pneumococcal pneumonia," *The Journal of Infectious Diseases*, vol. 176, no. 2, pp. 439–444, 1997.

[44] J. Chen, S. Sotome, J. Wang, H. Orii, T. Uemura, and K. Shinomiya, "Correlation of in vivo bone formation capability and in vitro differentiation of human bone marrow stromal cells," *Journal of Medical and Dental Sciences*, vol. 52, no. 1, pp. 27–34, 2005.

[45] V. Vacanti, E. Kong, G. Suzuki, K. Sato, J. M. Canty, and T. Lee, "Phenotypic changes of adult porcine mesenchymal stem cells induced by prolonged passaging in culture," *Journal of Cellular Physiology*, vol. 205, no. 2, pp. 194–201, 2005.

[46] J. U. Yoo, T. S. Barthel, K. Nishimura et al., "The chondrogenic potential of human bone-marrow-derived mesenchymal progenitor cells," *Journal of Bone & Joint Surgery*, vol. 80, no. 12, pp. 1745–1757, 1998.

[47] Z. Li, C. Liu, Z. Xie et al., "Epigenetic dysregulation in mesenchymal stem cell aging and spontaneous differentiation," *PLoS One*, vol. 6, no. 6, article e20526, 2011.

[48] A. R. Tan, E. Alegre-Aguarón, G. D. O'Connell et al., "Passage-dependent relationship between mesenchymal stem cell mobilization and chondrogenic potential," *Osteoarthritis and Cartilage*, vol. 23, no. 2, pp. 319–327, 2015.

[49] X.-H. Jing, L. Yang, X. J. Duan et al., "In vivo MR imaging tracking of magnetic iron oxide nanoparticle labeled, engineered, autologous bone marrow mesenchymal stem cells following intra-articular injection," *Joint, Bone, Spine*, vol. 75, no. 4, pp. 432–438, 2008.

[50] J. Chen, F. Wang, Y. Zhang et al., "In vivo tracking of superparamagnetic iron oxide nanoparticle labeled chondrocytes in large animal model," *Annals of Biomedical Engineering*, vol. 40, no. 12, pp. 2568–2578, 2012.

Hindawi
Stem Cells International
Volume 2017, Article ID 6319129, 10 pages
https://doi.org/10.1155/2017/6319129

Research Article

Influence of Different ECM-Like Hydrogels on Neurite Outgrowth Induced by Adipose Tissue-Derived Stem Cells

E. Oliveira,[1,2] R. C. Assunção-Silva,[1,2] O. Ziv-Polat,[3] E. D. Gomes,[1,2] F. G. Teixeira,[1,2] N. A. Silva,[1,2] A. Shahar,[3] and A. J. Salgado[1,2]

[1]*Life and Health Sciences Research Institute (ICVS), School of Medicine, University of Minho, Campus de Gualtar, 4710-057 Braga, Portugal*
[2]*ICVS/3B's-PT Government Associate Laboratory, Braga, Guimarães, Portugal*
[3]*NVR Research Ltd., Ness-Ziona, Israel*

Correspondence should be addressed to A. J. Salgado; asalgado@med.uminho.pt

Received 5 June 2017; Revised 22 August 2017; Accepted 18 September 2017; Published 3 December 2017

Academic Editor: Víctor Carriel

Copyright © 2017 E. Oliveira et al. This is an open access article distributed under the Creative Commons Attribution License, which permits unrestricted use, distribution, and reproduction in any medium, provided the original work is properly cited.

Mesenchymal stem cells (MSCs) have been proposed for spinal cord injury (SCI) applications due to their capacity to secrete growth factors and vesicles—secretome—that impacts important phenomena in SCI regeneration. To improve MSC survival into SCI sites, hydrogels have been used as transplantation vehicles. Herein, we hypothesized if different hydrogels could interact differently with adipose tissue-derived MSCs (ASCs). The efficacy of three natural hydrogels, gellan gum (functionalized with a fibronectin peptide), collagen, and a hydrogel rich in laminin epitopes (NVR-gel) in promoting neuritogenesis (alone and cocultured with ASCs), was evaluated in the present study. Their impact on ASC survival, metabolic activity, and gene expression was also evaluated. Our results indicated that all hydrogels supported ASC survival and viability, being this more evident for the functionalized GG hydrogels. Moreover, the presence of different ECM-derived biological cues within the hydrogels appears to differently affect the mRNA levels of growth factors involved in neuronal survival, differentiation, and axonal outgrowth. All the hydrogel-based systems supported axonal growth mediated by ASCs, but this effect was more robust in functionalized GG. The data herein presented highlights the importance of biological cues within hydrogel-based biomaterials as possible modulators of ASC secretome and its effects for SCI applications.

1. Introduction

The current care of SCI patients is mostly palliative. Thus, it is extremely important to develop new strategies that support both structural and functional restoration of the damaged or lost tissue. For this purpose, tissue engineering approaches, using biomaterials, stem cells, and often neurotrophic factors, are being extensively explored [1]. Biomaterials, particularly hydrogels, are interesting for SCI approaches mainly due to their physical properties that resemble central nervous system (CNS) soft tissues. Moreover, their porous structure allows molecule diffusion and the possibility to establish a three-dimensional (3D) environment that mimics the living tissues. These biomaterials are widely used to support cell transplantation [2]. For this purpose, natural hydrogels are an interesting tool, as they are mostly constituted by extracellular matrix (ECM) molecules or can be easily functionalized with them [3]. Among the variety of available natural hydrogels, this study will focus on the use of gellan gum, NVR-gel, and collagen as matrices for cell encapsulation. Gellan gum (GG), a linear anionic polysaccharide with a free carboxylic group per repeating units, was already reported to be biocompatible and nontoxic after injection in a hemisection SCI rat model [4]. Moreover, it was also shown to be suitable for functionalization, as its modification with a fibronectin-derived peptide (GRGDS) promoted higher cell adhesion and viability in comparison to unmodified GG [5]. Regarding NVR-gel, this is a biocompatible and biodegradable scaffold composed of hyaluronic acid (HA) and laminin [6]. While HA has a vital role in cell morphogenesis and proliferation [7], laminin provides an adhesive and growth-promoting substrate [6]. In fact, this

gel was shown to be an excellent 3D milieu for the growth of neuronal tissue in culture [6]. Finally, collagen has been reported as the main constituent of almost all ECMs. Together with its biocompatibility, collagen enables to form adhesive and permissive substrates for cell survival and neurite outgrowth [8]. This is supported by studies where, for example, neural stem/progenitor cells (NPCs) cultured on type I collagen hydrogel were found to develop functional synapses and form neuronal networks [9]. On the other hand, the use of stem cell-based therapies in SCI regenerative strategies has also shown interesting results. Within the different cell populations available, MSCs have been put forward as a possible choice [10, 11]. The most relevant feature of these cells is the active secretion of bioactive molecules (e.g., growth factors, cytokines, and exosomes), nowadays known as secretome. Indeed, studies have already demonstrated that after transplantation of MSCs (from different sources) on SCI models, neurotrophic factors such as brain-derived neurotrophic factor (BDNF), vascular endothelial factor (VEGF), interleukin-6 (IL-6), neurotrophin 3 (NT-3), basic fibroblast growth factor (bGFG), stem cell factor (SCF), hepatocyte growth factor (HGF), and glial cell line-derived neurotrophic factor (GDNF) were secreted, which was correlated with prominent increase of axonal regeneration and functional outcomes [3, 12, 13]. Despite these encouraging results, MSC transplantation still faces the problem of poor cell engraftment and survival in the lesion site [3]. Under this context, ECM-like hydrogels such as GG, NVR, and collagen could play a crucial role in overcoming these limitations. Indeed, by using these systems, it would be possible to extend cell survival within the injured site, as well as to modulate their behavior through the cues presented by the different cell adhesion peptides to MSCs. Having this in mind, in the present work, we aimed to evaluate the efficacy of the three referred natural hydrogels, namely, GG (functionalized with a fibronectin peptide), collagen, and NVR-gel in supporting the viability, metabolic activity, and gene expression of MSCs isolated from the adipose tissue 1 (adipose tissue-derived stem cells (ASCs)). Moreover, the effects of these hydrogels as modulators of ASC impact on axonal growth will be also addressed using dorsal root ganglion (DRG) explant cultures.

2. Materials and Methods

2.1. Adipose-Derived Stem Cell (ASC) Culture. Human ASCs (female, 25 years old, BMI = 27.8) were kindly provided by Professor Jeffrey Gimble (Tulane University Center for Stem Cell Research and Regenerative Medicine and LabCell LLC, New Orleans, Louisiana, USA) and cultured in α-MEM (Invitrogen, USA) medium [supplemented with sodium bicarbonate ($NaHCO^3$, Merck, USA), 10% of fetal bovine serum (FBS) (Biochrom AG, Germany), and 1% of penicillin-streptomycin antibiotic (Invitrogen, USA)] at 37°C and 5% CO^2. ASCs used and disclosed the following marker phenotypes: CD29: 93.63%; CD105: 97.09%; CD44: 87.50%; CD73: 92.86%; CD90: 88.99%; CD45: 2.11%; and CD34: 7.60%.

2.2. Hydrogel Preparation

2.2.1. Gellan Gum. Gellan gum (GG, Sigma, USA) was modified with the fibronectin-derived peptide (GRGDS) as previously described [3]. First, GG was dissolved in 2-(N-morpholino)ethanesulfonic acid (MES) buffer (100 mM, pH 5.5, Sigma, USA) and stirred for 48 h at 37°C. 4-(4,6-Dimethoxy-1,3,5-triazin-2-yl)-4-methylmorpholinium chloride (DMT-MM, Sigma, USA) and furfurylamine (Acros Organics, Belgium) were then added in a 4 : 1 M ratio (of each reagent relative to the eCOOH groups in gellan gum) and stirred at 37°C for 48 h. The solution was then dialyzed (Mw cutoff 12–14 kDa, Spectrum Labs, USA) alternately with distilled water and PBS (0.1 M, pH 7.2) for 5 days. After lyophilization, furan-modified GG (furan-GG) was obtained as a white powder.

The immobilization of GRGDS peptide (AnsSpect, USA), previously modified with a maleimide group (mal-GRGDS), into the furan-GG was performed by Diels-Alder chemistry, originating the GG-GRGDS. For that, furan-GG was dissolved in MES buffer (100 mM, pH 5.5) at 37°C (1.2 mg/ml). The mal-GRGDS was then added to furan-GG in a 5 : 1 maleimide : furan molar ratio and stirred at 37°C for 48 h. The mixture was dialyzed (Mw cutoff 12–14 kDa) for 5 days as described above. The water was then removed by lyophilization and GG-GRGDS was obtained as a white powder.

2.2.2. NVR-Gel. NVR-gel (NVR Labs, Israel) is mainly composed of two components: hyaluronic acid (HA, 3×10^3 KDa, BTG Polymers, Israel) and laminin (Sigma, USA). To prepare this hydrogel, HA 1% (*w*/*v*) and laminin were diluted in cell culture medium, at a concentration of 0.3% (*v*/*v*). The solution was then thoroughly mixed to obtain a liquid viscous hydrogel.

2.2.3. Collagen. Collagen gels were prepared as described by Allodi et al. [14]. Briefly, gels were prepared by mixing 450 μl of collagen type I (BD Biosciences, USA), 50 μl of Dulbecco's modified Eagle medium 10× (DMEM 10×, Sigma, USA), and 2 μl of 7.5% $NaHCO^3$ solution. Then, hydrogels were kept in the incubator for 2 h at 37°C and 5% CO^2 to allow the gelification process to occur.

2.3. Hydrogel Preparation and ASC Encapsulation

2.3.1. Gellan Gum. Prior to ASC encapsulation, the lyophilized GG-GRGDS was sterilized by UV light for 15 min. Then, GG-GRGDS was dissolved in ultrapure water at 1% (*w*/*v*) concentration and placed to stir at 40°C overnight. Next day, GG was dissolved in ultrapure water at 1% *w*/*v* concentration, placed to stir at 90°C for 30 min, and then sterilized by filtration. GG-GRGDS and GG were then mixed together in a 50 : 50 proportion. Just before cell encapsulation, calcium chloride [$CaCl^2$; 0.3% (*w*/*v*)] was added to the GG-GRGDS/GG mixture in a proportion of 1 : 10, to promote the ionic crosslinking of the hydrogel.

ASCs were obtained as previously described. Cells were encapsulated within the hydrogel by gently mixing the cell pellet with the desired volume of gel, at a concentration of 6×10^5 cells/ml until a homogeneous solution was obtained.

Table 1: PCR primers used to detect gene expression in ASCs, upon seeding in the three hydrogels.

Gene	Primer sequence	Amplicon length
HMBS	Forward 5′-CCTGGCCCACAGCATACAT-3′ Reverse 5′-TCGGGGAAACCTCAACACC-3′	155 bp
GDNF	Forward 5′-AGCCGCTGCAGTACCTAAAA-3′ Reverse 5′-CCAACCCAGAGAATTCCAGA-3′	150 bp
VEGF	Forward 5′-TTTCTTGCGCTTTCGTTTTT-3′ Reverse 5′-AGGCCAGCACATAGGAGAGA-3′	133 bp
NGF	Forward 5′-GTCTGTGGCGGTGGTCTTAT-3′ Reverse 5′-CAACAGGACTCACAGGAGCA-3′	115 bp
BDNF	Forward 5′-AGAAGAGGAGGCTCCAAAGG-3′ Reverse 5′-TGGCTGACACTTTCGAACAC-3′	145 bp

The hydrogel containing the cells was placed on cell culture wells in drops of 50 μl per chamber/well and cultured from 4 to 7 days.

2.3.2. NVR-Gel. After mixing the hydrogel with cell culture medium, a liquid viscous gel was obtained. The desired volume of hydrogel was added to the cells' pellet at a concentration of 6×10^5 cells/ml and mixed to uniformly distribute the cells. Then, 250 μl of the gel containing the ASCs was added to cell culture wells and kept in culture for 4 and 7 days.

2.3.3. Collagen. After collagen hydrogel gelification, the cell pellet was resuspended with the desired volume of hydrogel at a concentration of 6×10^5 cells/ml. The hydrogel containing the cells was placed on cell culture wells in 50 μl drops and placed in the incubator for 1.5 h at 37°C and 5% CO2 for the gelification process to occur. Cell culture medium was then added to the wells and kept in culture for 4 and 7 days.

2.4. MTS. The MTS assay relies on the reduction of the tetrazolium compound 3-(4,5-dimethylthiazol-2-yl)-5-(3-carboxymethoxyphenyl)-2-(4-sulfophenyl)-2H-tetrazolium (MTS, Promega, USA) to formazan by viable cells. After 7 days of culture, the cell culture medium was replaced by serum-free medium (DMEM, Invitrogen, USA), containing MTS in a 5 : 1 ratio and incubated for 3 hours at 37°C and 5% CO^2. For sample analysis, triplicates of each sample were placed in wells of a 96-well plate, allowing the optic density to be measured by spectrometry (at 490 nm) in a microplate reader.

2.5. Quantitative Real-Time PCR. After ASC encapsulation and culture on different hydrogels, a RT-PCR was performed to analyze the expression levels of specific genes involved in axonal growth, namely, BDNF, VEGF, NGF, and GDNF.

2.5.1. RNA Extraction. After 7 days of cell culture, the total RNA from ASCs encapsulated in the hydrogels was extracted. For that, 6 gels were combined to obtain a more reliable sample. Initially, 1 ml of Trizol solution (Life Technologies, USA) was added to the hydrogels containing the cells, and after a mechanical dissociation of the gels, a cell pellet was obtained. The samples were then collected in Eppendorf tubes. The cells' pellet was then incubated with chloroform (Sigma, USA) for 3 min at room temperature (RT) and centrifuged at 8000 rpm for 15 min, at 4°C. After this, the presence of three layers in the Eppendorf tube was possible to observe: an aqueous phase on top, an interphase, and an organic phase in the bottom. The aqueous phase, containing the RNA, was transferred into new Eppendorf tubes and precipitated by adding isopropanol (Carlos Erba Reagents, France). The samples were then left to rest for 10 min at RT. Afterwards, the samples were centrifuged (9000 rpm, 15 min, 4°C), the RNA pellets were washed with 75% ethanol and centrifuged again (5000 rpm, 5 min, 4°C). Then, the pellets were dissolved in nuclease-free water and the RNA quantification was performed using Nanodrop ND-1000 spectrophotometer (Alfagene, Portugal), to adjust the sample concentration to 500 ng/μl.

2.5.2. cDNA Transformation and Quantitative Real-Time PCR. The synthesis of the cDNA was performed using iScriptTM cDNA Synthesis Kit (BioRad, USA). First, 1 μg of purified RNA was used as a template and the volumes were normalized with nuclease-free water. A reaction mix containing the RNA sample, 5× iScript reaction mix, and iScript reverse transcriptase was prepared and added to the samples. Periods of sample incubation of 5 min at 25°C followed by 30 min at 42°C and 5 min at 85°C in a thermal cycler (Applied Biosystems, USA) were performed. To proceed with the quantitative gene expression analysis, the cDNA was subject to PCR amplification using Eva Green technology (Ssofast Evagreen Supermix, BioRad, USA) on the CFX96 Real-Time system (BioRad, USA).

Finally, a reaction solution was prepared by mixing 5 μl of Ssofast Evagreen Supermix, 10 μM of the primer respective to each tested gene, in forward and reverse, and 1 μl of cDNA. After adding the reaction solution to the template, specific cycling conditions were applied to samples, such as 30 s at 95°C of enzyme activation, followed by 40 cycles of 5 s at 95°C for denaturation, 5 s at 60°C for annealing, and 5 s at 72°C for extension step. The HMBS gene (XM_017017629.1) was the house-keeping gene herein used, and the tested genes were the BDNF (NG_011794.1), VEGF (AY500353.1), NGF (NG_007944.1), and GDNF (NG_011675.2), as described in Table 1.

2.6. DRG Coculture with ASCs in 3D Hydrogel-Based Environment. As previously described, ASCs were encapsulated within the hydrogels at a concentration of 6×10^5 cells/ml. Four replicates of 50 μl of each hydrogel were maintained in complete α-MEM for 24 hours, to let cells grow within the gel. After this time, DRGs from P5 Wistar-Han rat pups were dissected as previously described [15] and placed on top of the ASC-containing hydrogels. Cultures were kept for 7 days in neuron medium (Invitrogen, USA; neurobasal medium supplemented with B27, L-glutamine, glucose, and pen-strep). DRG culture on top of hydrogels without cells was used as control.

2.7. Immunocytochemistry and Phalloidin/DAPI Staining. After 4 and 7 days of cell culture, ASC and DRG cultures were prepared for phalloidin/DAPI staining and immunocytochemistry (ICC), respectively.

For ASC staining, phalloidin (Sigma, USA) was used to stain the F-actin filaments within the cells' cytoskeleton, while DAPI (Invitrogen, USA) was used to mark the cells' nucleus. Samples were fixed with 4% (*v*/*v*) paraformaldehyde (PFA) for 45 min at RT. After washing with PBS 1×, phalloidin (0.1 μg/ml; Sigma), associated with Alexa-Fluor 594, and DAPI (1 μg/ml; Invitrogen) were added to cell for 45 min at RT.

For ICC, an antibody for neurofilament (NF) was used to stain the intermediate filaments of DRG neurons. For that, the following antibodies were used: the mouse monoclonal anti-rat neurofilament 200 kDa (Millipore, USA) as the primary antibody and the Alexa fluor 488 goat anti-mouse IgG (H + L) (Invitrogen, USA) as the secondary antibody. Samples were fixed with 4% (*v*/*v*) PFA for 45 min at RT. For cell membrane permeabilization, samples were incubated with 0.3% Triton X-100 (Sigma, USA) for 10 min at RT and washed 3 times with PBS 1×. Samples were then incubated with a blocking buffer solution [PBS 1× containing 10% FBS] for 90 min at RT. Finally, samples were incubated with the primary antibody for 48 h at 4°C. After washing three times with PBS 1×, samples were incubated with the secondary antibody overnight at 4°C.

2.8. Quantification of Cell Densities and Axonal Growth. For cell density measurement and morphology analysis, ASC-containing hydrogels were imaged by confocal point-scanning microscopy (Olympus FV1000). The number of cells present in the hydrogels was inferred by counting the number of $DAPI^+$ cells in six regions taken at random in each gel sample, using the cell counter plugin of the ImageJ software.

For DRG axonal growth quantification, DRG cultures on top of the hydrogels were imaged by fluorescence microscopy (Olympus BX-61 Fluorescence Microscope, Olympus, Germany). Axonal growth was inferred by quantifying the area occupied by the neurites within the hydrogels. For that, three representative micrographs of each sample were taken and later analyzed using ImageJ software. The image scale was first set and converted to 8 bit and binary, which will convert the green fluorescence (neurofilament staining) into a black image with a white background. The body of the DRG was then excluded. Thereafter, through the "analyze particles" program's setting, the area occupied by the neurites was automatically calculated considering the image dark background as contrast.

2.9. Statistical Analysis. All statistical analyses were performed using GraphPad Prism (version 5.0; GraphPad Software, USA). Differences among groups were assessed using *t*-test or one way ANOVA test, followed by a Turkey post hoc. A p value of ≤ 0.05 (95% confidence level) was set as the criteria for statistical significance (*).

3. Results

3.1. ASC Survival and Metabolic Activity in the Three Matrices. In order to assess whether the GG-GRGDS, NVR-gel, and collagen have the capacity to promote ASC survival, viability, and proliferation, cells were encapsulated on the three hydrogels at a cell density of 6×10^5 cells/ml and cultured for 7 days in serum-containing α-MEM. 2D cultures were used as control. At the end of cell culture, phalloidin/DAPI staining was performed.

All hydrogels were found to support ASC survival and proliferation, as observed in Figures 1(a), 1(b), 1(c), and 1(d). ASCs disclose their typical spindle-like shape morphology. Nevertheless, cell behavior was different within each matrix, as the number of cells ($DAPI^+$ cells) in the three hydrogels and control was significantly different (Figure 1(e)).

In addition, a MTS assay was performed to assess the metabolic activity of ASCs in the three hydrogels. Results were presented as cell density/metabolic activity ratio (Figure 1(f)). The cells within the GG-GRGDS gels had a significantly higher metabolic activity when compared to 2D cultures, and NVR-gel, and collagen.

3.2. Pilot Screening on the Effects of GG-GRGDS, NVR-Gel, and Collagen on the Gene Expression of Neurotrophic Factors. ASC gene expression on some neurotrophic factors relevant for axonal growth—BDNF, VEGF, NGF, and GDNF—was analyzed using quantitative real-time PCR in cells that were encapsulated on the different hydrogels.

No statistical differences were observed among gene expression of ASCs in the different hydrogels for all the tested growth factors, as denoted in Figure 2. Nevertheless, BDNF and VEGF (Figures 1(a) and 1(b), resp.) appear to have a higher expression in ASCs cultured in collagen gels, which contrasts with lower expression profiles in GG-GRGDS and NVR-gel. In turn, NGF and GDNF mRNA levels (Figures 1(c) and 1(d), resp.) tends to be higher and very similar in these hydrogels, when compared to collagen.

3.3. Impact of ASCs on Axonal Growth: Role of ECM-Like Hydrogels. A DRG *in vitro* model of neurite/axonal growth was used to evaluate the impact of ASCs encapsulated on the different gels. For this purpose, ASCs were firstly encapsulated on the different gels, and DRGs were placed on top of it. After 7 days of culture in neuron medium, neurofilament staining was performed and DRG axonal growth was quantified as previously described. The above-referred conditions are represented in Figures 3 and 4.

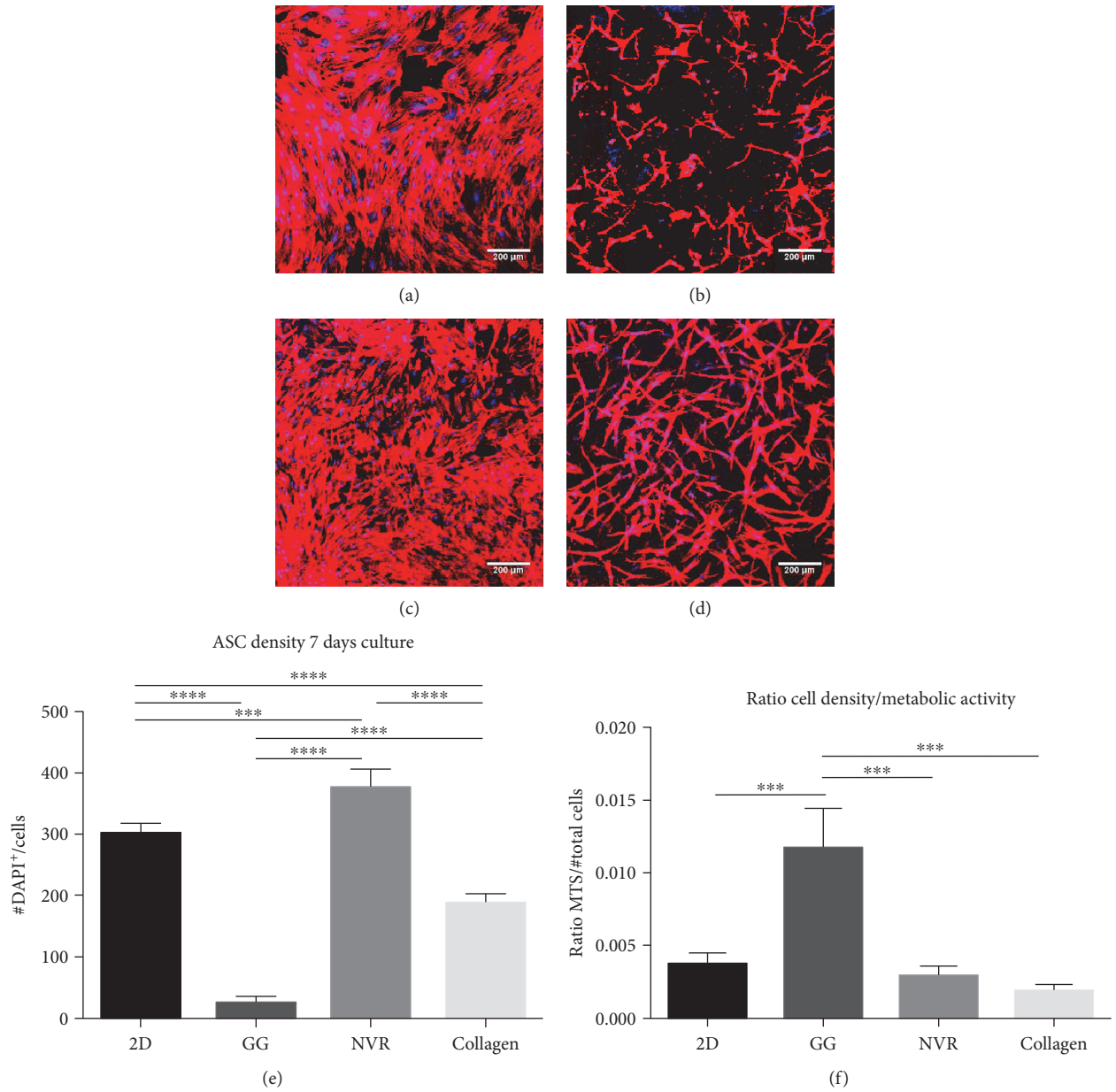

Figure 1: ASC encapsulation within the three matrices. ASC morphology was analyzed in (a) 2D cultures, (b) GG-GRGDS, (c) NVR-gel, and (d) collagen. Moreover, (e) cell density and (f) the ratio cell density/metabolic activity were also assessed in serum-containing α-MEM. Immunostaining for phalloidin (red) and DAPI (blue). Mean ± SD; $n = 4$ per condition; $p < 0.05$. Scale bar: 200 μm.

Upon quantification, DRG axonal growth was found to be promoted either by gel alone (GG: 53925.1 ± 33506.3; NVR: 996721 ± 706734; collagen: 813013 ± 301688) (Figures 4(a), 4(b), and 4(c)) and by gels plus cells (GG: 524567 ± 14206.1; NVR: $1.19 \times 10^6 \pm 631584$; collagen: $1.23 \times 10^6 \pm 648435$) (Figures 4(a), 4(b), and 4(c)). Even though GRGDS by itself was not able to promote high levels of neurite outgrowth, the addition of ASCs had a significant impact on its effect. Upon normalization against the respective controls, denoted in Figure 4(c), ASC-containing GG-GRGDS hydrogels were found to promote a robust and significant improvement of axonal growth (972.77 ± 26.34), while NVR and collagen shifts were marginal (119.72 ± 63.36; 151.52 ± 79.76, resp.).

These results suggest GG-GRGDS to be the most favorable for ASCs in the promotion of axonal growth by these cells.

4. Discussion

As previously stated, MSC transplantation is a promising therapy to tackle the complex and diversified events that occur in SCI, mainly due to their immunomodulatory capacity with prosurvival character and regenerative potential proven to be related with their secretome [11, 13, 16, 17]. However, the engraftment rate of transplanted cells in the lesion site is lower than the required to induce a regenerative

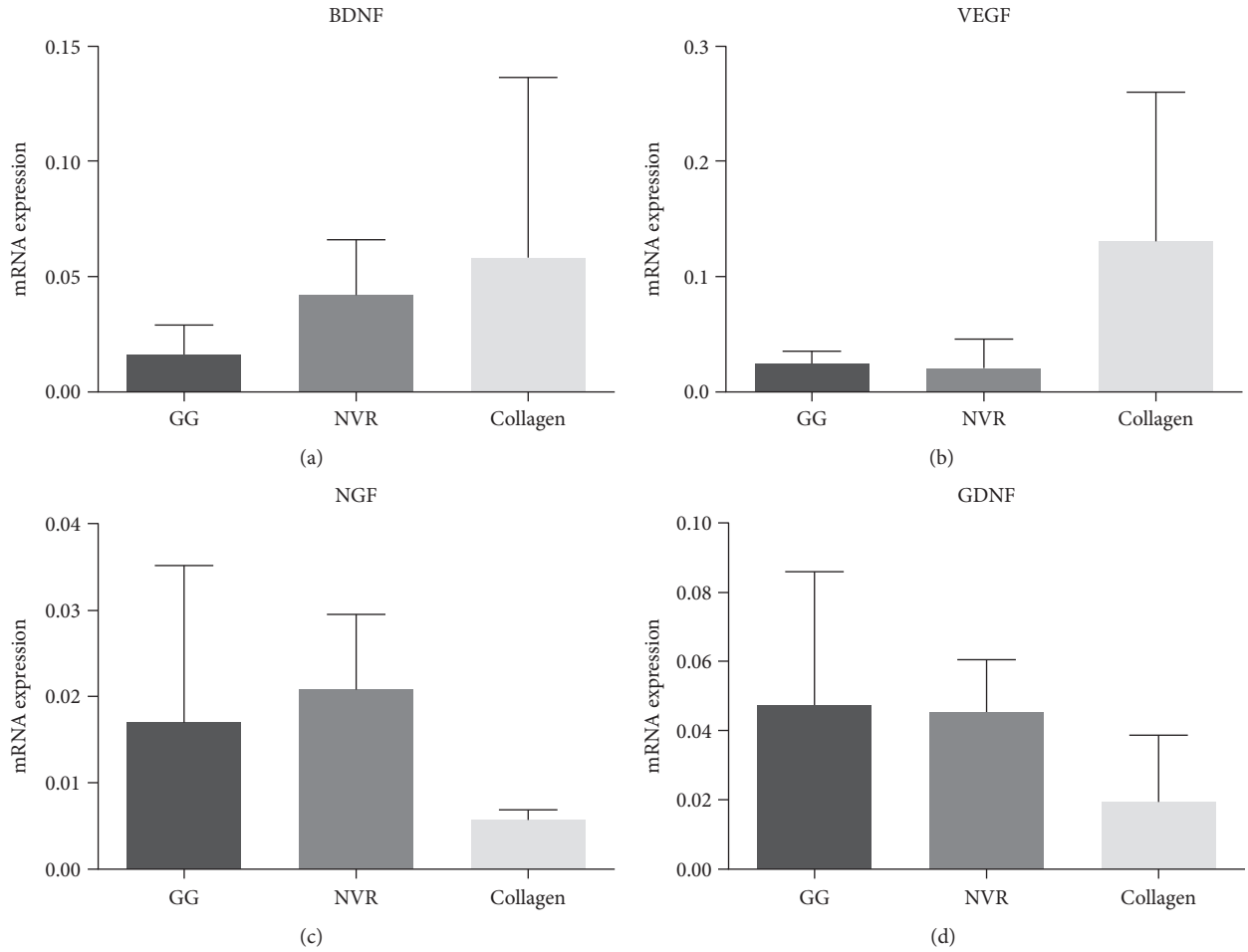

Figure 2: mRNA levels of BDNF, VEGF, NGF, and GDNF expression in ASCs cultured in GG-GRGDS, NVR-gel, and collagen after 7 days of cell culture. HMBS was the house-keeping gene herein used. Mean ± SD; $n = 3$.

response [18]. For that reason, hydrogels have been proposed as a substrate that promotes cell survival and proliferation and allows a constant secretion of molecules from MSCs in a local manner, thus dodging the need of repeated administrations [1].

In this study, we intended to test three different matrices—GG-GRGDS, NVR-gel, and collagen—as vehicles for ASCs. After encapsulating the cells in these hydrogels, all of them were found to support ASC survival, viability, and proliferation. As shown in Figures 1(a), 1(b), 1(c), and 1(d), ASCs were able to adhere to the 3D matrices, extending their processes and presenting their typical spindle-like shape morphology. Nevertheless, cells behave differently within each matrix, as can be inferred by differences observed in cell density after 7 days in culture (Figure 1(e)). In fact, the NVR-gel presented a statistically significant higher cell density when compared to 2D control and GG-GRGDS. Collagen follows NVR-gel, and the lowest cell density was observed for GG-GRGDS, all presenting statistical differences between them. The discrepancies observed in these results highlight the role of the ECM on cell adhesion, survival, and proliferation, besides demonstrating cell-type affinity to different ECM molecules. For example, the NVR-gel ability to promote higher cell proliferation is likely to be caused by the presence of the adhesion molecule laminin. In addition, this can also be triggered by the HA present in hydrogel's composition, which has high affinity to the cell surface receptor CD44 [19], documented to be present in MSCs [20]. In fact, Zhu et al. [21] evaluated the CD44-HA interaction in rat MSC migration and discovered that upon PDGF stimulation, CD44 expression in MSC was increased. Moreover, cell adhesion and migration was indeed proved to be dependent on that interaction.

As one of the main constituents of ECM, collagen is crucial for cell-cell and cell-ECM signaling and adhesion. Importantly, cell recognition of these ECM molecules is crucial for them to attach, survive, and proliferate. Therefore, this could explain why cells had easily proliferated in the collagen-based hydrogels. This is in accordance with a report that screened several proteins to uncover which molecules allowed a preferential binding of MSCs and the ones that avoided a strong adherence of fibroblasts. The results showed that MSCs bind with a higher efficiency to collagens (I, III, and IV) and laminin-111, when compared to fibroblasts. Moreover, the same study showed that both cell types bind with equally high efficiency to fibronectin. With this in mind, one can conclude that the presence of fibronectin peptides on the GG may justify the adherence,

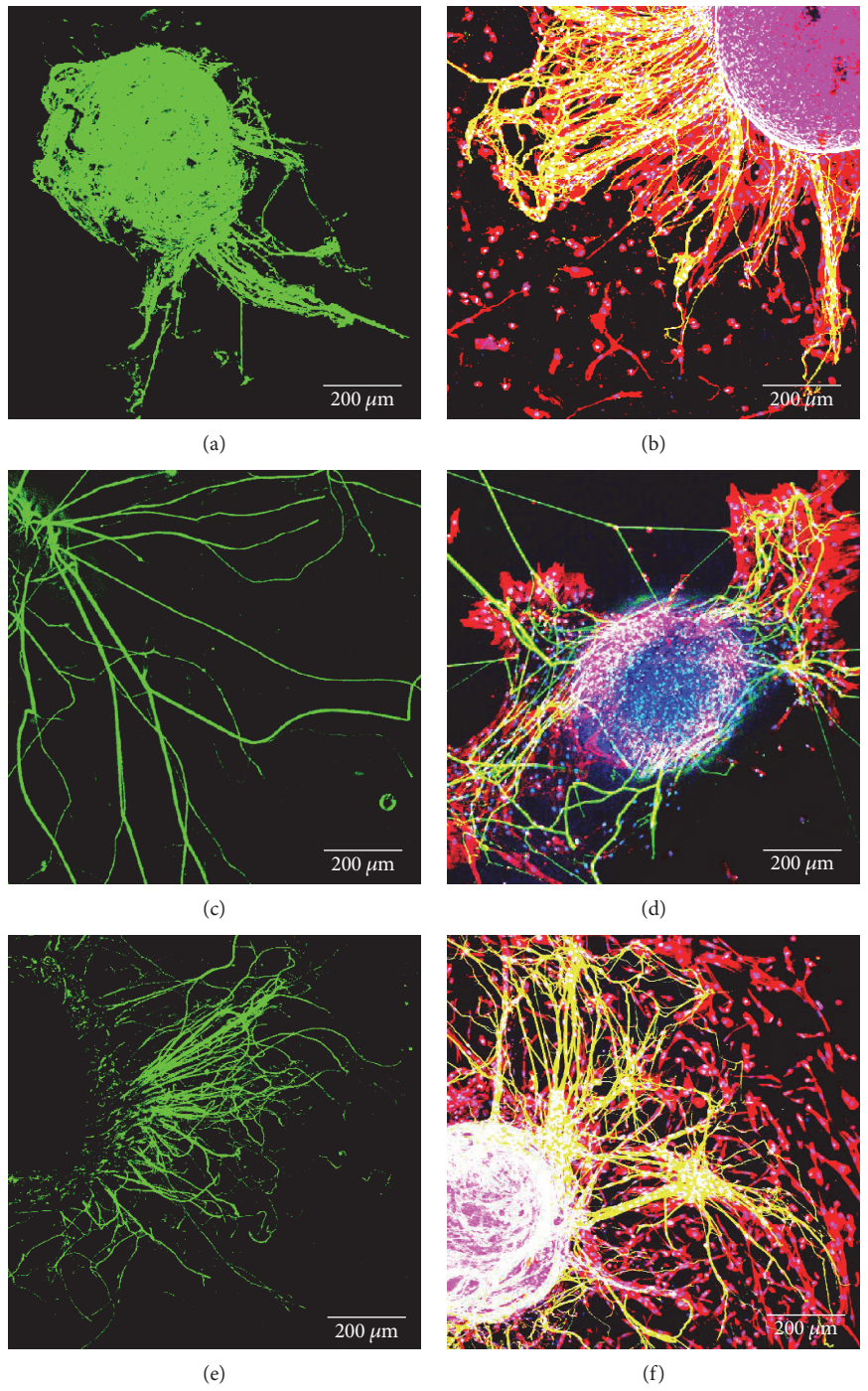

Figure 3: Coculture of ASC and DRG explants in serum-free conditions on GRGDS-GG (b), NVR-gel (d), and collagen (f). DRG monoculture on GG (a), NVR-gel (c), and collagen (e) was used as control. Immunostaining for neurofilament (green), phalloidin (red), and DAPI (blue). Scale bar: 200 μm.

survival, and typical morphology of the ASCs on this matrix. This was indeed observed in a study performed by Silva et al. [3], where encapsulated BM-MSCs in a GRGDS-modified GG revealed higher cell proliferation and metabolic activity than unmodified gels. Moreover, cell secretome was also positively influenced by the presence of the peptide, as BM-MSCs seeded in GG-GRGDS induced a higher metabolic viability and neuronal density of primary cultures of hippocampal neurons than those seeded in the regular GG. The reason why this hydrogel presented the lowest response of ASCs from the three tested hydrogels might be owed to the peptide concentration on the hydrogel, which may perhaps be lower than the necessary to attain the desired effect. In fact, as described by Silva et al. [3], the engraftment success for this molecule into the backbone of GG is around 30–35%, meaning that the GG-

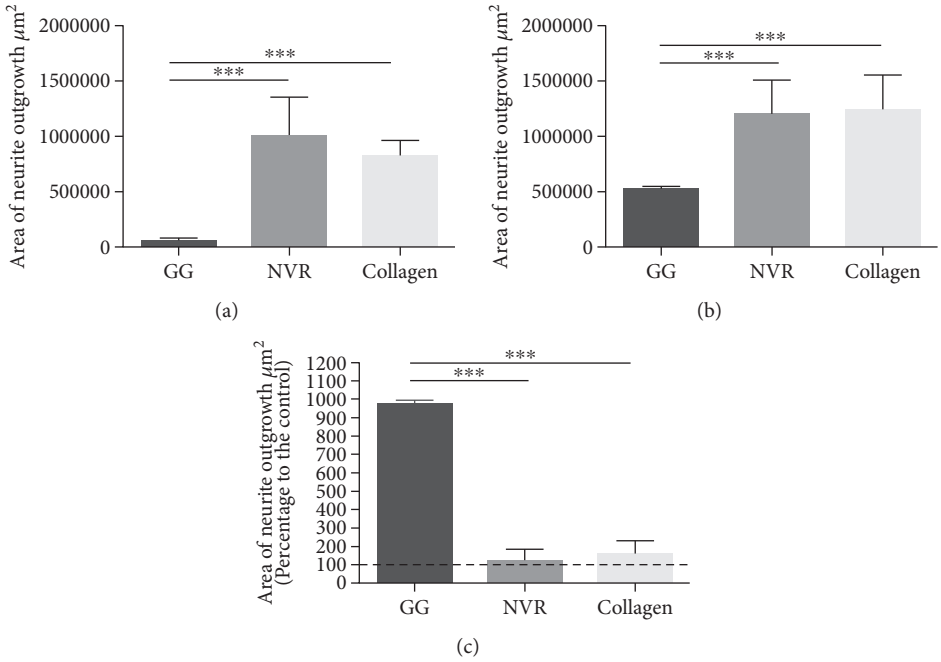

Figure 4: Quantification of the neurite outgrowth promoted by (a) hydrogels alone, (b) hydrogels plus ASCs, and (c) hydrogels plus ASCs regarding the respective controls. The mean area occupied by neurites (μm^2) was calculated using Neurite J plugin for ImageJ (NIH) software. Results presented as mean ± SD; $n = 4$ per condition.

GRGD hydrogel had decreased the levels of cell adhesion motifs when compared to collagen and NVR hydrogels.

Along with cell density measurements, the metabolic activity of ASCs in the three hydrogels was also observed to differ (Figure 1(f)). Interestingly, although GG-GRGDS presented the lowest cell density, the surviving cells had a significantly higher metabolic activity when compared with the remaining hydrogels and control. This is similar to the results obtained in the abovementioned study of Silva et al., as the presence of this peptide allowed BM-MSCs to survive within this modified GG hydrogel [3]. Regarding NVR-gel and collagen, ASC metabolic activity was very similar to control, suggesting no adverse effects of these hydrogels on ASCs. Nevertheless, the results obtained with the GG-GRGDS are of note. Altogether, these results indicate that the presence of different ECM molecules may exert varying responses on cellular functions by the same cell population. Moreover, they also show how ECM incorporation on scaffolds provides a higher cell response, which is advantageous for regenerative strategies using cell- and biomaterial-based therapies.

The observation that different hydrogels/ECM molecules influenced differently ASCs' viability and metabolic activity leads to question whether their gene expression on some neurotrophic factors relevant for axonal growth could also be different. For that reason, ASC mRNA levels of BDNF, VEGF, NGF, and GDNF were measured. BDNF, GDNF, and NGF belong to the neurotrophin family, which has an important role in neuronal survival and/or protection and axonal growth [22]. Some studies report BDNF to support motor and sensory neuron survival (neuroprotective effects) besides promoting the regeneration of axons in sensory and motor neurons [23]. On the other hand, it is known that GDNF enhances the survival and outgrowth of both motor and sensory neurons [6] as well as stimulates axon sparing and regeneration [24]. NGF is neuroprotective and promotes neurite outgrowth of sensory and sympathetic neurons *in vitro* and *in vivo* [25]. Finally, VEGF is a factor known to promote angiogenesis but recent proofs indicate that this factor has a neurotrophic and neuroprotective effect besides stimulating axonal outgrowth [26]. In line with the previous studies herein performed, ASCs' gene expression seems to differ in each matrix (Figure 2), although no statistical differences were observed. However, it is of note that the outcome of the gene expression analysis should not be directly assumed to the presence of the protein itself. So, further studies comprising protein analysis should be performed to confirm these results.

Altogether, the data obtained on hydrogels' effect on ASC behavior indicate that a modulation of the secretome by the different matrices may be occurring and that ASCs adapt their behavior according to the surrounding environment and to the presence of biological cues. According to the results obtained, it was possible to observe that GG by itself is not able to promote DRG neurite outgrowth, while NVR and collagen promote a 15-fold increase of axonal growth in comparison to GG (Figure 4(a)). Interestingly, when ASCs are present in the 3D system (Figure 4(b)), NVR and collagen present an increase on DRG neurite outgrowth of only 0.2× and 0.5×, respectively, in comparison to the growth observed in these gels alone. On the other hand, a significant 10-fold increase was observed on GG hydrogels in the presence of ASCs. The normalization of the growth of axons on the hydrogels containing ASCs to the respective controls enables a clear interpretation of these results. The potentiation of

neurite outgrowth by ASCs on GG can be explained by the higher level of cells' metabolic activity found within this hydrogel (Figure 1(f)). Consequently, cells might be able to secrete factors and molecules that help to compensate the initial difference observed between the three hydrogels. Altogether, these results point-out the GRGDS-GG matrix as the one to which ASCs adapt better and that potentiates their effects towards the promotion of axonal growth.

5. Conclusions

Spinal cord injury remains a physical, psychological, and economic problem, lacking regenerative therapies that translate into a complete and functional recovery of the patients. Numerous strategies have arisen for the treatment of SCI, but single therapy approaches were shown to be insufficient in successfully repairing the injured SC. For that reason, a combinatorial approach that acts in a synergistic arrangement can help overcome this problem, as it can enhance or avoid the limitations of the individual techniques. This work demonstrated that the use of hydrogels supports both the axonal growth and the ASC viability. The results from this study also revealed the importance of having biological cues, such as ECM molecules, to promote a more effective and pronounced effect on both the ASC and DRG cultures. Moreover, it appears that the ASCs vary their gene expression depending on the biological cues present on the hydrogels and that cells modulate their behaviour accordingly. A deeper understanding of the different interactions might give new insights for tissue engineering approaches and perhaps getting one step closer to a successful and functional recovery from SCI.

Conflicts of Interest

The authors declare that they have no conflicts of interest.

Authors' Contributions

E. Oliveira and R. C. Assunção-Silva contributed equally to this work.

Acknowledgments

This study is funded by *Prémios Santa Casa Neurociências*—Prize Melo e Castro for Spinal Cord Injury Research. This is also partially funded by EU-FP7-Health-2011-Collaborative Project 278612, Biohybrid—Templates for peripheral nerve regeneration, and Portuguese Foundation for Science and Technology (IF Development Grant to A. J. Salgado; postdoctoral fellowship to N. A. Silva—SFRH/BPD/97701/2013; PhD fellowships of R. C. Assunção-Silva and E. D. Gomes—PDE/BDE/113596/2015 and SFRH/BD/103075/2014, resp.). This article is a result of the project (NORTE-01-0145-FEDER-000013) supported by the Norte Portugal Regional Operational Programme (NORTE 2020), under the Portugal 2020 Partnership Agreement, through the European Regional Development Fund (ERDF); *Cofinanciado pelo ProgramaOperacional Regional do Norte(ON.2 SR&TD Integrated Program—NORTE-07-0124-FEDER-000021), ao abrigo do Quadro de Referência Estratégico Nacional (QREN), através do Fundo Europeude Desenvolvimento Regional (FEDER);* Projeto Estratégico—LA 26–2011-2012 and Projeto Estratégico—LA 26–2013-2014 cofinanciado por fundos nacionais, através da Fundação para a Ciência e a Tecnologia (PEst-C/SAU/LA0026/2011; PEst-C/SAU/LA0026/2013), e pelo Fundo Europeu de Desenvolvimento Regional (FEDER), através do COMPETE (FCOMP-01-0124-FEDER-022724; FCOMP-01-0124-FEDER-037298). The authors would like to thank Professor Jeffrey Gimble at the Tulane University Center for Stem Cell Research and Regenerative Medicine and LaCell LLC (New Orleans, Louisiana, USA) for kindly providing the ASCs used in this study.

References

[1] R. C. Assunção-Silva, E. D. Gomes, N. Sousa, N. A. Silva, and A. J. Salgado, "Hydrogels and cell based therapies in spinal cord injury regeneration," *Stem Cells International*, vol. 2015, Article ID 948040, 24 pages, 2015.

[2] A. J. Salgado, R. A. Sousa, J. S. Fraga et al., "Effects of starch/polycaprolactone-based blends for spinal cord injury regeneration in neurons/glial cells viability and proliferation," *Journal of Bioactive and Compatible Polymers*, vol. 24, no. 3, pp. 235–248, 2009.

[3] N. A. Silva, J. Moreira, S. Ribeiro-Samy et al., "Modulation of bone marrow mesenchymal stem cell secretome by ECM-like hydrogels," *Biochimie*, vol. 95, no. 12, pp. 2314–2319, 2013.

[4] N. A. Silva, A. J. Salgado, R. A. Sousa et al., "Development and characterization of a novel hybrid tissue engineering-based scaffold for spinal cord injury repair," *Tissue Engineering: Part A*, vol. 16, no. 1, pp. 45–54, 2010.

[5] N. A. Silva, M. J. Cooke, R. Y. Tam et al., "The effects of peptide modified gellan gum and olfactory ensheating glia cells on neural stem/progenitor cell fate," *Biomaterials*, vol. 33, no. 27, pp. 6345–6354, 2012.

[6] O. Ziv-Polat, A. Shahar, I. Levy et al., "The role of neurotrophic factors conjugated to iron oxide nanoparticles in peripheral nerve regeneration: in vitro studies," *BioMed Research International*, vol. 2014, Article ID 267808, 10 pages, 2014.

[7] E. R. Burnside and E. J. Bradbury, "Manipulating the extracellular matrix and its role in brain and spinal cord plasticity and repair," *Neuropathology and Applied Neurobiology*, vol. 40, no. 1, pp. 26–59, 2014.

[8] Y. S. Chen, C. L. Hsieh, C. C. Tsai et al., "Peripheral nerve regeneration using silicone rubber chambers filled with collagen, laminin and fibronectin," *Biomaterials*, vol. 21, no. 15, pp. 1541–1547, 2000.

[9] W. Ma, W. Fitzgerald, Q. Y. Liu et al., "CNS stem and progenitor cell differentiation into functional neuronal circuits in three-dimensional collagen gels," *Experimental Neurology*, vol. 190, no. 2, pp. 276–288, 2004.

[10] A. Hejcl, P. Lesný, M. Prádný et al., "Biocompatible hydrogels in spinal cord injury repair," *Physiological Research*, vol. 57, Supplement 3, pp. S121–S132, 2008.

[11] F. G. Teixeira, M. M. Carvalho, N. Sousa, and A. J. Salgado, "Mesenchymal stem cells secretome: a new paradigm for

central nervous system regeneration?," *Cellular and Molecular Life Sciences*, vol. 70, no. 20, pp. 3871–3882, 2013.

[12] K. Menezes, M. A. Nascimento, J. P. Gonçalves et al., "Human mesenchymal cells from adipose tissue deposit laminin and promote regeneration of injured spinal cord in rats," *PLoS One*, vol. 9, no. 5, article e96020, 2014.

[13] M. Pumberger, T. H. Qazi, M. C. Ehrentraut et al., "Synthetic niche to modulate regenerative potential of MSCs and enhance skeletal muscle regeneration," *Biomaterials*, vol. 99, pp. 95–108, 2016.

[14] I. Allodi, M. S. Guzmán-Lenis, J. Hernàndez, X. Navarro, and E. Udina, "In vitro comparison of motor and sensory neuron outgrowth in a 3D collagen matrix," *Journal of Neuroscience Methods*, vol. 198, no. 1, pp. 53–61, 2011.

[15] R. C. Assunção-Silva, C. C. Oliveira, O. Ziv-Polat et al., "Induction of neurite outgrowth in 3D hydrogel-based environments," *Biomedical Materials*, vol. 10, no. 5, article 051001, 2015.

[16] N. Nakano, Y. Nakai, T. B. Seo et al., "Characterization of conditioned medium of cultured bone marrow stromal cells," *Neuroscience Letters*, vol. 483, no. 1, pp. 57–61, 2010.

[17] A. J. Salgado, R. L. Reis, N. J. Sousa, and J. M. Gimble, "Adipose tissue derived stem cells secretome: soluble factors and their roles in regenerative medicine," *Current Stem Cell Research & Therapy*, vol. 5, no. 2, pp. 103–110, 2010.

[18] L. E. Kokai, K. Marra, and J. P. Rubin, "Adipose stem cells: biology and clinical applications for tissue repair and regeneration," *Translational Research*, vol. 163, no. 4, pp. 399–408, 2014.

[19] D. Docheva, C. Popov, W. Mutschler, and M. Schieker, "Human mesenchymal stem cells in contact with their environment: surface characteristics and the integrin system," *Journal of Cellular and Molecular Medicine*, vol. 11, no. 1, pp. 21–38, 2007.

[20] M. F. Taha and V. Hedayati, "Isolation, identification and multipotential differentiation of mouse adipose tissue-derived stem cells," *Tissue and Cell*, vol. 42, no. 4, pp. 211–216, 2010.

[21] H. Zhu, N. Mitsuhashi, A. Klein et al., "The role of the hyaluronan receptor CD44 in mesenchymal stem cell migration in the extracellular matrix," *Stem Cells*, vol. 24, no. 4, pp. 928–935, 2006.

[22] A. Hennigan, R. M. O'Callaghan, and A. M. Kelly, "Neurotrophins and their receptors: roles in plasticity, neurodegeneration and neuroprotection," *Biochemical Society Transactions*, vol. 35, pp. 424–427, 2007.

[23] J. Park, E. Lim, S. Back, H. Na, Y. Park, and K. Sun, "Nerve regeneration following spinal cord injury using matrix metalloproteinase-sensitive, hyaluronic acid-based biomimetic hydrogel scaffold containing brain-derived neurotrophic factor," *Journal of Biomedical Materials Research: Part A*, vol. 93, no. 3, pp. 1091–1099, 2010.

[24] M. Morano, S. Wrobel, F. Fregnan et al., "Nanotechnology versus stem cell engineering: in vitro comparison of neurite inductive potentials," *International Journal of Nanomedicine*, vol. 9, pp. 5289–5306, 2014.

[25] J. G. Boyd and T. Gordon, "Neurotrophic factors and their receptors in axonal regeneration and functional recovery after peripheral nerve injury," *Molecular Neurobiology*, vol. 27, no. 3, pp. 277–324, 2003.

[26] K. Jin, Y. Zhu, Y. Sun, X. O. Mao, L. Xie, and D. A. Greenberg, "Vascular endothelial growth factor (VEGF) stimulates neurogenesis in vitro and in vivo," *Proceedings of the National Academy of Sciences of the United States of America*, vol. 99, no. 18, pp. 11946–11950, 2002.

Hindawi
Stem Cells International
Volume 2017, Article ID 6597815, 13 pages
https://doi.org/10.1155/2017/6597815

Review Article

Xeno-Free Strategies for Safe Human Mesenchymal Stem/Stromal Cell Expansion: Supplements and Coatings

M. Cimino,[1,2,3] R. M. Gonçalves,[1,2,4] C. C. Barrias,[1,2,4] and M. C. L. Martins[1,2,4]

[1]*I3S, Instituto de Investigação e Inovação em Saúde, Universidade do Porto (UP), Porto, Portugal*
[2]*Instituto de Engenharia Biomédica (INEB), Universidade do Porto (UP), Porto, Portugal*
[3]*Faculdade de Engenharia, Universidade do Porto (UP), Porto, Portugal*
[4]*Instituto de Ciências Biomédicas Abel Salazar (ICBAS), Universidade do Porto (UP), Porto, Portugal*

Correspondence should be addressed to M. Cimino; maura.cimino@ineb.up.pt and M. C. L. Martins; cmartins@ineb.up.pt

Received 20 April 2017; Accepted 1 August 2017; Published 11 October 2017

Academic Editor: Miguel Alaminos

Copyright © 2017 M. Cimino et al. This is an open access article distributed under the Creative Commons Attribution License, which permits unrestricted use, distribution, and reproduction in any medium, provided the original work is properly cited.

Human mesenchymal stem/stromal cells (hMSCs) have generated great interest in regenerative medicine mainly due to their multidifferentiation potential and immunomodulatory role. Although hMSC can be obtained from different tissues, the number of available cells is always low for clinical applications, thus requiring *in vitro* expansion. Most of the current protocols for hMSC expansion make use of fetal bovine serum (FBS) as a nutrient-rich supplement. However, regulatory guidelines encourage novel xeno-free alternatives to define safer and standardized protocols for hMSC expansion that preserve their intrinsic therapeutic potential. Since hMSCs are adherent cells, the attachment surface and cell-adhesive components also play a crucial role on their successful expansion. This review focuses on the advantages/disadvantages of FBS-free media and surfaces/coatings that avoid the use of animal serum, overcoming ethical issues and improving the expansion of hMSC for clinical applications in a safe and reproducible way.

1. Introduction

Regenerative medicine aims to repair or replace tissue or organ functions, compromised due to aging, physical damage, congenital defects, or diseases. Cell-based therapies are based on the transplantation of freshly isolated or cultured cells into the site of injury. Those cells are frequently stem cells, which have the ability to self-renew and differentiate along multiple lineage pathways, and thus contribute to tissue repair/regeneration [1].

Among stem cells, human mesenchymal stem/stromal cells (hMSCs) have generated great interest because they are relatively easy to isolate, can be extensively expanded, and present multiple differentiation potential, namely, bone cells (osteocytes), cartilage cells (chondrocytes), and fat cells (adipocytes). Therefore, they are good candidates for cell-based therapeutic approaches towards several kinds of pathologies, such as myocardial infarction [2], graft-versus-host disease [3], Crohn's disease, neurodegenerative and muscle degenerative diseases [4], cartilage and meniscus repair [5], or stroke and spinal cord injury [6]. According to a study from Hart and colleagues, in February 2014 [7], 457 clinical trials involving hMSCs were registered worldwide being China the leader in this ranking. At the time of writing, the number of clinical trials raised until 706 (http://www.clinicaltrials.gov).

Human MSC can be derived from different tissues such as bone marrow (BM-hMSC), adult adipose tissue (AT-hMSC), and mobilized peripheral blood, as well as from placenta and umbilical cord blood (UC-hMSC), being BM the most common source in clinical use. However, hMSC prevalence in all these tissues is low, and the total amounts of isolated cells are insufficient for clinical applications. For example, BM contains approximately 1 in 3.4×10^4 bone cells [8], with total numbers generally decreasing with donor age [9]. The number of required BM-MSCs depends on the type of disease to treat, ranging, for example, from 2×10^6 cells/kg in graft-versus-host disease to 8×10^6 cells/kg in cardiomyopathy and to 10×10^6 cells/kg in respiratory distress syndrome (https://www.clinicaltrials.gov/). Thus, in order to have sufficient cell

Table 1: Successful clinical trials involving hMSC expanded *in vitro* with FBS-containing medium.

Type of disease	Treatment	Reference
Luminal Crohn's disease	Allogenic hMSCs	Forbes 2014 [101] (*)
Ischemic stroke	Autologous MSCs	Lee 2010 [102] (**)
Stroke injury	Autologous MSCs	Bang 2005 [103]
Amyotrophic lateral sclerosis	Intraspinal cord implantation	Mazzini 2008 [104]
Grade IV acute graft-versus-host disease	Haploidentical MSC	Le Blanc 2004 [105]
Brest cancer	Autologous MSCs	Koc 2000 [106]
Acute myocardial infarction	Autologous MSCs	Chen 2004 [107]

*Australia being a country with no incidence of BSE and vCJD, the use of certified FBS for hMSC ex vivo expansion is still accepted; **no adverse events in terms of zoonoses transmission were observed; however, since the vCJD latency period may last many years, long-term follow-up is needed.

Table 2: FBS use advantages and drawbacks.

Use of FBS as a supplement for cell culture	
Advantages	Disadvantages
Furnishes a cocktail of growth factors required for *in vitro* cell growth	Ill defined
Universal: suitable for all cell types	Lot-to-lot variability
	Possible contamination of the cell surface with xenogenic compounds that may influence cell behavior
	Possible microbiological contamination (virus, prions bacteria, endotoxins, and fungi)
	Economical: worldwide availability
	Ethical problems: requires the painful death of bovine fetuses

numbers for successful transplantation, isolated hMSC must be first expanded ex vivo, using effective and safe methods that maintain their key properties in a shorter period of time in order to avoid cell aging and possible contaminations [10].

Several controversies are related with the lack of common standard protocols for hMSC *in vitro* expansion. This is critical since culture conditions may have an impact on the transcriptome, proteome, and cellular organization of hMSCs, which will affect their engraftment and performance upon transplantation [11]. Discrepancy among laboratories includes the choice of basal media and the addition of supplementary factors. Moreover, hMSC being anchorage-dependent cells, culture surfaces are often coated with extracellular matrix (ECM) proteins or other commercially available cell adhesion factors, generating an additional element of discontinuity among expansion protocols. Finally, to reduce variability between preclinical trials, cell culture experiments must comply with good manufacturing practices (GMP) guidelines and every step of cell manipulation must be defined in standard operating procedures (SOP).

In this context, considerable efforts have been made to improve the ex vivo expansion of hMSC for clinical applications, at different levels. This review highlights the disadvantages associated with the use of fetal bovine serum (FBS) as a nutrient-rich medium supplement and focuses on the advantages/disadvantages of different xeno-free and/or serum-free supplements and surfaces/coatings for hMSC expansion.

2. Fetal Bovine Serum as a Supplement for hMSC *In Vitro* Expansion

MSC growth *in vitro* must be supported by the addition of a basal media such as Dulbecco's modified Eagle's medium (DMEM), α-modified minimum essential medium (α-MEM) [12], or media combinations such as 50 : 50 (v/v) of DMEM : HAM's nutrient mixture F12 [13] which generally include (i) biosynthetic precursors for cell anabolism, (ii) catabolic substrates for energy metabolism, (iii) vitamins and trace elements, and (iv) inorganic ions to maintain the pH and osmolarity of the culture [14]. This basal medium is further supplemented with FBS, a highly rich supplement that contains a cocktail of cell attachment proteins, growth factors, and other important biomolecules.

According to the description by Lalu et al. in 2012 [15], from 36 clinical studies involving hMSC, 27 used FBS as a media supplement and 5 used human serum while 4 did not specify the kind of supplement used. Table 1 describes some successful clinical trials almost without side effects where hMSCs were expanded in FBS-supplemented medium, even though there are many concerns regarding the use of FBS in terms of scientific ethical and economical disadvantages. These are summarized together with FBS advantages in Table 2.

FBS is an *ill-defined* supplement, with high inconsistency in terms of the quality and quantity of bioactive compounds [16]. Because of the great variability among different FBS

batches, preselection of specific lots is often required, which is costly, time consuming, and also hampers comparisons between different research groups [17]. For example, Knepper et al. showed that FBS from three different commercial sources vary on the relative amounts and apparent molecular weights of some transcription factors [18], while Zheng et al. showed that different lots of FBS had varying concentrations of proteins such as growth stimulatory and inhibitory factors, with obvious implications in cell growth rates [19].

When FBS is employed in hMSC expansion for cell therapies, there is also a strong concern regarding contamination with xenogenic compounds and microbiological contaminants, such us viruses, prions, bacteria, fungi, and endotoxins. Directive 2004/23/EC [20] and its recent implementation [21] specify safety measures to be taken into account during donation, procurement, testing, processing, preservation, storage, distribution, and use of human cells and tissues intended for human applications. A notable concern is the potential cross-specific or zoonic transmission of unknown pathogens related to the exposition of cells in culture to animal-derived compounds. Zoonoses bring the risk of virulent diseases such as anthrax, Q fever, and Creutzfeldt-Jakob disease (CJD), where a special concern regards the risk of bovine spongiform encephalopathies (BSE) transmission and its relation to the new variant CJD (vCJD) [22]. Recently, genetic material from bovine viral diarrhea (BVD) virus [23] and new viruses has been detected in bovine serum by massively parallel sequencing [24], a metagenomic technique that can identify viruses and other adventitious agents, without prior knowledge of their nature and being able to reveal either latent or silent infections. Moreover, bovine species of mycoplasma contaminants, often present in FBS, have been frequently isolated from cell cultures [25, 26], but these can be difficult to detect. In fact, batches of contaminated serum may effectively pass the test for mycoplasma as negative samples, as recently reported [27].

Regarding ethical concerns, FBS is harvested from bovine fetuses taken from pregnant cows during slaughter, by cardiac puncture and without any form of anesthesia [28]. During this procedure, fetuses undergo anoxia, a strong oxygen deficiency, and are exposed to pain and/or suffering in a procedure which may be considered ethically inhumane. Finally, the use of FBS in cell culture raises logistic and economic problems: around 1 to 3 fetuses are needed to produce just a liter of serum, implying high costs related to animal feeding, installation, and maintenance of the necessary infrastructures. Recently, an imminent increase of the FBS cost has been notified and justified according to the reduction in supply and the increased demand from life science and pharmaceutical customers. Considering the extensive spread of cell therapy industry, the demand of serum is likely to significantly exceed the amount of maximum worldwide serum availability [29].

3. FBS-Free Media Formulations for hMSC *In Vitro* Expansion

Suitable alternatives to FBS for hMSC expansion should ideally guarantee a well-defined composition, a reduced degree of contaminants, low production costs, extended shelf life, and easy availability. Different alternatives have been described in the literature, which can be broadly divided into (1) chemically defined media and (2) media supplemented with human blood derivatives (Table 3).

3.1. Chemically Defined Media. Chemically defined (CD) media include only components of known composition. Common strategies for the preparation of CD media have been amply described and validated [13]. In general, formulations for MSC culture consist of a basal media, as already discussed, to which different kinds of supplements are added. Until 15–30 years ago, supplements used in CD media, as highly purified hormones or growth factors, were often obtained from human or animal serum but, nowadays, with the advance of recombinant technologies, it is possible to produce a wide range of human proteins that allow the development of completely xeno-free CD media. Since hMSCs can be isolated from different sources and vary among different donors, the optimal CD media may have different specific requirements concerning medium supplements, which turns the development of a "universal" CD media into a challenging task.

Different CD media (serum free and/or xeno free) for hMSC are nowadays commercially available. For example, TheraPEAK™ MSCGM-CD™ (Lonza) and PowerStem (PAN Biotech GmbH) are able to support hMSC expansion and differentiation; however, CD105 expression may be significantly reduced after culture in those CD media in comparison with serum-supplemented medium [30]. Many of the currently available CD media require precoating of culture substrates with ECM proteins to support cell attachment (Section 4). For example, stemgro hMSC medium (Corning), when used in conjunction with the Corning CellBIND Surface (Section 4.6), enables hMSC attachment and growth comparable to that of serum-containing cultures, including maintenance of MSC multipotency. Another study [31] showed that proliferation of human BM-MSCs was successful on four different commercially available CD xeno-free media (MesenCult-XF, STEMPRO MSC SF, TheraPEAK MSCGM-CD, and Corning stemgro hMSC medium) and in particular upon seeding on a proprietary surface (Corning Synthemax Surface). The Corning medium, associated with the synthetic surface, was able to promote significantly higher long-term cell expansion than traditional serum-containing medium on tissue culture polystyrene (TCPS).

There are however some disadvantages associated with the use of CD media that might limit their wider application in clinical scale hMSC expansion. For example, even if databases of commercially available CD media are accessible online [14], their exact compositions are not specified by the suppliers. Cell-doubling times can vary among different CD media [31], and in some cases, cell morphology and size may differ and alterations in cell vacuoles may arise. Also, the quality/activity of biological compounds in the CD media formulations can generate variability among different batches compromising experiment reproducibility. The use of ECM-like coatings, often mandatory, may also raise some concerns, because of batch-to-batch variability,

Table 3: Xeno-free supplements for cell culture.

Human blood derivatives				Not human origin
Human serum (HS)	Human platelet lysate (hPL)	Human umbilical cord serum (hUCS)	Human plasma fractions (supplement for cell culture (SCC))	Chemically defined media (CD)
Advantages				
No ethical problems	No ethical problems	No ethical problems	No ethical problems	No ethical problems
No risk of xenogenic compound transmission	No risk of xenogenic compound transmission	No risk of xenogenic compound transmission	No risk of xenogenic compound transmission	No risk of xenogenic compound transmission
Easy and inexpensive procedure	Contains high level of GF	Easy and inexpensive procedure	GMP compliant: compatible with pharmaceutical grade advanced therapies	No risk of transmission of human diseases
		Contains high level of GF and proteins (transferrin, albumin, and fibronectin)	Little batch to batch variability (derived from an industrial plasma pool constituted from over 1000 donations)	
		Easy-available allogenic source	Provides cell growth and attachment factors	
			Lyophilized: convenient for transport and storage	
Disadvantages				
Variability between individual donations	Variability between individual donations	Variability between individual donations	Ongoing: further investigation will help to a better characterization	Cell specific
Possibility of transmission of human diseases	Possibility of transmission of human diseases	Possibility of transmission of human diseases		Ill-defined because it lacks of information provided by the companies
Low availability in terms of amount of donation	Low availability in terms of amount of donation	Low availability in terms of amount of donation		Development may be expensive and time consuming
Discrepancy of results in allogenic settings	Not well defined composition in terms of GF content			Cell-adaptation may be necessary
Quality in autologous settings may not be ideal	Quite laborious and expensive procedure			
Often requires the addition of cytokines and GF				

poor information about their protein content, potential immunogenicity of their components, and time-consuming coating procedure [12]. Often, guidelines for cell adaptation protocols are not provided, which can be a laborious, time-consuming process. Finally, as already stated, this type of media may result in nonoptimal cell growth, as compared to medium supplemented with serum or other animal-derived supplements, as reported in the literature in a study where the performance of different commercially available CD media was compared [32].

3.2. Human Blood Derivatives. Several "humanized" supplements derived from human blood have been proposed, namely, (1) autologous or allogeneic human serum (*hS*), (2) human platelet lysate (*hPL*), (3) umbilical cord blood serum (*hUCBS*), and, more recently, (4) industrial GMP human plasma derivatives (supplement for cell culture (*SCC*)). The use of each of these supplements will be described in more detail in the following sections.

3.2.1. Human Serum (hS). Human serum (hS) can be collected from autologous or allogenic whole blood donations. Autologous hS has been widely described for its positive effects on cell expansion. For example, medium supplemented with 10% *v*/*v* autologous hS was shown to be as efficient as the same amount of FBS for hMSC isolation and expansion, and even better as an inducer of osteogenic differentiation [33]. Yamamoto et al. [34] demonstrated that a patient's autologous hS could be used to expand bone marrow hMSC without compromising their potential for osteogenic differentiation. However, it may be problematic to collect a sufficient amount of autologous serum to propagate hMSC for clinical application. Moreover, depending on the patient, the quality of autologous serum may not be optimal, especially in those undergoing other types of therapies [11]. Also, a negative correlation between donor age and the outgrowth of cells from human trabecular bone was demonstrated in cultures supplemented with autologous serum [35] suggesting that the use of autologous serum is not suitable for elderly patients [36]. To try to overcome these drawbacks, Spees and coworkers demonstrated that, when cells are expanded in medium containing FBS and afterwards transferred to AHS^+ (autologous human serum supplemented with growth factors), the amount of FBS contaminants can be reduced in 99.99%, which could be used as a strategy to circumvent the low availability of autologous serum [37]. Nevertheless, Martin et al. demonstrated that hMSCs cultured with FBS were contaminated with xeno-derived carbohydrate N-glycolylneuraminic acid (NeuGc) [38, 39]. The subsequent replacement of FBS by hS was insufficient for achieving complete decontamination, since cells express bovine NeuGc on their surface, even after long periods of culture without FBS [40].

On the other hand, hS from allogenic donations can be associated with donor variability. Nevertheless, Witzeneder et al. suggested that pools of 6 donors are sufficient to reduce the variability among human blood samples [41]. However, results from stem cell expansion with allogenic hS still remain controversial, with both positive and negative outcomes described in the literature. For example, autologous serum plus recombinant basic fibroblast growth factor (bFGF) and three recombinant cytokines (Thrombopoietin, Stem Cell Factor, and FL or "Fms-related tyrosine kinase 3 ligand") have been shown to support expansion of primary marrow stromal cells [42]. Adipose tissue-derived MSC expanded with human allogenic serum pooled from 5 donors exhibited a more spindle-shaped morphology and increased motility than the same cells cultured on FBS, and a significantly higher proliferative rate [43]. Moreover, it has been demonstrated that human serum contains factors that, in comparison to FBS, exert dramatic effects on BM-MSC cell differentiation increasing the osteogenic and adipogenic activity of dexamethasone [44]. However, Anselme et al. [45] observed less formation of fibroblastic colony-forming units (CFU-F) when hMSCs were cultured in hS as compared to FBS-supplemented media. Nevertheless, BM-MSCs cultured in hS before transplantation were more efficient in the production of *in vivo* bone formation than the same cells cultured in FBS [46]. Aldahmash and colleagues [47] did not observe any significant differences in growth rates of an immortalized hMSC line during short-term (10 days) and long-term (100 days) culture in media supplemented with allogenic hS in comparison with FBS. Recently, Choi et al. compared the effects of different concentrations of autologous serum (1, 2, 5, and 10%) on expansion and adipogenic differentiation of AT-MSC using 10% FBS as a control. They found that cell isolation was successful without difference among media, while the proliferation potential follows the trend: 10% autologous serum > 10% FBS = 5% autologous serum > 2% autologous serum = 1% autologous serum [6].

3.2.2. Human Platelet Lysate (hPL). Human platelet lysate (hPL) can be obtained from blood platelets using different procedures, among which the most common is the freeze/thaw technique developed by Holmqvist and Westermark [48]. This procedure for platelet isolation from blood preserves their α granules, which contain a wide range of growth factors such as bFGF, epidermal growth factor (EGF), hepatic growth factor (HGF), insulin growth factor-1 (IGF-1), platelet-derived growth factor (PDGF), transforming growth factor-β1 (TGF-β1), and vascular endothelial growth factor (VEGF). In comparison to human serum, hPL contains higher levels of strong mitogens (e.g., EGF, PDGF, and TGF-β1), whereas the levels of IGF-1 and the protein content are lower due to the removal of immunoglobulins and albumin in the washing procedure [49]. In some studies, hPL has been more efficient than FBS regarding the expansion of hMSC, maintaining their differentiation potential as well as their immunosuppressive properties, namely, in the case of hMSC derived from adipose tissue [50]. Importantly, no difference between the use of freshly prepared and expired platelet concentrates has been observed regarding the proliferation potential and osteogenic differentiation of hMSC [51], suggesting that the bioactivity of this type of supplement is quite stable. The addition of exogenous growth factors has been commonly employed in FBS-supplemented culture to increase cell proliferation rates [52]. However, even if higher proliferation rates have been obtained in cultures

supplemented with FBS combined with bFGF, as compared to FBS only, those rates remained lower than the ones obtained in medium supplemented with 10% hPL [53]. Interestingly, hPL without the addition of anticoagulant forms a soft hydrogel, providing a three-dimensional (3D) scaffold, which has been described to increase *in vitro* expansion of hMSC by mimicking a more natural 3D context than the commonly used 2D polystyrene surfaces [50]. Finally, platelet derivatives have been already tested in clinical trials with good results for the treatment of tendinopathies and osteoarthritis [54, 55] and in hearth failure [56].

However, the use of hPL also presents some disadvantages. First, it is a supplement for cell culture that, similarly to FBS, is not precisely defined. A high variability exists between individual hPLs, as their composition is strongly dependent on donor-related factors, such us age, gender, blood group, and platelet individual counts [57]. Nevertheless, pooling different donations can reduce variability. Schallmoser et al. demonstrated that a pool of 15 donations can improve standardization [58]. Also, hPL isolation process may affect platelet degranulation and, consequently, growth factor content of hPLs. Additional variability may result from the filtering procedure, storage typology, or the content in heparin or anticoagulants [55]. Moreover, as observed for other human-derived media supplements, there is a concern regarding the possibility of immunological reactions, in allogenic settings, and transmission of human diseases. However, Castiglia et al. [59] recently described a method named *ihPL* (inactivated hPL), which ensures efficient generation of safe hPL batches, by virus inactivation through UVA light.

3.2.3. Human Umbilical Cord Blood Serum (hUCBS). Human umbilical cord blood serum (hUCBS) can be easily obtained following normal delivery, thus normally screened for the most common bacterial or viral contamination, and its use does not raise any ethical issues. It contains high levels of soluble growth factors and more than 60 proteins, namely, albumin, transferrin, and fibronectin (FN) in high concentrations, with different roles in cell growth and stem cell differentiation [12]. Phadnis et al. [60] demonstrated that BM-hMSC displayed a 32-fold increase in cell number 5 days after seeding in UCBS against a 10-fold increase in FBS culture conditions. Moreover, 10% UCBS has been proved to be more efficient in promoting hMSC osteogenic differentiation than 10% FBS because of its enhancement of osteocalcin promoter expression [61].

In general, UCBS can be considered advantageous as a cell culture supplement considering the easy availability of this allogeneic source, the easy and inexpensive isolation procedure [62], and the near absence of contaminants. On the other hand, some limitations must be considered, such as the high lot-to-lot variability, associated to donor-related features and the presence of adventitious agents that may eventually escape routine screening procedures.

3.2.4. Industrial GMP Human Plasma Derivatives (Supplement for Cell Culture (SCC)). A new type of supplement cell culture (SCC) has been recently described for *in vitro* cell expansion [63], consisting on a GMP pharmaceutical grade xeno-free human plasma-derived supplement. SCC is obtained from human plasma through cold-ethanol industrial fractionation [64]. Once plasma is collected from healthy donors at USA-based FDA-licensed plasmapheresis centers, plasma pools from over 1000 different donors are assembled in a single plasma unit. Every individual donation is tested for viral markers, and all plasma is tested, using nucleic acid techniques, for the presence of DNA or RNA from relevant pathogenic agents, in agreement with the European and American legislations. In addition, SCC production procedure includes a specific viral inactivation step (gamma irradiation) besides other purification steps with additional pathogen removal capacity [63].

SCC has already been successfully used as a supplement for *in vitro* cell culture to basal medium that supports culture of stem cells such as human embryonic stem cells (hES), induced pluripotent stem cells (iPSC) derived from human dermal fibroblast [65], and hMSCs [63]. When hMSCs were expanded in SCC (15% SCC reconstituted in basal medium (DMEM : HAM's nutrient mixture F12)) containing a cocktail of growth factors and other elements such as insulin, sodium selenite, and ethanolamine, cell yield was similar to the one obtained for hMSC expanded in commercial medium obtained from hMSC suppliers (Lonza Group and PromoCell). Moreover, SCC-supplemented medium maintained hMSC in an undifferentiated state during expansion and kept their capacity of adipogenic, chondrogenic, and osteogenic differentiation, under inducing conditions [63].

However, SCC being a supplement in very recent development, only few data are available in the literature regarding its potential use as an hMSC medium supplement. Thus, further investigations will help to a better characterization and improve additional applications. Its introduction in the market as other alternatives to FBS will show its potentiality as a supplement for *in vitro* cell expansion.

4. Surfaces and Coatings to Promote hMSC Attachment and Growth

Anchorage-dependent cells, such as hMSCs, are supported *in vivo* by the ECM, an assembly of many proteins and glycosaminoglycans (GAGs) that provides a 3D environment for their organization into tissues. Specific interactions between cell surface receptors and ligands on the ECM mediate intracellular signaling pathways and control gene expression, cytoskeletal organization, and cell morphology that are involved in key cellular activities such as cell adhesion, migration, proliferation, and differentiation [66].

When cells are cultured with FBS-supplemented medium, a protein layer readily adsorbs to the tissue culture polystyrene (TCPS) surface, the material generally used in the commercial cell culture flasks. This protein layer contains several adhesive proteins, such as fibronectin (FN) and vitronectin (VN) that are essential to mediate early stages of cell attachment [67], before cells are able to produce their own ECM [68]. In contrast, hMSC cultured in the absence of FBS does not properly attach to TCPS [69]. A common strategy for hMSC expansion in serum-free conditions is their

preincubation in FBS as a transient adaptation step to serum-free medium [69]. This process can confer to the cells the necessary elements for attachment. However, this is not acceptable in a GMP setting, demonstrating the need of identifying defined cell attachment factors and also designing new culture surfaces that support hMSC adhesion and proliferation, while maintaining its multipotency, in the absence of FBS.

4.1. Surface Coating with Cell-Adhesive Proteins. The simplest strategy to improve the attachment of hMSC in culture cell consists in precoating TCPS surfaces with purified adhesive proteins that can be isolated from human plasma or synthesized by recombinant technologies. Surface modification with a FN coating is probably the most widely used strategy for improving hMSC adhesion and proliferation in serum-free conditions. FN is a multifunctional, ECM glycoprotein that contains several functionally and structurally distinct domains, including cell-binding domains such as the RGD (Arg-Gly-Asp) sequence that are recognized by cell surface integrins, namely, $\alpha 5\beta 1$ and $\alpha v\beta 3$ [70]. Other coating proteins, such as laminin (LN), collagen type I (COL I) and collagen type IV (COL IV), and gelatin, also showed to improve hMSC adhesion and growth in serum-free medium [69]. In contrast, the number of attached hMSC on poly-D-lysine precoated surfaces was very low even when studies were performed in the presence of FBS [69]. Moreover, cells did not show their typical fibroblast-like spindled-shape morphology, which could be related with their low spreading capacity in this type of coating [71]. Ode et al. also reported that TCPS precoated with FN as well as COL I, II, III, and IV and fibrinogen (FG), but not with LN, induces hMSC adhesion and proliferation in serum-reduced conditions (0.1% *v*/*v* FBS) [72]. LN, an ECM protein especially abundant within the basal lamina of epithelial and endothelial tissues, has been described as an important mediator of cell attachment and migration [73]. Yet, the effect of LN-coated surfaces on hMSC adhesion and growth is not clear since opposite outcomes have been reported [69, 72, 74, 75]. Differences in hMSC behavior on LN-coated surfaces could be related with (i) protein conformation, which is dependent on the type of substrate, LN concentration, and incubation time; (ii) type of LN, as different forms have been identified; and (iii) disparities in terms of cell culture protocols, including the type of medium used.

Ogura et al. [76] also demonstrated that hMSC attachment and spreading on FN-coated dishes were increased when compared to albumin-coated dishes. This is not surprising since albumin, the protein that exists in higher concentration in serum and the first to reach and adsorb to most of the surfaces, is known by its nonadhesive characteristics [77].

Besides affecting hMSC attachment and proliferation, ECM protein coatings can also influence cell differentiation into specific lineages. For example, it is known that FN plays a pivotal role in hMSC osteogenic differentiation, while inhibiting adipogenesis [78]. VN and COL I coatings were also shown to induce MSC osteogenic differentiation [74, 78] through interaction with specific COL I receptor $\alpha_1\beta_1$ and VN receptor $\alpha_V\beta_3$ integrins. This fact was observed even in the absence of soluble osteogenic inducers [74]. LN-1 and LN-5 were shown to promote hMSC osteogenic differentiation in xeno-free conditions (human plasma and platelet extract) [79], but LN-5 suppress chondrogenic differentiation [75]. Since surface chemistry will influence the amount and conformation of the adsorbed protein layer and thus the exposure of specific integrin-binding sequences, the type of substrate used will affect hMSC differentiation profile even when the same protein coating was used [80].

TCPS coated with keratins, isolated from human hair, was recently suggested as an alternative to other most common adhesive proteins for hMSC *in vitro* expansion [81]. This protein contains the LDV (Leu-Asp-Val) cell adhesion motif recognized by cell membrane integrin $\alpha_4\beta_1$. Moreover, human hair keratins can be easily obtained in abundance even from an autologous source. However, more studies need to be performed in order to further validate its suitability for this kind of applications.

4.2. Surface Modifications to Promote Adequate Adsorption of Adhesive Proteins. The type of underlying substrate used for cell culture also influences hMSC adhesion and proliferation, since it dictates the nature, conformation, and orientation of adsorbed proteins and, consequently, the exposure of active ligands (cell-binding domains) for cell recognition and binding. Commercial cell culture flasks are commonly made of TCPS. These surfaces are obtained by modifying hydrophobic polystyrene surfaces, often by gas-plasma treatment, to turn them hydrophilic and negatively charged. This promotes the adsorption of serum attachment proteins such as FN and VN, in relation to other proteins such as albumin [82], providing better surfaces for subsequent cell adhesion.

In fact, it is currently well known that cell-binding domains of FN are hidden when the protein is in its native structure, becoming exposed upon adsorption on surfaces with adequate wettability and charge [83]. So, the effect of adsorbed FN on cell attachment largely depends on the properties of the underlying substrate. For example, Dolatshahi-Pirouz et al. demonstrated that although FN adsorption was higher on gold (Au) surfaces than on hydroxyapatite (HA) surfaces, the morphology of attached hMSC was more regular on HA. This was explained by the higher exposure of cell-binding domains on FN adsorbed on HA, which was confirmed using monoclonal antibodies directed against FN cell-binding domains [84]. The influence of surface wettability (hydrophilic versus hydrophobic surfaces) on selective adsorption of FN and VN from FBS and respective exposure of cell-binding domains was also studied using self-assembled monolayers (SAMs) prepared by mixing different ratios of OH- (hydrophilic-) and CH_3- (hydrophobic-) terminated alkanethiols [67]. hMSC adhesion and proliferation increased with the increase of surface hydrophilicity (increase of OH/CH_3) which was directly correlated with the increased exposure of cell-binding domains on adsorbed FN and VN [67]. However, Curran et al. [85] did not find differences in hMSC adhesion and viability among $-CH_3$, $-OH$, $-NH_2$, $-SH$, and $-COOH$ glass silane-modified surfaces in the presence of FBS. Nevertheless, they demonstrated that surface chemistry was able to modulate hMSC potential

of differentiation. They reported that only $-CH_3$ surfaces were able to maintain MSC phenotype, since cells were expanded without losing their differentiation skills under appropriated stimulus. NH_2 and −SH surfaces promoted osteogenesis differentiation while −OH and −COOH surfaces support chondrogenic differentiation even in basal conditions [85].

Although all these studies were performed in the presence of FBS, they highlight the importance of surface chemistry on the amount and conformation of adsorbed adhesive proteins, an essential step in the design of substrates for serum-free or xeno-free hMSC cultures.

4.3. Surface Chemical Modifications with Cell-Adhesive Peptides. Since the process of surface coating by simple protein adsorption does not provide a high level of control over the presentation of cell-binding domains, different strategies have been idealized to covalently immobilize cell-binding motifs (e.g., RGD) on a substrate [86, 87]. With this strategy, problems associated with surface coatings with proteins from animal or human origin can be overcome, since cells may directly bind to the functionalized substrate. Other advantages of chemically modified synthetic surfaces are their higher stability during storage and their low batch-to-batch variability.

An array with different RGD densities in a bioinert background was developed using different concentrations of the immobilized peptide sequence RGDSP (Arg-Gly-Asp-Ser-pro) on ethylene glycol-terminated SAMs. Results demonstrated that higher peptide densities induce higher MSC spreading and focal adhesion formation in the presence of FBS [88]. In fact, it is well known that although surfaces functionalized with RGD motifs can increase hMSC attachment and spreading, its efficacy strongly depends on its surface density [87] and patterning [89]. Surfaces functionalized with RGDs for xeno-free hMSC culture are already commercialized by BD Biosciences (Section 4.6).

4.4. Surface Coatings with Decellularized ECM. Single-protein coatings as the ones described above lack the complexity of cell-secreted ECM. Coatings with decellularized ECM can be used as an alternative to single proteins to improve cell growth and proliferation *in vitro* without the loss of their stem cell properties [90]. To obtain these coatings, hMSCs are cultured on tissue culture plates (or other substrate of interest) for enough time to allow cells to produce their own ECM, after which the coating is decellularized through appropriate processing, leaving only the ECM components. The decellularized ECM coating can be maintained in the original substrate, where subsequent hMSC populations can be directly cultured or can be collected and transferred to other substrate without losing its instructive potential [90].

Lai et al. described the characteristics of an ECM coating produced by hMSC before and after decellularization. Using confocal microscopy, it was possible to visualize the localization of COL I and III, FN, small leucine-rich proteoglycans such as biglycan and decorin, and major components of basement membrane such as the large molecular weight proteoglycan perlecan and LN [91].

A coating with ECM derived from human fetal MSC (fMSC) improved adult hMSC proliferation maintaining their multipotency, in comparison with ECM derived from adult MSC and TCPS. This fact could be related with the higher proliferation capacity of fMSC with associated higher amounts of ECM production [92]. These results are very promising for ex vivo expansion of hMSCs; however, they were not performed in xeno-free conditions. Moreover, the available amount of fMSCs associated with ethical issues could be a concern for this strategy.

The most commonly used decellularization processes are based on the detachment of intact cells using enzymatic processes or the lysis of cells using detergent compounds. However, all these processes have disadvantages, namely, the use of proteases such as trypsin, which can damage the ECM components, and the lysis of cells that can contaminate the resultant ECM with intracellular components. Rao Pattabhi et al. described a new decellularization protocol based on cold EDTA to remove intact cells from ECM without enzymes and detergents and with minimal ECM damage and contamination. They demonstrated that ECM derived from hMSCs obtained using this process enhances the proliferation of naive hMSC maintaining their potential for osteogenesis and adipogenesis [93].

However, all these assays were performed in standard medium containing FBS since their aim is the development of protocols that can enhance hMSC proliferation maintaining their multipotency. Thus, additional experiments are needed to adapt these strategies to xeno-free MSC cultures.

4.5. Surface Modification with GAGs. GAGs are ECM polysaccharides that are involved in a variety of extracellular and intracellular functions and are being widely explored for tissue engineering applications, when used both as surface coatings [94] and as 3D scaffolds for hMSC culture [95, 96].

Heparin is a linear GAG containing several sulphate and carboxyl groups, with a high negative charge density and with several well-characterized binding domains to different growth factors and ECM proteins, such as FGF-2, FN, VN, LN, COL, and bone morphogenetic proteins (BMP) [97, 98].

Heparin-functionalized surfaces may be engineered to attract and bind soluble growth factors, concentrating them on the surface, which avoids the need of using extra high concentrations of soluble growth factors during *in vitro* hMSC expansion. However, besides promoting hMSC adhesion and proliferation, these surfaces also induce osteogenic differentiation in standard culture medium [95]. This fact was associated with heparin ability to sequester from the culture medium not only proteins essential for hMSC adhesion (e.g., FN and VN) and proliferation (e.g., FGF2) but also proteins involved in osteogenic differentiation (e.g., BMPs) [99].

In a different approach, surfaces can be engineered to specifically sequester serum-borne heparin to cell-material interface and thus to attract and bind soluble growth factors. Heparin-binding surfaces were prepared by covalent immobilization of a small heparin-binding peptide (GGGKRTGQYKL) and the integrin-binding peptide (RGDSP) on bioinert SAMs. RGDSP was included to

Table 4: Commercially available coating strategies for hMSC *in vitro* culture.

Name	Company	Composition	Validation (cell types)
Soluble coatings			
CELLstart™	Thermo Fisher	Not disclosed	hMSC, human embryonic stem cells (hESC), and human neural stem cells (hNSC)
Nutristem MSC attachment solution	Biological industries	Affinity-purified human plasma fibronectin	BM-hMSC, AT-hMSC, UC-hMSC
Xuri MSC attachment solution	GE Healthcare	Affinity-purified human plasma fibronectin	Validated for human BM-hMSC, AT-hMSC, and UC-hMSC
Modified plasticware			
BD PureCoat™ ECM Mimetic Cultureware: collagen and fibronectin	Corning	Synthetic animal-free peptides covalently linked to a proprietary surface: (i) fibronectin-derived RGD peptide (ii) collagen I-derived peptide	BM-hMSC and AT-hMSC human umbilical cord blood-derived MSC (isolation)
Corning® Synthemax® Surface	Corning	Peptide acrylate coating functionalized with a vitronectin-derived peptide	Validated for hPSCs and other adult stem cell types

improve cell adhesion to bioinert SAMs. In the presence of FBS, these surfaces were able to enhance hMSC proliferation and osteogenic differentiation by amplifying the activity of endogenous FGF-2 and BMP, respectively [99].

However, it was also suggested that the upregulation of hMSC osteogenic differentiation could be related with heparin-induced alterations on FN conformation. Recent evidences pointed out that heparin induces a more extended conformation of fibrillar FN included in ECM scaffolds. Extended FN may expose hidden binding sites for many growth factors (e.g., FGF-2, BMP-2, and VEGF) that are fundamental on hMSC osteogenic differentiation [100].

4.6. Commercial Coatings and Modified Surfaces for MSC Culture. Different xeno-free protein-based coatings or modified culture surfaces for hMSC culture have been developed and are currently commercially available. Their use is nowadays widespread for hMSC *in vitro* expansion, especially when in combination with serum-free or chemically defined media. Some examples are described in Table 4, which is intended to be illustrative rather than all inclusive.

5. Conclusions

With impressive biological properties, hMSCs are nowadays considered one of the most promising cell types for cellular therapies, already demonstrated in many clinical trials using hMSC. Nevertheless, hMSCs are scarce and to achieve sufficient numbers for cell transplantation, an *in vitro* expansion step is required. This procedure requires improvements in order to guarantee a safe preparation of hMSC as therapeutic products.

Specific challenges concern the substitution of animal components such as FBS during hMSC *in vitro* expansion, since its uses raises scientific, economic, and ethical issues. To improve clinical use of hMSC for advanced therapies, cell culture/expansion under xeno-free conditions should be encouraged. Current strategies include the replacement of FBS with chemically defined media or human plasma derivatives such as hS, hUCBS, hPLs, and a more recent GMP-compliant supplement for cell culture (SCC). Beyond soluble components, recent investigations consist also in the development of refined culture surfaces for hMSC *in vitro* culture: in order to augment the adsorption of adhesive and/or growth-promoting agents, surfaces can be functionalized with adequate chemical groups and modified by immobilization of peptide ligands or whole ECM proteins such as GAGs and FN. However, most of these studies are being conducted in the presence of serum and additional experiments are needed to transpose these strategies to xeno-free MSC cultures.

In recent years, different promising experimental settings have been proposed towards clinical safety of hMSC ex vivo expansion and illustrated herein. However, there is still a lack of standardized protocols for this intent; thus, high-quality translation research and exchange among the numerous research groups interested in the field are demanded.

Conflicts of Interest

The authors declare that they have no conflicts of interest.

Acknowledgments

This work was financed by the European Union 7th Framework Program under the Marie Curie Initial Training Programme Network: IB2 (MC ITN-EID no. 317052[ABP1]), by Project NORTE-01-0145-FEDER-000012, supported by Norte Portugal Regional Operational Programme (NORTE 2020), under the PORTUGAL 2020 Partnership Agreement, through the European Regional Development Fund (ERDF) and by Fundo Europeu de Desenvolvimento Regional (FEDER) funds through the COMPETE 2020—Operacional Programme for Competitiveness and Internationalisation (POCI), Portugal 2020, and by Portuguese funds through Fundação para a Ciência e a Tecnologia (FCT)/Ministério da Ciência, Tecnologia e Ensino Superior in the framework of the project "Institute for Research and Innovation in Health

Sciences" (POCI-01-0145-FEDER-007274). Barrias C. C. (IF/00296/2015) and Gonçalves R. M. (IF/00638/2014) thank FCT for their IF research positions.

References

[1] S. L. Preston, M. R. Alison, S. J. Forbes, N. C. Direkze, R. Poulsom, and N. A. Wright, "The new stem cell biology: something for everyone," *Molecular Pathology*, vol. 56, no. 2, pp. 86–96, 2003.

[2] J. Otto Beitnes, E. Oie, A. Shahdadfar et al., "Intramyocardial injections of human mesenchymal stem cells following acute myocardial infarction modulate scar formation and improve left ventricular function," *Cell Transplantation*, vol. 21, no. 8, pp. 1697–1709, 2012.

[3] J. J. Auletta, S. K. Eid, P. Wuttisarnwattana et al., "Human mesenchymal stromal cells attenuate graft-versus-host disease and maintain graft-versus-leukemia activity following experimental allogeneic bone marrow transplantation," *Stem Cells*, vol. 33, no. 2, pp. 601–614, 2015.

[4] R. E. Newman, D. Yoo, M. A. LeRoux, and A. Danilkovitch-Miagkova, "Treatment of inflammatory diseases with mesenchymal stem cells," *Inflammation & Allergy Drug Targets*, vol. 8, no. 2, pp. 110–123, 2009.

[5] M. Horie, H. Choi, R. H. Lee et al., "Intra-articular injection of human mesenchymal stem cells (MSCs) promote rat meniscal regeneration by being activated to express Indian hedgehog that enhances expression of type II collagen," *Osteoarthritis and Cartilage*, vol. 20, no. 10, pp. 1197–1207, 2012.

[6] J. S. Choi, J. W. Leem, K. H. Lee et al., "Effects of human mesenchymal stem cell transplantation combined with polymer on functional recovery following spinal cord hemisection in rats," *Korean Journal Physiology & Pharmacology*, vol. 16, no. 6, pp. 405–411, 2012.

[7] M. L. Hart, M. L. Hart, J. Brun, K. Lutz, B. Rolauffs, and W. K. Aicher, "Do we need standardized, GMP-compliant cell culture procedures for pre-clinical in vitro studies involving mesenchymal stem/stromal cells?," *Journal of Tissue Science & Engineering*, vol. 5, no. 1, p. 1, 2014.

[8] H. Orbay, M. Tobita, and H. Mizuno, "Mesenchymal stem cells isolated from adipose and other tissues: basic biological properties and clinical applications," *Stem Cells International*, vol. 2012, Article ID 461718, 9 pages, 2012.

[9] M. Zaim, S. Karaman, G. Cetin, and S. Isik, "Donor age and long-term culture affect differentiation and proliferation of human bone marrow mesenchymal stem cells," *Annals of Hematology*, vol. 91, no. 8, pp. 1175–1186, 2012.

[10] K. Bieback, A. Hecker, T. Schlechter et al., "Replicative aging and differentiation potential of human adipose tissue-derived mesenchymal stromal cells expanded in pooled human or fetal bovine serum," *Cytotherapy*, vol. 14, no. 5, pp. 570–583, 2012.

[11] G. A. Tonti and F. Mannello, "From bone marrow to therapeutic applications: different behaviour and genetic/epigenetic stability during mesenchymal stem cell expansion in autologous and foetal bovine sera?," *The International Journal of Developmental Biology*, vol. 52, no. 8, pp. 1023–1032, 2008.

[12] C. Tekkatte, G. P. Gunasingh, K. M. Cherian, and K. Sankaranarayanan, ""Humanized" stem cell culture techniques: the animal serum controversy," *Stem Cells International*, vol. 2011, Article ID 504723, 14 pages, 2011.

[13] J. van der Valk, D. Brunner, K. De Smet et al., "Optimization of chemically defined cell culture media–replacing fetal bovine serum in mammalian in vitro methods," *Toxicology In Vitro*, vol. 24, no. 4, pp. 1053–1063, 2010.

[14] D. Brunner, J. Frank, H. Appl, H. Schöffl, W. Pfaller, and G. Gstraunthaler, "Serum-free cell culture: the serum-free media interactive online database," *ALTEX*, vol. 27, no. 1, pp. 53–62, 2010.

[15] M. M. Lalu, L. McIntyre, C. Pugliese et al., "Safety of cell therapy with mesenchymal stromal cells (SafeCell): a systematic review and meta-analysis of clinical trials," *PLoS One*, vol. 7, no. 10, article e47559, 2012.

[16] U. Bjare, "Serum-free cell culture," *Pharmacology & Therapeutics*, vol. 53, no. 3, pp. 355–374, 1992.

[17] J. Wappler, B. Rath, T. Läufer, A. Heidenreich, and K. Montzka, "Eliminating the need of serum testing using low serum culture conditions for human bone marrow-derived mesenchymal stromal cell expansion," *Biomedical Engineering Online*, vol. 12, p. 15, 2013.

[18] P. A. Knepper, C. S. Mayanil, W. Goossens, D. C. McLone, and E. Hayes, "The presence of transcription factors in fetal bovine sera," *In Vitro Cellular & Developmental Biology - Animal*, vol. 34, no. 2, pp. 170–173, 1998.

[19] X. Zheng, H. Baker, W. S. Hancock, F. Fawaz, M. McCaman, and E. Pungor Jr., "Proteomic analysis for the assessment of different lots of fetal bovine serum as a raw material for cell culture. Part IV. Application of proteomics to the manufacture of biological drugs," *Biotechnology Progress*, vol. 22, no. 5, pp. 1294–1300, 2006.

[20] The European Parliament and the Council of the European Union, "Directive 2004/23/EC of the European Parliament and of the council on setting standards of quality and safety for the donation, procurement, testing, processing, preservation, storage and distribution of human tissues and cells," *Official Journal of the European Union*, vol. 7.4, 2004L 102/48-58.

[21] The European Commission, "Commission Directive (EU) 2015/566 of 8 April 2015 implementing directive 2004/23/EC as regards the procedures for verifying the equivalent standards of quality and safety of imported tissues and cells," *Official Journal of the European Union*, vol. 9.4, no. 56–68, 2015L 93/56.

[22] P. A. De Sousa, G. Galea, and M. Turner, "The road to providing human embryo stem cells for therapeutic use: the UK experience," *Reproduction*, vol. 132, no. 5, pp. 681–689, 2006.

[23] T. F. Pinheiro de Oliveira, A. A. Fonseca Jr., M. F. Camargos et al., "Detection of contaminants in cell cultures, sera and trypsin," *Biologicals*, vol. 41, no. 6, pp. 407–414, 2013.

[24] M. Wisher, "Virus risk mitigation for raw materials," *Bioprocess International*, vol. 11, no. 9, pp. 37–39, 2013.

[25] L. Nikfarjam and P. Farzaneh, "Prevention and detection of mycoplasma contamination in cell culture," *Cell Journal*, vol. 13, no. 4, pp. 203–212, 2012.

[26] S. Rottem and M. F. Barile, "Beware of mycoplasmas," *Trends in Biotechnology*, vol. 11, no. 4, pp. 143–151, 1993.

[27] H. M. Windsor, G. D. Windsor, and J. H. Noordergraaf, "The growth and long term survival of Acholeplasma laidlawii in media products used in biopharmaceutical manufacturing," *Biologicals*, vol. 38, no. 2, pp. 204–210, 2010.

[28] C. E. Jochems, J. B. van der Valk, F. R. Stafleu, and V. Baumans, "The use of fetal bovine serum: ethical or scientific problem?,"

Alternatives to Laboratory Animals, vol. 30, no. 2, pp. 219–227, 2002.

[29] D. A. Brindley, N. L. Davie, E. J. Culme-Seymour, C. Mason, D. W. Smith, and J. A. Rowley, "Peak serum: implications of serum supply for cell therapy manufacturing," *Regenerative Medicine*, vol. 7, no. 1, pp. 7–13, 2012.

[30] P. Mark, M. Kleinsorge, R. Gaebel et al., "Human mesenchymal stem cells display reduced expression of CD105 after culture in serum-free medium," *Stem Cells International*, vol. 2013, Article ID 698076, 8 pages, 2013.

[31] P. J. Dolley-Sonneville, L. E. Romeo, and Z. K. Melkoumian, "Synthetic surface for expansion of human mesenchymal stem cells in xeno-free, chemically defined culture conditions," *PLoS One*, vol. 8, no. 8, article e70263, 2013.

[32] S. Gottipamula, M. S. Muttigi, S. Chaansa et al., "Large-scale expansion of pre-isolated bone marrow mesenchymal stromal cells in serum-free conditions," *Journal of Tissue Engineering and Regenerative Medicine*, vol. 10, no. 2, pp. 108–119, 2016.

[33] N. Stute, K. Holtz, M. Bubenheim, C. Lange, F. Blake, and A. R. Zander, "Autologous serum for isolation and expansion of human mesenchymal stem cells for clinical use," *Experimental Hematology*, vol. 32, no. 12, pp. 1212–1225, 2004.

[34] N. Yamamoto, M. Isobe, A. Negishi et al., "Effects of autologous serum on osteoblastic differentiation in human bone marrow cells," *Journal of Medical and Dental Sciences*, vol. 50, no. 1, pp. 63–69, 2003.

[35] Y. Shigeno and B. A. Ashton, "Human bone-cell proliferation in vitro decreases with human donor age," *Journal of Bone and Joint Surgery*, vol. 77, no. 1, pp. 139–142, 1995.

[36] S. Jung, K. M. Panchalingam, L. Rosenberg, and L. A. Behie, "*Ex vivo* expansion of human mesenchymal stem cells in defined serum-free media," *Stem Cells International*, vol. 2012, Article ID 123030, 21 pages, 2012.

[37] J. L. Spees, C. A. Gregory, H. Singh et al., "Internalized antigens must be removed to prepare hypoimmunogenic mesenchymal stem cells for cell and gene therapy," *Molecular Therapy*, vol. 9, 2004.

[38] M. J. Martin, A. Muotri, F. Gage, and A. Varki, "Human embryonic stem cells express an immunogenic nonhuman sialic acid," *Nature Medicine*, vol. 11, no. 2, pp. 228–232, 2005.

[39] N. Hashii, N. Kawasaki, Y. Nakajima et al., "Study on the quality control of cell therapy products. Determination of N-glycolylneuraminic acid incorporated into human cells by nano-flow liquid chromatography/Fourier transformation ion cyclotron mass spectrometry," *Journal of Chromatography A*, vol. 1160, no. 1-2, pp. 263–269, 2007.

[40] A. Heiskanen, T. Satomaa, S. Tiitinen et al., "N-glycolylneuraminic acid xenoantigen contamination of human embryonic and mesenchymal stem cells is substantially reversible," *Stem Cells*, vol. 25, no. 1, pp. 197–202, 2007.

[41] K. Witzeneder, A. Lindenmair, C. Gabriel et al., "Human-derived alternatives to fetal bovine serum in cell culture," *Transfusion Medicine and Hemotherapy*, vol. 40, no. 6, pp. 417–423, 2013.

[42] M. Yamaguchi, F. Hirayama, S. Wakamoto et al., "Bone marrow stromal cells prepared using AB serum and bFGF for hematopoietic stem cells expansion," *Transfusion*, vol. 42, no. 7, pp. 921–927, 2002.

[43] A. Kocaoemer, S. Kern, H. Klüter, and K. Bieback, "Human AB serum and thrombin-activated platelet-rich plasma are suitable alternatives to fetal calf serum for the expansion of mesenchymal stem cells from adipose tissue," *Stem Cells*, vol. 25, no. 5, pp. 1270–1278, 2007.

[44] R. O. Oreffo, A. S. Virdi, and J. T. Triffitt, "Modulation of osteogenesis and adipogenesis by human serum in human bone marrow cultures," *European Journal of Cell Biology*, vol. 74, no. 3, pp. 251–261, 1997.

[45] K. Anselme, O. Broux, B. Noel et al., "In vitro control of human bone marrow stromal cells for bone tissue engineering," *Tissue Engineering*, vol. 8, no. 6, pp. 941–953, 2002.

[46] S. A. Kuznetsov, M. H. Mankani, and P. G. Robey, "Effect of serum on human bone marrow stromal cells: ex vivo expansion and in vivo bone formation," *Transplantation*, vol. 70, no. 12, pp. 1780–1787, 2000.

[47] A. Aldahmash, M. Haack-Sørensen, M. Al-Nbaheen, L. Harkness, B. M. Abdallah, and M. Kassem, "Human serum is as efficient as fetal bovine serum in supporting proliferation and differentiation of human multipotent stromal (mesenchymal) stem cells in vitro and in vivo," *Stem Cell Reviews*, vol. 7, no. 4, pp. 860–868, 2011.

[48] O. Holmqvist and B. Westermark, *Blood Platelet Lysate, Method of Its Preparation and a Cell Culture Medium Containing Said Blood Platelet*, European Patent Office, 1994.

[49] C. Rauch, E. Feifel, E. M. Amann et al., "Alternatives to the use of fetal bovine serum: human platelet lysates as a serum substitute in cell culture media," *ALTEX*, vol. 28, no. 4, pp. 305–316, 2011.

[50] G. Walenda, H. Hemeda, R. K. Schneider, R. Merkel, B. Hoffmann, and W. Wagner, "Human platelet lysate gel provides a novel three dimensional-matrix for enhanced culture expansion of mesenchymal stromal cells," *Tissue Engineering Part C, Methods*, vol. 18, no. 12, pp. 924–934, 2012.

[51] S. M. Jonsdottir-Buch, R. Lieder, and O. E. Sigurjonsson, "Platelet lysates produced from expired platelet concentrates support growth and osteogenic differentiation of mesenchymal stem cells," *PLoS One*, vol. 8, no. 7, article e68984, 2013.

[52] K. Hanada, J. E. Dennis, and A. I. Caplan, "Stimulatory effects of basic fibroblast growth factor and bone morphogenetic protein-2 on osteogenic differentiation of rat bone marrow-derived mesenchymal stem cells," *Journal of Bone and Mineral Research*, vol. 12, no. 10, pp. 1606–1614, 1997.

[53] C. Doucet, I. Ernou, Y. Zhang et al., "Platelet lysates promote mesenchymal stem cell expansion: a safety substitute for animal serum in cell-based therapy applications," *Journal of Cellular Physiology*, vol. 205, no. 2, pp. 228–236, 2005.

[54] M. Sanchez, E. Anitua, G. Orive, I. Mujika, and I. Andia, "Platelet-rich therapies in the treatment of orthopaedic sport injuries," *Sports Medicine*, vol. 39, no. 5, pp. 345–354, 2009.

[55] A. Dugrillon, H. Eichler, S. Kern, and H. Klüter, "Autologous concentrated platelet-rich plasma (cPRP) for local application in bone regeneration," *International Journal of Oral and Maxillofacial Surgery*, vol. 31, no. 6, pp. 615–619, 2002.

[56] J. Bartunek, A. Behfar, D. Dolatabadi et al., "Cardiopoietic stem cell therapy in heart failure: the C-CURE (cardiopoietic stem cell therapy in heart failure) multicenter randomized trial with lineage-specified biologics," *Journal of the American College of Cardiology*, vol. 61, no. 23, pp. 2329–2338, 2013.

[57] M. Lohmann, G. Walenda, H. Hemeda et al., "Donor age of human platelet lysate affects proliferation and differentiation

of mesenchymal stem cells," *PLoS One*, vol. 7, no. 5, article e37839, 2012.

[58] K. Schallmoser and D. Strunk, "Generation of a pool of human platelet lysate and efficient use in cell culture," *Methods in Molecular Biology*, vol. 946, pp. 349–362, 2013.

[59] S. Castiglia, K. Mareschi, L. Labanca et al., "Inactivated human platelet lysate with psoralen: a new perspective for mesenchymal stromal cell production in good manufacturing practice conditions," *Cytotherapy*, vol. 16, no. 6, pp. 750–763, 2014.

[60] S. M. Phadnis, M. V. Joglekar, V. Venkateshan, S. M. Ghaskadbi, A. A. Hardikar, and R. R. Bhonde, "Human umbilical cord blood serum promotes growth, proliferation, as well as differentiation of human bone marrow-derived progenitor cells," *In Vitro Cellular & Developmental Biology - Animal*, vol. 42, no. 10, pp. 283–286, 2006.

[61] J. Jung, N. Moon, J. Y. Ahn et al., "Mesenchymal stromal cells expanded in human allogenic cord blood serum display higher self-renewal and enhanced osteogenic potential," *Stem Cells and Development*, vol. 18, no. 4, pp. 559–571, 2009.

[62] R. Victor, P. A. Rao, V. A. Rao et al., "Use of umbilical cord serum in chromosomal studies," *International Journal of Human Genetics*, vol. 7, no. 2, pp. 163–166, 2007.

[63] J. M. Díez, E. Bauman, R. Gajardo, and J. I. Jorquera, "Culture of human mesenchymal stem cells using a candidate pharmaceutical grade xeno-free cell culture supplement derived from industrial human plasma pools," *Stem Cell Research & Therapy*, vol. 6, no. 1, p. 28, 2015.

[64] E. J. Cohn, L. E. Strong, W. Hughes et al., "Preparation and properties of serum and plasma proteins. IV. A system for the separation into fractions of the protein and lipoprotein components of biological tissues and fluids1a,b,c,d," *Journal of the American Chemical Society*, vol. 68, pp. 459–475, 1946.

[65] I. Rodriguez-Piza, Y. Richaud-Patin, R. Vassena et al., "Reprogramming of human fibroblasts to induced pluripotent stem cells under xeno-free conditions," *Stem Cells*, vol. 28, 2010.

[66] E. Hohenester and J. Engel, "Domain structure and organisation in extracellular matrix proteins," *Matrix Biology*, vol. 21, no. 2, pp. 115–128, 2002.

[67] C. C. Barrias, M. C. Martins, G. Almeida-Porada, M. A. Barbosa, and P. L. Granja, "The correlation between the adsorption of adhesive proteins and cell behaviour on hydroxyl-methyl mixed self-assembled monolayers," *Biomaterials*, vol. 30, no. 3, pp. 307–316, 2009.

[68] B. Li, C. Moshfegh, Z. Lin, J. Albuschies, and V. Vogel, "Mesenchymal stem cells exploit extracellular matrix as mechanotransducer," *Scientific Reports*, vol. 3, p. 2425, 2013.

[69] S. Jung, A. Sen, L. Rosenberg, and L. A. Behie, "Identification of growth and attachment factors for the serum-free isolation and expansion of human mesenchymal stromal cells," *Cytotherapy*, vol. 12, no. 5, pp. 637–657, 2010.

[70] E. F. Plow, T. A. Haas, L. Zhang, J. Loftus, and J. W. Smith, "Ligand binding to integrins," *The Journal of Biological Chemistry*, vol. 275, no. 29, pp. 21785–21788, 2000.

[71] L. Qian and W. M. Saltzman, "Improving the expansion and neuronal differentiation of mesenchymal stem cells through culture surface modification," *Biomaterials*, vol. 25, no. 7-8, pp. 1331–1337, 2004.

[72] A. Ode, G. N. Duda, J. D. Glaeser et al., "Toward biomimetic materials in bone regeneration: functional behavior of mesenchymal stem cells on a broad spectrum of extracellular matrix components," *Journal of Biomedical Materials Research Part A*, vol. 95, no. 4, pp. 1114–1124, 2010.

[73] K. J. Hamill, A. S. Paller, and J. C. Jones, "Adhesion and migration, the diverse functions of the laminin $\alpha 3$ subunit," *Dermatologic Clinics*, vol. 28, no. 1, pp. 79–87, 2010.

[74] R. M. Salasznyk, W. A. Williams, A. Boskey, A. Batorsky, and G. E. Plopper, "Adhesion to vitronectin and collagen I promotes osteogenic differentiation of human mesenchymal stem cells," *Journal of Biomedicine & Biotechnology*, vol. 2004, no. 1, pp. 24–34, 2004.

[75] J. Hashimoto, Y. Kariya, and K. Miyazaki, "Regulation of proliferation and chondrogenic differentiation of human mesenchymal stem cells by laminin-5 (laminin-332)," *Stem Cells*, vol. 24, no. 11, pp. 2346–2354, 2006.

[76] N. Ogura, M. Kawada, W. J. Chang et al., "Differentiation of the human mesenchymal stem cells derived from bone marrow and enhancement of cell attachment by fibronectin," *Journal of Oral Science*, vol. 46, no. 4, pp. 207–213, 2004.

[77] S. N. Rodrigues, I. C. Gonçalves, M. C. Martins, M. A. Barbosa, and B. D. Ratner, "Fibrinogen adsorption, platelet adhesion and activation on mixed hydroxyl-/methyl-terminated self-assembled monolayers," *Biomaterials*, vol. 27, no. 31, pp. 5357–5367, 2006.

[78] D. Salzig, J. Leber, K. Merkewitz, M. C. Lange, N. Köster, and P. Czermak, "Attachment, growth, and detachment of human mesenchymal stem cells in a chemically defined medium," *Stem Cells International*, vol. 2016, Article ID 5246584, 10 pages, 2016.

[79] F. Mittag, E. M. Falkenberg, A. Janczyk et al., "Laminin-5 and type I collagen promote adhesion and osteogenic differentiation of animal serum-free expanded human mesenchymal stromal cells," *Orthopedic Reviews*, vol. 4, no. 4, article e36, 2012.

[80] J. E. Phillips, T. A. Petrie, F. P. Creighton, and A. J. García, "Human mesenchymal stem cell differentiation on self-assembled monolayers presenting different surface chemistries," *Acta Biomaterialia*, vol. 6, no. 1, pp. 12–20, 2010.

[81] P. Hartrianti, L. Ling, L. M. Goh et al., "Modulating mesenchymal stem cell behavior using human hair keratin-coated surfaces," *Stem Cells International*, vol. 2015, Article ID 752424, 9 pages, 2015.

[82] B. Mattiasson, A. Kumar, and I. Y. Galeaev, Eds., *Macroporous Polymers: Production Properties and Biotechnological/Biomedical Applications*, CRC Press, 2009.

[83] M. Bergkvist, J. Carlsson, and S. Oscarsson, "Surface-dependent conformations of human plasma fibronectin adsorbed to silica, mica, and hydrophobic surfaces, studied with use of atomic force microscopy," *Journal of Biomedical Materials Research, Part A*, vol. 64, no. 2, pp. 349–356, 2003.

[84] A. Dolatshahi-Pirouz, T. H. Jensen, K. Kolind et al., "Cell shape and spreading of stromal (mesenchymal) stem cells cultured on fibronectin coated gold and hydroxyapatite surfaces," *Colloids and Surfaces, B: Biointerfaces*, vol. 84, no. 1, pp. 18–25, 2011.

[85] J. M. Curran, R. Chen, and J. A. Hunt, "The guidance of human mesenchymal stem cell differentiation in vitro by controlled modifications to the cell substrate," *Biomaterials*, vol. 27, no. 27, pp. 4783–4793, 2006.

[86] M. Mrksich, "What can surface chemistry do for cell biology?," *Current Opinion in Chemical Biology*, vol. 6, no. 6, pp. 794–797, 2002.

[87] A. A. Sawyer, K. M. Hennessy, and S. L. Bellis, "Regulation of mesenchymal stem cell attachment and spreading on hydroxyapatite by RGD peptides and adsorbed serum proteins," *Biomaterials*, vol. 26, no. 13, pp. 1467–1475, 2005.

[88] J. T. Koepsel and W. L. Murphy, "Patterning discrete stem cell culture environments via localized self-assembled monolayer replacement," *Langmuir*, vol. 25, no. 21, pp. 12825–12834, 2009.

[89] X. Wang, K. Ye, Z. Li, C. Yan, and J. Ding, "Adhesion, proliferation, and differentiation of mesenchymal stem cells on RGD nanopatterns of varied nanospacings," *Organogenesis*, vol. 9, no. 4, pp. 280–286, 2013.

[90] M. L. Decaris and J. K. Leach, "Design of experiments approach to engineer cell-secreted matrices for directing osteogenic differentiation," *Annals of Biomedical Engineering*, vol. 39, no. 4, pp. 1174–1185, 2011.

[91] Y. Lai, Y. Sun, C. M. Skinner et al., "Reconstitution of marrow-derived extracellular matrix ex vivo: a robust culture system for expanding large-scale highly functional human mesenchymal stem cells," *Stem Cells and Development*, vol. 19, no. 7, pp. 1095–1107, 2010.

[92] C. P. Ng, A. R. Sharif, D. E. Heath et al., "Enhanced ex vivo expansion of adult mesenchymal stem cells by fetal mesenchymal stem cell ECM," *Biomaterials*, vol. 35, no. 13, pp. 4046–4057, 2014.

[93] S. Rao Pattabhi, J. S. Martinez, and T. C. S. Keller, "Decellularized ECM effects on human mesenchymal stem cell stemness and differentiation," *Differentiation: Research in Biological Diversity*, vol. 88, no. 4-5, pp. 131–143, 2014.

[94] B. E. Uygun, S. E. Stojsih, and H. W. Matthew, "Effects of immobilized glycosaminoglycans on the proliferation and differentiation of mesenchymal stem cells," *Tissue Engineering Part A*, vol. 15, no. 11, pp. 3499–3512, 2009.

[95] D. S. Benoit, A. R. Durney, and K. S. Anseth, "The effect of heparin-functionalized PEG hydrogels on three-dimensional human mesenchymal stem cell osteogenic differentiation," *Biomaterials*, vol. 28, no. 1, pp. 66–77, 2007.

[96] L. Gilmore, S. Rimmer, S. L. McArthur, S. Mittar, D. Sun, and S. MacNeil, "Arginine functionalization of hydrogels for heparin binding-a supramolecular approach to developing a pro-angiogenic biomaterial," *Biotechnology and Bioengineering*, vol. 110, no. 1, pp. 296–317, 2013.

[97] R. Padera, G. Venkataraman, D. Berry, R. Godavarti, and R. Sasisekharan, "FGF-2/fibroblast growth factor receptor/heparin-like glycosaminoglycan interactions: a compensation model for FGF-2 signaling," *The FASEB Journal*, vol. 13, no. 13, pp. 1677–1687, 1999.

[98] A. Varki, R. D. Cummings, J. D. Esko et al., *Essentials of Glycobiology*, Cold Spring Harbor Laboratory Press, New York, NY, USA, 2nd edition, 2009.

[99] G. A. Hudalla, N. A. Kouris, J. T. Koepsel, B. M. Ogle, and W. L. Murphy, "Harnessing endogenous growth factor activity modulates stem cell behavior," *Integrative Biology (Camb)*, vol. 3, no. 8, pp. 832–842, 2011.

[100] B. Li, Z. Lin, M. Mitsi, Y. Zhang, and V. Vogel, "Heparin-induced conformational changes of fibronectin within the extracellular matrix promote hMSC osteogenic differentiation," *Biomaterials Science*, vol. 3, no. 1, pp. 73–84, 2015.

[101] G. M. Forbes, M. J. Sturm, R. W. Leong et al., "A phase 2 study of allogeneic mesenchymal stromal cells for luminal Crohn's disease refractory to biologic therapy," *Clinical Gastroenterology and Hepatology*, vol. 12, no. 1, pp. 64–71, 2014.

[102] J. S. Lee, J. M. Hong, G. J. Moon et al., "A long-term follow-up study of intravenous autologous mesenchymal stem cell transplantation in patients with ischemic stroke," *Stem Cells*, vol. 28, no. 6, pp. 1099–1106, 2010.

[103] O. Y. Bang, J. S. Lee, P. H. Lee, and G. Lee, "Autologous mesenchymal stem cell transplantation in stroke patients," *Annals of Neurology*, vol. 57, no. 6, pp. 874–882, 2005.

[104] L. Mazzini, K. Mareschi, I. Ferrero et al., "Stem cell treatment in amyotrophic lateral sclerosis," *Journal of the Neurological Sciences*, vol. 265, no. 1-2, pp. 78–83, 2008.

[105] K. Le Blanc, I. Rasmusson, B. Sundberg et al., "Treatment of severe acute graft-versus-host disease with third party haploidentical mesenchymal stem cells," *Lancet*, vol. 363, no. 9419, pp. 1439–1441, 2004.

[106] O. N. Koc, S. L. Gerson, B. W. Cooper et al., "Rapid hematopoietic recovery after coinfusion of autologous-blood stem cells and culture-expanded marrow mesenchymal stem cells in advanced breast cancer patients receiving high-dose chemotherapy," *Journal of Clinical Oncology*, vol. 18, no. 2, pp. 307–316, 2000.

[107] S. L. Chen, W. W. Fang, F. Ye et al., "Effect on left ventricular function of intracoronary transplantation of autologous bone marrow mesenchymal stem cell in patients with acute myocardial infarction," *The American Journal of Cardiology*, vol. 94, no. 1, pp. 92–95, 2004.

Hindawi
Stem Cells International
Volume 2017, Article ID 1764523, 12 pages
https://doi.org/10.1155/2017/1764523

Research Article

Tissue Engineering to Repair Diaphragmatic Defect in a Rat Model

G. P. Liao,[1] Y. Choi,[1,2] K. Vojnits,[1,2] H. Xue,[1] K. Aroom,[1] F. Meng,[1,2] H. Y. Pan,[1,2,3] R. A. Hetz,[1] C. J. Corkins,[1] T. G. Hughes,[1] F. Triolo,[1] A. Johnson,[4] Kenneth J. Moise Jr,[4] K. P. Lally,[1] C. S. Cox Jr.,[1,2] and Y. Li[1,2,3]

[1]*Department of Pediatric Surgery, University of Texas, McGovern Medical School at Houston, Houston, TX, USA*
[2]*Center for Stem Cell and Regenerative Medicine, University of Texas Health Science Center at Houston (UT Health), Houston, TX 77030, USA*
[3]*Department of Orthopaedic Surgery, University of Texas, McGovern Medical School at Houston, Houston, TX, USA*
[4]*Department of Obstetrics, Gynecology, and Reproductive Sciences, University of Texas, McGovern Medical School at Houston, Houston, TX 77030, USA*

Correspondence should be addressed to C. S. Cox Jr.; charles.s.cox@uth.tmc.edu and Y. Li; yong.li.1@uth.tmc.edu

Received 2 March 2017; Revised 16 May 2017; Accepted 25 May 2017; Published 27 August 2017

Academic Editor: Heidi Declercq

Copyright © 2017 G. P. Liao et al. This is an open access article distributed under the Creative Commons Attribution License, which permits unrestricted use, distribution, and reproduction in any medium, provided the original work is properly cited.

Tissue engineering is an emerging strategy for repairing damaged tissues or organs. The current study explored using decellularized rat diaphragm scaffolds combined with human amniotic fluid-derived multipotent stromal cells (hAFMSC) to provide a scaffold, stem cell construct that would allow structural barrier function during tissue ingrowth/regeneration. We created an innovative cell infusion system that allowed hAFMSC to embed into scaffolds and then implanted the composite tissues into rats with surgically created left-sided diaphragmatic defects. Control rats received decellularized diaphragm scaffolds alone. We found that the composite tissues that combined hAFMSCs demonstrated improved physiological function as well as the muscular-tendon structure, compared with the native contralateral hemidiaphragm of the same rat. Our results indicate that the decellularized diaphragm scaffolds are a potential support material for diaphragmatic hernia repair and the composite grafts with hAFMSC are able to accelerate the functional recovery of diaphragmatic hernia.

1. Introduction

Tissue engineering technologies have developed rapidly in the last decade. Several successful bioengineered tissues are undergoing evaluation in clinical trials. Recently, decellularized tissue has been used as a scaffold to grow organs, including a functional heart, lung, intestines, and other organs [1, 2]. The process of decellularization can remove resident cells from the donor organs or tissues using detergent and mechanical agitation, leaving a three-dimensional (3D) extracellular matrix (ECM) scaffold that can be reseeded with new progenitor cells or composites [3–5]. The benefits of decellularized ECM scaffolds include preservation of the natural organ architecture as well as maintenance of microvascular networks [4, 6, 7]. Thus, decellularized scaffolds have gained popularity and are becoming a common scaffold for whole organ regeneration. In larger organs with intact macrovasculature, recellularization with stem cells can be accomplished by intravascular infusion. In smaller tissues, this is more difficult. To overcome this in our model, we developed a perfusion apparatus to allow pressurized donor cell infusion into an ECM scaffold.

Congenital diaphragmatic hernia (CDH) is a congenital diaphragmatic defect associated with pulmonary hypertension and cardiopulmonary failure that continues to present a challenge for neonatologists and pediatric surgeons [8–10]. While the incidence of CDH varies between 1 : 2000–4000 live births, the hospital costs exceeds 100 times the cost of an uncomplicated birth [11]. Small defects described as types A and B by the Congenital Diaphragmatic Hernia Study Group can be repaired primarily [12]. However, larger types C and D defects require patch repair [13]. Although the early mortality associated with CDH has decreased to 5–10% due to improved neonatal intensive care,

the long-term morbidity associated with patch repairs remains significant, including musculoskeletal chest wall deformities (67%), scoliosis (13%) as well as small bowel obstruction (13%), and failure to thrive (78%) with many infants at less than 50% percentile in weight at 24 months post discharge [14, 15]. In the last decade, clinical and preclinical investigators have been investigating the use of biological patches for CDH repair and have included lyophilized dura, small intestine submucosa (SIS), and acellular dermis (Alloderm®) [16–18]. Biological patches alone have failed due to lack of tissue ingrowth with subsequent resorption of the patches, poor immediate strength, rupture, neighbor tissue adhesions, and fibrosis. Tissue-engineered patches for CDH repair seek to improve biomechanical compatibility while reducing recurrent hernia [18–23]. Decellularized ECM scaffolds have the potential of regenerating the structure and function of their native tissue over commercially available matrices from other tissues. Those decellularized ECM scaffolds have been used in combination with stem cells to construct composite tissues that have been utilized successfully in tissue repair, including diaphragmatic repair [23–25]. While the current practice of PTFE/Gore-tex® patch repair is reasonably effective with acceptable rates of recurrence and infection, a simple biologic tissue could represent an advantage, especially on the large diaphragmatic defects.

In the current study, we explored using a biological patch comprised of decellularized ECM scaffolds from rat diaphragms seeded with human amniotic fluid-derived multipotent stromal cells (hAFMSC), to repair a surgical diaphragmatic defect in a rat model. Structural and functional measures were used to define treatment outcome. We aimed to test whether a decellularized ECM scaffold recellularized with amniotic-derived stem cells can construct a functional composite tissue for diaphragmatic defect repair in a rat model.

2. Materials and Methods

2.1. Decellularized ECM Scaffolds from Rat Diaphragms. The procedure of tissue decellularization is to effectively remove cellular components and residual DNA, but keep the physicochemical structure of the ECM to support seeding cells' survival in a 3D architecture [25, 26]. Our protocol includes (1) excision of the rat hemidiaphragm in a sterile environment; (2) put the diaphragm in a tube with 40 mL PBS (50 mL, BD); (3) transfer the diaphragm into a 50 mL tube prefilled with 0.5% SDS; (4) attach tube to rocker (Nutator, number 421105, Beckton Dickinson, MD) and rotate for 0.5/sec for 24 hours; (5) transfer the diaphragm to a fresh tube prefilled with 0.5% sodium dodecyl sulfate (SDS) and rotate for 24 hours; (6) transfer the decellularized tissue into a 50 mL tube with sterile PBS and wash during rotation for 24 hours; and (7) leave the tissue in PBS and store at 4°C.

2.2. Mechanical Testing for Rat Diaphragm or Decellularized ECM Scaffolds. Six Sprague Dawley (SD) adult rats (female, 150–175 grams, approximately 7-8 weeks old, Charles River Lab.) were used to biotype donor diaphragms. After successful decellularization, the rat diaphragm ECM tissues were prepared as 5 mm wide × 10 mm long strips and mounted in a physiological perfusion chamber, interfaced to a force transducer that measures contractile force via a multitier Power Lab monitor (Experimetria Ltd. Balatonfured, Hungary). Once the tissue is mounted on the transducer, the hook and thread connected to the transducer are pulled taut so any subsequent contractions pull the force transducer down, displacing the sensor. This displacement, enhanced by the amplifier, is then graphically displayed on the computer screen versus time. Maximum force readings of ~6.0 grams were set for these measurements, since over 6.0 tears the ECM scaffolds.

2.3. Transmission Electron Microscopy (TEM) Scans for Decellularized ECM Scaffolds. Samples of ECM scaffolds were fixed with a TEM preparing solution containing 3% glutaraldehyde plus 2% paraformaldehyde in 0.1 M cacodylate buffer (pH 7.3), for 1 hour at ambient temperature, and then washed with cacodylate buffer (0.1 M, pH 7.3) for 3 × 10 minutes. After fixation, the samples were sequentially treated with Millipore-filtered 1% aqueous tannic acid for 30 minutes and 1% aqueous uranyl acetate for 1 hour in the dark. Then, the samples were dehydrated with a series of increasing concentrations of ethanol for 5 minutes each and then transferred to a series of increasing concentrations of hexamethyldisilazane (HMDS, 5 minutes each) and air-dried overnight. Samples were mounted on to double-stick carbon tabs (Ted Pella, Inc., Redding, CA), which had been previously mounted on to aluminum specimen mounts (Electron Microscopy Sciences, Ft. Washington, PA), and then coated under vacuum using a Balzer MED 010 evaporator (Technotrade International, Manchester, NH) with platinum alloy for a thickness of 25 nm and then immediately flash carbon coated under vacuum. The samples were transferred to a desiccator for examination at a later date. All samples were read in a JSM-5910 scanning electron microscope (JEOL, USA, Inc., Peabody, MA) at an accelerating voltage of 5 kV.

2.4. hAFMSC Isolation and Identification. hAFMSCs were isolated via amniocentesis (2–5 mL) from pregnant women (18 years and older, at least 16 weeks 0/7 days pregnant in sterile fashion during routine diagnostic amniocenteses from patients at the Texas Center for Maternal and Fetal Treatment (Institutional Review Board HSC-MS-111-0593). These samples were stored at 5°C after collection and processed within 48 hours from procurement (Institutional Biosafety Committee). Sample processing, including the isolation and expansion, was carried out in an ISO7 human cell production facility, in compliance with current good manufacturing practice (cGMP) guidelines of the Food and Drug Administration (FDA). These cells were identified based on their surface markers by immunostaining with flow cytometry analysis. We selected one donor-derived hAFMSC for the current study (from a 33-year-old healthy Caucasian female, nonhispanic donor at gestational age 20 weeks). The selected hAFMSCs were prelabeled with green fluorescent protein (GFP) as a track

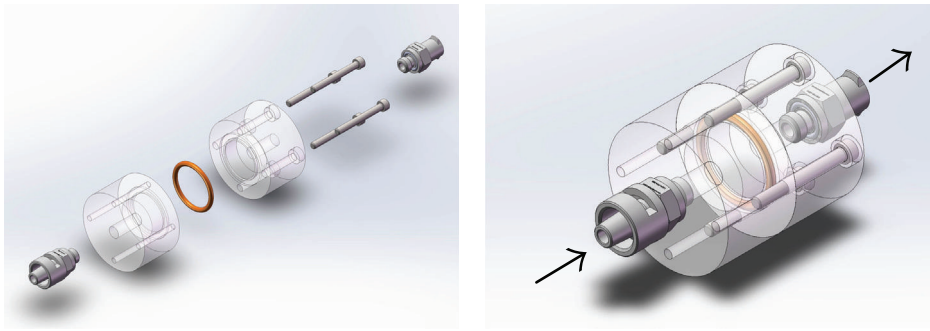

(a) (b)

Figure 1: A scheme design of cellular infusion system. Two acrylic cylindrical paths allow pressurized perfusion of cell containing medium through a scaffold that results in cell seeding of the various layers of the scaffold. (a) Infusion system components. (b) Medium flow direction.

marker by using a lentivirus vector (Invitrogen) according to the manufacturer's instruction.

Following expansion, the aliquots were stored in liquid nitrogen for further studies. To confirm immunophenotype and differentiation capacity, hAFMSCs were tested for hallmarks via cell surface markers: CD90, CD73, CD45, CD34, CD29, CD106, CD10, CD13, HLA-ABC, and HLA-DR by flow cytometry, consistent with the International Society for Cellular Therapy (ISCT) definition of mesenchymal stem cells (MSCs) cell surface markers. We also evaluated their multiple-differentiation abilities in vitro, including osteogenic, adipogenic, chondrogenic, and myogenic differentiation, as described by others and in our previous reports [27–31].

2.5. Design and Creation of an Infusion System for Cell Seeding. An infusion system was designed to create a uniform distribution of donor cells within a scaffold (Figure 1). The flow/medium influence is able to transport donor cells and distribute into the deep portion of decellularized ECMs. Briefly, donor diaphragm ECM scaffolds (adult female rats) were sandwiched in an infusion chamber, with media and cells pushed across the scaffold via hydrostatic pressure. The chamber consists of two pieces of polycarbonate, a sealing O-ring, luer connector fittings, and a set of machine screws to secure the polycarbonate pieces together. An exploded and assembled view of a CAD model of the device is shown in Figures 1(a) and 1(b), respectively. The polycarbonate pieces were milled from stock $1''$ rod to create a small fluid chamber, a through-hole down the center, several through-holes circumferentially, and a small groove to allow for proper seating of the O-ring. The center through-holes were threaded to accept a luer fitting. The circumferential holes of one of the polycarbonate parts were also threaded to accept the clamping screws. After machining, the parts were vapor polished using dichloromethane to improve optical transparency of the device. For each ECM, we seeded it in 1×10^4 fAFMSC (diluted in 1 mL PBS); subsequently, those composite tissues were transported (4°C) for surgery to repair the diaphragm defects created in the rat model.

2.6. Surgical Repair Diaphragmatic Defect in a Rat Model. All surgical procedures were approved by the Animal Welfare Committee (AWC) of the McGovern School of Medicine University of Texas Medical School at Houston (Protocol number AWC-12-080). SD rats (used number of rats: $n = 40$; 150–175 grams, 7 weeks old, female, Charles River Lab.) were anesthetized with 4% isoflurane and underwent endotracheal intubation under direct visualization. The animals were then placed on a heated operating platform and connected to a volume-controlled ventilator at a rate of 85 breaths per minute and tidal volume of 10 cc/kg with 2% maintenance isoflurane. After the appropriate anesthetic plane was confirmed by toe pinch, the rats were then sterilely prepared and draped to expose the upper thorax and abdomen. A 1.5 cm midline incision was created, beginning just inferior to the level of the xiphoid process. After entering the abdomen, a self-retaining abdominal wall retractor was used to expose the liver and diaphragm. A 3-0 chromic suture was then passed through the xiphoid and skin and secured in a sterile fashion to a fixed retractor to further expose the diaphragm.

Electrocautery was used to detach the falciform ligament, and a fined tooth forceps was used to grasp the center of the left hemidiaphragm, providing inferior gentle retraction away from the thoracic cavity; a small defect allowed insertion of the tip of the electrocautery device to breach the negative pressure of the thoracic cavity. An 18-gauge angiocather serving as a chest tube was then introduced into the thoracic cavity under direct visualization. A $1.2 \times 1.2\ \text{cm}^2$ circular diameter defect (about 75% tendon and 25% muscle-like tissues represent a total of ~40% of the total hemidiaphragm) was created in the left hemidiaphragm using electrocautery, and the experimental patch was sutured to the diaphragm in an underlay fashion with 2-3 mm overlap using 4-6 interrupted 5-0 Prolene@ sutures. The repair procedure is shown in Figures 2(a) and 2(b).

To close the abdomen, the pneumothorax was evacuated with a 10 cc syringe. Cefazolin (60 mg/kg) was administered directly to the peritoneum, and 0.25% bupivacaine infiltrated into the peritoneum and subcutaneous tissues along the incision. The incision was then closed with 4-0 Vicyrl@ sutures in two layers.

2.7. Biomechanical Stretch Testing. Currently, there are no methods that have been reported for testing diaphragmatic functions. We created a physiological test for rat

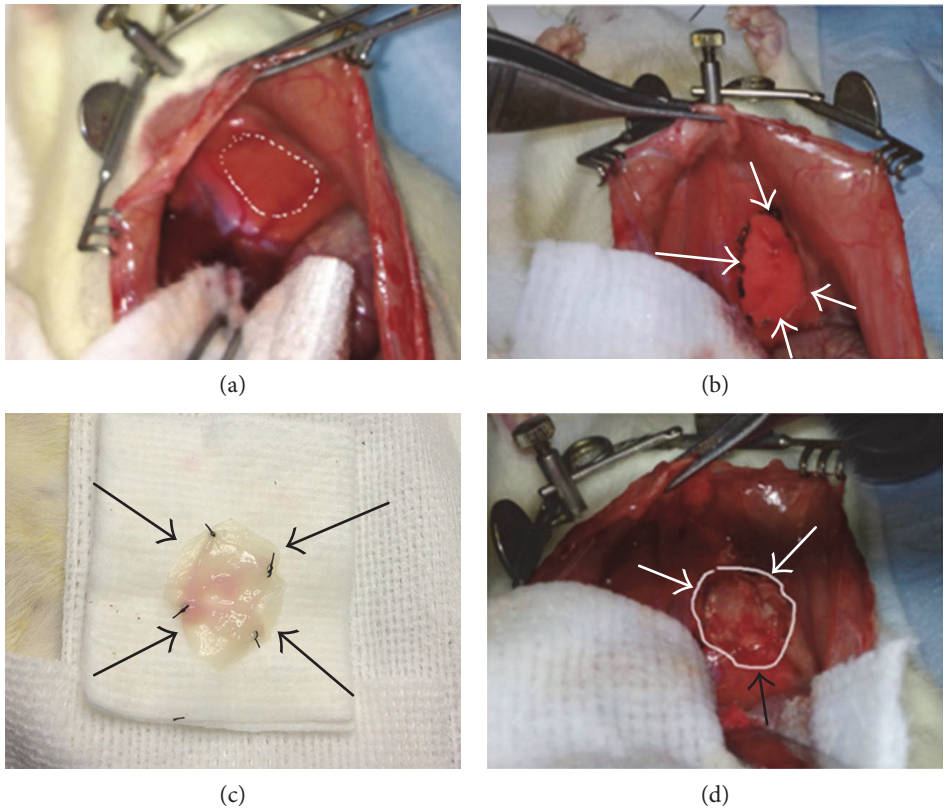

FIGURE 2: The surgical procedure to create the diaphragmatic defect and repair. (a) The rat diaphragm is explored through an abdominal approach, and the surgical defect is created. (b) A standardized defect size of 1.2×1.2 cm in the left side of the diaphragm is created. (c) A composite engineered tissue is prepared for implantation. (d) Complete repair of the defect by a composite engineered tissue.

diaphragmatic function based on our previous reports of skeletal muscle functional tests [32–34], via an electric stimulation to measure the rat diaphragm contractility ex vivo. At 4 and 6 months postsurgery, rats were anesthetized with 4% isoflurane and the chest and abdomen were exposed using a single midline incision. The sternum was bisected two rib levels above the diaphragm and carried posteriorly to the spine. After cardiac puncture, the segment of the dissected ribcage was then removed en bloc to include the entire diaphragm. The ribcage was trimmed so that the diaphragm was supported by just one rib level and placed in Kreb's solution. The diaphragm was then bisected to form two triangular segments, the right segment representing native diaphragm and the left representing the patch. Each triangle segment had a rib as the base and the central tendon at the apex. Both segments were then attached to a muscle stimulation platform to support a rib on one end. The segment was then passed through two metallic rings to create a uniform electric field. A 5-0 silk suture was then tied to the central tendon at the apex of the triangular segment. Each platform, containing one diaphragm segment was placed and secured to an organ bath containing Kreb's solution and connected to an oxygen supply. The sutures were then tied to a precalibrated cantilever for force transduction using LabChart ADInstruments software (Colorado Springs, CO). The diaphragm segments were prestretched to 1.0 gram and stimulated with 10 volts to generate a baseline force versus time curve. The diaphragm segments were then allowed to equilibrate for 30–45 minutes to allow for maximal recovery of force generation, and sequential stimuli are given with 1.0 gram prestretch; the contractile force was measured. The elasticity of the tissue segments was also measured by sequentially elongating the tissue segments by 1.0 mm increments and measuring both the passive or stimulated maximum force for each incremental stretch.

2.8. Histological Analysis. The repaired diaphragms were biopsied, and the biopsied sites were selected from the repaired edge parts, for histological analysis. Serial 8–10 microcryostat sections were performed for histological analyses. Hematoxylin and Eosin (H&E) staining identified the muscle tissue. Trichrome staining was used to analyze the collagen content (reflecting tendon-like tissue formation) of the repaired site tissues. The tissue slides were processed as specified in the manufacturer's protocol (Masson's Trichrome Stain Kit, K7228 IMEB, Inc.); thus, the nuclei were stained black, muscle fibers were stained red, and all collagen was stained blue. For immunohistochemistry, we used 10% horse serum (HS) to block nonspecific background binding and then applied rabbit anti-Nestin (1 : 100, Santa Cruz Biotechnology) and biotin-conjugated CD31 (1 : 150, Chemicon). Secondary fluorescent antibodies (1 : 500, anti-rabbit-594 and 1 : 800, Streptavidin-594) were applied, and then 4′,6-diamidino-2-phenylindole (DAPI, Sigma) was used to stain nuclei as described in our previous reports [35, 36].

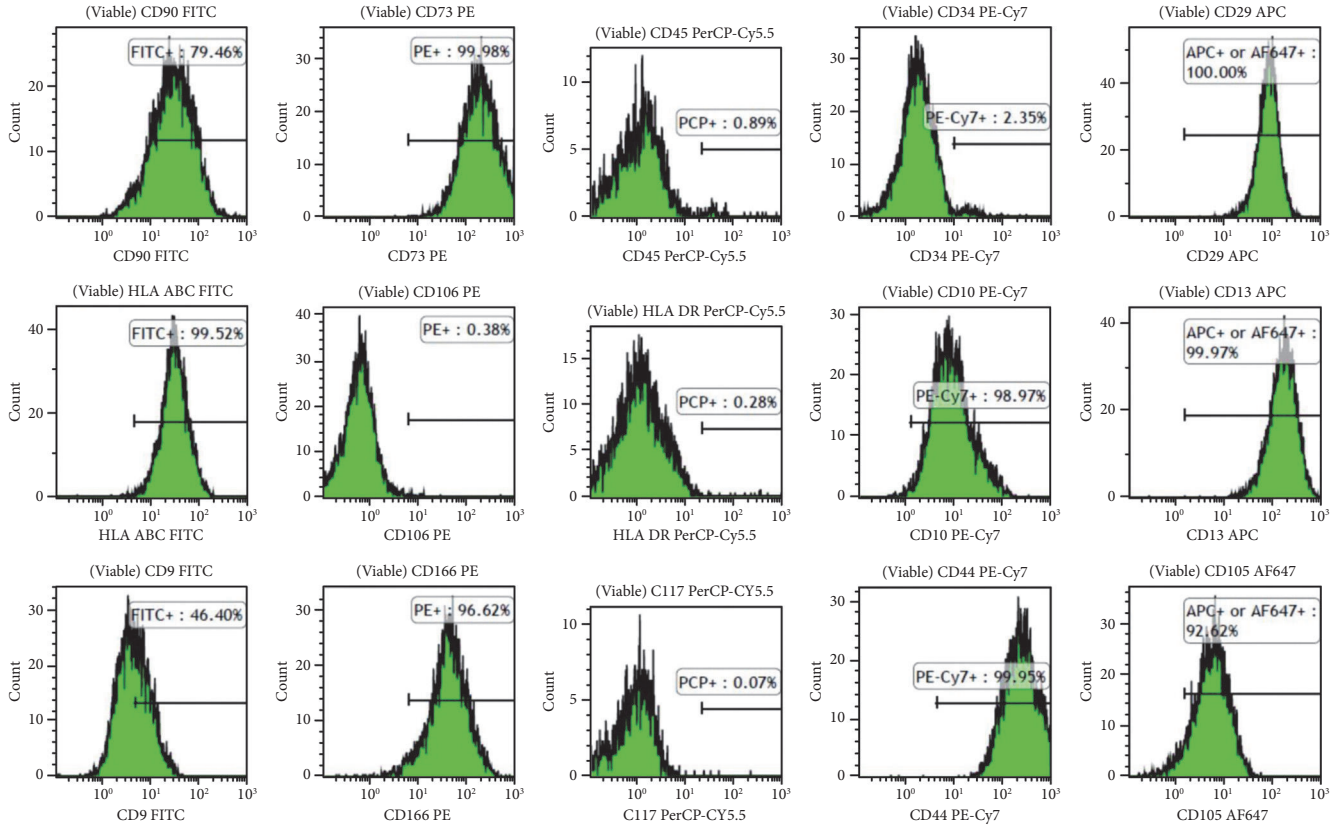

Figure 3: Flow cytometry analysis for hAFMSCs. hAFMSCs used for the current experiments that expressed surface markers as the percentage of viable singlets gated showed 100% CD29, 79.5% CD90, 0.9% CD45, 100% CD73, 2.4% CD34, 100% CD13, 99.5% HLA-ABC, 0.3% HLA-DR, 0.4% CD106, 99%, CD10, 92.6% CD105, 46.4% CD9, 0.1% CD117, 96.6% CD166, and 99.9% CD44.

Negative controls were performed concurrently with all immunohistochemical staining. Immunofluorescent results were visualized using fluorescent microscopy (Nikon microscope, Nikon, Melville, New York). We also captured fluorescent images from 3 to 5 different locations/slide by using the 20x objective and FITC or DSRED channels without recording DAPI. Then, images were analyzed using ImageJ software (NIH, USA), measuring the mean grey values of the threshold area. Data were collected in Excel for further analyses. The resultant values represented the mean of 3 experimental and 4 biological replicates.

2.9. Statistical Analysis. The statistical significance of differences between the groups of surgical treatment and control nonsurgery diaphragms was determined by using one-way analysis of variance (ANOVA) tests. Once finding a significance, for example, p values <0.05%, post hoc analysis was performed using Fisher's least significant difference (LSD) correction. Statistical significance was considered with a $p < 0.05$.

3. Results

3.1. Isolation and Characterization of Human Amniotic Fluid-Derived Multipotent Stromal Cells (hAFMSCs). We obtained the human donor-derived hAFMSCs from a healthy 33-year-old Caucasian female, at gestational age 20 weeks. In brief, the human amniotic fluid was centrifuged at 400g for 15 minutes and the pellet was resuspended in complete TheraPEAK xeno-free mesenchymal stem cell growth medium (Lonza, Basel, CH) supplemented with 20% allogeneic pooled human AB serum (Valley Biomedical, Winchester, VA), 5 ng/mL basic fibroblast growth factor (CellGenix, Portsmouth, NH), and 50 μg/mL gentamicin (Irvine Scientific, Santa Ana, CA) and the cells were cultured at 37°C in a 5% CO_2 and 95% RH environment. The expansion was carried out under the same conditions changing the medium every 3–5 days. Upon reaching 80–90% confluence, cells were passaged by lifting with TrypLE Express xeno-free reagent (Thermo Fisher Scientific, Waltham, MA) and plating at a cell density of 900–1000 cells/cm^2. Cells were cryopreserved in CryoStor CS10 medium (Biolife Solutions, Bothell, WA). Prior to transplantation, passage 3 cells were thawed, washed, and incubated in antibiotic-free medium and tested for mycoplasma, sterility (gram stain and 14 day aerobic and anaerobic cultures), endotoxin, and immunophenotype.

These human donor-derived hAFMSCs were subsequently identified based on their surface markers through flow cytometry analysis, as in our previous reports [27, 29]. These cells were released for infusion upon meeting specific release criteria, including the following immunophenotype: <5% CD34+, CD45+, CD117, HLA-DR cells; >90% CD29+, CD73+, CD44+, CD13, CD166 cells, negative mycoplasma,

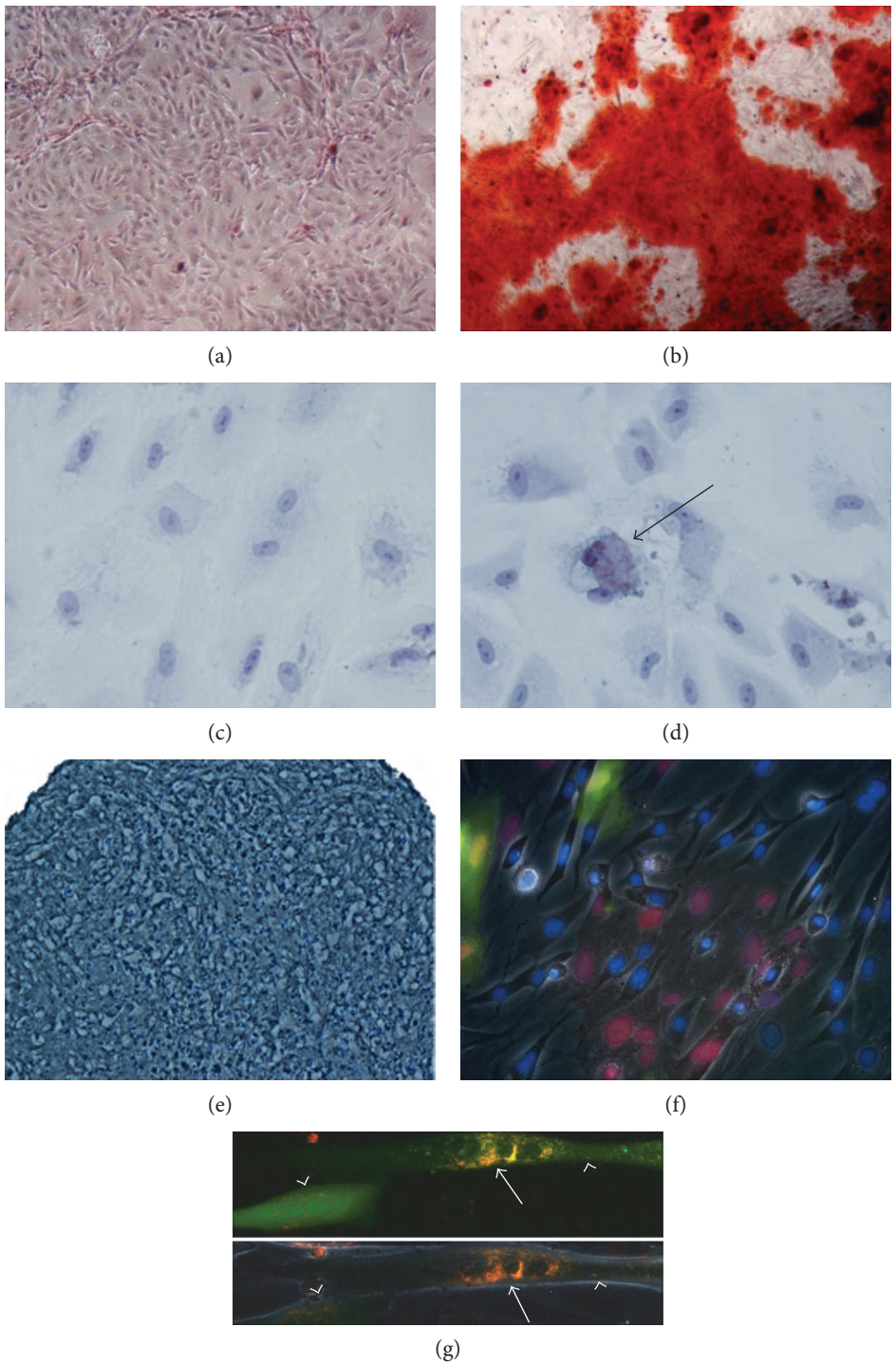

Figure 4: Multiple-differentiation potentials of hAFMSCs in vitro. Osteogenic differentiation of hAFMSC induction for 5 days, stained with Alizarin red: (a) noninduced control hAFMSCs and (b) induced hAFMSCs cultured in osteogenic medium containing BMP4. Adipogenesis of hAFMSCs after induction: (c) noninduced control hAFMSCs and (d) induced hAFMSCs within adipogenic medium for 5 days, as shown by positive Oil red O (arrows' cells). (e) Chondrogenic differentiation of hAFMSCs within chondrogenesis medium with Toluidine blue staining in vitro. Using a coculture system, the same number of both myoblasts (arrows, C2C12-prelabeled red dye-bits) and hAFMSCs (arrowheads, pre-GFP-labeled, green) were 1 : 1 mixed (f), per placing on to one dish. The fused multinucleated myotubes could be detected at 4 days after coculturing, in which some of the myotubes were positive for both red dye and green-GFP together (g). Results suggested that the myogenic differentiation potential via the myotube-fusion occurred between myoblasts and hAFMSCs.

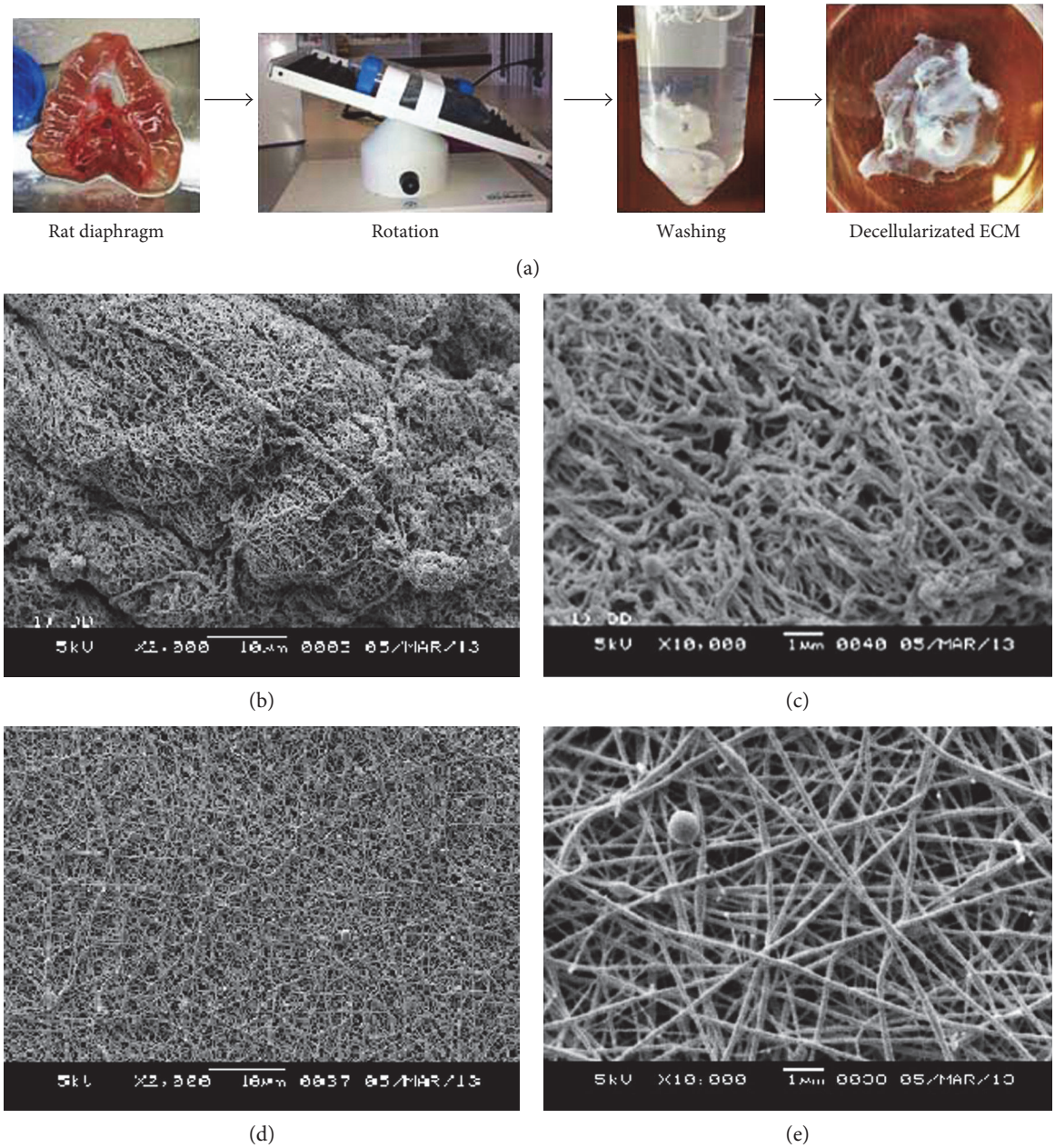

Figure 5: (a) A procedure of decellularization of rat diaphragm. (b, c) Results of TEM scan for the normal rat diaphragms. (d, e) Results of TEM scan for the decellularizated ECM scaffolds of rat diaphragms.

and gram stain. The immunophenotyping results of the lots used in this work are shown in Figure 3. Those hAFMSCs also demonstrated tri-lineage differentiation potential, including osteogenic, adipogenic, chondrogenic, and myogenic differentiation (Figure 4) [27, 29, 37].

3.2. Tissue Decellularization and Cellular Infusion In Vitro. The ECM scaffold tissues were identified histologically by H&E or DAPI staining to verify the lack of surviving resident cells after decellularization (Figure 5). TEM examination for the ECM scaffolds also indicated that there were no changes in tissue structure or architecture before (Figures 5(a) and 5(b)) and after (Figures 5(c) and 5(d)) decellularization. We selected a suitable size of ECM scaffold to develop the composite tissue to allow diaphragmatic defect repair with donor hAFMSCs by using our infusion system in vitro (Figures 6(a)–6(c)).

The ECM scaffold was spread across one of the polycarbonate pieces and covered with the O-ring as shown in Figure 6(a). The second polycarbonate phalange art was placed on top of the O-ring and scaffold. The clamping screws were uniformly tightened to compress the scaffold and O-ring against the polycarbonate pieces to create a fluid-tight seal. A 5 mL syringe was loaded with a volume of

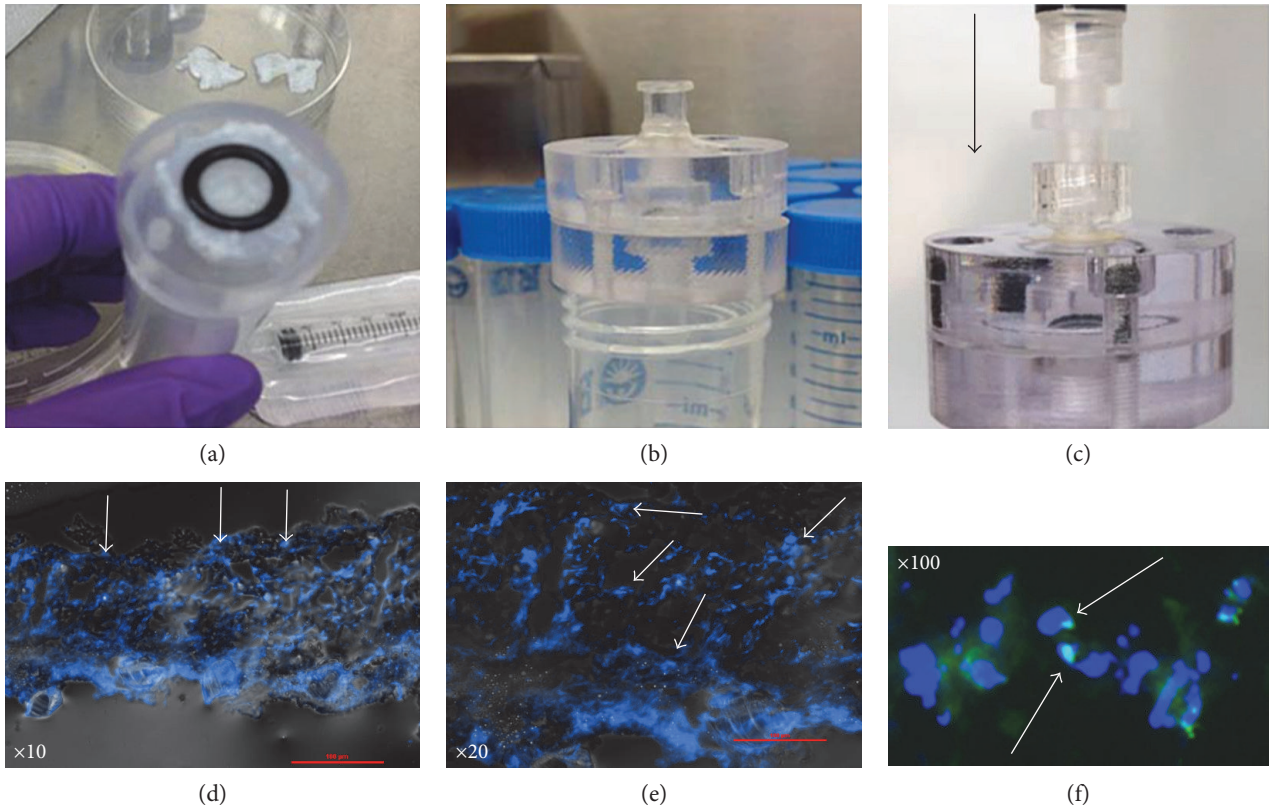

Figure 6: The process of cellular infusion in vitro. (a) A decellularized ECM scaffold is placed onto the top of an infusion chamber. (b) Position and fix ECM scaffold. (c) Begin infusing donor cells with culture medium into a decellularized ECM scaffold. (d, e) Histological analysis of cell distribution into scaffold by using DAPI staining. (f) Distribution test of fluorescent GFP-labeled donor cells in the ECM scaffold after completing infusion.

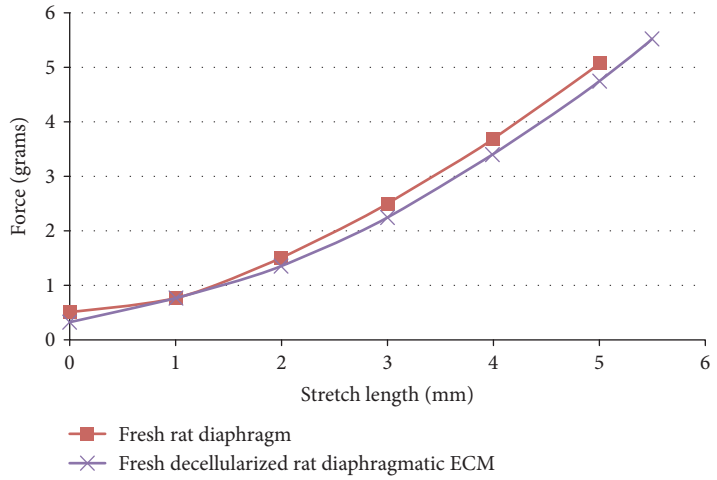

Figure 7: Modeling testing for the decellularized ECM scaffolds in vitro. Within the maximum stretch distance of 6.0 mm and maximum force of 6.0 grams applied to the ECM scaffolds, the results showed the similarity of stress/strain between the fresh rat diaphragms and the decellularized ECM scaffolds of rat diaphragms.

donor cells, and a T luer fitting was affixed to the end of the syringe. An analog pressure gauge was attached to the T fitting, with the third end inserted into the infusion device. A syringe was attached to the device without the T fitting and pressure gauge (Figure 6(c)). A constant hydrostatic pressure was applied by manually pushing on the syringe and monitoring the pressure gauge. The pressure was maintained at constant levels for various durations. With histological analysis, we detected that the perfusion system could improve donor cell implantation into the scaffold,

Table 1

	Decell ± SEM (n)	Decell + hAFMSCs ± SEM (n)	p value
Max force (% native)	50 ± 8% (9)	77 ± 8% (7)	0.03
Modular strength (P-T, MPa)	1.4 ± 0.1 (13)	1.2 ± 0.0 (11)	0.05

shown by DAPI staining (Figures 6(d) and 6(e)) and the tracking of the GFP-labeled cells (Figure 6(f)).

3.3. Stress/Strain Testing for Rat Diaphragm or Decellularized ECM Scaffolds. Figure 7 shows that the decellularized ECM of rat diaphragms developed a tension (> 90%) similar to that freshly isolated rat diaphragms.

3.4. Physiological Recovery after Natural Repair of the Diaphragmatic Defect. We tested the contractile force generation of all patch repaired tissues and contralateral control diaphragmatic tissues. Tissue contractile testing by single pulse (maximum force) stimulation and testing of modular strength, for example, train pulses (T-P) stimulation, were recorded separately. Single pulse stimulation of explanted hemidiaphragms repaired with the composite patch generated 77 ± 8% of the contralateral hemidiaphragm force compared to 50 ± 8% with the decellularized ECM scaffolds of rat diaphragms patch alone ($p = 0.03$). However, the composite patch hemidiaphragms had closer to normal (1.0 MPa) modular tensile strength at 1.2 ± 0.0 MPa than hemidiaphragms repaired with the decellularized ECM scaffolds patch at 1.4 ± 0.1 MPa ($p = 0.05$) (Table 1).

3.5. Histological Analyses of Healing Diaphragms. The repaired diaphragm was composed of filled and regenerated muscle tissues (center nuclei myofibers, Figure 8(a)), and a segment of repaired diaphragm demonstrated tendon-like tissues (trichrome staining blue colors, Figure 8(b)). These regenerated tissues were built with supporting decellularized ECM scaffolds. With immunostaining, we have discovered that the new diaphragm tissues were developed with innervation (ingrowth peripheral nerves) and vascularization (Figures 9(a) and 9(b)) four months after tissue repair. These immunohistochemical stains were analyzed by using ImageJ software, measuring the minimum, maximum, and the mean grey values of the threshold area (Figures 9(a) and 9(b)). Decellularized ECM tissue with cell compositions resulted in the higher number of densities in both vascular (CD31, Figure 9(a)) and neuronal (Nestin, Figure 9(b)) positive cells, indicating accelerated cellular infiltration and regeneration compared to the group of decellularized ECM scaffolds alone.

4. Discussion

It has been suggested that the combination of biomaterial scaffolds with stem cells can accelerate tissue regeneration and result in tissue repair with natural structural and functional properties [38, 39]. However, challenges remain in

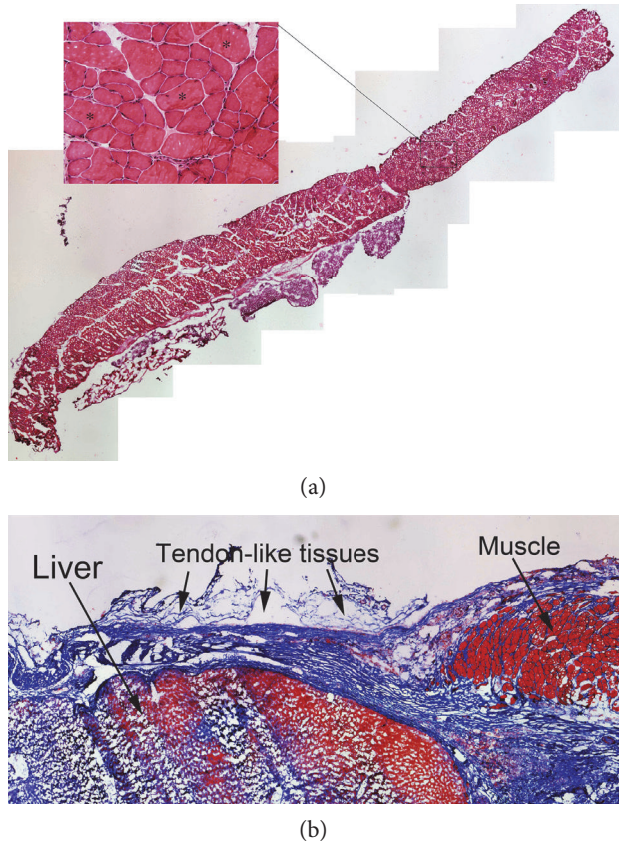

(a)

(b)

Figure 8: H&E staining to identify the muscular-tendon regrowth in the rat diaphragmatic defect. (a) Regenerated muscle tissue within the ECM scaffold after repairing diaphragmatic defect four months later. (b) Tendon-like tissue (arrows, blue tissue) can be detected connecting new muscle tissue within the repaired rat diaphragm. ∗ indicates central nuclei of regenerative muscle fibers; arrows indicates tendon-like tissue.

distributing cells into 3D scaffolds during the tissue engineering processes [36, 40]. Several methods have been tested for seeding stem cells into scaffolds, such as the use of 3D printers, growth factors, or chemical stimulation, and coculture scaffolds with stem cells in vitro [35, 41–43]. In this study, we used a cell infusion system that could successfully deliver donor cells into a 3D ECM scaffold, to build a composite tissue in vitro. Though, the decellularized ECM scaffold alone can be used to repair the tissue defect in rat diaphragms, the composite tissues that combined scaffold and hAFMSC improved the healing of the diaphragmatic defects physiologically and histologically. Similar studies of skeletal muscle or heart tissue repair using engineered tissues have indicated that the composite tissues with stem cells could accelerate healing processes and improve functional tissue recovery [21, 36, 44–46]. Additionally, the benefit of hAFMSCs is autologous cell sourcing to minimize immune responses. Further, there is an ample time window of ~2 months to allow expansion of the donor hAFMSCs for use at the time of birth.

We measured the diaphragmatic function using electrical stimulation ex vivo. These innovative results reflect the recovery of muscle, tendon, neuron-muscular-junction,

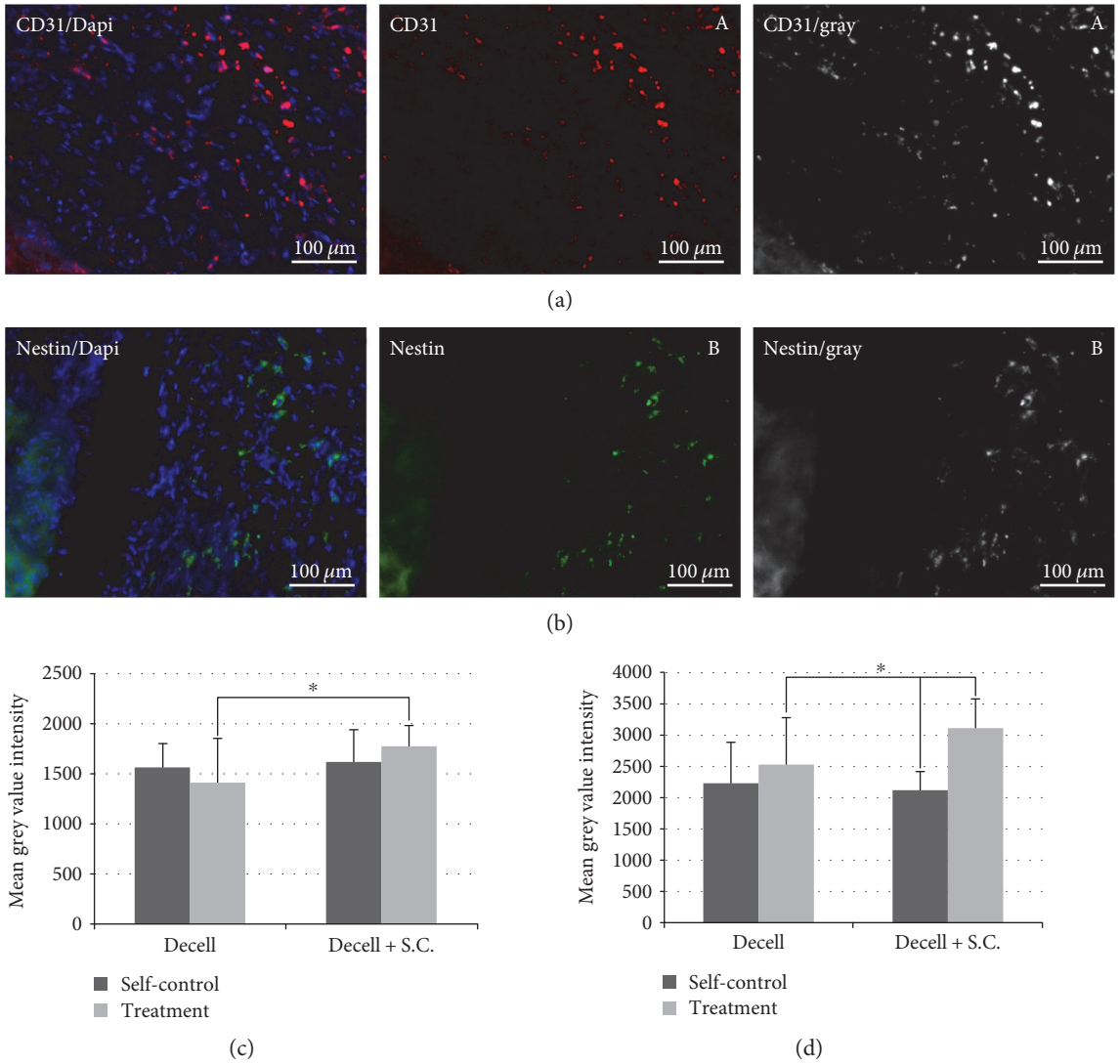

Figure 9: Immunohistochemical analysis of the regrowth tissues within the rat diaphragm. (a) CD31 positive cells (red) represent the vascularity that can be detected within the repaired rat diaphragmatic tissue. (b) Nerve regeneration can be evaluated by Nestin staining (green) within the implanted ECM scaffolds. We also measured the expression level of CD31 (A) and Nestin (B) through quantities of their gray fluorescence. The measurements indicated the revascularization (c) and reinnervation (d) that occurred in the repaired defect. $^{*}p < 0.05$.

and muscle-tendon-junction within the engineered tissues. Moreover, the result of electrical stimulation was confirmed by histological analysis. In physiological terms, the composite patches demonstrated maximum contractile force and tensile properties closer to native tissues as compared to decellularized ECM scaffolds alone. Histological results also indicated that the use of decellularized ECM scaffolds alone or composite tissues could repair the defects with different levels of revascularization. We noted a difference in Nestin staining between decellularized ECM scaffolds and the composite tissues, potentially representing never ingrowth. Although there was no mechanical failure or reherniation, there is potential for these scaffolds to be mechanically inadequate when scaling up to models such as pigs or humans. We are currently investigating the use of decellularized ECM scaffolds seeded with hAFMSCs, combined with other matrices, such as natural silks or biomaterials to improve the initial tensile properties following implantation and scaling up to porcine models. Additionally, improved seeding methods may be required for larger patches, possibly via a sandwich (ECM-cells-ECM) composite tissue. The strategy to use more than one layer of decellularized ECM scaffolds of diaphragms to potentially support the repair of large diaphragmatic defects or emergency uses is clinically relevant.

5. Conclusion

The native decellularized ECM scaffold from rat diaphragms can be used as a support material for repairing rat diaphragmatic defects. However, the composite biological patches that combine decellularized ECM scaffolds with human amniotic fluid-derived multipotent stromal cells (hAFMSCs) could improve diaphragmatic biomechanical function and modular tensile strength. The repair with composite tissues is also associated with improved innervation, vasculogenesis, and muscular-tendon regrowth.

Conflicts of Interest

No financial conflict of interest exists in the current study.

Acknowledgments

The authors would like to thank Ms. Zhengmai Mao for the technical assistance in fluorescence imaging and Dr. Karen Uray and her team for the help on physiological tests. This project was funded through the Texas Emerging Technology Fund (ETF).

References

[1] B. Lin, J. Kim, Y. Li et al., "High-purity enrichment of functional cardiovascular cells from human iPS cells," *Cardiovascular Research*, vol. 95, no. 3, pp. 327–335, 2012.

[2] T. Y. Lu, B. Lin, J. Kim et al., "Repopulation of decellularized mouse heart with human induced pluripotent stem cell-derived cardiovascular progenitor cells," *Nature Communications*, vol. 4, p. 2307, 2013.

[3] F. Pati, J. Jang, D. H. Ha et al., "Printing three-dimensional tissue analogues with decellularized extracellular matrix bioink," *Nature Communications*, vol. 5, p. 3935, 2014.

[4] C. Quint, Y. Kondo, R. J. Manson, J. H. Lawson, A. Dardik, and L. E. Niklason, "Decellularized tissue-engineered blood vessel as an arterial conduit," *Proceedings of the National Academy of Sciences of the United States of America*, vol. 108, no. 22, pp. 9214–9219, 2011.

[5] J. K. Kular, S. Basu, and R. I. Sharma, "The extracellular matrix: structure, composition, age-related differences, tools for analysis and applications for tissue engineering," *Journal of Tissue Engineering*, vol. 5, 2014.

[6] B. E. Uygun, A. Soto-Gutierrez, H. Yagi et al., "Organ reengineering through development of a transplantable recellularized liver graft using decellularized liver matrix," *Nature Medicine*, vol. 16, no. 7, pp. 814–820, 2010.

[7] J. Halper and M. Kjaer, "Basic components of connective tissues and extracellular matrix: elastin, fibrillin, fibulins, fibrinogen, fibronectin, laminin, tenascins and thrombospondins," *Advances in Experimental Medicine and Biology*, vol. 802, pp. 31–47, 2014.

[8] K. P. Lally, M. S. Paranka, J. Roden et al., "Congenital diaphragmatic hernia. Stabilization and repair on ECMO," *Annals of Surgery*, vol. 216, no. 5, pp. 569–573, 1992.

[9] S. R. Hofmann, K. Stadler, A. Heilmann et al., "Stabilisation of cardiopulmonary function in newborns with congenital diaphragmatic hernia using lung function parameters and hemodynamic management," *Klinische Pädiatrie*, vol. 224, no. 4, pp. e1–e10, 2012.

[10] E. Danzer and H. L. Hedrick, "Controversies in the management of severe congenital diaphragmatic hernia," *Seminars in Fetal & Neonatal Medicine*, vol. 19, no. 6, pp. 376–384, 2014.

[11] F. Abdullah, Y. Zhang, C. Sciortino et al., "Congenital diaphragmatic hernia: outcome review of 2,173 surgical repairs in US infants," *Pediatric Surgery International*, vol. 25, no. 12, pp. 1059–1064, 2009.

[12] K. Tsao, P. A. Lally, K. P. Lally, and G. Congenital Diaphragmatic Hernia Study, "Minimally invasive repair of congenital diaphragmatic hernia," *Journal of Pediatric Surgery*, vol. 46, no. 6, pp. 1158–1164, 2011.

[13] K. Tsao and K. P. Lally, "The congenital diaphragmatic hernia study group: a voluntary international registry," *Seminars in Pediatric Surgery*, vol. 17, no. 2, pp. 90–97, 2008.

[14] T. Jancelewicz, L. T. Vu, R. L. Keller et al., "Long-term surgical outcomes in congenital diaphragmatic hernia: observations from a single institution," *Journal of Pediatric Surgery*, vol. 45, no. 1, pp. 155–160, 2010.

[15] A. Safavi, A. R. Synnes, K. O'Brien et al., "Multi-institutional follow-up of patients with congenital diaphragmatic hernia reveals severe disability and variations in practice," *Journal of Pediatric Surgery*, vol. 47, no. 5, pp. 836–841, 2012.

[16] V. C. Koot, J. H. Bergmeijer, and J. C. Molenaar, "Lyophylized dura patch repair of congenital diaphragmatic hernia: occurrence of relapses," *Journal of Pediatric Surgery*, vol. 28, no. 5, pp. 667-668, 1993.

[17] L. Dalla Vecchia, S. Engum, B. Kogon, E. Jensen, M. Davis, and J. Grosfeld, "Evaluation of small intestine submucosa and acellular dermis as diaphragmatic prostheses," *Journal of Pediatric Surgery*, vol. 34, no. 1, pp. 167–171, 1999.

[18] D. O. Fauza, "Tissue engineering in congenital diaphragmatic hernia," *Seminars in Pediatric Surgery*, vol. 23, no. 3, pp. 135–140, 2014.

[19] S. A. Steigman, J. T. Oh, N. Almendinger, P. Javid, D. LaVan, and D. Fauza, "Structural and biomechanical characteristics of the diaphragmatic tendon in infancy and childhood: an initial analysis," *Journal of Pediatric Surgery*, vol. 45, no. 7, pp. 1455–1458, 2010.

[20] C. G. Turner, J. D. Klein, S. A. Steigman et al., "Preclinical regulatory validation of an engineered diaphragmatic tendon made with amniotic mesenchymal stem cells," *Journal of Pediatric Surgery*, vol. 46, no. 1, pp. 57–61, 2011.

[21] S. M. Kunisaki, J. R. Fuchs, A. Kaviani et al., "Diaphragmatic repair through fetal tissue engineering: a comparison between mesenchymal amniocyte- and myoblast-based constructs," *Journal of Pediatric Surgery*, vol. 41, no. 1, pp. 34–39, 2006.

[22] D. O. Fauza, J. J. Marler, R. Koka, R. A. Forse, J. E. Mayer, and J. P. Vacanti, "Fetal tissue engineering: diaphragmatic replacement," *Journal of Pediatric Surgery*, vol. 36, no. 1, pp. 146–151, 2001.

[23] E. A. Gubareva, S. Sjoqvist, I. V. Gilevich et al., "Orthotopic transplantation of a tissue engineered diaphragm in rats," *Biomaterials*, vol. 77, pp. 320–335, 2016.

[24] D. M. Faulk, J. D. Wildemann, and S. F. Badylak, "Decellularization and cell seeding of whole liver biologic scaffolds composed of extracellular matrix," *Journal of Clinical and Experimental Hepatology*, vol. 5, no. 1, pp. 69–80, 2015.

[25] H. R. Davari, M. B. Rahim, N. Tanideh et al., "Partial replacement of left hemidiaphragm in dogs by either cryopreserved or decellularized heterograft patch," *Interactive Cardiovascular and Thoracic Surgery*, vol. 23, no. 4, pp. 623–629, 2016.

[26] S. Sart, Y. Yan, Y. Li et al., "Crosslinking of extracellular matrix scaffolds derived from pluripotent stem cell aggregates modulates neural differentiation," *Acta Biomaterialia*, vol. 30, pp. 222–232, 2016.

[27] M. T. Harting, F. Jimenez, H. Xue et al., "Intravenous mesenchymal stem cell therapy for traumatic brain injury," *Journal of Neurosurgery*, vol. 110, no. 6, pp. 1189–1197, 2009.

[28] M. T. Harting, L. E. Sloan, F. Jimenez, J. Baumgartner, and C. S. Cox Jr., "Subacute neural stem cell therapy for traumatic

brain injury," *The Journal of Surgical Research*, vol. 153, no. 2, pp. 188–194, 2009.

[29] T. Menge, M. Gerber, K. Wataha et al., "Human mesenchymal stem cells inhibit endothelial proliferation and angiogenesis via cell-cell contact through modulation of the VE-cadherin/beta-catenin signaling pathway," *Stem Cells and Development*, vol. 22, no. 1, pp. 148–157, 2013.

[30] C. A. Gregory, W. G. Gunn, A. Peister, and D. J. Prockop, "An Alizarin red-based assay of mineralization by adherent cells in culture: comparison with cetylpyridinium chloride extraction," *Analytical Biochemistry*, vol. 329, no. 1, pp. 77–84, 2004.

[31] I. Sekiya, B. L. Larson, J. T. Vuoristo, J. G. Cui, and D. J. Prockop, "Adipogenic differentiation of human adult stem cells from bone marrow stroma (MSCs)," *Journal of Bone and Mineral Research*, vol. 19, no. 2, pp. 256–264, 2004.

[32] Y. S. Chan, Y. Li, W. Foster et al., "Antifibrotic effects of suramin in injured skeletal muscle after laceration," *Journal of Applied Physiology*, vol. 95, no. 2, pp. 771–780, 2003.

[33] W. Foster, Y. Li, A. Usas, G. Somogyi, and J. Huard, "Gamma interferon as an antifibrosis agent in skeletal muscle," *Journal of Orthopaedic Research*, vol. 21, no. 5, pp. 798–804, 2003.

[34] S. Negishi, Y. Li, A. Usas, F. H. Fu, and J. Huard, "The effect of relaxin treatment on skeletal muscle injuries," *The American Journal of Sports Medicine*, vol. 33, no. 12, pp. 1816–1824, 2005.

[35] W. Wang, H. Pan, K. Murray, B. S. Jefferson, and Y. Li, "Matrix metalloproteinase-1 promotes muscle cell migration and differentiation," *The American Journal of Pathology*, vol. 174, no. 2, pp. 541–549, 2009.

[36] J. Ma, K. Holden, J. Zhu, H. Pan, and Y. Li, "The application of three-dimensional collagen-scaffolds seeded with myoblasts to repair skeletal muscle defects," *Journal of Biomedicine & Biotechnology*, vol. 2011, Article ID 812135, 9 pages, 2011.

[37] D. J. Prockop, I. Sekiya, and D. C. Colter, "Isolation and characterization of rapidly self-renewing stem cells from cultures of human marrow stromal cells," *Cytotherapy*, vol. 3, no. 5, pp. 393–396, 2001.

[38] L. Wang, J. A. Johnson, D. W. Chang, and Q. Zhang, "Decellularized musculofascial extracellular matrix for tissue engineering," *Biomaterials*, vol. 34, no. 11, pp. 2641–2654, 2013.

[39] D. Seliktar, "Designing cell-compatible hydrogels for biomedical applications," *Science*, vol. 336, no. 6085, pp. 1124–1128, 2012.

[40] P. Friedl, E. Sahai, S. Weiss, and K. M. Yamada, "New dimensions in cell migration," *Nature Reviews Molecular Cell Biology*, vol. 13, no. 11, pp. 743–747, 2012.

[41] Y. Tan, Y. Zhang, and M. Pei, "Meniscus reconstruction through coculturing meniscus cells with synovium-derived stem cells on small intestine submucosa—a pilot study to engineer meniscus tissue constructs," *Tissue Engineering Part A*, vol. 16, no. 1, pp. 67–79, 2010.

[42] D. Stone, M. Phaneuf, N. Sivamurthy, F. W. LoGerfo, and W. C. Quist, "A biologically active VEGF construct in vitro: implications for bioengineering-improved prosthetic vascular grafts," *Journal of Biomedical Materials Research*, vol. 59, no. 1, pp. 160–165, 2002.

[43] K. M. Stroka, Z. Gu, S. X. Sun, and K. Konstantopoulos, "Bioengineering paradigms for cell migration in confined microenvironments," *Current Opinion in Cell Biology*, vol. 30, pp. 41–50, 2014.

[44] P. Akhyari, H. Aubin, P. Gwanmesia et al., "The quest for an optimized protocol for whole-heart decellularization: a comparison of three popular and a novel decellularization technique and their diverse effects on crucial extracellular matrix qualities," *Tissue Engineering Part C, Methods*, vol. 17, no. 9, pp. 915–926, 2011.

[45] P. L. Sanchez, M. E. Fernandez-Santos, S. Costanza et al., "Acellular human heart matrix: a critical step toward whole heart grafts," *Biomaterials*, vol. 61, pp. 279–289, 2015.

[46] S. Da Sacco, R. E. De Filippo, and L. Perin, "Amniotic fluid as a source of pluripotent and multipotent stem cells for organ regeneration," *Current Opinion in Organ Transplantation*, vol. 16, no. 1, pp. 101–105, 2011.

Hindawi
Stem Cells International
Volume 2017, Article ID 4740709, 11 pages
https://doi.org/10.1155/2017/4740709

Review Article

The Use of Adipose-Derived Stem Cells in Selected Skin Diseases (Vitiligo, Alopecia, and Nonhealing Wounds)

Agnieszka Owczarczyk-Saczonek,[1] Anna Wociór,[2] Waldemar Placek,[1] Wojciech Maksymowicz,[3] and Joanna Wojtkiewicz[2,4,5]

[1]*Department of Dermatology, Sexually Transmitted Diseases and Clinical Immunology, University of Warmia and Mazury in Olsztyn, Olsztyn, Poland*
[2]*Foundation for Nerve Cell Regeneration, University of Warmia and Mazury in Olsztyn, Olsztyn, Poland*
[3]*Department of Neurology and Neurosurgery, Faculty of Medical Sciences, University of Warmia and Mazury in Olsztyn, Olsztyn, Poland*
[4]*Department of Pathophysiology, Faculty of Medical Sciences, University of Warmia and Mazury in Olsztyn, Olsztyn, Poland*
[5]*Laboratory for Regenerative Medicine, Faculty of Medical Sciences, University of Warmia and Mazury in Olsztyn, Olsztyn, Poland*

Correspondence should be addressed to Agnieszka Owczarczyk-Saczonek; aganek@wp.pl

Received 25 February 2017; Revised 3 June 2017; Accepted 18 June 2017; Published 21 August 2017

Academic Editor: Andrzej Lange

Copyright © 2017 Agnieszka Owczarczyk-Saczonek et al. This is an open access article distributed under the Creative Commons Attribution License, which permits unrestricted use, distribution, and reproduction in any medium, provided the original work is properly cited.

The promising results derived from the use of adipose-derived stem cells (ADSCs) in many diseases are a subject of observation in preclinical studies. ADSCs seem to be the ideal cell population for the use in regenerative medicine due to their easy isolation, nonimmunogenic properties, multipotential nature, possibilities for differentiation into various cell lines, and potential for angiogenesis. This article reviews the current data on the use of ADSCs in the treatment of vitiligo, various types of hair loss, and the healing of chronic wounds.

1. Introduction

Brown and white adipose tissue is a source of mesenchymal stem cells, specifically adipose-derived stem cells (ADSCs). It is an inexpensive, unlimited reservoir of stem cells. From 300 ml of adipose tissue, $2\text{-}3 \times 10^8$ ADSCs can be obtained. This is between 100 and 1000 times more than the mesenchymal stem cells from the bone marrow [1–4]. In addition, they can be easily obtained with no ethical dilemmas pertaining to their use [5, 6]. Moreover, the high content of ADSCs in adipose tissue precludes the need for long in vitro culture, which reduces the risk of chromosomal abnormalities [7].

In 2001, researchers at the University of California, Los Angeles described the isolation of a new population of adult stem cells from liposuctioned adipose tissue. These cells were given the name of processed lipoaspirate or PLA cells due to their derivation from processed lipoaspirate tissue obtained through cosmetic surgery. Since then, intensive studies in the use of regenerative medicine have begun. The term PLA cell has now been replaced with the term adipose-derived stem cells or ASCs to give the field some sort of conformity in terms of nomenclature. By and large, the method of ADSC isolation from lipoaspirates using this enzymatic method has not changed significantly [2, 8–10]. Typical isolation procedures for ASCs involve digestion of the lipoaspirated tissue with collagenase and subsequent centrifugation, then a high-density stromal vascular fraction is produced. Subculturing is then performed to detach the ADSCs from the primary adipocytes [8, 9].

2. Physiology of ADSCs

ADSCs are heterogeneous, no specific marker for them has been identified, and the location of stem cells in adipose

tissue is difficult to determine. However, most of them occur in the perivascular regions. The morphology of ADSCs resemble fibroblasts, consisting of a large endoplasmic reticulum and nuclei [9]. ADSCs do not have a specific marker and the expression of antigens is similar to bone marrow MSCs: CD10, CD13, CD29, CD34, CD44, CD54, CD71, CD49b, CD90, CD105, CD117, and STRO-1. However, they do not express the hematopoietic markers, such as CD14, CD16, CD31, CD45, CD56, CD61, CD62E, CD104, CD106, CD144, the endothelial cell markers CD31, CD144, and von Willebrand factor [9, 11, 12]. Moreover, they are privileged cells with reduced immunogenicity; therefore, there is no expression of HLA-DR [13, 14].

ADSCs may also be a precursor of chondrocytes, osteocytes, muscle cells, neurons, and fibroblasts as well as keratinocytes under proper conditions. However, their most important function is the stimulation of surrounding cells to differentiate into specialized cells under the influence of certain growth factors [15–17]. It has been shown that the ADSCs are even necessary for the activation of epidermal stem cells in the skin [18]. Their exogenous administration mobilizes other stem cells, including the stem cells of the epidermis from the "bulge" region of the hair follicle. This action is based on the production of growth factors, including epidermal growth factor (EGF), fibroblast growth factor (FGF-β), hepatocyte growth factor (HGF), transforming growth factor (TGF-β), vascular endothelial growth factor (VEGF), keratinocyte growth factor (KGF), granulocyte-macrophage colony-stimulating factor (GM-CSF), stromal factor 1-alpha, and cytokines, such as IL-6, 8, 11, 12, and TGF-α. This paracrine secretion of cytokines explains their high concentrations in obese patients [11, 15, 17]. ADSCs also inhibit the production of proinflammatory cytokines, enhance the production of anti-inflammatory IL-10, and stimulate the regulatory T cells [11, 19]. They also stimulate angiogenesis by differentiation in endothelial cells. ADSCs can protect against apoptosis, which offers great opportunities for their use in regenerative medicine [3, 4, 11, 20]. Expression of the receptor for PDGF and CD10 is constant, regardless of the number of passages [15, 21]. Traktuev et al. showed that cells with the CD34+/CD31 phenotype have the ability to stabilize the endothelial network in vitro and stabilize neovascularization in vivo [15, 22]. In addition, perivascular ADSCs (CD146+) also function as a niche for hematopoietic stem cells in vitro [22].

Of particular interest is platelet-derived growth factor-D (PDGF-D), which is secreted by the ADSCs. It is a mitogen for mesenchymal cells, which induces the transformation of cells and also accelerates tumor growth, but its role is not quite understood. Kim et al. showed that PDGF-D and PDGF receptor β are expressed in ADSCs, but PDGF-B is not. PDGF-D can increase the proliferation and migration of ADSCs for the generation of mitochondrial reactive oxygen species (MTRose) and by controlling mRNA expression of various growth factors (VEGF, FGF-1, FGF5, EGF, leukemia inhibitory factor, inhibin, and IL-11) [15, 23].

Cultured ADSCs from this niche have ultrastructural features similar to primitive MSCs (large nucleus, immature cytoplasmic organelles). Although Rubio et al. reported that human ADSCs can undergo malignant transformation during long passages of more than four months, five years later, the authors were not able to reproduce the phenomenon of transformation, most likely due to contamination artifacts [24].

ADSCs have an antioxidant effect. They can capture free radicals and heat shock protein in ischemia status. Research has revealed that during the aging processes and in diabetes, the function of ADSCs is impaired [2, 25].

Vitamins can affect the proliferation of ADSCs. The addition of folic acid and vitamin B12 slightly increases their activity in cell culture, while vitamin C significantly stimulates ADSCs in a dose-dependent manner. Vitamin C increases the expression of the mRNA of HGF, VEGF, bFGF, and KGF [15].

There are some differences in the physiological and biological features of ADSCs derived from different anatomical sites. Siciliano et al. compared the characteristics of stem cells from mediastinal fat and skin. Subcutaneous ADSCs demonstrated greater proliferation and differentiation capacity, an increased IL-6 secretion, and a smaller VEGF-C than ADSCs isolated from the mediastinum. ADSCs from the mediastinum showed a higher proangiogenic potential [26]. On the other hand, ADSCs from the visceral fat have a reduced susceptibility to apoptosis, and ADSCs from the pericardium, omentum, and groin have a different phenotype [27].

Obesity has an influence on the differentiation potential and immunogenicity of ADSCs. The study by Perez et al. demonstrated that stem cells derived from murine and human nonobese sources had increased sensitivity to insulin and can inhibit lipolysis during differentiation into mature adipocytes. In contrast, cells isolated from obese patients showed an impaired uptake of glucose, insulin resistance, and less antilipolytic effect of insulin. Moreover, they released a greater amount of proinflammatory cytokines (mainly TNF-α) and showed disturbances in the production of adiponectin [28].

Interestingly, the preferred factor for proliferation, migration, and differentiation of the ADSCs is hypoxia (an oxygen concentration of 1–5%). Hypoxia induces the expression of HIF-1α (hypoxia-inducible factor 1-α) and increases the production of growth factors, particularly VEGF, bFGF, and HGF which are involved in neovascularization [15, 16]. This phenomenon is observed in obesity. Local hypoxia in the adipose tissue induces the formation of free radicals (ROS) and leads to the secretion of growth factors which stimulate the formation of new blood vessels [15].

Pachon-Pena et al. have also found that obese-derived hADSCs demonstrate increased proliferation and migration capacity, but decreased lipid droplet accumulation, which is correlated with a higher expression of human leukocyte antigen- (HLA-) II, a cluster of CD106 differentiation, and a lower expression of CD29. Of interest, adipogenic differentiation modified CD106, CD49b, and HLA-ABC surface protein expression, which was dependent on the donor's BMI. Moreover, low oxygen tension increased proliferation and migration of lean but not obese hASCs, which was correlated with an altered CD36 and CD49b immunophenotypic profile [29]. Moreover, in obesity, ADSCs indicate changes

in their transcriptomic profile (set of mRNA molecules present in a particular point of a cell) with a loss of plasticity, simultaneously showing an increasing similarity to the adipocyte phenotype [15, 30].

Currently, ADSCs are used in aesthetic dermatology for skin rejuvenation, to correct wrinkles, to correct facial lipoatrophy, and even to improve erections. They are described in the treatment of perianal fistulas in Crohn's disease, bone grafts, and type 1 diabetes [20, 31]. However, the therapeutic use of ADSCs is still experimental.

3. Vitiligo

Vitiligo is a disorder caused by the loss of melanocytes. Repigmentation of vitiligo depends on available melanocytes from three possible sources: from the hair follicle unit which is the main provider of pigment cells, from the border of vitiligo lesions, and from unaffected melanocytes within depigmented areas [32]. Melanocytes rarely undergo mitosis without growth factors; therefore, mitogenic factors are used in transplantation treatments for this disease [33, 34]. Repigmentation occurs due to the migration of melanocyte stem cells (MelSCs) located in the lower part of the hair follicle (infundibulum). Therefore, this process starts perifolliculary [33–36].

ADSCs can be a source of growth factors for melanocytes cultured in the presence of keratinocytes. Lim et al. showed efficacy in mice and Sprague-Dawley rats after administration of human melanocytes alone or enriched with human ADSCs. Better results have been shown with a coadministration of melanocytes and ADSCs, which were grown separately and then mixed in a ratio of 1 : 1, 1 : 2, or 1 : 3, as compared to the administration of pure melanocytes alone [33].

Although the interaction between ADSCs and melanocytes are well known, in the study of Kim et al., an increase in the secretion of HGF by ADSCs after prior exposure to bFGF or EGF was demonstrated [37]. They showed that the proliferation and migration of melanocytes were significantly stimulated by coculturing the ADSCs in comparison with monoculture melanocytes. This may be related to the presence of bFGF and melanocyte growth factor (MGF) produced by ADSCs [37]. The ratio of melanocytes with positive expression of TRP-2, E-cadherin, and N-cadherin were significantly increased in the cocultures with ADSCs compared to keratinocyte and melanocyte monocultures. Melanocytes with a positive expression of TRP-2 (tautomerase dopachrome) are considered to be melanocyte precursors, but TRP-1 positive is considered to be diverse and mature [37, 38]. This is an important result, because the greater the number of immature melanocytes, the better clinical outcomes. In addition, cadherin-calcium-dependent cell adhesion receptors take part in cell-cell interactions. E-cadherin determines the adhesion between keratinocytes and melanocytes, and N-cadherin facilitates the contact between fibroblasts and melanocytes. They also play a role in the differentiation of melanocytes [37, 39]. These studies have confirmed that cultures with ADSCs increase the proliferation and migration of melanocytes, while reducing their differentiation [37].

4. Alopecia

Multipotent stem cells can regenerate hair follicles and sebaceous glands in the skin. The stem cells can be used to regenerate hair growth in a number of therapeutic methods:

(i) the reversal of pathological mechanisms that contributes to hair loss (androgenetic alopecia);

(ii) complete regeneration of hair follicles with "bulge";

(iii) neogenesis of hair follicles with a stem cell culture [40, 41].

The newest therapeutic option is the use of ADSCs. Fukuoka and Suga used them in 22 patients (11 men and 11 women) with alopecia. The cells were administered intradermally every 3 to 5 weeks (6 sessions), controlling the growth of hair using a trichogram. They observed significant improvement in both female and male patients [42].

Hair follicles are surrounded by subcutaneous fat cells and skin, which make up the interfollicular dermal macroenvironment, important in maintaining normal cell growth in the region bulges and hair follicles [18, 43]. Moreover, ADSCs are necessary for the activation of epidermal stem cells [18]. Their action is based primarily on the secretion of growth factors, such as VEGF which regulates hair growth and the size of the hair follicle by stimulating angiogenesis, HGF which is engaged in the length of the phases of the hair cycle, PDGF which induces and maintains the anagen phase, and IGF-1 which controls the cycle of hair growth and hair cell differentiation [42, 44–47]. ADSCs stimulate angiogenesis and enhance blood supply to the hair papilla cells. They also have immunomodulatory and immunosuppressive effects through direct interactions between the cells and secrete prostaglandin E2 (PGE2), leukemia inhibitory factor (LIF), and kynurenine [18]. Huang et al. studied the effect of ADSCs on papilla cells of the hair. During the cell culture, the hair retained its own markers. After adding ADSCs (isolated from rats), characteristics common to coculture were observed. There were mixed papilla and medulla cells with ADSCs. The core and the inner shell of the outer coat also contained ADSCs. The best results were achieved in the second cocultures [44].

It was also shown that subcutaneous adipose tissue played an important role in the extension of the anagen phase. There was a proliferation of progenitor cells, which were adipocytes in the transition from the telogen phase to the anagen phase of the hair follicle [43, 44]. The layer thickness of subcutaneous adipocytes during active hair growth (anagen) increased significantly compared to their amount in the resting phase (telogen) [18, 43]. ADSCs stimulated hair follicle cells via peroxisome proliferator-activated receptor, which has been detected in three isoforms (PPARα, PPARγ, and PPARδ) [44]. In contrast, mature adipocytes have a negative effect on the proliferation of hair follicles, as well as the proliferation of fibroblasts surrounding the follicle in the cocultures [18, 48].

Interestingly, changing the properties of the adipocyte cell lines may cause skin and hair disorders. Lipid metabolism

may lead to defects in the structure of the skin and its functions. Overexpression of human apolipoprotein C1 (APOC1) with hyperlipidemia in transgenic mice results in abnormal hair growth correlated with the expression of the human APOC1 gene in the skin [18, 49].

Musina et al. assessed the influence of hypoxia as a stimulating factor for ADSCs to secrete growth factors. Subcutaneous injection induces the anagen phase in mice, as well as increases the proliferation of human follicular cells, keratinocytes, and hair papillae. Under the influence of hypoxia, there is an increased secretion of insulin-like growth factor binding protein- (IGFBP-) 1 and 2, M-CSF, M-CSF receptor, PDGF-β, VEGF, and decreased EGF secretion [12].

Unfortunately, the studies proved that the two-dimensional (2D) culture of the papilla cells lose their ability to form the hair (trichogenicity) and require a spheroidal form (3D) in culture [50, 51], Table 1.

5. Chronic Wounds

Damage to the skin leads to debilitating effects forming wounds. A wound is defined as a disruption of the normal anatomic structure and functional integrity of the skin. Chronic or nonhealing wounds are wounds that do not progress through the normal wound healing process, resulting in an open laceration of varying degrees of severity [9, 52]. Impaired healing is often associated with ischemia, diabetes mellitus, tumor, venous and pressure ulcers, and severe infections, and it can be the cause of reduced quality of life, disability, and even death [9, 53]. Therefore, wound healing remains a major challenge, and there is a need to develop treatments for improved therapy. Among the various strategies, the most promising seems to be the use of stem cells. This process remains a challenge to date and causes debilitating effects with tremendous suffering. Recent advances in tissue engineering approaches in the area of cell therapy have provided promising treatment options to meet the challenges of impaired skin wound healing [9].

Wound healing is a complex process, covering four mutually overlapping phases: hemostasis, inflammation, proliferation, and remodeling [5, 54, 55]. For the proper process to proceed, all steps must occur in the correct order and time [9]. In many chronic wounds, the elongation inflammatory phase leads to the damage of normal tissues, the production of an excessive amount of proinflammatory cytokines, and the prolonged presence of neutrophils, which causes the degradation of the extracellular matrix (ECM) due to an increase in the secretion of matrix metalloproteinases (MMPs) [9, 56].

Restoring the integrity of the skin involves several cell types, extracellular matrix components, and cytokines [57]. It is believed that what is physiologically responsible for the renewal of epidermal stem cells is located only in the basal layer of the epidermis. However, after damage to the skin, stem cells "bulge" in the region of the hair follicle and take additional responsibility for skin regeneration, particularly in the initial stage [4, 58].

Cell cultures enriched with stem and progenitor cells can be administered to patients via various methods: a direct application on the wound (e.g., as a suspension), injectable (arteriography), intravenous administration, or application of the culture on the appropriate biological scaffold. The most populous cells are the autologous progenitor cells of the epidermis. Current research is focused on bone marrow and adipose-derived stem cells being used in wound healing [4, 58].

ADSCs are involved in the process of healing indirectly by secreting a number of growth factors (IGF, TGF-β1, VEGF, HGF, and FGF2) with a paracrine action that activates keratinocytes and fibroblasts of the skin by stimulating the processes of neovascularization through the generation of anti-inflammatory cytokines, as well as having antioxidant and antiapoptotic effects [14, 36, 59, 60]. ADSCs release wound healing factors and can stimulate recruitment, migration, and proliferation of endogenous cells in the wound environment. The studies suggest that ASCs can affect other cell types specifically in skin tissue via the paracrine method [9]. They may also be directly transformed into fibroblasts and keratinocytes.

Human ADSCs can be converted to epithelial cells expressing the characteristics of cytokeratins 5, 14, 19, and α6; integrins; and even desmoglein 3 [60, 61]. They can also differentiate into fibroblast cells, demonstrating not only their morphological similarity but also their ability to also express cell surface proteins including vimentin and fibronectin [60]. An important feature of the ADSCs is that they produce an antioxidant that protects fibroblasts from oxidative stress [36]. One of the factors that induce ADSCs to increase secretion of growth factors and antiapoptotic factors is hypoxia at the wound site. It has been shown that culturing the ADSCs under hypoxic conditions improves their ability to bind to the adhesion molecules (ICAM-1, VCAM-1), which leads to faster neovascularization, increased production of bFGF, and increased ADSC proliferation [9, 16, 36, 62]. A recent study provides evidence that stromal cell-derived factor-1 (SDF-1) can increase the therapeutic effect of ADSCs in cutaneous chronic wounds. It may protect against cell apoptosis in hypoxic and serum-free conditions through activation of the caspase signaling pathway in ADSCs [63].

The first attempts at healing chronic wounds were performed using ADSCs from lipoaspirate, even without culturing in vitro [9]. This technique is commonly used in aesthetic medicine, avoiding the manipulation that might influence their biological functioning. The simplest method is the application of a component of the adipose tissue-derived multicellular stromal vascular fraction (SVF), after enzymatic digestion and centrifugation of lipoaspirate [64, 65]. SVF is a heterogeneous population of MNCs that include ADSCs of the mesenchymal phenotypes (analogous to MSCs), endothelial progenitor cells (EPCs), hemopoietic progenitors, monocytes, leukocytes, and pericytes. Pericytes are the most important for angiogenesis, and they stabilize nascent blood vessels [65–67].

The administration of wound single-cell suspensions often leads to the formation of aggregates and islet necrosis which can occur after cell injection. Monolayer-cultured cells are poorly retained in local transplantations, nullifying the therapeutic intent or resulting in unexpected stem cell behaviors [68, 69]. Then, the low cell engraftment efficiency by

Table 1: List of past and present clinical adipose-derived stem cell trials in alopecia [80].

Number	Study	Application method	Conditions	Phase	Trial institution/sponsor and country	NCT number and duration period
(1)	The Effect of Allogeneic Human Adipose Derived Stem Cell Component Extract on Androgenic Alopecia	Stem cell component extract	Androgenic alopecia	III	Pusan National University Hospital, South Korea	NCT02594046 2015-2016
(2)	Adipose Tissue Derived Stem Cell Based Hair Restoration Therapy for Androgenetic Alopecia (AGA)	Stem cells with platelet-rich plasma	Androgenic alopecia	II	King Edward Medical University, Pakistan	NCT02865421 2016–2018
(3)	Biocellular-Cellular Regenerative Treatment Scaring Alopecia and Alopecia Areata (SAAA)	PRP concentration, emulsification tSVF	Alopecia areata Scarring alopecia		Regeneris Medical, USA	NCT03078686 2017–2019
(4)	AGA Biocellular Stem/Stromal Hair Regenerative Study (STRAAND)	Emulsified adipose-derived tissue stromal vascular fraction with platelet-rich plasma	Hair disease	I, II	Healeon Medical Inc./Ministry of Health, Honduras	NCT02849470 2016–2018

Table 2: List of past and present clinical adipose-derived stem cell trials on chronic wound [80].

Number	Study	Application method	Conditions	Phase	Trial institution/sponsor and country	NCT number and duration period
(1)	Adipose derived Regenerative Cellular Therapy of Chronic Wounds	Injections to the wound	Venous ulcer, diabetic foot, pressure ulcer	II	Tower Outpatient Clinic, Los Angeles, California, USA	NCT02092870 2013–2015
(2)	ADSCs and Pressure Ulcers	Injections (stromal vascular fraction) to rim around the venous stasis of the wound	Chronic venous stasis wounds	I	Sanford Plastic and Reconstructive Surgery Clinic, Sioux Falls, USA	NCT02961699 2017–2020
(3)	ADSCs and Pressure Ulcers	Injected into a fibrin sealant applicator and applied to the wound	Pressure ulcer	I	Mayo Clinic, Florida, USA	NCT02375802 2015–2017
(4)	Safety of Adipose-Derived Stem Cell Stromal Vascular Fraction	Injections with or without unprocessed autologous fat (fresh or cryopreserved)	Abnormally healing wounds, scars, and soft tissue defects	I	AdiSave Inc., Canada	NCT02590042 2015–2019
(5)	Assessment of the Efficacy and Tolerance of Sub-cutaneous Re-injection of Autologous Adipose-derived REGEnerative Cellsin the Local Treatment of Neuropathic Diabetic Foot ulcERs (REGENDER)	Injections to the wound	Diabetic foot ulcer	II	Assistance Publique Hopitaux De Marseille, France	NCT02866565 2017–2019
(6)	Treatment of Hypertensive Leg Ulcer by Adipose Tissue Grafting	Adipose tissue grafting (lipofilling)	Hypertensive leg ulcer	I	University Hospital, Caen, France	NCT01932021 2013–2014
(7)	Safety of ALLO-ASC-DFU in the Patients with Diabetic Foot Ulcers	ALLO-ASC-DFU	Diabetic foot ulcer	I	Asan Medical Center, Seoul, South Korea	NCT02394886 2014–2015
(8)	The Role of Lipoaspirate Injection in the Treatment of Diabetic Lower Extremity Wounds and Venous Stasis Ulcers	Injection of lipoaspirate	Diabetic wounds, venous stasis wounds	—	Washington DC Veterans Affairs Medical Center, USA	NCT00815217 2009–2010
(9)	Allogeneic ADSCs and Platelet-Poor Plasma Fibrin Hydrogel to Treat the Patients With Burn Wounds	Applied by surface application over perforated (1 : 3) autologous skin graft	Second- or third-degree burns	I, II	The Kyiv City Clinical Hospital, Ukraine	NCT03113747 2015–2018
(10)	Safety of ADSCs Stromal Vascular Fraction	Injections (stromal vascular fraction) to the wound fresh or cryopreserved autologous fat	Abnormally healing wounds, scars, and soft tissue defects	I	Forest Hill Institute of Aesthetic Plastic Surgery, Toronto, Ontario, Canada	NCT02590042 2015–2019
(11)	Child's Adipose Cells: Capacity of Tissue Regeneration	Adipose tissue sample in children < 10 y.	A nude mouse model of skin burn	—	CHU de Toulouse-Purpan, Tolouse, France	NCT02779205 2015–2017
(12)	A Study to Evaluate the Safety of ALLO-ASC-DFU in the Subjects With Deep Second-degree Burn Wound	A hydrogel sheet containing allogenic ASC	Deep second-degree burn wound patients	I	Hallym University of Medical Center, Seoul, Republic of Korea	NCT02394873 2015

Table 2: Continued.

Number	Study	Application method	Conditions	Phase	Trial institution/sponsor and country	NCT number and duration period
(13)	ADSCs for the Treatment of Perianal Fistula in Crohn Disease: A Pilot Study (ASPEFIC1)	ADSC injection	Perianal fistula Crohn's disease	II	Papa Giovanni XXIII Hospital, Italy	NCT02403232 2014–2018
(14)	Autologous Cultured Adipose-Derived Stem Cells (ANTG-ASC) on Complex and Crohn's Fistula	ADSC injection	Perianal fistula Crohn's disease	II	Seoul National University Hospital, Republic of Korea	NCT01314092 2011–2016
(15)	Adipose-Derived Stem Cells to Treat Complex Perianal Fistulas	ADSC injection and dressing with fibrin glue	Perianal fistulas	I	General Surgery Department, Hospital Universitario La Paz, Spain	NCT01020825 2009–2011

injection approach has significantly limited the clinical translation of stem cell therapies [70]. Some techniques use matrices like atelocollagen or the scaffolding of silk fibroin-chitosan suspension ADSCs [71, 72]. Sivan et al. used fibrin and fibronectin to construct an in vitro niche and the mimicking of an in vivo provisional matrix, which plays a dual role in the support of hemostasis, accelerates cell attachment and growth, and is responsible for the increased survival of differentiated cells [73].

Nowadays, researchers are focused on the three-dimensional (3D) culture systems of ADSCs to build multicellular constructs with an extracellular matrix (ECM) and to demonstrate better therapeutic efficacy [68, 69]. The study by Cerqueira et al. used human ADSCs with an extracellular matrix (ECM) as a natural tissue glue that was applied to three layers to form a 3D structure (these are known as "technique sheets"). Then, they were transferred to wounds in mice, obtained by the complete excision of the skin. Restoration of the skin was observed with the formation of new hair follicles and vessels. This resulted in a greater stability of transplanted ADSCs, through cell-cell and cell-ECM interactions. The sheet technique greatly improves the efficiency of transplanted ADSCs [14]. Feng et al. describe a simple method for the 3D culture of adipose-derived stem/stromal cells (ADSCs) which prepares them into a ready-to-use injectable. They transferred suspensions of monolayer-cultured ASCs to a syringe containing hyaluronic acid gel (a naturally derived ECM component) and then incubated the syringe as a 3D culture vessel (microspheroids of human ADSCs). They confirmed high therapeutic efficacy in pathological wound repair in vivo [68]. However, central necrosis was reported when spheroids of mesenchymal stem cells reached a diameter of 200 μm in a suspension-rocking culture system [63, 68]. There are high hopes for a new technology that uses a semi-interpenetrated polymer network (semi-IPN) structure. It was developed by combining this polymer with hyaluronic acid (HA), leading to an in situ cross-linkable hydrogel with significantly increased porosity, enhanced swelling behavior, and improved cell adhesion and viability in both 2D and 3D cell culture models [74].

The next step in the current research is looking for additional materials that may resemble a physiological niche for stem cells to enhance cell retention. Conditioned media for ADSCs have been reported to enhance angiogenesis, enhance epithelialization, and affect recruitment or proliferation of macrophages and endothelial progenitor cells during the healing process [75]. Dong et al. have developed a method of using an injectable poly(ethylene glycol) (PEG)-gelatin hydrogel with highly tunable properties. Murine ADSCs can be easily encapsulated into the hydrogel, which supports ADSC growth and maintains their stemness. This method significantly improves cell retention, enhances angiogenesis, and accelerates wound closure using a murine wound healing model. Then, the injectable PEG-gelatin hydrogel can be used for regulating stem cell behaviors in 3D culture or to deliver cells for wound healing and other tissue regeneration applications [70]. It was found that long-term cell viability could be achieved for both in vitro (21 days) and in vivo (14 days) studies. With ADSCs, this hydrogel system showed potential as a bioactive hydrogel dressing for wound healing [75].

On the basis of many studies, the best wound healing is achieved by using ADSCs with platelet-rich plasma (PRP). Their presence has caused more rapid proliferation of fibroblasts and keratinocytes in vitro [57, 76–78]. PRP is a source of growth factors, necessary for healing, such as PDGF, TGF, IGF, and EGF. They are concentrated in the platelets. In addition, PRP can act as a scaffold for other types of cells such as mesenchymal stem cells [57, 76, 79]. On the other hand, higher concentrations of PRP in vitro culture can slow down the rate of regeneration due to proteolytic enzymes (PRP-collagenase, elastase, and cathepsin) which inhibit cell growth. The best results have been achieved after using a maximum 10% PRP [57, 78].

Healing of chronic cutaneous wounds and ulcers is troublesome and may require the use of skin substitutes. Adipose-derived stem cells have immense potential as an autologous cell source for treating wounds and regenerating skin, Table 2.

6. Conclusions

ADSCs appear as the ideal cell population for the use in regenerative medicine:

(i) they are unlimited in supply and easily obtainable from adipose tissue;

(ii) they are autologous, nonimmunogenic cells;

(iii) they have a multipotential nature and easily differentiable into various cell lines;

(iv) they have a significant potential of angiogenesis;

(v) they can be easily cultured and have high affinity for 3D scaffolds [2, 56, 60].

Conflicts of Interest

The authors declare that there is no conflict of interest regarding the publication of this paper.

References

[1] A. Owczarczyk-Saczonek, W. Placek, and W. Maksymowicz, "The importance and use of stem cells in dermatology," *Przegląd Dermatologiczny*, vol. 103, no. 4, pp. 309–315, 2016.

[2] W. Beeson, E. Woods, and R. Agha, "Tissue engineering, regenerative medicine, and rejuvenation in 2010: the role of adipose-derived stem cells," *Facial Plastic Surgery*, vol. 27, no. 4, pp. 378–387, 2011.

[3] M. Koźlik and P. Wójcicki, "The use of stem cells in plastic and reconstructive surgery," *Advances in Clinical and Experimental Medicine*, vol. 23, no. 6, pp. 1011–1017, 2014.

[4] K. S. Ogliari, D. Marinowic, D. E. Brum, and F. Loth, "Stem cells in dermatology," *Anais Brasileiros de Dermatologia*, vol. 89, no. 2, pp. 286–292, 2014.

[5] M. Cherubino, J. P. Rubin, N. Miljkovic, A. Kelmendi-Doko, and K. G. Marra, "Adipose-derived stem cells for wound

healing applications," *Annals of Plastic Surgery*, vol. 66, no. 2, pp. 210–215, 2011.

[6] E. H. Kim and C. Y. Heo, "Current applications of adipose-derived stem cells and their future perspectives," *World Journal of Stem Cells*, vol. 26, no. 1, pp. 65–68, 2014.

[7] B. G. Jeon, B. M. Kumar, E. J. Kang et al., "Characterization and comparison of telomere length, telomerase and reverse transcriptase activity and gene expression in human mesenchymal stem cells and cancer cells of various origins," *Cell and Tissue Research*, vol. 345, no. 1, pp. 149–161, 2011.

[8] H. M. Chung, C. H. Won, and J. H. Sung, "Responses of adipose-derived stem cells during hypoxia: enhanced skin-regenerative potential," *Expert Opinion on Biological Therapy*, vol. 9, no. 12, pp. 1499–1508, 2009.

[9] W. U. Hassan, U. Greiser, and W. Wang, "Role of adipose-derived stem cells in wound healing," *Wound Repair Regeneration Journal*, vol. 22, no. 3, pp. 313–325, 2014.

[10] M. Zhu, S. Heydarkhan-Hagvall, M. Hedrick, P. Benhaim, and P. Zuk, "Manual isolation of adipose-derived stem cells from human lipoaspirates," *Journal of Visualized Experiments*, no. 79, article e50585, 2013.

[11] A. Bajek, N. Gurtowska, J. Olkowska, L. Kazmierski, M. Maj, and T. Drewa, "Adipose-derived stem cells as a tool in cell-based therapies," *Archivum Immunologiae et Therapiae Experimentalis (Warsz)*, vol. 64, no. 6, pp. 443–454, 2016.

[12] R. Musina, E. Bekchanova, and G. Sukhikh, "Comparison of mesenchymal stem cells obtained from different human tissues," *Bulletin of Experimental Biology and Medicine*, vol. 139, no. 4, pp. 504–509, 2005.

[13] P. Niemeyer, J. Vohrer, H. Schmal et al., "Survival of human mesenchymal stromal cells from bone marrow and adipose tissue after xenogenic transplantation in immunocompetent mice," *Cytotherapy*, vol. 10, no. 8, pp. 784–795, 2008.

[14] M. T. Cerqueira, R. P. Pirraco, T. C. Santos et al., "Human adipose stem cells cell sheet constructs impact epidermal morphogenesis in full-thickness excisional wounds," *Biomacromolecules*, vol. 14, no. 11, pp. 3997–4008, 2013.

[15] W. S. Kim, J. Han, S. J. Hwang, and J. H. Sung, "An update on niche composition, signaling and functional regulation of the adipose-derived stem cells," *Expert Opinion on Biological Therapy*, vol. 14, no. 8, pp. 1091–1102, 2014.

[16] W. S. Kim, B. S. Park, and J. H. Sung, "The wound-healing and antioxidant effects of adipose-derived stem cells," *Expert Opinion on Biological Therapy*, vol. 9, no. 7, pp. 879–887, 2009.

[17] B. S. Park, W. S. Kim, J. S. Choi et al., "Hair growth stimulated by conditioned medium of adipose-derived stem cells is enhanced by hypoxia: evidence of increased growth factor secretion," *BioMed Research International*, vol. 31, no. 1, pp. 27–34, 2010.

[18] P. Zhang, R. E. Kling, S. K. Ravuri et al., "A review of adipocyte lineage cells and dermal papilla cells in hair follicle regeneration," *Journal of Tissue Engineering*, vol. 27, no. 5, article 2041731414556850, 2014.

[19] E. Gonzalez-Rey, M. A. Gonzalez, N. Varela et al., "Human adipose-derived mesenchymal stem cells reduce inflammatory and T cell responses and induce regulatory T cells in vitro in rheumatoid arthritis," *Annals of the Rheumatic Diseases*, vol. 69, no. 1, pp. 241–248, 2010.

[20] U. Skalska, E. Kontny, M. Prochorec-Sobieszek, and W. Maśliński, "Intra-articular adipose-derived mesenchymal stem cells from rheumatoid arthritis patients maintain the function of chondrogenic differentiation," *Rheumatology (Oxford)*, vol. 51, no. 10, pp. 1757–1764, 2012.

[21] Y. J. Ryu, T. J. Cho, D. S. Lee, J. Y. Choi, and J. Cho, "Phenotypic characterization and in vivo localization of human adipose-derived mesenchymal stem cells," *Molecules and Cells*, vol. 35, no. 6, pp. 557–564, 2013.

[22] D. O. Traktuev, D. N. Prater, S. Merfeld-Clauss et al., "Robust functional vascular network formation in vivo by cooperation of adipose progenitor and endothelial cells," *Circulation Research*, vol. 104, no. 12, pp. 1410–1420, 2009.

[23] J. Hye Kim, S. Gyu Park, W. K. Kim, S. U. Song, and J. H. Sung, "Functional regulation of adipose-derived stem cells by PDGF-D," *Stem Cells*, vol. 33, no. 2, pp. 542–556, 2015.

[24] D. Rubio, J. Garcia-Castro, M. C. Martin et al., "Spontaneous human adult stem cell transformation," *Cancer Research*, vol. 65, no. 8, pp. 3035–3039, 2005.

[25] J. M. Gimble, Z. E. Floyd, and B. A. Bunnell, "The 4th dimension and adult stem cells: can timing be everything?," *Journal of Cellular Biochemistry*, vol. 107, no. 4, pp. 569–578, 2009.

[26] C. Siciliano, A. Bordin, M. Ibrahim et al., "The adipose tissue of origin influences the biological potential of human adipose-stromal cells isolated from mediastinal and subcutaneous fat depots," *Stem Cell Research*, vol. 17, no. 2, pp. 342–351, 2016.

[27] V. Russo, C. Yu, P. Belliveau, A. Hamilton, and L. E. Flynn, "Comparison of human adipose-derived stem cells isolated from subcutaneous, omental, and intrathoracic adipose tissue depots for regenerative applications," *Stem Cells Translational Medicine*, vol. 3, no. 2, pp. 206–217, 2014.

[28] L. M. Pérez, A. Bernal, N. San Martín, M. Lorenzo, S. Fernández-Veledo, and B. G. Gálvez, "Metabolic rescue of obese adipose-derived stem cells by Lin28/Let7 pathway," *Diabetes*, vol. 62, no. 7, pp. 2368–2379, 2013.

[29] G. Pachón-Peña, C. Serena, M. Ejarque et al., "Obesity determines the immunophenotypic profile and functional characteristics of human mesenchymal stem cells from adipose tissue," *Stem Cells Translational Medicine*, vol. 5, no. 4, pp. 464–475, 2016.

[30] B. Onate, G. Vilahur, S. Camino-Lopez et al., "Stem cells isolated from adipose tissue of obese patients show changes in their transcriptomic profile that indicate loss in stemcellness and increased commitment to an adipocyte-like phenotype," *BMC Genomics*, vol. 14, p. 625, 2013.

[31] M. Tobita, H. Orbay, and H. Mizuno, "Adipose-derived stem cells: current findings and future perspectives," *Discovery Medicine*, vol. 11, no. 57, pp. 160–170, 2011.

[32] R. Falabella, "Vitiligo and the melanocyte reservoir," *Indian Journal of Dermatology*, vol. 54, no. 4, pp. 313–318, 2009.

[33] W. S. Lim, C. H. Kim, J. Y. Kim, B. R. Do, E. J. Kim, and A. Y. Lee, "Adipose-derived stem cells improve efficacy of melanocyte transplantation in animal skin," *Biomolecules & Therapeutic (Seoul)*, vol. 22, no. 4, pp. 328–333, 2014.

[34] K. Vinay and S. Dogra, "Stem cells in vitiligo: current position and prospects," *Pigment International*, vol. 1, no. 1, pp. 8–12, 2014.

[35] M. Aziz Jalali, B. Jafari, M. Isfahani, and M. A. Nilforoushzadeh, "Treatment of segmental vitiligo with normal-hair follicle autograft," *The Medical Journal of the Islamic Republic of Iran*, vol. 27, no. 4, pp. 210–214, 2013.

[36] J. H. Lee and D. E. Fisher, "Melanocyte stem cells as potential therapeutics in skin disorders," *Expert Opinion on Biological Therapy*, vol. 14, no. 11, pp. 1569–1579, 2014.

[37] J. Y. Kim, C. D. Park, J. H. Lee, C. H. Lee, B. R. Do, and A. Y. Lee, "Co-culture of melanocytes with adipose-derived stem cells as a potential substitute for co-culture with keratinocytes," *Acta Dermato-Venereologica*, vol. 92, no. 1, pp. 16–23, 2012.

[38] N. V. Botchkareva, V. A. Botchkarev, and B. A. Gilchrest, "Fate of melanocytes during development of the hair follicle pigmentary unit," *Journal of Investigative Dermatology Symposium Proceedings*, vol. 8, no. 1, pp. 76–79, 2003.

[39] L. D. Derycke and M. E. Bracke, "N-cadherin in the spotlight of cell-cell adhesion, differentiation, embryogenesis, invasion and signalling," *The International Journal of Developmental Biology*, vol. 48, no. 5-6, pp. 463–476, 2004.

[40] K. Asakawa, K. E. Toyoshima, N. Ishibashi et al., "Hair organ regeneration via the bioengineered hair follicular unit transplantation," *Scientific Reports*, vol. 2, p. 424, 2012.

[41] M. E. Balañá, H. E. Charreau, and G. J. Leirós, "Epidermal stem cells and skin tissue engineering in hair follicle regeneration," *World Journal of Stem Cell*, vol. 7, no. 4, pp. 711–727, 2015.

[42] H. Fukuoka and H. Suga, "Hair regeneration treatment using adipose-derived stem cell conditioned medium: follow-up with trichograms," *Eplasty*, vol. 26, no. 15, p. 10, 2015.

[43] E. Festa, J. Fretz, R. Berry et al., "Adipocyte lineage cells contribute to the skin stem cell niche to drive hair cycling," *Cell*, vol. 146, no. 5, pp. 761–771, 2011.

[44] C. F. Huang, Y. J. Chang, Y. Y. Hsueh et al., "Assembling composite dermal papilla spheres with adipose-derived stem cells to enhance hair follicle induction," *Science Reports*, vol. 23, no. 6, article 26436, 2016.

[45] I. Hwang, K. A. Choi, H. S. Park et al., "Neural stem cells restore hair growth through activation of the hair follicle niche," *Cell Transplantology*, vol. 25, no. 8, pp. 1439–1451, 2016.

[46] A. Rezza, R. Sennett, M. Tanguy, C. Clavel, and M. Rendl, "PDGF signalling in the dermis and in dermal condensates is dispensable for hair follicle induction and formation," *Experimental Dermatology*, vol. 24, no. 6, pp. 468–470, 2015.

[47] K. Yano, L. F. Brown, and M. Detmar, "Control of hair growth and follicle size by VEGF-mediated angiogenesis," *The Journal of Clinical Investigation*, vol. 107, no. 4, pp. 409–417, 2001.

[48] N. Misago, S. Toda, H. Sugihara, H. Kohda, and Y. Narisawa, "Proliferation and differentiation of organoid hair follicle cells co-cultured with fat cells in collagen gel matrix culture," *British Journal of Dermatolology*, vol. 139, no. 1, pp. 40–48, 1998.

[49] M. C. Jong, M. J. Gijbels, V. E. Dahlmans et al., "Hyperlipidemia and cutaneous abnormalities in transgenic mice overexpressing human apolipoprotein C1," *The Journal of Clinical Investigation*, vol. 101, no. 1, pp. 145–152, 1998.

[50] B. M. Kang, M. H. Kwack, M. K. Kim, J. C. Kim, and Y. K. Sung, "Sphere formation increases the ability of cultured human dermal papilla cells to induce hair follicles from mouse epidermal cells in a reconstitution assay," *Journal of Investigative Dermatology*, vol. 132, no. 1, pp. 237–239, 2012.

[51] C. H. Seo, M. H. Kwack, S. H. Lee, M. K. Kim, J. C. Kim, and Y. K. Sung, "Poor capability of 3D-cultured adipose-derived stem cells to induce hair follicles in contrast to 3D-cultured dermal papilla cells," *Annals of Dermatology*, vol. 28, no. 5, pp. 662–665, 2016.

[52] G. Marfia, S. E. Navone, C. D. Vito et al., "Mesenchymal stem cells: potential for therapy and treatment of chronic non-healing skin wounds," *Organogenesis*, vol. 11, no. 4, pp. 183–206, 2015.

[53] D. Tartarini and E. Mele, "Adult stem cell therapies for wound healing: biomaterials and computational models," *Front Bioengineering Biotechnology*, vol. 11, no. 3, p. 206, 2016.

[54] A. Gosain and L. A. DiPietro, "Aging and wound healing," *World Journal of Surgery*, vol. 28, no. 3, pp. 321–326, 2004.

[55] H. J. You and S. K. Han, "Cell therapy for wound healing," *Journal of Korean Medicine Science*, vol. 29, no. 3, pp. 311–319, 2014.

[56] S. Akita, H. Yoshimoto, K. Akino et al., "Early experiences with stem cells in treating chronic wounds," *Clinics in Plastic Surgery*, vol. 39, no. 3, pp. 281–292, 2012.

[57] T. Stessuk, M. B. Puzzi, E. A. Chaim et al., "Platelet-rich plasma (PRP) and adipose-derived mesenchymal stem cells: stimulatory effects on proliferation and migration of fibroblasts and keratinocytes in vitro," *Archives of Dermatology Research*, vol. 308, no. 7, pp. 511–520, 2016.

[58] M. Pikuła, P. Langa, P. Kosikowska, and P. Trzonkowski, "Stem cells and growth factors in wound healing," *Postepy Higieny i Medycyny Doswiadczalnej (Online)*, vol. 69, pp. 874–885, 2015.

[59] W. S. Kim, B. S. Park, J. H. Sung et al., "Wound healing effect of adipose-derived stem cells: a critical role of secretory factors on human dermal fibroblasts," *Journal of Dermatological Science*, vol. 48, no. 1, pp. 15–24, 2007.

[60] Y. Shingyochi, H. Orbay, and H. Mizuno, "Adipose-derived stem cells for wound repair and regeneration," *Expert Opinion on Biologic Therapy*, vol. 15, no. 9, pp. 1285–1292, 2015.

[61] U. Sivan, K. Jayakumar, and L. K. Krishnan, "Constitution of fibrin-based niche for in vitro differentiation of adipose-derived mesenchymal stem cells to keratinocytes," *Bioresearch Open Access*, vol. 3, pp. 339–347, 2014.

[62] P. J. Amos, A. M. Bailey, H. Shang, A. J. Katz, M. B. Lawrence, and S. M. Peirce, "Functional binding of human adipose-derived stromal cells: effects of extraction method and hypoxia pretreatment," *Annales of Plastic Surgery*, vol. 60, no. 4, pp. 437–444, 2008.

[63] Q. Li, Y. Guo, F. Chen, J. Liu, and P. Jin, "Stromal cell-derived factor-1 promotes human adipose tissue-derived stem cell survival and chronic wound healing," *Experimental and Therapeutic Medicine*, vol. 12, no. 1, pp. 45–50, 2016.

[64] P. Bourin, B. A. Bunnell, L. Casteilla et al., "Stromal cells from the adipose tissue-derived stromal vascular fraction and culture expanded adipose tissue-derived stromal/stem cells: a joint statement of the International Federation for Adipose Therapeutics and Science (IFATS) and the International Society for Cellular Therapy (ISCT)," *Cytotherapy*, vol. 15, no. 6, pp. 641–648, 2013.

[65] M. H. Carstens, A. Gómez, R. Cortés et al., "Non-reconstructable peripheral vascular disease of the lower extremity in ten patients treated with adipose-derived stromal vascular fraction cells," *Stem Cell Research*, vol. 18, pp. 14–21, 2017.

[66] P. J. Amos, H. Shang, A. M. Bailey, A. Taylor, A. J. Katz, and S. M. Peirce, "IFATS collection: the role of human adipose-derived stromal cells in inflammatory microvascular remodeling and evidence of a perivascular phenotype," *Stem Cells*, vol. 26, pp. 2682–2690, 2008.

[67] A. Nguyen, J. Guo, D. A. Banyard et al., "Stromal vascular fraction: a regenerative reality? Part 1: current concepts and

review of the literature," *Journal of Plastic Reconstructive and Aesthetic Surgery*, vol. 69, pp. 170–179, 2016.

[68] J. Feng, K. Mineda, S. H. Wu et al., "An injectable non-cross-linked hyaluronic-acid gel containing therapeutic spheroids of human adipose-derived stem cells," *Scientific Reports*, vol. 8, no. 1, p. 1548, 2017.

[69] I. S. Park, P. S. Chung, and J. C. Ahn, "Enhanced angiogenic effect of adipose-derived stromal cell spheroid with low-level light therapy in hind limb ischemia mice," *Biomaterials*, vol. 35, pp. 9280–9289, 2014.

[70] Y. Dong, A. Sigen, M. Rodrigues et al., "Injectable and tunable gelatin hydrogels enhance stem cell retention and improve cutaneous wound healing," *Advanced Functional Materials*, vol. 27, no. 24, article 1606619, 2017.

[71] S. P. Huang, C. H. Huang, J. F. Shyu et al., "Promotion of wound healing using adipose-derived stem cells in radiation ulcer of a rat model," *Journal of Biomedical Science*, vol. 22, p. 51, 2013.

[72] J. Yang, M. Yamato, C. Kohno et al., "Cell sheet engineering: recreating tissues without biodegradable scaffolds," *Biomaterials*, vol. 26, no. 33, pp. 6415–6422, 2005.

[73] U. Sivan, K. Jayakumar, and L. K. Krishnan, "Constitution of fibrin-based niche for in vitro differentiation of adipose-derived mesenchymal stem cells to keratinocytes," *BioResearch Open Access*, vol. 1, no. 6, pp. 339–347, 2014.

[74] Y. Dong, W. Hassan, Y. Zheng et al., "Thermoresponsive hyperbranched copolymer with multi acrylate functionality for in situ cross-linkable hyaluronic acid composite semi-IPN hydrogel," *Journal of Material Science: Materials in Medicine*, vol. 23, no. 1, pp. 25–35, 2012.

[75] Y. Dong, W. Hassan, R. Kennedy et al., "Performance of an in-situ formed bioactive hydrogel dressing from a PEG-based hyperbranched multi-functional copolymer," *Acta Biomaterialia*, vol. 10, no. 5, pp. 2076–2085, 2014.

[76] N. Kakudo, T. Minakata, T. Mitsui, S. Kushida, F. Z. Notodihardjo, and K. Kusumoto, "Proliferation-promoting effect of platelet-rich plasma on human adipose-derived stem cells and human dermal fibroblasts," *Plastic and Reconstructive Surgery*, vol. 122, pp. 1352–6130, 2008.

[77] E. Raposio, N. Bertozzi, N. Bonomini et al., "Adipose-derived stem cells added to platelet-rich plasma for chronic skin ulcer therapy," *Wounds*, vol. 28, no. 4, pp. 126–131, 2016.

[78] L. F. Marques, T. Stessuk, I. C. Camargo, N. Sabeh Junior, L. Santosdos, and J. T. Ribeiro-Paes, "Platelet-rich plasma (PRP): methodological aspects and clinical applications," *Platelets*, vol. 26, no. 2, pp. 101–113, 2014.

[79] J. A. Greenspoon, S. G. Moulton, P. J. Millett, and M. Petri, "The role of platelet rich plasma (PRP) and other biologics for rotator cuff repair," *Open Orthopedy Journal*, vol. 21, no. 10, pp. 309–314, 2016.

[80] ClinicalTrials.gov, downloading from: https://clinicaltrials.gov/.

Hindawi
Stem Cells International
Volume 2017, Article ID 8309256, 9 pages
https://doi.org/10.1155/2017/8309256

Research Article

In Vivo Articular Cartilage Regeneration Using Human Dental Pulp Stem Cells Cultured in an Alginate Scaffold: A Preliminary Study

Manuel Mata,[1,2,3] Lara Milian,[1,3] Maria Oliver,[1,3] Javier Zurriaga,[4] Maria Sancho-Tello,[1,3] Jose Javier Martin de Llano,[1,3] and Carmen Carda[1,3,5]

[1]*Department of Pathology, Faculty of Medicine and Odontology, University of Valencia, Blasco Ibáñez Avenue 15, 46010 Valencia, Spain*
[2]*Centro de Investigación Biomédica en Red de Enfermedades Respiratorias (CIBERES), Monforte de Lemos Avenue, 3-5, Pabellón 11, 28029 Madrid, Spain*
[3]*Fundación para la Investigación del Hospital Clínico de la Comunidad Valenciana (INCLIVA), Blasco Ibañez Avenue 15, 46010 Valencia, Spain*
[4]*Hospital Clinico Universitario de Valencia, Blasco Ibañez Avenue 17, 46010 Valencia, Spain*
[5]*Centro de Investigación Biomédica en Red en Bioingeniería Biomateriales y Nanomedicina (CIBERBBN), Monforte de Lemos Avenue, 3-5, Pabellón 11, 28029 Madrid, Spain*

Correspondence should be addressed to Manuel Mata; manuel.mata@uv.es

Received 27 April 2017; Accepted 4 July 2017; Published 16 August 2017

Academic Editor: Víctor Carriel

Copyright © 2017 Manuel Mata et al. This is an open access article distributed under the Creative Commons Attribution License, which permits unrestricted use, distribution, and reproduction in any medium, provided the original work is properly cited.

Osteoarthritis is an inflammatory disease in which all joint-related elements, articular cartilage in particular, are affected. The poor regeneration capacity of this tissue together with the lack of pharmacological treatment has led to the development of regenerative medicine methodologies including microfracture and autologous chondrocyte implantation (ACI). The effectiveness of ACI has been shown *in vitro* and *in vivo*, but the use of other cell types, including bone marrow and adipose-derived mesenchymal stem cells, is necessary because of the poor proliferation rate of isolated articular chondrocytes. In this investigation, we assessed the chondrogenic ability of human dental pulp stem cells (hDPSCs) to regenerate cartilage *in vitro* and *in vivo*. hDPSCs and primary isolated rabbit chondrocytes were cultured in chondrogenic culture medium and found to express collagen II and aggrecan. Both cell types were cultured in 3% alginate hydrogels and implanted in a rabbit model of cartilage damage. Three months after surgery, significant cartilage regeneration was observed, particularly in the animals implanted with hDPSCs. Although the results presented here are preliminary, they suggest that hDPSCs may be useful for regeneration of articular cartilage.

1. Introduction

Osteoarthritis (OA) is a complex systemic disease in which the whole joint, including the synovium, articular cartilage, subchondral bone, tendons, and muscles, is affected [1]. OA can be idiopathic or initiated by aging, trauma, malformations, or inflammatory disease [2, 3]. As it affects up to 10% of males and 18% of females greater than 48 yr of age, OA is becoming a serious health problem, and currently established therapies for OA insufficiently address the clinical need [1].

The loss of articular cartilage distinctive of OA is characterized by proteolytic degradation of the chondral matrix, which induces the release of cytokines including interleukin 6 (IL-6), IL-1β, and tumor necrosis factor alpha (TNF-α), leading to secretion of matrix-degrading enzymes from chondrocytes, further propagating tissue breakdown [4, 5]. The limited regeneration capacity of articular cartilage generally leads to formation of fibrocartilage-like scar tissue, which replaces the native hyaline cartilage matrix [6].

Current pharmacological agents for the treatment of OA involve anti-inflammatory drugs including cyclooxygenase

2-selective or nonselective nonsteroidal anti-inflammatory drugs as well as TNF-α-binding antibodies or IL-1 inhibitors [7–9]. However, the potential for these compounds to improve the structural damage is limited, and the development of novel immune modulation strategies will be necessary to alter the progression of OA [6].

Nonpharmacological regenerative techniques have been developed for regeneration of articular cartilage according to the 3R paradigm: reconstruction, repair, and replacement [10]. Microfracture as well as autogenic (mosaicplasty) and allogenic tissue transplantation has shown positive results in short term but poor outcomes in long term, resulting in poor hyaline cartilage regeneration that is replaced by fibrocartilage [11, 12]. Autologous chondrocyte implantation has shown better results in terms of regeneration not only in experimental studies but also in clinical trials in which this methodology has been compared with microfracture [13].

The principal limitations associated with the use of autologous cartilage include the poor proliferation of autologous chondrocytes as well as the source limitation and morbidity of the extraction process. It has been previously shown that a higher cellular content induces better tissue repair [14, 15]. Native articular cartilage has a cell density of 1.4×10^7/cm, corresponding to 5–10% of the cartilage volume, but this cell density is difficult to replicate *in vitro* [16]. For this reason, other sources for cartilage repair have been evaluated, including bone marrow mesenchymal stem cells (MSCs) or adipose stem cells [17, 18], which have been considered top candidates for cartilage regeneration because of their ability to generate functional cartilage tissue [11].

Human dental pulp stem cells (hDPSCs) are self-renewing MSCs residing within the perivascular niche of the dental pulp [19–21] thought to originate from the cranial neural crest and express both MSC and neural stem cell markers [22]. hDPSCs are easily obtained from extracted third molars, and under specific conditions, they can differentiate *in vitro* into a variety of cell types including neurons, odontoblasts, osteoblasts, adipocytes, and chondrocytes [23, 24]. Nevertheless, their ability to regenerate articular cartilage *in vivo* is poorly understood.

The culture environment dramatically influences chondrogenesis. It has been shown that the three-dimensional environment provided by hydrogels improves cartilage formation [11]. Several hydrogel sources, including proteins such as collagen, elastin, fibrin, and silk fibroin; polysaccharides such as chitosan, chondroitin sulfate, and hyaluronic acid; and seaweed polysaccharides such as alginate, agarose, carrageenan, and ulvan, have been used for cartilage repair [11]. Algal polysaccharides such as alginate have been considered for cartilage regeneration because of their sulfate groups, chemical affinity for mammalian glycosaminoglycans, and lack of interaction with cell integrins that help retain the rounded shape of cultured cells, enhancing chondrogenesis [25, 26].

The objective of this study was to assess the effectiveness of hDPSCs in the regeneration of articular cartilage *in vivo*. hDPSCs and rabbit articular chondrocytes were isolated, characterized, and cultured in a 3% alginate scaffold, and the scaffolds were implanted in an experimental rabbit model of a full-depth chondral joint defect. The results presented here demonstrate the chondrogenic capacity of hDPSCs and suggest their use in cartilage regeneration.

2. Materials and Methods

2.1. Cell Culture and Experimental Design. Rabbit primary articular chondrocytes and hDPSCs were used in this study. Chondrocytes were isolated as described previously [27]. Briefly, articular cartilage was obtained from the knee joints of donor rabbits following sacrifice by a lethal intravenous injection of anesthetic into the auricular vein (500 mg/iv sodium thiopental; thiobarbital, B. Braun Medical, Barcelona, Spain). The cartilage was dissected from the subchondral bone, finely diced, and washed with Dulbecco's modified Eagle's medium (DMEM; Thermo Fisher Scientific, Fife, WA, USA) supplemented with 100 U penicillin, 100 μg streptomycin (Biological Industries, Kibbutz Beit HaEmek, Israel), and 0.4% fungizone (Gibco/Thermo Fisher Scientific). The diced cartilage was digested with different enzymes in the supplemented DMEM. The cartilage was first incubated with 0.5 mg/mL hyaluronidase (Sigma-Aldrich, St. Louis, MO, USA) in a shaking water bath at 37°C for 30 min. The hyaluronidase was removed, and 1 mg/mL pronase (VWR International, Barcelona, Spain) was added. After incubation in a shaking water bath at 37°C for 60 min, the cartilage pieces were washed with supplemented DMEM. The medium was removed, 0.5 mg/mL collagenase-IA (Sigma-Aldrich) was added, and digestion was continued overnight in a shaking water bath at 37°C. The resulting cell suspension was filtered through a 70 μm-pore nylon filter (BD Biosciences, San Jose, CA, USA) to remove tissue debris. Cells were centrifuged and washed with DMEM supplemented with 10% fetal bovine serum (FBS; Thermo Fisher Scientific). Finally, isolated cells were used immediately for chondrocyte culture by placing them in T75 culture flasks (Becton-Dickinson, East Rutherford, NJ, USA) at a high density in DMEM supplemented with 10% FBS and 50 μg/mL ascorbic acid (Sigma-Aldrich) at 37°C in a 5% CO_2-humidified atmosphere.

hDPSCs were isolated as described previously [28]. Donors provided informed consent. The study was conducted in accordance with the Declaration of Helsinki and applicable local regulatory requirements and laws. All procedures were approved by the Ethics Committee of the University Clinical Hospital of Valencia (Spain). The dental pulp of human third molars was gently removed under sterile conditions using cow horn forceps with a small excavator and immersed in culture tubes filled with medium. The specimens were then divided into small pieces using a bistoury knife, immersed in Hanks solution (Gibco), and incubated for 2 h at 37°C in 5% CO_2. The supernatant medium was removed, and 0.1% type IV collagenase (Sigma-Aldrich) was added for 15 min, followed by centrifugation at 1500 rpm for 10 min. The supernatant was removed, and the cells were plated in 25 cm^3 flasks in DMEM (Nunc, Sigma-Aldrich, Madrid, Spain) containing penicillin/streptomycin, 10% FBS (Sigma-Aldrich, Madrid, Spain),

amphotericin B, and 0.1% L-glutamine. The medium was replaced every 4 d. Once the cells reached confluence, flow cytometry was performed.

Rabbit chondrocytes and hDPSCs were cultured in chondral differentiation medium, which was composed of DMEM with 1% insulin-transferrin-sodium selenite medium supplement (BD Biosciences, Madrid, Spain) and 50 μg/mL ascorbic acid for up to 6 wk. Chondrocyte differentiation was evaluated by immunofluorescence using specific antibodies against collagens I (COLI) and II (COLII) and aggrecan (ACAN). Changes in cell morphology were evaluated by fluorescence using rhodamine-conjugated phalloidin.

For *in vivo* experiments, 3% alginate hydrogels containing nondifferentiated primary chondrocytes or hDPSCs were constructed and implanted in rabbit knees. The following experimental groups were evaluated: control (alginate only), alginate containing chondrocytes, and alginate-containing hDPSCs. Three months after surgery, the animals were sacrificed, and a histopathological study of the knees was performed using the contralateral knee of each animal as a control. Three different animals were used in each experimental group.

2.2. Flow Cytometric Characterization of hDPSCs. hDPSCs were characterized using a FACSCalibur equipped with a 488 nm Argon laser and a 635 nm red diode laser (Becton Dickinson, Madrid, Spain) as described previously [29]. Experimental data were analyzed using CellQuest software (Becton Dickinson, Madrid, Spain). To exclude debris, samples were gated based on light-scattering properties in the side-scattered and forward-scattered light modes, and 10,000 events per sample within this gate (R1) were collected, using the medium setting for the sample flow rate. The following markers were evaluated: CD29 (Alexa Fluor® 488), CD31 (PE/Cy7), CD44 (PE/Cy5), CD45 (Pacific Blue™), CD105 (APC), and CD146 (PE).

2.3. Immunofluorescence Staining of Collagen I, Collagen II, and Aggrecan. Expression of COLI, COLII, and ACAN was determined in cell culture using specific antibodies (Sigma-Aldrich, Madrid, Spain). The cells were cultured on poly-L-lysine-coated cover slides in chondrogenic culture medium for up to 6 wk as described above. Then, they were fixed with 4% paraformaldehyde in phosphate-buffered saline (PBS) pH 7.4 for 10 min. Once washed, the cells were permeabilized with 0.1% Triton X-100 in PBS for 5 min, and after three washes, they were incubated for 30 min with blocking solution (1% bovine serum albumin (BSA) and 1.1% Tween-20 in PBS). The cells were then incubated with the appropriate primary antibody (diluted in antibody diluent at 1 : 100 for COLI and ACAN and 1 : 500 for COLII) overnight at 4°C. After three washes, cells were incubated with 1 : 200 secondary anti-mouse (COLI and ACAN) or anti-rabbit (COLII) FITC-conjugated antibody (Sigma-Aldrich, Madrid, Spain). After the final washes, the nuclei were stained with 4′,6-diamidino-2-phenylindole (DAPI), and the samples were analyzed using the Leica DM2500 fluorescence microscope (Leica, Wetzlar, Germany).

2.4. Fluorescence Staining of F-Actin. F-Actin was evaluated using rhodamine-conjugated phalloidin (Molecular Probes, Thermo Fisher Scientific). Cells were cultured on cover slides, grown to subconfluence, washed with PBS pH 7.4, and fixed in 3.7% formaldehyde solution in PBS for 10 min at room temperature. The cells were permeabilized with 0.1% Triton X-100 in PBS for 3–5 min. To reduce nonspecific background staining, samples were preincubated with PBS containing 1% BSA for 20–30 min. Next, each sample was stained for 20 min with 5 μL phalloidin methanol stock solution diluted in 200 μL PBS. Finally, after washing the samples, the nuclei were stained with DAPI and analyzed using the Leica DM2500 fluorescence microscope.

2.5. Preparation of Alginate Hydrogels. To prepare alginate scaffolds, a 3% alginate solution was prepared in sterile PBS (Sigma-Aldrich, Madrid, Spain). The alginate solution was filtered through a sterile 0.2 μM syringe filter and stored at 4°C until use. To polymerize the alginate, 50 μL 0.5 M $CaCl_2$ prepared in water was added to the bottom of a 24-well culture plate. The alginate solution was warmed at 37°C, and 500 μL was added to the $CaCl_2$ solution. The plate was incubated for 30 min at room temperature and then for another 30 min at 4°C. The polymerized scaffold was then covered with 500 μL culture medium and incubated at 37°C in 5% CO_2. In the experimental groups containing cells, a suspension of 2×10^6 cells/mL in prewarmed alginate solution was prepared, and polymerization was performed as described above.

2.6. Scaffold Implantation of Animals. Two-month-old male New Zealand rabbits, weighing 1.5–2.0 kg, were obtained from Granjas San Bernardo S.L. (Tulebra, Spain), quarantined for 7 d, and maintained under conventional housing conditions, with appropriate bedding and free access to water and food. Rabbits were kept in standard single cages under controlled temperature and light conditions.

Spanish guidelines for the care and use of laboratory animals were observed. The study protocol was approved by the Ethics Committee of the University of Valencia according to law 86/609/EEC and 214/1997 and decree 164/1998 of the Generalitat Valenciana Government.

Rabbits were preanesthetized by subcutaneous injection of 15 mg/kg ketamine (ketolar; Pfizer, Madrid, Spain) and intramuscular injection of 0.1 mg/kg medetomidine (Domitor; Pfizer) and prepared for surgery (washed, shaved, etc.). General anesthesia was induced with 4% isoflurane using a specially designed mask and maintained by administration of 1.5% isoflurane with O_2 (2 L/min). The surgical site was sterilized with iodine solution, and nonsterile areas were covered with sterile drapes. Surgeons wore sterile coats and gloves, and all instruments were sterilized beforehand and kept sterile during surgery. An arthrotomy at the knee joint was performed through a medial longitudinal parapatellar incision. The medial capsule was incised and the patella laterally dislocated. A 3 mm steel trephine was used to create a defect of 3 mm in diameter and 1 mm deep in the central articular surface of the femoral trochlear groove, which resulted in subchondral bone injury and removal of articular

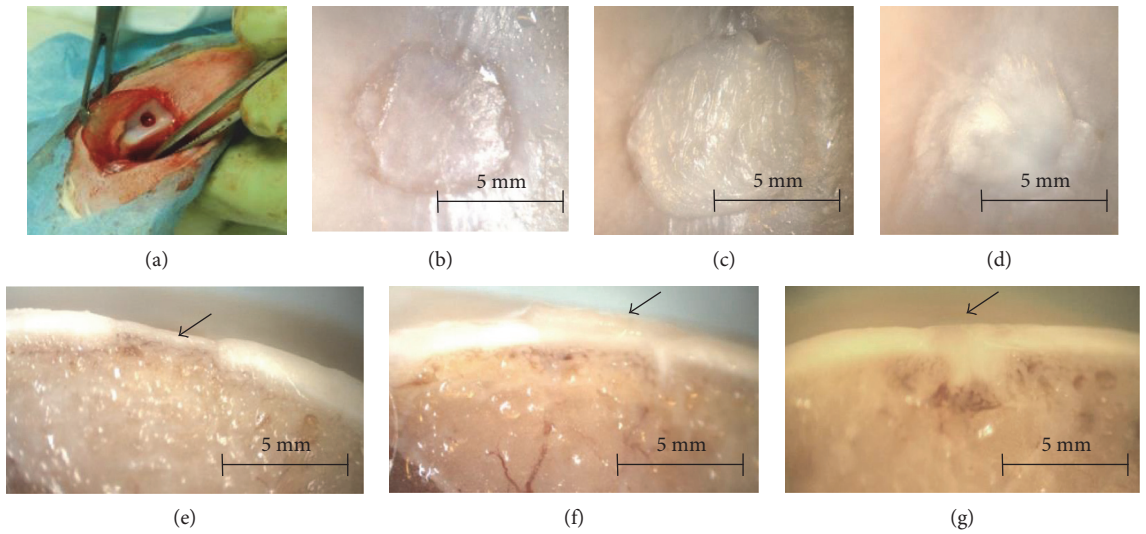

Figure 1: Osteochondral defects of 3 mm were generated in the knees of rabbits (a) and covered with alginate alone (b, e), alginate containing 2×10^6 rabbit primary chondrocytes (c, f), or alginate containing 2×10^6 hDPSCs (d, g). The animals were sacrificed 3 months after surgery. Representative macroscopic images of the animals ($n = 3$) are shown.

cartilage (Figure 1(a)). The defect was cleaned and rinsed with sterile saline, and scaffolds were laid in the defect and aligned with the surrounding articular surface. Control animals were subjected to the same operation, but no scaffold was implanted in the cartilage defect. The arthrotomy and skin were sutured with continuous stitches of 4/0 Coated Vicryl (Johnson and Johnson, New Brunswick, NJ, USA). Macroscopic pictures were taken throughout the surgical procedure using a Leica DC150 camera. After removal of the conformed anesthesia mask, rabbits were returned to their cages and allowed free activity. Postoperative analgesia consisted of intramuscular injection of 3 mg/kg dexketoprofen (Enantyum; Menarini, Florence, Italy) on the day of surgery, followed by the same dose every 24 h for 3 d. Three months after surgery, intramuscular injection of 3 mg/kg gentamicin (Genta-Gobens; Laboratorios Normon, Madrid, Spain) was administered as antibiotic prophylaxis. This time point was chosen based on previous studies using the same animal model [27].

2.7. Histological Studies. Morphology was evaluated following standard histological procedures. Briefly, rabbit articulation specimens were rinsed with PBS and fixed with 4% formaldehyde at room temperature for 5 d. Samples were rinsed with PBS and immersed in OSTEOSOFT decalcifier solution (Merck, Whitehouse Station, NJ, USA) for 5 wk at room temperature. Specimens were cut through the middle of the scaffold, the diameter of which measured approximately 3 mm, and each half was embedded in paraffin separately, generating 5 μm thick sections, which were stained with hematoxylin and eosin. Stained sections were analyzed under an optical microscope (DM 4000B; Leica) and photographed using the Leica DFC 420 camera. Collagen fiber orientation was analyzed under polarized light using an optical microscope (DM 4000B; Leica) as described previously [12].

Type I and II collagen expression were evaluated by immunohistochemistry using specific mouse anti-human antibodies (C2456 Sigma, dilution 1 : 150 and CP18 Calbiochem, dilution 1 : 100). Sections were deparaffined and rehydrated through graded ethanol, rinsed in distilled water, and treated with 0.3% H_2O_2 and 10% normal horse serum to block endogenous peroxidase and nonspecific binding, respectively. Antigen retrieval for type I and type II collagen was performed by proteinase k incubation for 10 min. Dako envision amplification system (Cytomation Envision System-labelled polymer-HRP anti-mouse) was used, followed by development with 3,3′-diaminobenzidine (Dako, Barcelona, Spain) as chromogen according to the manufacturer's instructions, which originated a brown staining in immunoreactive structures. Sections were finally counterstained with Mayer's hematoxylin (Sigma-Aldrich, Madrid, Spain).

2.8. Data Presentation. All experiments were performed in triplicate. The histopathological study was performed in a double-blinded manner, and the figures presented in the manuscript are representative images.

3. Results

3.1. Differentiation of Rabbit Primary Chondrocytes In Vitro. Rabbit primary chondrocytes were isolated and cultured as described in Materials and Methods. Cells were then cultured in proliferation or differentiation culture medium for up to 6 wk. Cell morphology was evaluated using rhodamine-conjugated phalloidin, while COLI, COLII, and ACAN expression were analyzed by immunofluorescence. The results are summarized in Figure 2. Chondrocytes grown in proliferation medium demonstrated a stellate mesenchymal morphology with marked F-actin stress fibers (Figure 2(a)) as well as expression of type I collagen

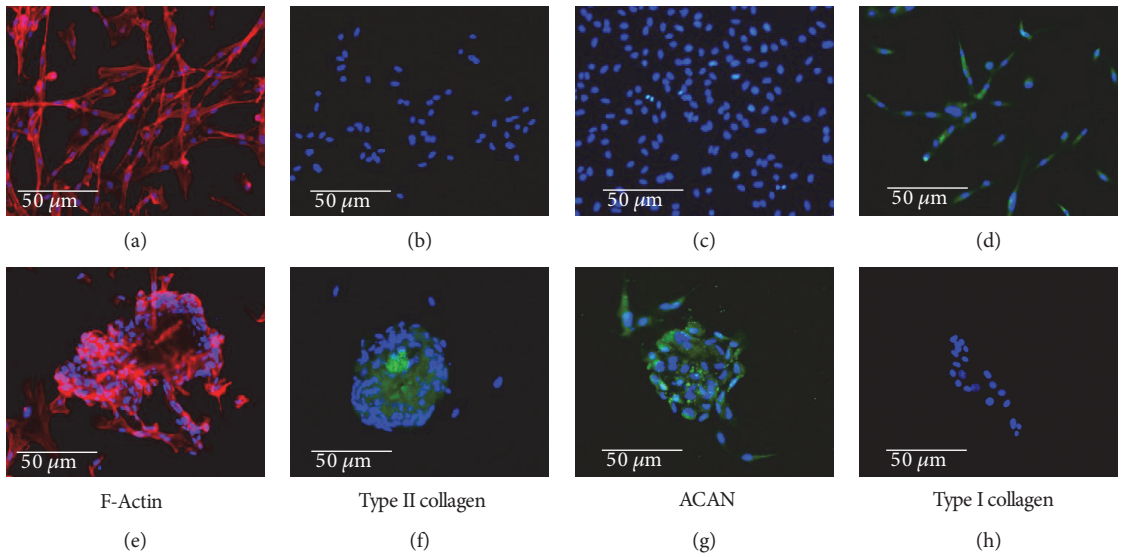

Figure 2: Rabbit primary articular chondrocytes were isolated and cultured in proliferation (a–d) or differentiation culture medium (e–h) for up to 6 weeks. F-Actin expression (a, e) was analyzed by microscopy fluorescence using rhodamine-conjugated phalloidin, and collagen II (COLII; (b, f)), aggrecan (ACAN; (c, g)), and collagen I (COLI; (d, h)) expression were analyzed by immunofluorescence. In all panels, cell nuclei were stained with 4′,6-diamidino-2-phenylindole (DAPI). Microphotographs are representative fields of three independent experiments.

(Figure 2(d)). The shape of cells cultured in chondral differentiation medium changed dramatically to a rounded morphology (Figure 2(f)), with diminished fibrillary actin. These changes correlated with significant expression of COLII and ACAN (Figures 2(g) and 2(h)). No expression of COLI was detected (Figure 2(i)).

3.2. Characterization and Differentiation of hDPSCs In Vitro. hDPSCs were cultured and analyzed by flow cytometry for CD29, CD44, CD105, and CD146 expression. Nearly 98% of the cells analyzed were positive for CD29, CD44, CD105, and CD146 but negative for CD31 and CD45.

The cells were grown in proliferation or differentiation culture medium for up to 6 wk, and the results are summarized in Figure 3. Cells cultured in differentiation medium displayed a more rounded morphology compared with those cultured in proliferation medium. Nevertheless, this change was not as evident as that in primary chondrocytes (Figures 3(a) and 3(e)). No expression of COLI and lower expression of COLII were observed (Figures 3(f) and 3(g)), although significant expression of ACAN was evident (Figure 3(d)).

3.3. Chondrocytes and hDPSCs Induce Joint Cartilage Regeneration In Vivo. To determine if cultured cells can induce cartilage regeneration, a well-established rabbit model of articular regeneration was used [27]. Alginate scaffolds with or without chondrocytes or hDPSCs at a density of 2×10^6 cells/mL were manufactured and implanted in the knees of rabbits. The animals were sacrificed 3 months after surgery, and the joints were evaluated. Rabbit joints were evaluated macroscopically, and representative results are shown (Figures 1(b), 1(c), 1(d), 1(e), 1(f), and 1(g)). Animals with alginate implants showed a significant loss of articular cartilage with an appreciable sinking of the articular surface (Figures 1(b) and 1(e)). Alginate containing primary chondrocytes resulted in a clear regeneration of articular cartilage, which appeared to protrude into the articular cavity (Figures 1(c) and 1(f), arrow). Similar results were observed with alginate containing hDPSCs, except with less evident protrusion into the joint cavity (Figures 1(d) and 1(g)).

Histological analysis revealed a marked loss of articular cartilage in rabbits implanted with alginate only (Figures 4(b) and 4(f)) compared to that in control animals (Figures 4(a) and 4(e)). This loss of cartilage was clearly diminished in animals implanted with alginate containing either chondrocytes (Figures 4(c) and 4(g)) or hDPSCs (Figures 4(d) and 4(h)). These animals exhibited marked regeneration of articular cartilage, characterized by the formation of new isogenic chondral groups and new chondral matrix, although this was more evident in animals implanted with hDPSCs compared with chondrocytes. Polarized light microscopy was used to analyze the arrangement of chondral matrix fibers. A pronounced disturbance in collagen fiber arrangement was observed in the animals implanted with alginate only compared with animals implanted with alginate containing chondrocytes or hDPSCs, in which the fiber disposition was more similar to that of native cartilage (Figures 4(i), 4(j), 4(k), and 4(l)). Immunohistochemistry was used to evaluate type I and II collagen expression. In the animals in which only alginate was used to repair the lesion, a lower expression of type II collagen was observed compared to that in control animals (Figures 4(m) and 4(n)). In both experimental groups in which chondrocytes and hDPSCs were used in combination with alginate, a higher expression of type II collagen was observed (Figures 4(o) and 4(p)). No significant expression of type

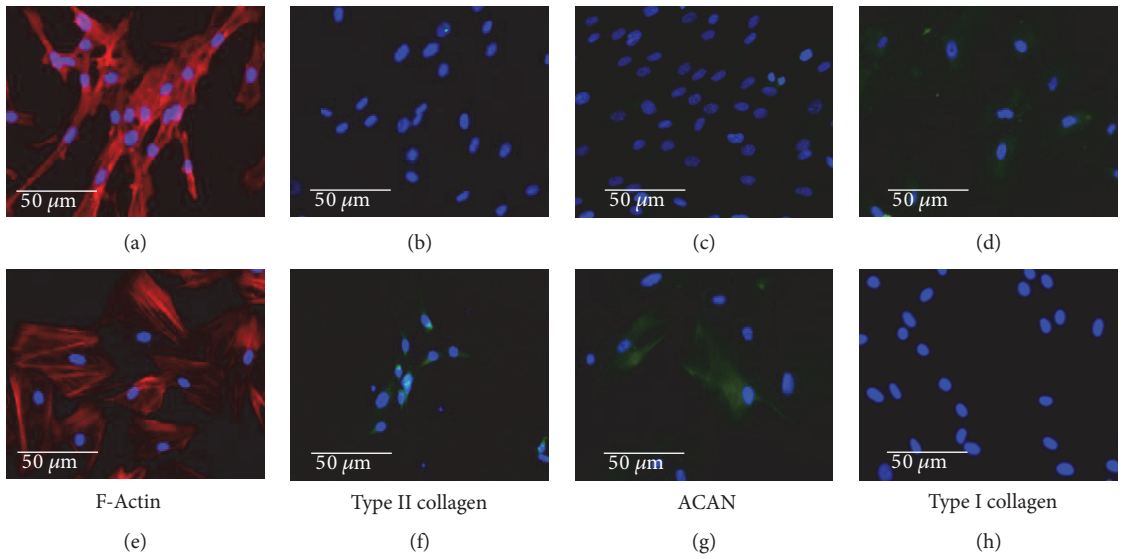

Figure 3: Human dental pulp stem cells (hDPSCs) were isolated and cultured in proliferation (a–d) or chondrocyte differentiation culture medium (e–h) for up to 6 weeks. F-Actin expression (a, e) was analyzed by fluorescence microscopy using rhodamine-conjugated phalloidin, and COLII (b, f), ACAN (c, g), and COLI (d, h) expression were analyzed by immunofluorescence. In all panels, cell nuclei were stained with DAPI. Microphotographs are representative fields of three independent experiments.

I collagen was found in the articular cartilage of animals analyzed (data not shown).

4. Discussion

OA is considered an inflammatory systemic disease in which all joint components are affected. It is characterized by a progressive degeneration of articular cartilage and nonreversible replacement of this cartilage with nonfunctional fibrocartilage. Articular cartilage is an avascular connective tissue, resulting in poor regenerative capacity [30]. The prevalence of OA increases every year as a consequence of the aging population, and it is considered a serious health problem with no effective pharmacological treatment [6].

According to the International Cartilage Repair Society, microfracture, autologous chondrocyte implantation, and osteochondral autographs result in certain degrees of short-term success for OA treatment [1]. The success of autologous chondrocyte implantation has been demonstrated not only at the experimental level but also in clinical trials, and autologous chondrocyte implantation has shown benefits comparable to those of other options such as microfracture [13]. However, this option suffers from a number of limitations primarily related to the extraction source (cartilage biopsy, which is not exempt from morbidity) and the poor regeneration capacity of chondrocytes, which can make it impossible to obtain the minimum number of cells needed for tissue regeneration [31, 32]. These limitations have stimulated researchers to investigate the use of other cell types. Among them, MSCs of different origin, including bone marrow or adipose, have been evaluated because of their capacity to regenerate cartilage [33].

Recently, dental pulp has gained interest as a source of MSCs. Human dental pulp contains several types of stem cells including hDPSCs, periodontal ligament stem cells, stem cells from apical papilla, and dental follicle progenitor cells [19, 21, 34, 35]. hDPSCs are characterized by a high-proliferative capacity while maintaining the ability to differentiate into multiple lineages [23]. Although these cells have been investigated for their potential to differentiate into chondrocytes *in vitro* [36], their regeneration of cartilage *in vivo* is poorly understood. Here, we found that after growth for 6 wk in chondrocyte differentiation culture medium, hDPSCs express ACAN. Nevertheless, only low expression of COLII was detected. This could be due to the length of time in culture; ACAN is expressed earlier than COLII, so it is possible that an increase in COLII would be seen after longer time points. A second possibility is the culture environment. It has been demonstrated by different groups that a three-dimensional environment is critical for chondrocyte differentiation [11]. Moreover, Nemeth et al. demonstrated that DPSCs form three-dimensional spheroids show significant upregulation of chondrogenic gene markers when cultured in hydrogel scaffolds of composite methacrylated gelatin-hyaluronic acid [37]. Among the different hydrogels used for cartilage regeneration, alginate has been successful for the generation of cartilage [11]. For this reason, we cultured cells in alginate hydrogels to evaluate their ability to regenerate articular cartilage *in vivo*. We used a well-established *in vivo* model of articular cartilage damage [27] and primary isolated chondrocytes as a reference group. Our results demonstrate the importance of using different cells (chondrocytes or mesenchymal cells) to obtain appropriate cartilage regeneration. Animals in which only alginate was implanted demonstrated poor regeneration with loss of cartilage tissue compared with those in which chondrocytes or hDPSCs were also implanted. We observed improved tissue regeneration as well as a smoother articular surface when hDPSCs were used instead of primary chondrocytes,

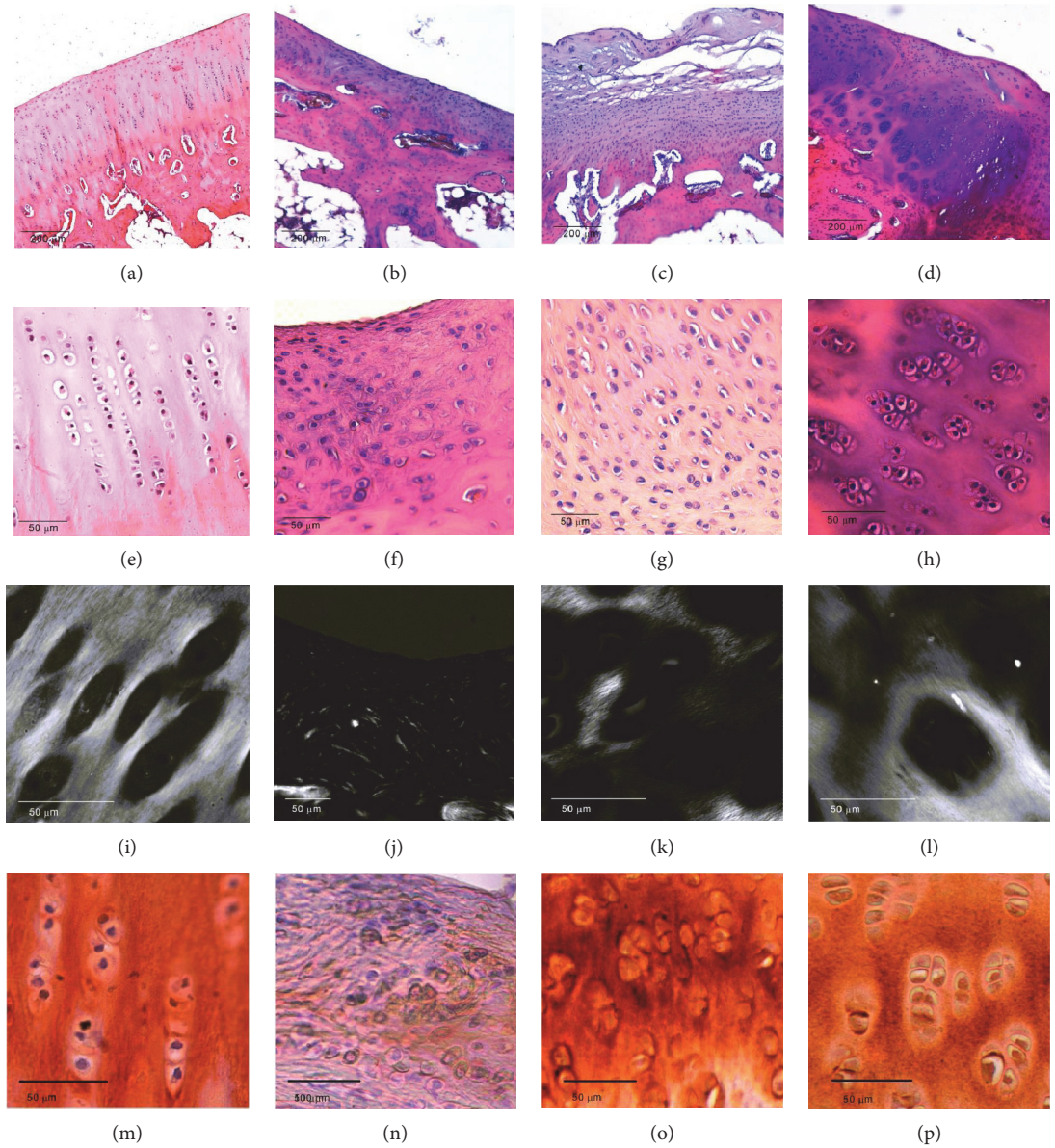

Figure 4: Osteochondral defects of 3 mm were generated in the knees of rabbits and covered with alginate alone (b, f, j, n), alginate containing 2×10^6 rabbit primary chondrocytes (c, g, k, o), or alginate containing 2×10^6 hDPSCs (d, h, l, p). The animals were sacrificed 3 months after surgery. Knees were fixed with 4% formaldehyde, immersed in OSTEOSOFT decalcifier solution for 5 wk at room temperature, and embedded in paraffin. The resulting 5 μm-thick sections were stained with hematoxylin and eosin and analyzed under normal (a–h), polarized (i–l) light using an optical microscope. Immunohistochemistry analysis of type II collagen is represented in panels m–p. Histological images of control animals (a, e, i, m) are also represented. Representative microscopic images of $n = 3$ animals are shown.

which may be due to the anti-inflammatory effects of hDPSCs (discussed below).

Although the results presented here suggest that hDPSCs are useful for cartilage regeneration, it is important to note that this is a preliminary study. On the one hand, it will be important to further our understanding of the mechanisms involved in hDPSC-induced regeneration. These cells have been shown to inhibit the characteristic inflammatory processes underlying OA [38]. In fact, administration of culture medium conditioned by hDPSCs has confirmed beneficial effects on OA [39]. On the other hand, it will also be important to analyze the composition of the regenerated tissue and to extend this study to other animal models of OA. Despite these limitations, the results shown here are novel and support the use of dental pulp as an accessible source of mesenchymal cells, which may be used instead of primary chondrocytes because of their better proliferation and cartilage-regeneration capacity.

Conflicts of Interest

The authors declare no conflicts of interest.

Acknowledgments

Grants MAT2016-76039-C4-2-R (Maria Sancho-Tello and Carmen Carda) and PI16-01315 (Manuel Mata) were from the Ministry of Economy and Competitiveness of the Spanish Government and the Instituto de Salud Carlos III. CIBER-BBN and CIBERER are funded by the VI National R&D&I Plan 2008–2011, Iniciativa Ingenio 2010, Consolider Program, CIBER Actions and financed by the Instituto de Salud Carlos III with the assistance of the European Regional Development Fund.

References

[1] A. Mobasheri, G. Kalamegam, G. Musumeci, and M. E. Batt, "Chondrocyte and mesenchymal stem cell-based therapies for cartilage repair in osteoarthritis and related orthopaedic conditions," *Maturitas*, vol. 78, no. 3, pp. 188–198, 2014.

[2] A. L. Clutterbuck, A. Mobasheri, M. Shakibaei, D. Allaway, and P. Harris, "Interleukin-1β-induced extracellular matrix degradation and glycosaminoglycan release is inhibited by curcumin in an explant model of cartilage inflammation," *Annals of the New York Academy of Sciences*, vol. 1171, pp. 428–435, 2009.

[3] F. Berenbaum, "Osteoarthritis as an inflammatory disease (osteoarthritis is not osteoarthrosis!)," *Osteoarthritis and Cartilage*, vol. 21, no. 1, pp. 16–21, 2013.

[4] F. David, J. Farley, H. Huang, J. P. Lavoie, and S. Laverty, "Cytokine and chemokine gene expression of IL-1β stimulated equine articular chondrocytes," *Veterinary Surgery*, vol. 36, no. 3, pp. 221–227, 2007.

[5] J. Martel-Pelletier, "Pathophysiology of osteoarthritis," *Osteoarthritis and Cartilage*, vol. 12, Supplement A, pp. S31–S33, 2004.

[6] N. Fahy, E. Farrell, T. Ritter, A. E. Ryan, and J. M. Murphy, "Immune modulation to improve tissue engineering outcomes for cartilage repair in the osteoarthritic joint," *Tissue Engineering Part B: Reviews*, vol. 21, no. 1, pp. 55–66, 2015.

[7] W. Zhang, R. W. Moskowitz, G. Nuki et al., "OARSI recommendations for the management of hip and knee osteoarthritis, part II: OARSI evidence-based, expert consensus guidelines," *Osteoarthritis and Cartilage*, vol. 16, no. 2, pp. 137–162, 2008.

[8] G. Verbruggen, R. Wittoek, B. Vander Cruyssen, and D. Elewaut, "Tumor necrosis factor blockade for the treatment of erosive osteoarthritis of the interphalangeal finger joints: a double blind, randomized trial on structure modification," *Annals of the Rheumatic Diseases*, vol. 71, no. 6, pp. 891–898, 2012.

[9] B. Rintelen, K. Neumann, and B. F. Leeb, "A meta-analysis of controlled clinical studies with diacerein in the treatment of osteoarthritis," *Archives of Internal Medicine*, vol. 166, no. 17, pp. 1899–1906, 2006.

[10] A. M. Haleem and C. R. Chu, "Advances in tissue engineering techniques for articular cartilage repair," *Operative Techniques in Orthopaedics*, vol. 20, pp. 76–89, 2010.

[11] E. G. Popa, R. L. Reis, and M. E. Gomes, "Seaweed polysaccharide-based hydrogels used for the regeneration of articular cartilage," *Critical Reviews in Biotechnology*, vol. 35, no. 3, pp. 410–424, 2015.

[12] R. Baba, T. Onodera, D. Momma et al., "A novel bone marrow stimulation technique augmented by administration of ultra-purified alginate gel enhances osteochondral repair in a rabbit model," *Tissue Engineering Part C: Methods*, vol. 21, no. 12, pp. 1263–1273, 2015.

[13] D. Saris, A. Price, W. Widuchowski et al., "Matrix-applied characterized autologous cultured chondrocytes versus microfracture: two-year follow-up of a prospective randomized trial," *The American Journal of Sports Medicine*, vol. 42, no. 6, pp. 1384–1394, 2014.

[14] L. V. Gulotta, S. Chaudhury, and D. Wiznia, "Stem cells for augmenting tendon repair," *Stem Cells International*, vol. 2012, Article ID 291431, 7 pages, 2012.

[15] J. Iwasa, M. Ochi, Y. Uchio, K. Katsube, N. Adachi, and K. Kawasaki, "Effects of cell density on proliferation and matrix synthesis of chondrocytes embedded in atelocollagen gel," *Artificial Organs*, vol. 27, no. 3, pp. 249–255, 2003.

[16] M. D. Buschmann, Y. A. Gluzband, A. J. Grodzinsky, J. H. Kimura, and E. B. Hunziker, "Chondrocytes in agarose culture synthesize a mechanically functional extracellular matrix," *Journal of Orthopaedic Research*, vol. 10, no. 6, pp. 745–758, 1992.

[17] R. Kuroda, K. Ishida, T. Matsumoto et al., "Treatment of a full-thickness articular cartilage defect in the femoral condyle of an athlete with autologous bone-marrow stromal cells," *Osteoarthritis and Cartilage*, vol. 15, no. 2, pp. 226–231, 2007.

[18] T. Rada, R. L. Reis, and M. E. Gomes, "Adipose tissue-derived stem cells and their application in bone and cartilage tissue engineering," *Tissue Engineering Part B: Reviews*, vol. 15, no. 2, pp. 113–125, 2009.

[19] S. Gronthos, M. Mankani, J. Brahim, P. G. Robey, and S. Shi, "Postnatal human dental pulp stem cells (DPSCs) *in vitro* and *in vivo*," *Proceedings of the National Academy of Sciences of the United States of America*, vol. 97, no. 25, pp. 13625–13630, 2000.

[20] S. Gronthos, J. Brahim, W. Li et al., "Stem cell properties of human dental pulp stem cells," *Journal of Dental Research*, vol. 81, no. 8, pp. 531–535, 2002.

[21] M. Miura, S. Gronthos, M. Zhao et al., "SHED: stem cells from human exfoliated deciduous teeth," *Proceedings of the National Academy of Sciences of the United States of America*, vol. 100, no. 10, pp. 5807–5812, 2003.

[22] K. Sakai, A. Yamamoto, K. Matsubara et al., "Human dental pulp-derived stem cells promote locomotor recovery after complete transection of the rat spinal cord by multiple neuro-regenerative mechanisms," *The Journal of Clinical Investigation*, vol. 122, no. 1, pp. 80–90, 2012.

[23] K. Chen, H. Xiong, N. Xu, Y. Shen, Y. Huang, and C. Liu, "Chondrogenic potential of stem cells from human exfoliated deciduous teeth *in vitro* and *in vivo*," *Acta Odontologica Scandinavica*, vol. 72, no. 8, pp. 664–672, 2014.

[24] J. Dai, J. Wang, J. Lu et al., "The effect of co-culturing costal chondrocytes and dental pulp stem cells combined with exogenous FGF9 protein on chondrogenesis and ossification in engineered cartilage," *Biomaterials*, vol. 33, no. 31, pp. 7699–7711, 2012.

[25] J. Vera, J. Castro, A. Gonzalez, and A. Moenne, "Seaweed polysaccharides and derived oligosaccharides stimulate defense responses and protection against pathogens in plants," *Marine Drugs*, vol. 9, no. 12, pp. 2514–2525, 2011.

[26] A. Steward, Y. Liu, and D. Wagner, "Engineering cell attachments to scaffolds in cartilage tissue engineering," *Journal of Metals*, vol. 63, pp. 74–82, 2011.

[27] M. Sancho-Tello, F. Forriol, P. Gastaldi et al., "Time evolution of in vivo articular cartilage repair induced by bone marrow stimulation and scaffold implantation in rabbits," *The International Journal of Artificial Organs*, vol. 38, no. 4, pp. 210–223, 2015.

[28] J. M. Soria, M. Sancho-Tello, M. A. Esparza et al., "Biomaterials coated by dental pulp cells as substrate for neural stem cell differentiation," *Journal of Biomedical Materials Research Part A*, vol. 97, no. 1, pp. 85–92, 2011.

[29] Macouillard-Poulletier de Gann, M. A. Belaud-Rotureau, P. Voisin et al., "Flow cytometric analysis of mitochondrial activity *in situ*: application to acetylceramide-induced mitochondrial swelling and apoptosis," *Cytometry*, vol. 33, no. 3, pp. 333–339, 1998.

[30] R. Williams, I. M. Khan, K. Richardson et al., "Identification and clonal characterization of a progenitor cell subpopulation in normal human articular cartilage," *PLoS One*, vol. 5, no. 10, article e13246, 2010.

[31] M. Jakob, O. Démarteau, D. Schäfer et al., "Specific growth factors during the expansion and redifferentiation of adult human articular chondrocytes enhance chondrogenesis and cartilaginous tissue formation *in vitro*," *Journal of Cellular Biochemistry*, vol. 81, no. 2, pp. 368–377, 2001.

[32] K. von der Mark, V. Gauss, H. von der Mark, and P. Müller, "Relationship between cell shape and type of collagen synthesized as chondrocytes lose their cartilage phenotype in culture," *Nature*, vol. 267, no. 5611, pp. 531-532, 1977.

[33] E. A. Makris, A. H. Gomoll, K. N. Malizos, J. C. Hu, and K. A. Athanasiou, "Repair and tissue engineering techniques for articular cartilage," *Nature Reviews Rheumatology*, vol. 11, no. 1, pp. 21–34, 2015.

[34] B. M. Seo, M. Miura, S. Gronthos et al., "Investigation of multipotent postnatal stem cells from human periodontal ligament," *Lancet*, vol. 364, no. 9429, pp. 149–155, 2004.

[35] W. Sonoyama, Y. Liu, D. Fang et al., "Mesenchymal stem cell-mediated functional tooth regeneration in swine," *PLoS One*, vol. 1, article e79, 2006.

[36] N. Nuti, C. Corallo, B. M. Chan, M. Ferrari, and B. Gerami-Naini, "Multipotent differentiation of human dental pulp stem cells: a literature review," *Stem Cell Reviews*, vol. 12, no. 5, pp. 511–523, 2016.

[37] C. L. Nemeth, K. Janebodin, A. E. Yuan, J. E. Dennis, M. Reyes, and D. H. Kim, "Enhanced chondrogenic differentiation of dental pulp stem cells using nanopatterned PEG-GelMA-HA hydrogels," *Tissue Engineering Part A*, vol. 20, no. 21-22, pp. 2817–2829, 2014.

[38] P. Lohan, O. Treacy, K. Lynch et al., "Culture expanded primary chondrocytes have potent immunomodulatory properties and do not induce an allogeneic immune response," *Osteoarthritis and Cartilage*, vol. 24, no. 3, pp. 521–533, 2016.

[39] J. Ishikawa, N. Takahashi, T. Matsumoto et al., "Factors secreted from dental pulp stem cells show multifaceted benefits for treating experimental rheumatoid arthritis," *Bone*, vol. 83, pp. 210–219, 2016.

Hindawi
Stem Cells International
Volume 2017, Article ID 4206187, 10 pages
https://doi.org/10.1155/2017/4206187

Research Article

Ex Vivo Expansion of Human Limbal Epithelial Cells Using Human Placenta-Derived and Umbilical Cord-Derived Mesenchymal Stem Cells

Sang Min Nam,[1] Yong-Sun Maeng,[2] Eung Kweon Kim,[3,4] Kyoung Yul Seo,[3] and Helen Lew[1]

[1]*Department of Ophthalmology, CHA Bundang Medical Center, CHA University, Seongnam, Republic of Korea*
[2]*Department of Obstetrics and Gynecology, Institute of Women's Life Medical Science, Yonsei University College of Medicine, Seoul, Republic of Korea*
[3]*Department of Ophthalmology, Institute of Vision Research, Severance Hospital, Yonsei University College of Medicine, Seoul, Republic of Korea*
[4]*Corneal Dystrophy Research Institute, Yonsei University College of Medicine, Seoul, Republic of Korea*

Correspondence should be addressed to Kyoung Yul Seo; seoky@yuhs.ac and Helen Lew; eye@cha.ac.kr

Received 12 May 2017; Accepted 4 July 2017; Published 15 August 2017

Academic Editor: Miguel Alaminos

Copyright © 2017 Sang Min Nam et al. This is an open access article distributed under the Creative Commons Attribution License, which permits unrestricted use, distribution, and reproduction in any medium, provided the original work is properly cited.

Ex vivo culture of human limbal epithelial cells (LECs) is used to treat limbal stem cell (LSC) deficiency, a vision loss condition, and suitable culture systems using feeder cells or serum without animal elements have been developed. This study evaluated the use of human umbilical cord or placenta mesenchymal stem cells (C-MSCs or P-MSCs, resp.) as feeder cells in an animal/serum-free coculture system with human LECs. C-/P-MSCs stimulated LEC colony formation of the stem cell markers (p63, ABCG2) and secreted known LEC clonal growth factors (keratinocyte growth factor, β-nerve growth factor). Transforming growth factor-β-induced protein (TGFBIp), an extracellular matrix (ECM) protein, was produced by C-/P-MSCs and resulted in an increase in $p63^+$ $ABCG2^+$ LEC colonies. TGFBIp-activated integrin signaling molecules (FAK, Src, and ERK) were expressed in LECs, and TGFBIp-induced LEC proliferation was effectively blocked by a FAK inhibitor. In conclusion, C-/P-MSCs enhanced LEC culture by increasing growth of the LSC population by secreting growth factors and the ECM protein TGFBIp, which is suggested to be a novel factor for promoting the growth of LECs in culture. C-/P-MSCs may be useful for the generation of animal-free culture systems for the treatment of LSC deficiency.

1. Introduction

The limbus, where corneal epithelial stem cells reside, is the narrow zone between the cornea and the bulbar conjunctiva. Damage to the limbus results in limbal stem cell deficiency (LSCD), which causes severe vision loss by painful opacification of the otherwise transparent cornea. For LSCD treatment, transplantation of in vitro cultured limbal epithelial cell (LEC) sheets grown on various culture substrates has shown success in terms of ocular surface reconstruction and improved vision [1]. Therefore, it will be essential to determine a suitable culture system using different carriers of the sheet, culture medium, or feeder layer.

Murine 3T3 feeder layer cells increase the colony-forming efficiency of LECs and produce a robust sheet by unclear mechanisms [2]. However, the use of xenologic 3T3 cells may expose human LECs to mouse pathogens, presenting ethical and safety issues. To avoid xenogenic contamination, human dermal fibroblasts, human bone marrow mesenchymal stem cells (BM-MSCs), human limbal mesenchymal cells, and human adipose tissue-derived MSCs have been used as replaceable feeder cells [2–5]. Human MSCs express various genes that maintain or promote the proliferation of LECs, for example, pleiotrophin, epiregulin, cystatin C, hepatocyte growth factor (HGF), keratinocyte growth factor (KGF), and insulin-like growth factor 1a in adipose

tissue-derived MSCs and KGF, HGF, and N-cadherin in BM-MSCs [2, 3]. Human umbilical cord or placenta MSCs (C-MSCs or P-MSCs, resp.) may also be candidate feeder cells but, to the best of our knowledge, have not been tested in LEC culture.

Compared with BM-MSCs, a collection of human C-/P-MSCs is noninvasive and considered ethically acceptable, because the human placenta is discarded postpartum [6]. MSCs are abundant in the placenta but rare in the adult bone marrow [6]. In addition, the number of BM-MSCs significantly decreases with age [6]. C-/P-MSCs can be obtained efficiently, because P-MSCs grow faster and more robustly in culture than do BM-MSCs, and a substantial number of C-MSCs can be obtained after several passages [7, 8]. A feeder layer of C-MSCs also showed a nontumorigenic effect in embryonic stem cells by downregulating c-myc signaling [9].

With LSCD LEC sheet therapy, the percentage of $p63^+$ cells in culture is positively associated with the clinical outcome [10]. p63 sustains the proliferative potential of limbal stem cells (LSCs) and is expressed in holoclones [10–12]. ATP-binding cassette subfamily G member 2 (ABCG2) is the most useful marker of LSCs [12]. In this study, the potential of C-/P-MSCs in LEC culture was assessed according to $p63^+$ and $ABCG2^+$ colony formation. In addition, a new effective factor, transforming growth factor-β-induced protein (TGFBIp), was shown to be secreted by C-/P-MSCs, and a potential signaling pathway stimulating LEC proliferation is suggested.

2. Materials and Methods

2.1. LEC Culture. Limbal epithelial sheets were isolated from human corneoscleral rims after penetrating keratoplasty. This study was approved by the Institutional Review Board of Severance Hospital (Seoul, Republic of Korea). A human corneoscleral rim was incubated at 4°C for 10 h in CnT-PR medium (CELLnTec, Bern, Switzerland) containing 50 mg/mL dispase II (Roche, Indianapolis, IN, USA) and 100 mM sorbitol (Sigma-Aldrich, St. Louis, MO, USA). Under a dissection microscope, a loose limbal epithelial sheet was separated using a spatula, as described previously [13]. The limbal epithelial sheet was cultured on a 1 : 20 diluted Matrigel (Sigma-Aldrich)-coated plate in CnT-PR medium.

2.2. MSC Culture. P-MSCs (passage 6) and C-MSCs (passage 5) were provided by CHA Biotech (Seongnam, Republic of Korea). Preparation and characterization of both cell types have been described previously [14]. MSCs were cultured on a 150 mm culture dish in minimum essential medium-(MEM-) alpha (Gibco, Carlsbad, CA, USA) and 10% fetal bovine serum (FBS; Gibco).

2.3. Preparation of MSC-Conditioned Medium and the Colony-Forming Unit Assay. Confluent P-MSC or C-MSC cultures were grown in MEM-alpha without FBS for 24 hours, and the media were collected and centrifuged to remove cells and debris. The conditioned medium was added to CnT-PR medium at a 1 : 1 ratio. LECs (4×10^3) were seeded on a 1 : 20 diluted Matrigel-coated 60 mm dish containing conditioned medium and incubated for 10 days. The colonies were then fixed with 4% paraformaldehyde and stained with hematoxylin and eosin. The number of colony-forming units (CFU) in each dish was counted in four different microscopic fields of view. Experiments were performed in triplicate for each medium condition.

2.4. Coculture of MSCs and LECs. Cell culture inserts (Transwell; polycarbonate, 0.4 μm pore size; Corning, NY, USA) were coated with 1 : 20 diluted Matrigel, and 3×10^3 LECs were seeded on the inserts. In addition, 7×10^4 P-MSCs or C-MSCs were seeded as feeder cells in the bottom well of the paired wells and cocultured with LECs in CnT-PR medium for 10 days. Both P-MSCs and C-MSCs were tested in experiments using coculture. A CFU assay for LECs was performed as described above.

2.5. Immunocytochemical Analysis of LEC Colonies. LEC colonies were washed in phosphate-buffered saline (PBS), blocked with 5% donkey serum in an antibody dilution buffer consisting of PBS and 0.1% Triton X-100, incubated overnight with the primary antibody (p63 [Cell Signaling, Beverly, MA, USA] or ABCG2 [Abcam, Cambridge, MA, USA]) at 4°C, and labeled with a fluorescein-conjugated secondary antibody (Molecular Probes, Leiden, Netherlands). The colonies were then observed under a fluorescence microscope (Olympus, Tokyo, Japan).

2.6. Proteins Secreted by the MSCs. Protein levels in the MSC and LEC coculture medium were measured using enzyme-linked immunosorbent assay (ELISA) kits: human KGF quantikine ELISA kit (DKG00, R&D Systems, Minneapolis, MN, USA), human β IG H3 ELISA kit (TGFBI) (ab155426; Abcam), human EGF ELISA kit (ELH-EGF-001, THP; RayBiotech, Vienna, Austria), and human NGF-β ELISA kit (K0331220; Koma Biotech, Seoul, Republic of Korea). ELISAs were performed in triplicate for each sample, and coculture was performed in triplicate for each type of MSC.

2.7. Effect of TGFBIp on LEC Growth and Colony Formation. The 3-(4,5-dimethylthiazol-2-yl)-2,5-diphenyltetrazolium bromide (MTT) assay was used to evaluate LEC proliferation following TGFBIp treatment. LECs were seeded at 2×10^4/well in 96-well culture plates in CnT-PR medium. After 24 hours, the cells were then treated with human TGFBIp (Sino Biological Inc., 10569-H08H, Beijing, China) at different concentrations ranging from 0–10 μg/mL. Following TGFBIp treatment (24, 48, and 72 h), 20 μL MTT labeling reagent (5 mg/mL) was added to each well. The media were removed 4 hours later, 150 μL dimethyl sulfoxide (DMSO) was added to each well, and the absorbance was measured at 570 nm.

A CFU assay was performed for LECs treated with TGFBIp. LECs (4×10^3) were seeded on a 1 : 20 diluted Matrigel-coated 60 mm dish containing CnT-PR medium and TGFBIp (10 μg/mL). After 10 days of culture, the colony numbers were counted and the expression of p63 and ABCG2 was analyzed as described above.

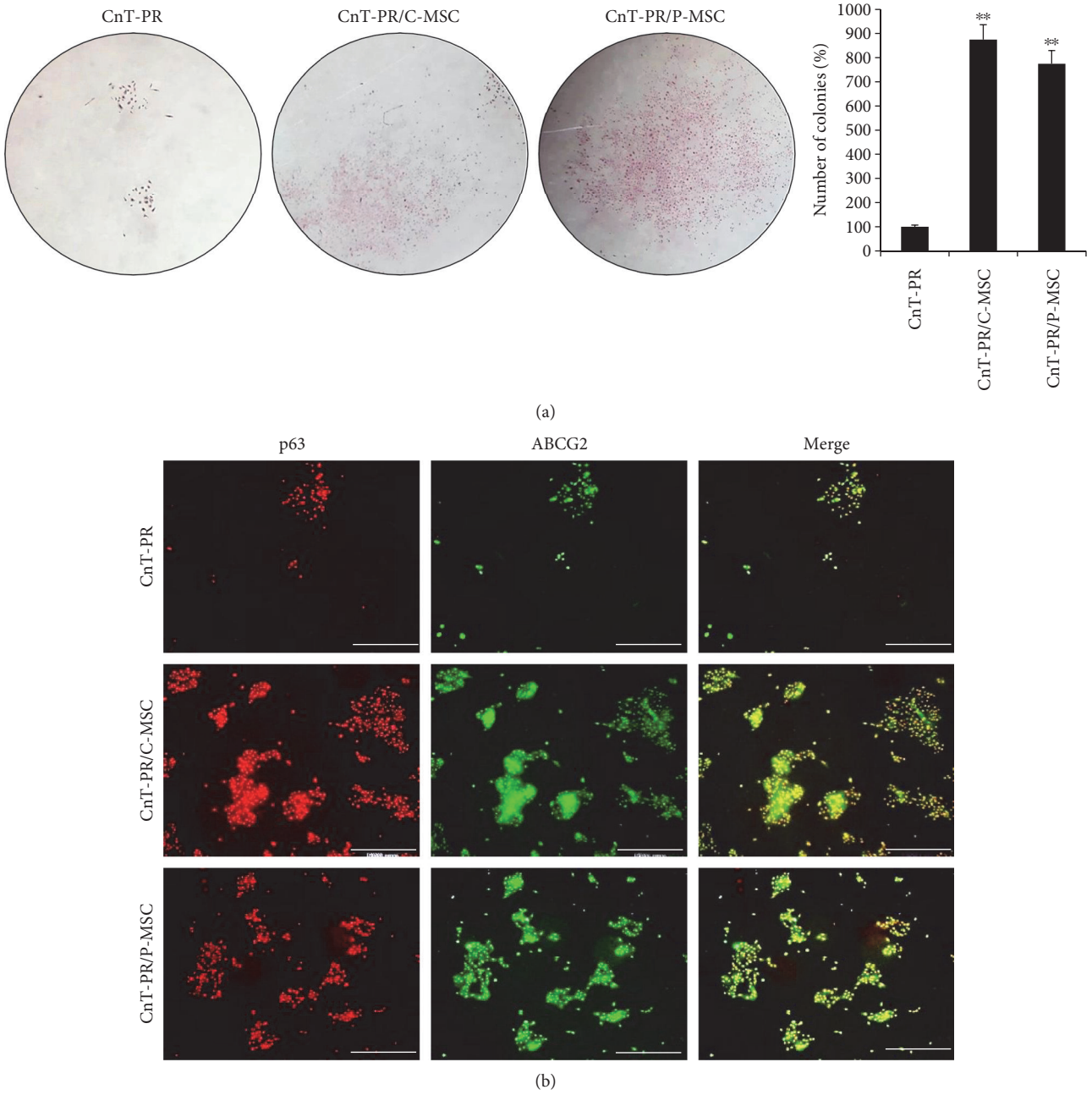

Figure 1: Colony-forming unit assay of conditioned medium from C-MSC or P-MSC. Microscopic analysis following hematoxylin and eosin (H&E) staining (a; magnification: ×10) and immunofluorescence analysis of p63 and ABCG2 (b; white bar indicates 500 μm) are shown. Error bars represent the standard deviation of the mean. $^{**}P < 0.01$, compared with the control medium, CnT-PR (Student's t-test). C-MSC: umbilical cord-derived mesenchymal stem cell; P-MSC: placenta-derived mesenchymal stem cell; ABCG2: ATP-binding cassette subfamily G member 2.

2.8. Western Blotting of Signaling Pathway Members Induced by TGFBIp. LECs (2×10^5/well) were seeded onto 60 mm plates. After 24 hours, cells were treated with TGFBIp (10 μg/mL) for various periods (5, 10, 15, 30, and 60 minutes). Cells were harvested using radio immunoprecipitation assay buffer; the resulting cell lysates were subjected to sodium dodecyl sulfate-polyacrylamide gel electrophoresis, and proteins from the gel were transferred onto polyvinylidene difluoride membranes. The blocked membranes were incubated with the appropriate primary antibody (anti-human, phosphorylated Src, phosphorylated AKT, extracellular signal-regulated kinase [ERK], phosphorylated ERK [pERK], focal adhesion kinase [FAK], or phosphorylated FAK [1 : 1000 dilution, Cell Signaling Technology Inc., Danvers, MA, USA]), and the immunoreactive bands were visualized using an enhanced chemiluminescence immunoblotting system (GE Healthcare, Buckinghamshire, UK). The intensity of a protein band was quantified by densitometry of immunoblots.

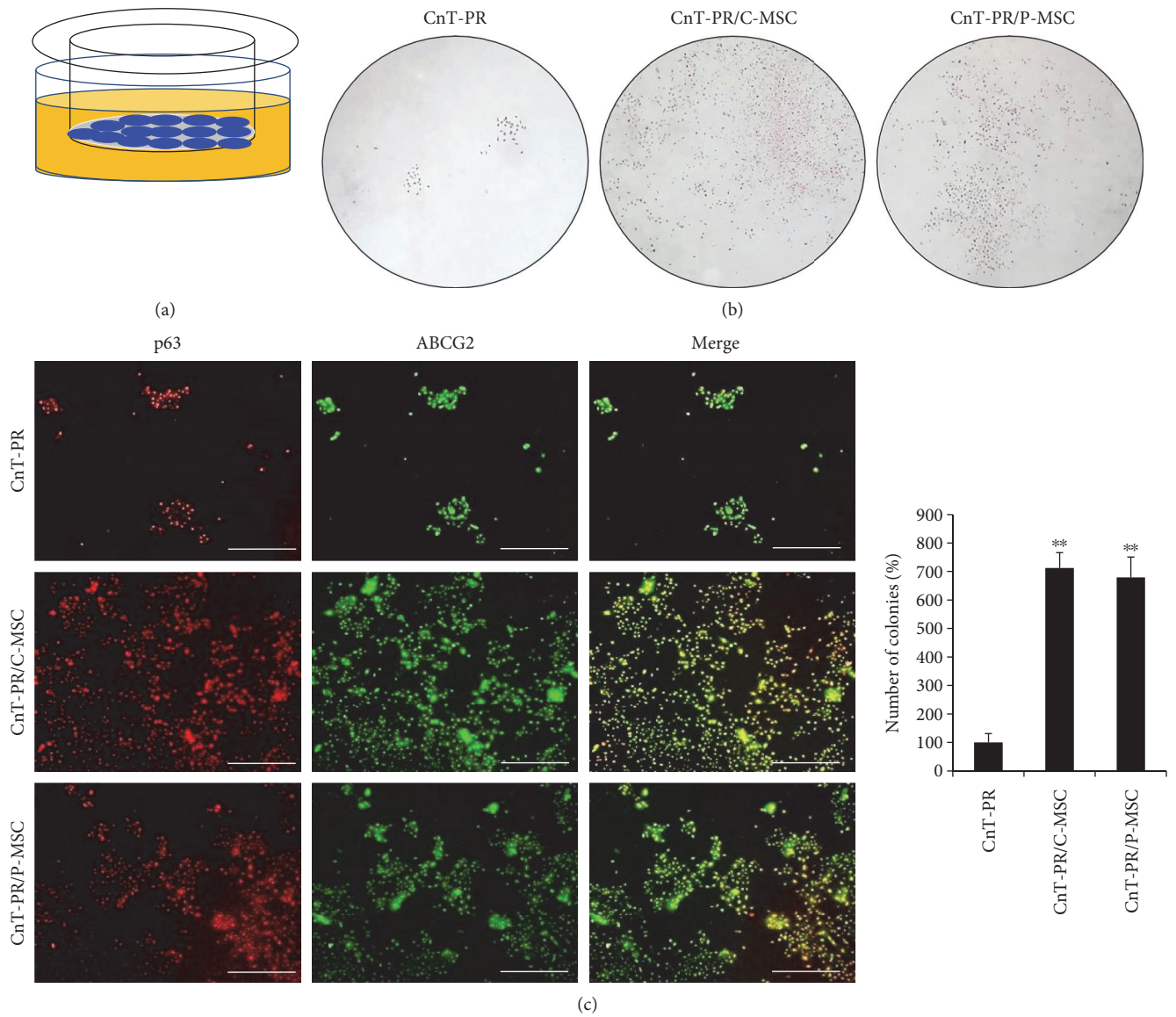

Figure 2: Coculture of MSCs and limbal epithelial cells (LECs) and colony-forming unit assay. Schematic of the coculture system containing LECs (blue in the insert) and MSCs (not shown). Yellow indicates medium. (a) Microscopic analysis following H&E staining (b; magnification: ×10) and immunofluorescence of p63 and ABCG2 (c; white bar indicates 500 μm) are shown. Error bars represent the standard deviation of the mean. $^{**}P < 0.01$, compared with the control medium, CnT-PR (Student's t-test). C-MSC: umbilical cord-derived mesenchymal stem cell; P-MSC: placenta-derived mesenchymal stem cell; ABCG2: ATP-binding cassette subfamily G member 2.

2.9. FAK Inhibitor and LEC Proliferation Assay. LECs were seeded at 2×10^4/well in 96-well culture plates. The cells were incubated in CnT-PR medium for 24 hours and preincubated for 40 minutes with or without 1 μM CAS 4506-66-5 (FAK inhibitor 14, Sigma-Aldrich). The cells were then treated with 10 μg/mL human TGFBIp (Sino Biological Inc., 10569-H08H). Following TGFBIp treatment (24, 48, and 72 hours), 20 μL MTT labeling reagent (5 mg/mL) was added to each well. The media were removed 4 hours later, 150 μL DMSO was added to each well, and the absorbance was measured at 570 nm.

3. Results

3.1. Promotion of $p63^+$ $ABCG2^+$ LEC Colonies by C- or P-MSCs. C- or P-MSCs were tested in two different systems, conditioned medium and coculture systems. First, conditioned media from both C-MSC and P-MSC cultures increased the number of LEC colonies compared with the basal medium, CnT-PR (Figure 1). In addition, almost all of the colonies were positive for p63 and ABCG2 (Figure 1). Because ABCG2 is a marker of LSCs and p63 is correlated with positive clinical outcomes, some factors in the conditioned medium may promote a positive clinical effect by promoting the growth of $p63^+$ and $ABCG2^+$ cells. A Transwell coculture system was designed: in this convenient system, C-/P-MSCs did not contact LECs directly, but LECs were continuously exposed to factors secreted from C-/P-MSCs (Figure 2). In this system, elements were directly transferred from C-/P-MSCs to LECs. In both C-MSC and P-MSC coculture systems, the number of colonies increased in

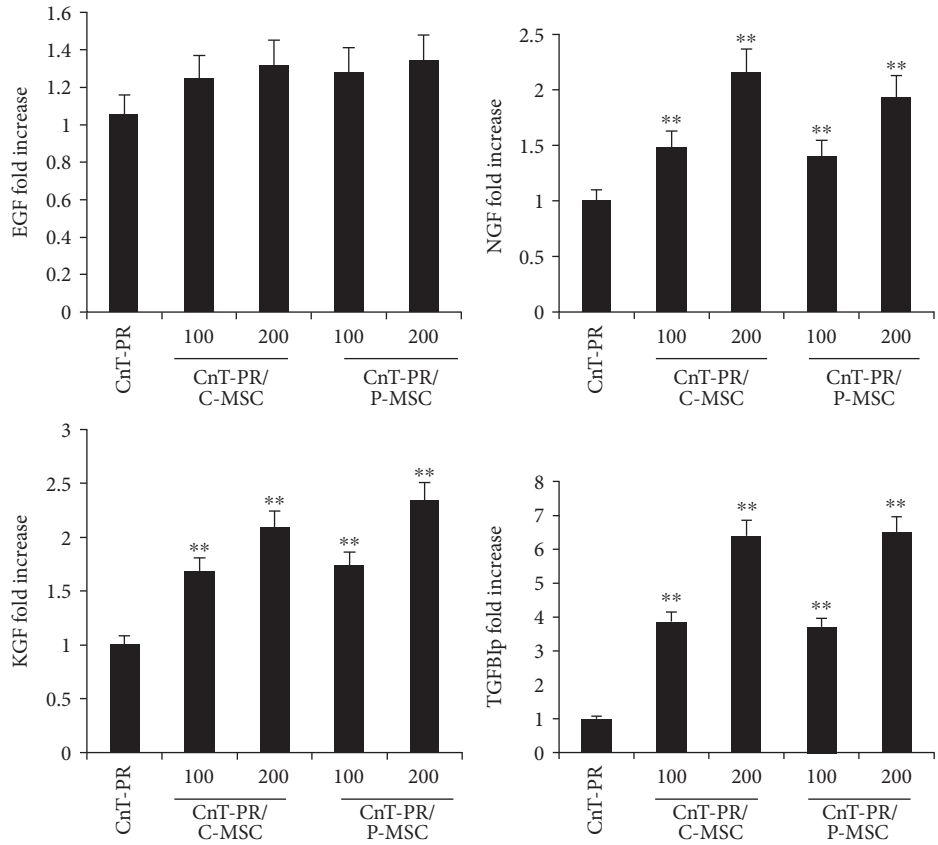

Figure 3: Human protein levels in the supernatant of the coculture medium, detected by the enzyme-linked immunosorbent assay. C-MSCs or P-MSCs were cultured with limbal epithelial cells. The control medium was CnT-PR, and each supernatant was tested in two different volumes: 100 μL and 200 μL. $^{**}P < 0.01$, compared with the control medium, CnT-PR (Student's t-test). Error bars represent the standard deviation of the mean. C-MSC: umbilical cord-derived mesenchymal stem cell; P-MSC: placenta-derived mesenchymal stem cell; EGF: epidermal growth factor; NGF: nerve growth factor; KGF: keratinocyte growth factor; TGFBIp: transforming growth factor-β-induced protein.

comparison to that of colonies in CnT-PR medium, and nearly all of the colonies were positive for p63 and ABCG2 (Figure 2). However, the number of colonies generated was not greater in the coculture system compared with conditioned medium (Figures 1 and 2). Because only CnT-PR medium was used in the coculture system, the increase in the number of LEC colonies appeared to be caused by factors secreted by C-/P-MSCs. In contrast, the conditioned medium consisted of MEM-alpha, CnT-PR, and elements secreted by C-/P-MSCs. Therefore, secreted factors in the conditioned medium and the coculture system promoted the formation of $p63^+$ $ABCG2^+$ LEC colonies. Although both C-MSCs and P-MSCs were cultured in CnT-PR medium without serum in the coculture system, their functions were comparable when grown in MEM-alpha medium with serum.

3.2. β-NGF, KGF, and TGFBIp Were Present at Higher Levels in the Coculture System. To determine the factors secreted by C-/P-MSCs, the supernatant obtained from the coculture medium was analyzed by ELISA to detect human epidermal growth factor (EGF), KGF, β-nerve growth factor (β-NGF), and TGFBIp. EGF, KGF, and β-NGF stimulate clonal growth of LSCs, and TGFBIp was chosen as a novel candidate [15]. In both C-MSC and P-MSC coculture media, EGF was not significantly elevated compared with that in CnT-PR medium alone (Figure 3). In contrast, KGF, β-NGF, and TGFBIp were detected at higher levels in both C-MSC and P-MSC coculture media compared with CnT-PR medium alone (Figure 3). The concentration of TGFBIp was remarkably high compared with that of KGF and β-NGF in both C-MSC and P-MSC coculture media (Figure 3). Based on these findings, KGF, β-NGF, and TGFBIp, but not EGF, may have been responsible for the increase in $p63^+$ $ABCG2^+$ LEC colonies.

3.3. TGFBIp Promoted Colony Formation and Proliferation of LECs via FAK and ERK Signaling. To confirm the effect of TGFBIp, a LEC proliferation assay was performed, and the results revealed that TGFBIp promoted proliferation of LECs in a dose-dependent manner up to 10 μg/mL at three different time points (Figure 4(a)). TGFBIp was added to CnT-PR medium at 10 μg/mL, and the TGFBIp-containing medium resulted in more colonies than did the control medium; the majority of which were $p63^+$ and $ABCG2^+$ (Figures 5(a) and 5(b)).

To determine which signaling pathways are involved in TGFBIp-induced LEC proliferation, different intracellular signaling molecules were analyzed. TGFBIp interacts with

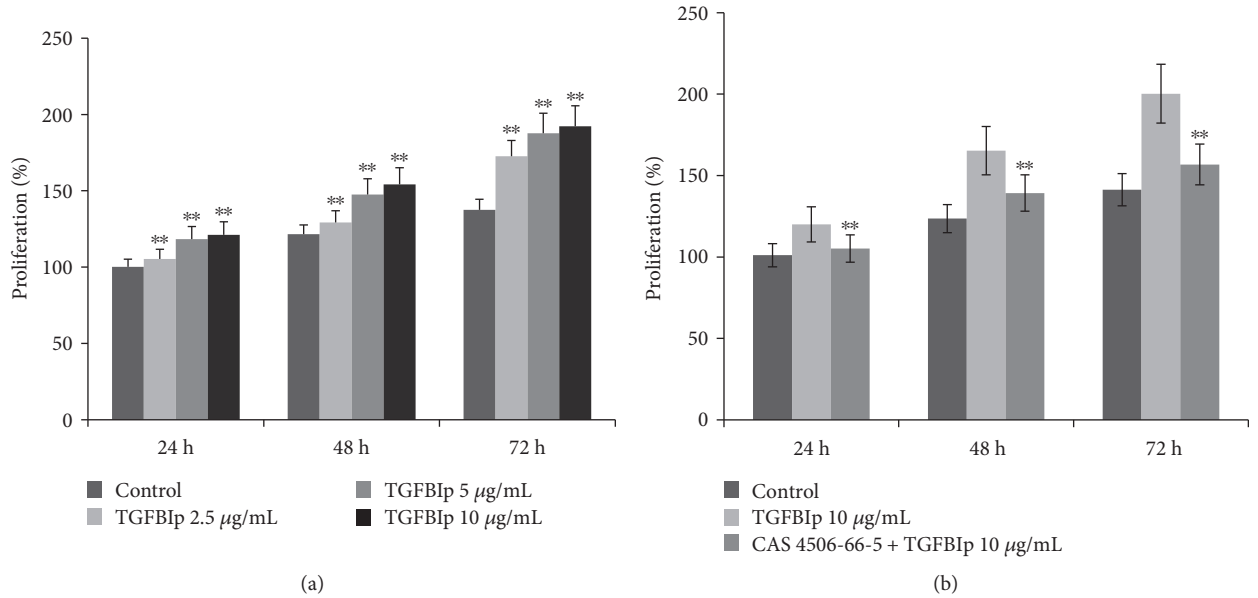

Figure 4: Effect of TGFBIp on limbal epithelial cell (LEC) proliferation. LECs were incubated with TGFBIp (0–10 μg/mL) for 72 h (a). LECs were preincubated with or without the FAK inhibitor CAS 4506-66-5 (1 μM) and then stimulated with TGFBIp (10 μg/mL) for 72 h (b). Cell proliferation was assessed by the MTT assay. Error bars represent the standard deviation of the mean. $^{**}P < 0.01$, compared with the control medium, TGFBIp 0 μg/mL (Student's t-test). TGFBIp: transforming growth factor-β-induced protein.

integrins with multiple motifs, including the C-terminal RGD motif, and activates integrin-associated proteins, such as FAK and Src [16]. As a result, FAK promotes cell proliferation via ERK signaling or cell survival via AKT activation [16]. The expression of FAK, SRC, ERK, and AKT were evaluated by Western blotting following incubation with TGFBIp-containing (10 μg/mL) CnT-PR medium. Phosphorylation of FAK, SRC, and ERK was increased by TGFBIp stimulation, while AKT phosphorylation was unaffected (Figure 6). To investigate the significance of the FAK signaling pathway, LECs were pretreated with a FAK inhibitor (CAS 4506-66-5) and stimulated with TGFBIp. LEC proliferation by TGFBIp was effectively blocked by CAS 4506-66-5 at three different time points (Figure 4(b)). Overall, TGFBIp stimulated LEC proliferation, which was suppressed by CAS 4506-66-5, and the formation of $p63^+$ $ABCG2^+$ LEC colonies, suggesting that TGFBIp may act on LECs via integrins.

4. Discussion

Factors secreted by human C-/P-MSCs promoted the formation of $p63^+$ $ABCG2^+$ colonies in LEC culture. The levels of KGF, β-NGF, and TGFBIp were elevated in C-/P-MSC coculture media, and TGFBIp stimulated LEC proliferation via the FAK, Src, and ERK signaling pathways.

CnT-PR is a serum-free medium developed for progenitor cell-targeted growth with good colony-forming ability [15]. However, in LEC culture, serum-free CnT-PR is unsuccessful for LSC transplantation, as serum support seems to be essential [17, 18]. Vitronectin and fibronectin, ECM proteins present in FBS, are important for the initial attachment of LECs [19]. For clinical use, animal-free culture techniques have been developed using autologous serum, and these have shown promising clinical results [20]. In this study, serum was removed from the C-/P-MSC culture medium 24 hours before adding it to CnT-PR medium to generate the conditioned medium. Coculture with C-/P-MSCs was also performed under serum-free conditions as only CnT-PR medium was used. Under both serum-free conditions, the number of the $p63^+$ $ABCG2^+$ LEC colonies was increased compared with that under the use of CnT-PR medium alone, which implied that C-/P-MSCs enhanced the LEC culture system for LSCD treatment in the absence of serum (Figures 1 and 2).

Human epidermal keratinocytes generate three types of clonogenic cells, holoclones, meroclones, and paraclones, which have different proliferative capacities [21]. Holoclone-forming cells have the ability to self-renew and high proliferative potential; they are human squamous epithelial stem cells located in the limbus but not in the central cornea [10, 21]. p63 is a marker of holoclones, and quantitative immunodetection of p63 is used as a validation method before grafting in LSCD patients [10, 22]. Success of LEC transplantation is associated with the percentage of p63-positive cells (p63%) in culture; the success rate is 78% if p63% > 3% but only 11% if p63% $\leqq$ 3% [10]. Therefore, the increase in $p63^+$ LEC colony number by C-/P-MSCs could improve LEC transplantation.

3T3 fibroblasts have been introduced as feeder cells [23]. Because 3T3 fibroblasts are effective without directly contacting LECs, soluble factors derived from 3T3 fibroblasts may be involved in the promotion of LSCs [24]. Hence, the Transwell coculture system may be clinically applicable and potentially involve soluble factors from the MSCs (Figure 2). In addition, the Transwell coculture system helps to avoid mixing problems with feeder cells

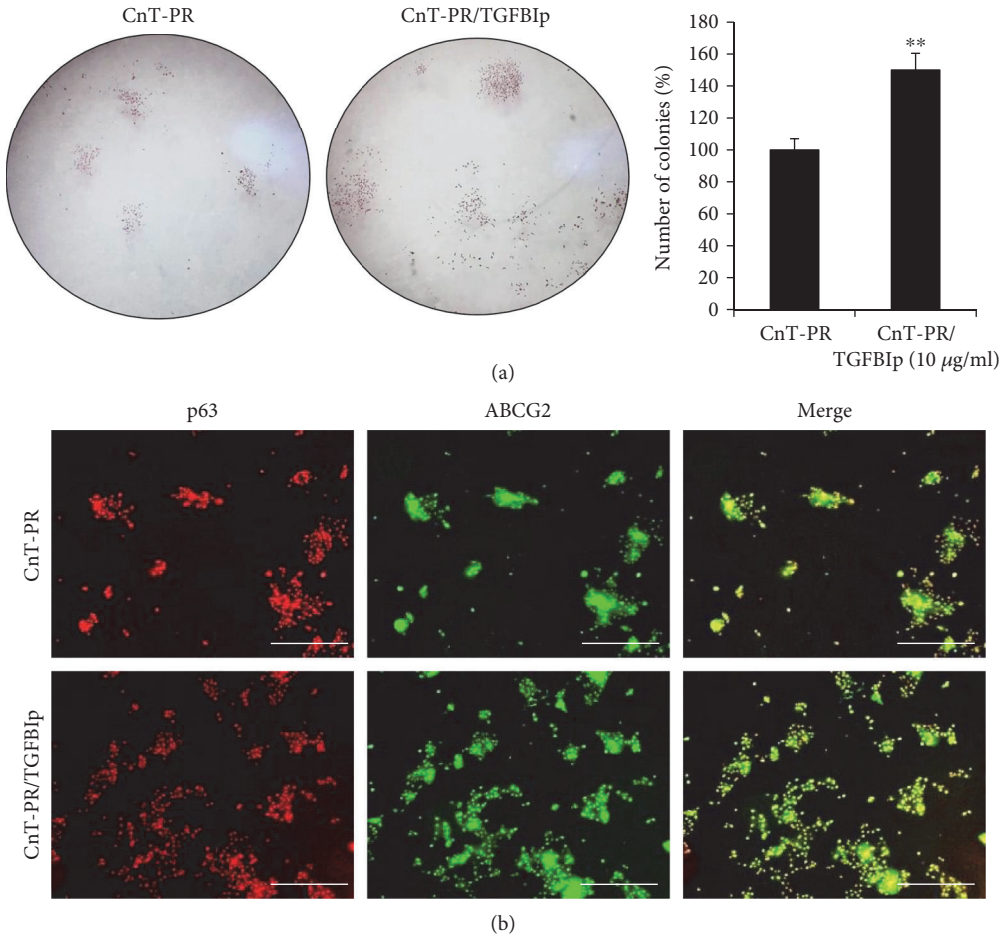

Figure 5: Colony-forming unit assay of limbal epithelial cell (LEC) after treatment with TGFBIp. Microscopic analysis following H&E staining (a; magnification: ×10) and immunofluorescence of p63 and ABCG2 (b; white bar indicates 500 μm) are shown. Error bars represent the standard deviation of the mean. $^{**}P < 0.01$, compared with the control medium, CnT-PR (Student's t-test). TGFBIp: transforming growth factor-β-induced protein.

because transplantable LECs on the insert can be cultured separately. The importance of soluble factors was reaffirmed by the C-/P-MSC-conditioned medium (Figure 1). In comparison with conditioned medium, the coculture system provides fresh MSC-derived factors to the LECs. However, the coculture conditions may not be perfect for MSCs, for which serum-free CnT-PR medium was used. For the conditioned medium, C-/P-MSCs were cultured with serum and MEM-alpha. As a result, the colony formation ability of the coculture system was not superior but comparable with that of the conditioned medium (Figures 1 and 2).

The soluble factors KGF and β-NGF, but not EGF, were present at higher levels in the coculture medium compared with the CnT-PR control medium (Figure 3). KGF and EGF stimulate clonal growth of human LECs more than do HGF and other growth factors [15]. Expression of KGF in human MSCs has been reported in LEC culture, but EGF and β-NGF have not been investigated [2, 3]. KGF is highly expressed in limbal fibroblasts, and the basal layers of the limbal epithelium express the KGF receptor [25]. KGF increases p63 expression in human LECs, and human LSCs may require KGF expression to maintain an undifferentiated state [25]. However, KGF does not inhibit the differentiation of LECs, which may be beneficial for the culture of LEC sheets that include both undifferentiated and differentiated cell layers [25, 26]. In contrast, EGF inhibits the expression of differentiation markers in corneal epithelial cells [26]. The NGF receptor, TrkA, is also expressed in limbal epithelial basal cells, and β-NGF exhibits an additive effect with EGF on the promotion of LEC growth rate [15]. β-NGF signaling favors LSC survival and is important for the expansion of limbal epithelial progenitor cells; a high level of NGF is present in the human amniotic membrane, and LEC expansion on the amniotic membrane is significantly retarded by blocking NGF signaling [27].

TGFBIp was detected at much higher concentrations in C-/P-MSC coculture medium compared with CnT-PR control medium, and it promoted LEC colony formation and proliferation (Figures 3, 4(a), and 5). To the best of our knowledge, the effect of TGFBIp on LEC colony formation has not yet been reported. TGFBIp is an ECM protein detected in various cell types, including MSCs

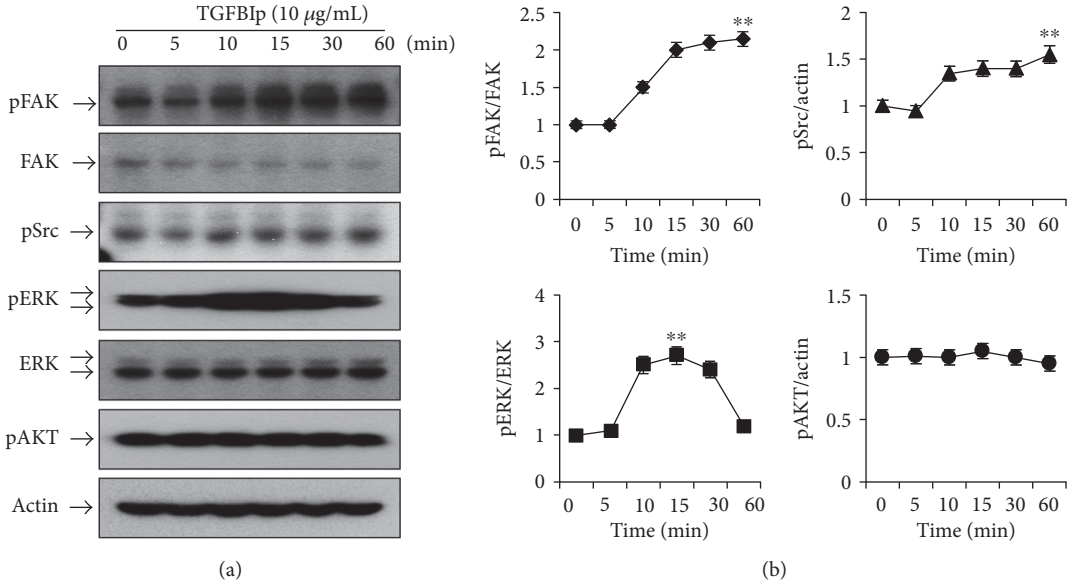

Figure 6: Effects of TGFBIp on the FAK, Src, and ERK signaling pathways in limbal epithelial cells (LECs). Representative Western blotting images (a) and densitometric analyses (b). LECs were treated with TGFBIp (10 μg/mL) for the indicated periods of time, and cell lysates were subjected to Western blot analysis. The relative ratios were normalized by arbitrarily setting the phosphorylation ratio at 0 minute as 1. Analyses were performed in triplicate. Error bars represent the standard error of the mean. $^{**}P < 0.01$, compared with the ratio at 0 minute (Student's t-test). TGFBIp: transforming growth factor-β-induced protein; FAK: focal adhesion kinase; ERK: extracellular signal-regulated kinase.

and corneal epithelial cells [28–30]. TGFBIp participates in diverse processes including cell adhesion and migration and contributes to wound healing in human corneal epithelial cells [28, 30]. TGFBIp has multiple integrin-binding motifs including Arg-Gly-Asp (RGD), NKDIL (sequence of peptide), and EPDIM (sequence of peptide) and interacts with other ECM molecules, such as collagen, fibronectin, laminin, or glycosaminoglycan [29, 30]. Therefore, TGFBIp would be able to function as a linker protein connecting the ECM and integrins. LECs express several integrins that can interact with TGFBIp, such as $\alpha 3\beta 1$, $\alpha v\beta 5$, and $\alpha 6\beta 4$ [30, 31]. TGFBIp may create favorable conditions for LEC attachment during culture, resulting in increased colony formation.

The LEC integrins $\alpha 3\beta 1$ and $\alpha 6\beta 4$ may function in cell survival and proliferation when activated by TGFBIp [31]. Integrins cooperate with other growth factors or cytokine receptors by transactivation, coordination, modulation, and compartmentalization [32]. In addition, $\beta 1$ and $\beta 4$ are highly expressed in LSCs and may be important for maintaining the stem cell population [31, 33]. Integrins play an important role in the regulation of stem cell function including stem cell proliferation, self-renewal, and cell division orientation [33]. Consequently, TGFBIp may promote LEC cell proliferation and $p63^+$ $ABCG2^+$ colony formation.

In intracellular integrin signaling, FAK associates with integrin and plays a key role in the formation of a signaling complex with other molecules [34]. The activated dual kinase FAK-Src complex functions to promote cell migration, proliferation, and survival [16]. Crk-associated substrate and c-Jun N-terminal kinase (JNK) are involved in cell migration, ERK and cyclin D1 are important for cell cycle progression, and phosphatidylinositol 3-kinase (PI3K) and AKT are involved in FAK-dependent cell survival [16, 34]. In the TGFBIp-dependent pathway, $\alpha v\beta 5$ integrin triggers phosphorylation and activation of FAK, paxillin, AKT, and ERK and mediates the adhesion and migration of vascular smooth muscle cells [35]. Coculture with mouse embryonic stem cells enhances the adhesion, migration, and proliferation of rabbit corneal epithelial cells via the integrin $\beta 1$-FAK-AKT pathway [36]. In the present study, TGFBIp activated FAK, Src, and ERK signaling, but not AKT signaling, in human LECs (Figure 6). Because TGFBIp-dependent LEC proliferation was effectively suppressed by a FAK inhibitor (Figure 4(b)), FAK activation by integrin might be an essential step for TGFBIp action in LECs, although the importance of Src and ERK remains to be assessed. This study showed that TGFBIp was secreted by C-/P-MSCs and TGFBIp activity in LECs required FAK activation. ERK has been shown to regulate the migration of immortalized human corneal epithelial cells during wound healing by modulating the phosphorylation of FAK and paxillin [37]. Therefore, ERK may not be a downstream mediator of FAK.

5. Conclusions

Human C-/P-MSCs supported the LSC population in LEC culture by secreting growth factors and ECM proteins such as TGFBIp. We have shown that TGFBIp regulates LECs possibly via integrin signaling. Human C-/P-MSCs can be obtained safely and efficiently and may help in the

development of an animal-free LEC culture system for the treatment of LSCD.

Conflicts of Interest

The authors declare no conflicts of interest. Eung Kweon Kim is a medical advisory board member of Avellino Lab USA.

Authors' Contributions

Kyoung Yul Seo and Helen Lew contributed equally to this work.

Acknowledgments

This research was supported by a grant from the Korea Health Technology R&D Project through the Korea Health Industry Development Institute, funded by the Ministry of Health & Welfare, Republic of Korea (Grant no. HI14C1607).

References

[1] I. Mariappan, S. Maddileti, S. Savy et al., "In vitro culture and expansion of human limbal epithelial cells," *Nature Protocols*, vol. 5, no. 8, pp. 1470–1479, 2010.

[2] M. Omoto, H. Miyashita, S. Shimmura et al., "The use of human mesenchymal stem cell-derived feeder cells for the cultivation of transplantable epithelial sheets," *Investigative Ophthalmology and Visual Science*, vol. 50, no. 5, pp. 2109–2115, 2009.

[3] H. Sugiyama, K. Maeda, M. Yamato et al., "Human adipose tissue-derived mesenchymal stem cells as a novel feeder layer for epithelial cells," *Journal of Tissue Engineering and Regenerative Medicine*, vol. 2, no. 7, pp. 445–449, 2008.

[4] X. Zhang, H. Sun, X. Li, X. Yuan, L. Zhang, and S. Zhao, "Utilization of human limbal mesenchymal cells as feeder layers for human limbal stem cells cultured on amniotic membrane," *Journal of Tissue Engineering and Regenerative Medicine*, vol. 4, no. 1, pp. 38–44, 2010.

[5] S. M. Sharma, T. Fuchsluger, S. Ahmad et al., "Comparative analysis of human-derived feeder layers with 3T3 fibroblasts for the ex vivo expansion of human limbal and oral epithelium," *Stem Cell Reviews and Reports*, vol. 8, no. 3, pp. 696–705, 2012.

[6] Z. Miao, J. Jin, L. Chen et al., "Isolation of mesenchymal stem cells from human placenta: comparison with human bone marrow mesenchymal stem cells," *Cell Biology International*, vol. 30, no. 9, pp. 681–687, 2006.

[7] T. Nagamura-Inoue and H. He, "Umbilical cord-derived mesenchymal stem cells: their advantages and potential clinical utility," *World Journal of Stem Cells*, vol. 6, no. 2, pp. 195–202, 2014.

[8] S. Barlow, G. Brooke, K. Chatterjee et al., "Comparison of human placenta- and bone marrow-derived multipotent mesenchymal stem cells," *Stem Cells and Development*, vol. 17, no. 6, pp. 1095–1107, 2008.

[9] D. C. Ding, Y. H. Chang, W. C. Shyu, and S. Z. Lin, "Human umbilical cord mesenchymal stem cells: a new era for stem cell therapy," *Cell Transplantation*, vol. 24, no. 3, pp. 339–347, 2015.

[10] P. Rama, S. Matuska, G. Paganoni, A. Spinelli, M. D. Luca, and G. Pellegrini, "Limbal stem-cell therapy and long-term corneal regeneration," *New England Journal of Medicine*, vol. 363, no. 2, pp. 147–155, 2010.

[11] C. Blanpain and E. Fuchs, "p63: revving up epithelial stem-cell potential," *Nature Cell Biology*, vol. 9, no. 7, pp. 731–733, 2007.

[12] U. Schlotzer-Schrehardt and F. E. Kruse, "Identification and characterization of limbal stem cells," *Experimental Eye Research*, vol. 81, no. 3, pp. 247–264, 2005.

[13] E. M. Espana, A. C. Romano, T. Kawakita, M. D. Pascuale, R. Smiddy, and S. C. Tseng, "Novel enzymatic isolation of an entire viable human limbal epithelial sheet," *Investigative Ophthalmology and Visual Science*, vol. 44, no. 10, pp. 4275–4281, 2003.

[14] M. J. Kim, K. S. Shin, J. H. Jeon et al., "Human chorionic-plate-derived mesenchymal stem cells and Wharton's jelly-derived mesenchymal stem cells: a comparative analysis of their potential as placenta-derived stem cells," *Cell and Tissue Research*, vol. 346, no. 1, pp. 53–64, 2011.

[15] E. A. Meyer-Blazejewska, F. E. Kruse, K. Bitterer et al., "Preservation of the limbal stem cell phenotype by appropriate culture techniques," *Investigative Ophthalmology and Visual Science*, vol. 51, no. 2, pp. 765–774, 2010.

[16] S. K. Mitra and D. D. Schlaepfer, "Integrin-regulated FAK-Src signaling in normal and cancer cells," *Current Opinion in Cell Biology*, vol. 18, no. 5, pp. 516–523, 2006.

[17] N. Zakaria, T. Possemiers, S. N. Dhubhghaill et al., "Results of a phase I/II clinical trial: standardized, non-xenogenic, cultivated limbal stem cell transplantation," *Journal of Translational Medicine*, vol. 12, no. 1, p. 58, 2014.

[18] S. Gonzalez, L. Chen, and S. X. Deng, "Comparative study of xenobiotic-free media for the cultivation of human limbal epithelial stem/progenitor cells," *Tissue Engineering Part C: Methods*, vol. 23, no. 4, pp. 219–227, 2017.

[19] J. G. Steele, G. Johnson, H. J. Griesser, and P. A. Underwood, "Mechanism of initial attachment of corneal epithelial cells to polymeric surfaces," *Biomaterials*, vol. 18, no. 23, pp. 1541–1551, 1997.

[20] V. S. Sangwan, S. Basu, G. K. Vemuganti et al., "Clinical outcomes of xeno-free autologous cultivated limbal epithelial transplantation: a 10-year study," *British Journal of Ophthalmology*, vol. 95, no. 11, pp. 1525–1529, 2011.

[21] U. Schlotzer-Schrehardt, "Clonal analysis of limbal epithelial stem cell populations," *Methods in Molecular Biology*, vol. 1014, pp. 55–64, 2013, Chapter 3.

[22] R. Hayashi, M. Yamato, H. Takayanagi et al., "Validation system of tissue-engineered epithelial cell sheets for corneal regenerative medicine," *Tissue Engineering Part C: Methods*, vol. 16, no. 4, pp. 553–560, 2010.

[23] A. J. Shortt, G. A. Secker, M. D. Notara et al., "Transplantation of ex vivo cultured limbal epithelial stem cells: a review of techniques and clinical results," *Survey of Ophthalmology*, vol. 52, no. 5, pp. 483–502, 2007.

[24] S. C. Tseng, S. Y. Chen, Y. C. Shen, W. L. Chen, and F. R. Hu, "Critical appraisal of ex vivo expansion of human limbal epithelial stem cells," *Current Molecular Medicine*, vol. 10, no. 9, pp. 841–850, 2010.

[25] H. Miyashita, S. Yokoo, S. Yoshida et al., "Long-term maintenance of limbal epithelial progenitor cells using rho

kinase inhibitor and keratinocyte growth factor," *Stem Cells Translational Medicine*, vol. 2, no. 10, pp. 758–765, 2013.

[26] S. E. Wilson, Y. G. He, J. Weng, J. D. Zieske, J. V. Jester, and G. S. Schultz, "Effect of epidermal growth factor, hepatocyte growth factor, and keratinocyte growth factor, on proliferation, motility and differentiation of human corneal epithelial cells," *Experimental Eye Research*, vol. 59, no. 6, pp. 665–678, 1994.

[27] A. Touhami, M. Grueterich, and S. C. Tseng, "The role of NGF signaling in human limbal epithelium expanded by amniotic membrane culture," *Investigative Ophthalmology and Visual Science*, vol. 43, no. 4, pp. 987–994, 2002.

[28] Y. S. Maeng, G. H. Lee, B. Lee, S. I. Choi, T. I. Kim, and E. K. Kim, "Role of TGFBIp in wound healing and mucin expression in corneal epithelial cells," *Yonsei Medical Journal*, vol. 58, no. 2, pp. 423–431, 2017.

[29] Y. S. Maeng, Y. J. Choi, and E. K. Kim, "TGFBIp regulates differentiation of EPC (CD133(+) C-kit(+) Lin(-) cells) to EC through activation of the Notch signaling pathway," *Stem Cells*, vol. 33, no. 6, pp. 2052–2062, 2015.

[30] M. P. Ween, M. K. Oehler, and C. Ricciardelli, "Transforming growth factor-beta-induced protein (TGFBI)/(betaig-H3): a matrix protein with dual functions in ovarian cancer," *International Journal of Molecular Sciences*, vol. 13, no. 8, pp. 10461–10477, 2012.

[31] M. A. Stepp, "Corneal integrins and their functions," *Experimental Eye Research*, vol. 83, no. 1, pp. 3–15, 2006.

[32] M. F. Brizzi, G. Tarone, and P. Defilippi, "Extracellular matrix, integrins, and growth factors as tailors of the stem cell niche," *Current Opinion in Cell Biology*, vol. 24, no. 5, pp. 645–651, 2012.

[33] S. J. Ellis and G. Tanentzapf, "Integrin-mediated adhesion and stem-cell-niche interactions," *Cell and Tissue Research*, vol. 339, no. 1, pp. 121–130, 2010.

[34] B. D. Cox, M. Natarajan, M. R. Stettner, and C. L. Gladson, "New concepts regarding focal adhesion kinase promotion of cell migration and proliferation," *Journal of Cellular Biochemistry*, vol. 99, no. 1, pp. 35–52, 2006.

[35] B. H. Lee, J. S. Bae, R. W. Park, J. E. Kim, J. Y. Park, and I. S. Kim, "betaig-h3 triggers signaling pathways mediating adhesion and migration of vascular smooth muscle cells through alphavbeta5 integrin," *Experimental and Molecular Medicine*, vol. 38, no. 2, pp. 153–161, 2006.

[36] J. Zhou, F. Chen, J. Xiao et al., "Enhanced functional properties of corneal epithelial cells by coculture with embryonic stem cells via the integrin beta1-FAK-PI3K/Akt pathway," *International Journal of Biochemistry and Cell Biology*, vol. 43, no. 8, pp. 1168–1177, 2011.

[37] S. Teranishi, K. Kimura, and T. Nishida, "Role of formation of an ERK-FAK-paxillin complex in migration of human corneal epithelial cells during wound closure in vitro," *Investigative Ophthalmology and Visual Science*, vol. 50, no. 12, pp. 5646–5652, 2009.